Combination of ALK and MEK inhibitors for the treatment of ALK-positive non-small cell lung cancer

Nensi Shrestha

A thesis submitted for the degree of

Doctor of Philosophy

at the University of Otago, Dunedin,

New Zealand.

November 2020

This thesis is dedicated to my father, Upendra Lal Shrestha
and mother, Manjala Shrestha.

ABSTRACT

Anaplastic lymphoma kinase (ALK)-positive non-small cell lung cancer (NSCLC) most commonly arises through Echinoderm microtubule-associated protein like 4 (EML4)-ALK chromosomal fusion and is associated with younger aged patients with non-smoking or light smoking history. Patients harbouring EML4-ALK fusion oncoprotein are highly sensitive to ALK-tyrosine kinase inhibitors (TKIs). Crizotinib, a first generation ALK-TKI, was approved by the Food and Drug Administration (FDA) for the treatment of ALK-positive NSCLC patients. Crizotinib has demonstrated superior efficacy compared to standard platinum-based chemotherapy with longer progression-free survival and a higher objective response rate. However, the clinical benefit of crizotinib (and other ALK inhibitors) is limited due to the development of acquired resistance typically within a year of therapy. Mechanism of resistance includes copy number gain, secondary mutations in ALK, or activation of bypass signalling pathways Thus, this study investigated the possibility of improving the efficacy of ALK inhibition, and overcoming resistance, by employing the combined effect of ALK inhibitor, crizotinib and MEK inhibitor, selumetinib in both crizotinib naïve (H3122) and crizotinib resistant (CR-H3122) ALK-positive non-small cell lung cancer cells.

The combination of crizotinib and selumetinib significantly decreased the cell viability of both H3122 and CR-H3122 cells. The mechanism behind this synergistic effect of combination treatment was due to the marked suppression of RAS/MAPK signalling pathway that led to a decrease in cell proliferation and increase in apoptosis. Cell cycle analysis showed that the combination treatment significantly increased the percentage of cells in the G1 phase by ≥ 8 % compared to either single drug treatment. And this was mediated by an increase in expression of p27 (≥ 1.2-fold) and a decrease in cyclin D1 expression (≥ 80%) by the combination treatment compared to either of single drug treatment. Similarly, there was a significant increase in the percentage of apoptotic cells (≥ 17%) with combination treatment compared to either of single drug treatment.

The drug combination elicited greater than 3-fold increase in expression of Bim compared to crizotinib alone that in turn upregulated the expression of cleaved caspase and cleaved PARP.

Furthermore, the efficacy of combination treatment in xenograft model of ALK-positive NSCLC was investigated. Results showed that crizotinib (25 mg/kg) and selumetinib (25 mg/kg) decreased the tumour volume by 52 % and 59 %, respectively compared to vehicle control. Interestingly, their combination further markedly reduced tumour volume compared to both crizotinib and selumetinib monotherapy. Moreover, the preclinical toxicity study on Balb/c mice demonstrated that both the single and combined treatment of crizotinib and selumetinib were non-toxic at the dose of 25 mg/kg with values of alanine transaminase (ALT) (< 80 U/L) and creatinine (< 2 mg/dL) within the normal range. Also, the combination treatment did not modulate the activity of the two drugs major metabolizing enzyme CYP3A.

In summary, the finding in this thesis supports the hypothesis that marked inhibition of tumour growth can be obtained by the combination of ALK inhibitor with MEK inhibitor and thus can be a potential strategy in the treatment of ALK-positive NSCLC. This study further raises the possibility of gaining the benefit of combination treatment by the use of a sufficient dose of MEK inhibitor alone in crizotinib resistant NSCLC. In addition to this, the study identifies Bim, PARP and cyclin dependent kinase (CDK) as the druggable target for possible triple drug therapy.

ACKNOWLEDGMENTS

I would like to express my deepest gratitude to my primary supervisor, Associate Professor John C Ashton for his constant support, guidance, and encouragement during my PhD study. He has been always there to patiently listen and discuss my research plan and inspired me to think outside of the box. His guidance in writing my paper and thesis really helped me write in concisely and reply the scientific message to the readers. I could not have wished for having a better supervisor for my PhD.

I am sincerely grateful to my co-supervisor, Professor Rhonda J Rosengren. Her support and guidance were indispensable for my doctoral study. I am immensely thankful to her for teaching me animal handling techniques and providing valuable comments for my manuscripts and thesis.

I wish to express deep gratitude to the University of Otago for providing me with doctoral scholarship. I am also thankful to the Division of Health Sciences, Elizabeth Jean Trotter Postgraduate Research Travelling Scholarship in Biomedical Sciences and New Zealand Federation of Graduate Women Inc (NZFGW) for providing the travel grant to attend conferences.

I would like to thank Mhairi for teaching me laboratory skill and sharing knowledge. I really appreciate your kind and helpful gesture.

I would like to sincerely thank my facilitator Associate Professor Roslyn Kemp for support and encouragement as well as making sure that I have the resources and good working environment during my PhD.

I would like to thank Dr Greg Giles for teaching me how to use fluorescence spectrofluorometer and allowing me to use the instrument for my PhD project. I would also like to thank Dr Sarah Baird for providing Cisplatin for my project.

I am grateful to all staff members at the department of pharmacology and toxicology for their support during my PhD study.

I am thankful to all the members of Ashton and Rosengren lab for their support and motivation during my PhD journey. Specially I am grateful to Abigail and Rebecca for their support during animal study. I would also like to

thank Orleans for his generous help to solve H and E staining problem. I would like to thank Zabeen Lateef for teaching me tail vein injection. I am grateful to Priyal for her support for PCR and sequencing.

A big thank you to my colleagues and friends at department of pharmacology and toxicology: Orleans, Jackmil, Jakeb, Anita, Houman, Gowthami, Risha, Abigail, Steph, Mayur, Geetanjali, Zohaib, Jessie, Priyal, Shakil, Lucy for sharing good time and humour.

A special thanks to my friends and seniors in Dunedin: Prabhat, Sarala, Vikash, Reena, Bishal, Pooja, Prakash, Sweta, Sandesh, Shakti, Rakesh, Binod uncle and family and, Gagan and family. Special thanks to Dunedin Nepalese Society for making me feel like home away from home.

Finally, I would like to express my deepest gratitude to my parents for their unconditional love, support, and motivation throughout my life. Thank you for always believing in me and encouraging me to follow my dreams. I would like to thank my parent-in-law and family for their support, love and care. A special thank you to my chirma, Ranjana, my sister, Nikita and my brother, Nimesh for their love, trust and support. I must express big thanks to my lovely husband and best friend, Sudeep for his immense support, care, love, motivation, and encouragement in each step of my life. You are my pillar of strength without whom I cannot imagine to be where I am today.

PUBLICATIONS

THAT HAVE ARISEN FROM WORK ASSOCIATED WITH THIS THESIS

International peer-reviewed journals

Published

- **Shrestha, N.**, Bland, A. R., Bower, R. L., Rosengren, R., & Ashton, J. (2020). Inhibition of MEK alone and in combination with ALK inhibition suppresses tumor growth in a mouse model of ALK positive lung cancer. *Journal of Pharmacology and Experimental Therapeutics.*

- **Shrestha, N.**, Nimick, M., Dass, P., Rosengren, R. J., & Ashton, J. C. (2019). Mechanisms of suppression of cell growth by dual inhibition of ALK and MEK in ALK-positive non-small cell lung cancer. *Scientific reports*, 9(1), 1-12.

- **Shrestha, N.**, Lateef, Z., Martey, O., Bland, A. R., Nimick, M., Rosengren, R., & Ashton, J. C. (2019). Does the mouse tail vein injection method provide a good model of lung cancer?. *F1000Research*, 8.

Oral Presentations

- **Shrestha N**, Nimick M, Rosengren RJ, Ashton, JC. *Induction of G1 cell cycle arrest and apoptosis in ALK-positive lung cancer cells by the combination of ALK and MEK inhibitor*. School of Biomedical Sciences (BMS) Postgraduate Colloquium Programme 2019, Dunedin, New Zealand
- **Shrestha N**, Nimick M, Rosengren RJ, Ashton, JC. *MAPK/ERK pathway and ALK inhibition has synergistic cytotoxicity in crizotinib resistant EML4-ALK-positive lung cancer*. The Australian Society of Clinical and Experimental Pharmacologist and Toxicologists (ASCEPT) New Zealand 2018 Annual Scientific Meeting, Queenstown, New Zealand
- **Shrestha N**, Nimick M, Rosengren RJ, Ashton, JC. *MAPK/ERK pathway and ALK inhibition has synergistic cytotoxicity in crizotinib resistant EML4-ALK-positive lung cancer.* School of Biomedical Sciences (BMS) Postgraduate Colloquium Programme 2018, Dunedin, New Zealand.

Poster Presentations

- **Shrestha N**, Bland AR, Bower RL, Nimick M, Rosengren RJ, Ashton, JC. *Antitumor activity of crizotinib in combination with selumetinib in in vitro and in vivo models of ALK-positive lung cancer.* Cell Symposia: Hallmarks of Cancer 2019, Seattle, USA

- **Shrestha N**, Bland AR, Bower RL, Nimick M, Rosengren RJ, Ashton, JC. *Toxicity and Efficacy of crizotinib and selumetinib combination therapy in in vivo xenograft model of ALK-positive lung cancer.* New Zealand Medical Sciences Congress (MEDSCI) 2019, Queenstown, New Zealand

- **Shrestha N**, Nimick M, Rosengren RJ, Ashton, JC. *Synergistic cytotoxicity through MAPK/ERK pathway and ALK inhibition in crizotinib resistant EML4-ALK-positive lung cancer.* International Association for Study of Lung Cancer (IASLC) 19th World Conference on Lung Cancer 2018, Toronto, Canada

- **Shrestha N**, Bland AR, Nimick M, Rosengren RJ, Ashton, JC. *Novel Strategies for the Treatment of Crizotinib Resisitant EML4-ALK+ Lung Cancer.* School of Biomedical Sciences (BMS) Postgraduate Colloquium Programme 2018, Dunedin, New Zealand

- **Shrestha N**, Bland AR, Nimick M, Rosengren RJ, Ashton, JC. *Novel Strategies for the Treatment of Crizotinib Resisitant EML4-ALK+ Lung Cancer.* Society of Toxicology (SOT) 57th Annual Meeting and ToxExpo 2018, San Antonio, Texas, USA

TABLE OF CONTENTS

LIST OF FIGURES

LIST OF TABLES

LIST OF EQUATIONS

ABBREVIATIONS

4EBP1	4E-binding protein 1
AC	adenocarcinoma
AEC	Animal Ethics Committee
AKT	protein kinase B
ALCL	anaplastic large cell lymphoma
ALK	anaplastic lymphoma kinase
ALT	alanine aminotransferase
ANOVA	analysis of variance
Apaf-1	apoptosis protease activating factor
APS	ammonium persulphate
ATP	adenosine triphosphate
AUC	area under the curve
BAD	Bcl-2 associated dead promoter
Bak	Bcl-2 antagonist/killer-1
Bax	Bcl-2-associated X protein
BBB	blood brain barrier
BCA	bicinchoninic acid
Bcl-2	B-cell lymphoma-2
BH3	Bcl-2 homology 3
BID	twice a day
BRAF	B-raf proto-oncogene, serine/threonine kinase
BSA	bovine serum albumin
CAK	CDK activating kinase
CAP	College of American Pathologist
CD105	endoglin
CDKN2A	cyclin dependent kinase inhibitor 2A
CDKs	cyclin dependent kinases
CI	combination index
CK5	cytokeratin 5
CK6	cytokeratin 6

CKIs	cyclin dependent kinase inhibitors
Cmax	peak plasma concentration
CSF	cerebrospinal fluid
CYP	cytochrome P450
DAB	3′ 3-diaminobenzidine
DAG	diacylglycerol
DDR2	discoidin domain-containing receptor 2
DFS	disease free survival
dH_2O	distilled water
DIABLO	direct inhibitor of apoptosis-binding protein with low pI
DISC	death-inducing signalling complex
DMSO	dimethyl Sulfoxide
DPX	dibutyl phthalate, in mounting medium
EDTA	ethylenediaminetetraacetic acid
EGF	epidermal growth factor
EGFR	epidermal growth factor receptor
EMEM	European Medicines Evaluation Agency
EML4	echinoderm microtubule-associated protein-like 4
ERK	extracellular signal-regulated kinase
FACS	fluorescein-activated cell sorting
FADD	Fas-associated death domain
FAM 150	heparin, augumentor α and β
FasL	fatty acid synthetase ligand
FasR	fatty acid synthetase receptor
FBS	foetal bovine serum
FDA	Food and Drug Administration
FGF	fibroblast growth factor
FGR1	fibroblast growth factor receptor 1
FISH	fluorescence *in situ* hybridisation
FLT3	fms like tyrosine kinase 3
FOXO	Forkhead box on

G1-S-G2-M phase	first gap-synthesis-second gap-mitotic phase
GEFs	guanine nucleotide exchange factors
GI_{50}	growth inhibitory concentration
Grb2	growth factor receptor bound protein 2
GSK-3	glycogen synthase kinase 3
GTP	guanosine-5'-triphosphate
H and E	haematoxylin and eosin staining
HCL	hydrochloric acid
HELP	hydrophobic echinoderm microtubule associated protein-like protein
HEPES	4-(2-hydroxyethyl)-1-piperazineethanesulfonic acid
HER2	human epidermal growth factor receptor 2
HTRU	Hercus Taieri Resource Unit
IAPs	inhibitors of apoptosis proteins
IASLC	International Association for Study of Lung Cancer
IC_{50}	concentration that kills 50% of cells.
ICAD	DNase caspase activated deoxyribonuclease
IGFR	insulin like growth factor receptor
IgG	immunoglobulin
IHC	immunohistochemistry
IP3	inositol-1,4,5-triphosphate
IRS- 1	insulin receptor substrate-1
IV	intravenous
JAK-STAT	janus activated kinase-signal transducer and activator of transcription
KCL	potassium chloride
KEAP1	kelch-like ECH-associated protein 1
KIF5B	kinesin family member 5B
KLC1	kinesin light chain 1
KRAS	kirsten rat sarcoma viral oncogene homolog
LCC	large cell carcinoma
LDCT	low dose computed tomography
LDLa	lipoprotein class A

MAM	receptor protein tyrosine phosphatase Mu
MAPK	mitogen-activated protein kinase
MDM2	murine double minute 2
MEK1/2	marker extraction kernel 1/2
MET	hepatocyte growth factor receptor
MK	midkine
MTD	maximum tolerated dose
mTOR	mammalian target of rapamycin
mTORC2	mammalian target of rapamycin complex 2
MVD	microvessel density
NaCl	sodium chloride
NADPH	nicotinamide adenine dinucleotide phosphate
NCCN	National Comprehensive Cancer Network
NF1	neurofibromin 1
NGS	next-generation sequencing
NPM	nucleophosmin
NSCLC	non-small cell lung cancer
OCT	optimal cutting temperature
ORR	objective response rate
OS	overall survival
PARP	poly (ADP-ribose) polymerase
PBS	phosphate buffer saline
PDGFR	platelet-derived growth factor receptor
PDK1	phosphoinositide dependent kinase 1
pERK	phosphorylated ERK
PET	positron emission tomography
PFS	progression free survival
PH	pleckstrin homology
PI	propidium iodide
PI3K	phosphoinositide 3-kinase
PIP	phosphatidylinositol monophosphate
PIP_2	phosphatidylinosito-4-5-bisphosphate

PIP_3	phosphatidylinosito-3-4-5-triphosphate
PKC	protein kinase C
PLCγ	phospholipase C gamma
PMSF	phenylmethanesulfonyl fluoride
PTB	phosphotyrosine binding
PTEN	phosphatase and tensin homolog
PTN	pleiotrophin
PTPN3	phosphatase nonreceptor type 3
PVDF	polyvinylidene fluoride
RB1	retinoblastoma protein
RET	rearranged during transfection
ROS1	ROS proto-oncogene 1, receptor tyrosine kinase
RPMI	Roswell Park Memorial Institute Medium
RSKs	ribosomal S6 kinases
RTK	receptor tyrosine kinase
RT-PCR	reverse transcriptase-polymerase chain reaction
S6K1	ribosomal protein S6 kinase beta-1 70kD
SCC	small cell carcinoma
SCID	severe combined immunodeficiency
SCLC	small cell lung cancer
SDS	sodium dodecyl sulphate
SDS-PAGE	Sodium-dodecylsulphate-polyacrylamide gel
SEM	standard error of mean
SH2	Src homology 2
SH3	Src homology 3
Smac	second mitochondria-derived activator of caspase
SNP	single-nucleotide polymorphism
SRB	sulforhodamine B
STK11	serine/threonine kinase 11
$t_{1/2}$	terminal half life
TBS	tris-buffered saline
TBST	tween Tris-buffered saline

TCA	trichloro acetic acid
TdT	terminal deoxynucleotidyl transferase
TEMED	N, N, N, N-tetramethyethylene diamine
TGF	TRK-fused gene
TGF	transforming growth factor
TKI	tyrosine kinase inhibitor
TNF	tumour necrosis factor receptor
TNFα	tumor necrosis factor alpha
TP53	tumour protein p53
TPR	translocated promoter region
TRADD	TNF receptor-associated death domain
TRAIL-R	TNF-related apoptosis-inducing ligand receptor
Tris-HCL	trizma hydrochloride
TSC2	tuberous sclerosis protein 2
TTF1	thyroid transcription factor
TUNEL	terminal dUTP Nick-End Labelling
U/L	international unit per litre
UGT	uridine-diphosphate glucuronosyltransferase
VEGF	vascular endothelial growth factor
VEGFR	vascular endothelial growth factor receptor

Chapter 1: Introduction

1.1. Lung cancer

1.1.1. Epidemiology

The incidence and mortality from lung cancer have risen over the last century. Lung cancer has revolutionised from a rare and obscure disease to the most common cancer (Rubin, 1991). In 1912, Alder reported 374 cases of primary lung cancer that constituted only 0.5% of total cancer cases (Alder, 1912). In 2012, lung cancer was reported to be the most prevalent cancer worldwide, accounting for 13% (1.8 million new cases) of total cancer cases. There were approximately 1.6 million lung cancer deaths (19.4% of total deaths) making it the most lethal type of cancer globally (Ferlay et al., 2015). In United States, 228,150 new cases of lung cancer (116,440 in men and 111,710 in women) and 142,670 deaths from lung cancer (76,650 in men and 66,020 in women) are expected to occur in 2019 (Siegel et al., 2019). In New Zealand, lung cancer is the leading cause of cancer mortality with higher deaths than breast, prostate and melanoma combined. Ministry of Health, New Zealand has reported 2037 new cases and 1659 deaths from lung cancer in 2013. Additionally, the incidence and mortality from lung cancer are higher in Maori compared to non-Maori populations (Lung Foundation NZ, 2020).

1.1.2. Etiology and risk factors

The principal risk factor for lung cancer is smoking and the use of tobacco products accounts for up to 90% of lung cancer cases (de Groot et al., 2018; Hecht, 1999). Other contributing factors include occupational and environmental exposures such as asbestos, silica, chromium, nickel, radon gas, arsenic, ionising radiation, polycyclic aromatic hydrocarbons and air pollutions (Alberg et al., 2002; De Matteis et al., 2008). History of lung diseases such as chronic obstructive pulmonary disease COPD, chronic bronchitis, pneumonia and family history of lung cancer is associated with increased risk of lung cancer (Brenner et al., 2011; Cote et al., 2012). Genetic and epigenetic alteration can also increase the susceptibility to lung cancer. Inherited cancer syndromes due to rare germline

mutation in p53, retinoblastoma, reduction in DNA repair capacity due to germ line alteration in nucleotide excision repair genes: ERCC1, single-nucleotide polymorphism (SNP) variation at 15q24-15q25, loss of heterozygosity at chromosomal region 3p21.3 (RASSF1A), 3p14.2 (FHIT), 9p21 (p16) and 17p13 (p53) and germ line mutation in receptor tyrosine kinases (RTKs) such as epidermal growth factor receptor (EGFR) are associated with higher lung cancer susceptibility (Bell et al., 2005; Hung et al., 2008; Hwang et al., 2003; Sanders et al., 1989; Spitz et al., 2003; Yu et al., 2008).

1.1.3. Diagnosis and staging

Lung cancer is a highly invasive and rapidly metastasising cancer. (Herbst, Heymach, & Lippman, 2008). The outcome of lung cancer depends on the stage of diagnosis. While the early diagnosis of the diseases results in longer survival, the majority of lung cancers are diagnosed at an advanced stage (70-80% at stage III-IV) leading to poor prognosis and survival (Nesbitt et al., 1995; Walters et al., 2013). Five-year survival rate for lung cancer (all stages combined) is around 19% (Siegel et al., 2019). The late diagnosis of lung cancer is due to the nonspecific nature of symptoms. Diagnostic approaches including chest X-ray, low dose computed tomography (LDCT), positron emission tomography (PET) imaging and histological examination of tumour biopsies are commonly used (Gridelli et al., 2015). LDCT demonstrated greater benefit with 20% reduction in lung cancer mortality while chest x-ray with or without sputum had no benefit in reduction of mortality (Humphrey et al., 2004; National Lung Screening Trial Research et al., 2011). Furthermore, accurate clinical staging of lung cancer is important in determining the optimal treatment strategy. Clinical staging of lung cancer is based on the TNM system by International Association for Study of Lung Cancer (IASLC) where T describes size and extension of primary tumour, N describes the regional lymph node involvement and M describes distant metastasis. The updated 8th edition of TNM classification and staging of lung cancer was implemented from 2018 and details are presented in Table 1.1 (Goldstraw et al., 2016; Lim et al., 2018).

Table 1.1 The 8th Edition of TNM classification and staging of Lung cancer
Adapted from (Goldstraw et al., 2016). Permission obtained from Elsevier.

8th T/M Descriptor	N0	N1	N2	N3
T1a	IA1	IIB	IIIA	IIIB
T1b	IA2	IIB	IIIA	IIIB
T1c	IA3	IIB	IIIA	IIIB
T2a	IB	IIB	IIIA	IIIB
T2b	IIA	IIB	IIIA	IIIB
T3	IIB	IIIA	IIIB	IIIC
T4	IIIA	IIIA	IIIB	IIIC
M1a	IVA	IVA	IVA	IVA
M1b	IVA	IVA	IVA	IVA
M1c	IVB	IVB	IVB	IVB

Abbreviations: T, primary tumour; N, Regional lymph nodes; M, distant metastasis; T1a, Tumour ≤ 1 cm; T1b, Tumour > 1-2 cm; T1c, Tumour > 2- 3 cm; T2a, Tumour> 3 – 4 cm; T2b, Tumour > 4 – 5 cm; T3, Tumour >5-7 cm; T4, Tumour > 7 cm; M1a, pleural or pericardial nodule(s) or separate tumour nodule(s) in a contralateral lobe or malignant pleural or pericardial effusion; M1b, Single extrathoracic metastasis; M1c, Multiple extrathoracic metastases in one or more organs; N0, No regional node metastasis; N1, Metastasis in ipsilateral pulmonary or hilar nodes; N2, Metastasis in ipsilateral mediastinal or subcarinal nodes; N3, Metastasis in contralateral mediastinal, hilar, or supraclavicular nodes

1.1.4. Histopathology and classification

Lung cancer is a heterogeneous disease with diverse histological and molecular subtypes. Lung cancer is broadly classified into small-cell lung cancer (SCLC) and non-small-cell lung cancer (NSCLC) (Herbst et al., 2008). SCLC is a highly aggressive cancer accounting for 15% of total lung cancer cases. SCLC is characterised by high mitotic index, higher vascularisation, early metastasis, mutation in tumour suppressor genes and oncogenes (Bunn et al., 2016; Gazdar et al., 2017; George et al., 2015). It is predominantly associated with smoking and derived from neuroendocrine cells or neuroendocrine progenitors in the lung (Karachaliou et al., 2016; Park et al., 2011).

NSCLC occurs in the remaining 85% of all lung cancer cases. Based on histology, NSCLC is further divided into adenocarcinoma (AC), squamous-cell carcinoma (SCC), and large-cell carcinoma (LCC) (Herbst et al., 2008; Travis et al., 2015; Travis et al., 2013). Adenocarcinoma is the most common NSCLC that accounts for approximately 40% of all lung cancers. AC arises from alveolar or bronchiolar epithelial cells and is often located in peripheral airways. It has glandular differentiation and expresses biomarkers such as thyroid transcription

factor 1 (TTF1), napsin A, and keratin 7 (Duma et al., 2019; Langer et al., 2010; Noguchi et al., 1995). It is commonly observed in young (<40 years old), female, non-smokers (Sun S, 2007). Squamous-cell carcinoma accounts for around 30% of lung cancers. SCC is localised in the central part of the lung, near the main airway and is related to smoking (Duma et al., 2019; Kenfield et al., 2008). SCC has squamous differentiation and expresses biomarkers such as p40, cytokeratin 5 (CK5), cytokeratin 6 (CK6) (Chen et al., 2014; Takamochi et al., 2016). LCC accounts for 10% of total lung cancers. It has large peripheral masses and is poorly differentiated (Duma et al., 2019; Patz, 2000) and is also associated with smoking (Muscat et al., 1997).

1.2. Molecular alteration of NSCLC

Molecular and genomic profiling of lung tumour samples has identified subsets of molecular alterations including oncogenes and tumour suppressor genes that provide an understanding of tumorigenesis and are excellent biomarkers and targets for cancer therapy (Fujimoto & Wistuba, 2014). The frequency of these alterations depends on factors such as smoking history, age, sex, and race (Nagashima et al., 2013; Riely et al., 2008; Sun et al., 2010). Adenocarcinoma demonstrated high rates of somatic mutation with 8.9 mutations per DNA megabase (Collisson et al., 2014). Genetic alterations such as point mutation, somatic copy number alteration and genomic translocation have been reported. These include: gain of function mutation in oncogenic drivers such as epidermal growth factor receptor (EGFR), kirsten rat sarcoma viral oncogene homolog (KRAS), B-raf proto-oncogene, serine/threonine kinase (BRAF), human epidermal growth factor receptor 2 (HER2), hepatocyte growth factor receptor (MET), phosphoinositide 3 kinase (PI3KC), loss of function mutation in tumour suppressor such as tumour protein p53 (TP53), phosphatase and tensin homolog (PTEN), retinoblastoma protein (RB1), neurofibromin 1 (NF1), serine/threonine kinase 11 (STK11), cyclin-dependent kinase inhibitor 2A (CDKN2A), and kelch-like ECH-associated protein 1 (KEAP1), structural rearrangement (translocation, inversion) of anaplastic lymphoma kinase (ALK), ROS proto-oncogene 1, receptor tyrosine kinase (ROS1) and rearranged during transfection (RET), amplification of proto-oncogenes such as MET, fibroblast growth factor receptor 1 (FGR1), discoidin domain-containing receptor 2 (DDR2) (Bergethon et al., 2012; Collisson et al., 2014; Ding et al., 2008; Imielinski et al., 2012; Paez et al., 2004; Sanchez-Cespedes et al., 2002; Takahashi et al., 1989). The frequency of molecular alteration in NSCLC and potential drugs are summarised in Table 1.2. Genetic alterations aberrantly activate proto-oncogenes resulting in a deleterious effect on protein function and on downstream signalling pathways that plays a critical role in regulating cellular functions including proliferation and apoptosis (Collisson et al., 2014). Therefore, understanding the complex

molecular biology of NSCLC is important for the development of personalised therapy that can produce a superior clinical outcome in NSCLC patients.

1.2.1. Receptor tyrosine kinase

Most of the oncogenic mutations that have been proven to be important in lung cancer are associated with RTKs. These are single pass transmembrane receptors that are essential components of signal transduction pathways. RTKs belong to the family of protein tyrosine kinase and are key regulators of a cellular process such as cell growth, differentiation, migration, motility, metabolism and survival (Hubbard & Miller, 2007; Schlessinger, 2000). All RTKs have an extracellular region, a single transmembrane helix and an intracellular tyrosine kinase domain. They catalyse the transfer of the phosphoryl group of ATP to tyrosine residues on target proteins and mediate cell to cell communications (Hubbard, 1999; Hunter, 1998). Ligand binding to RTKs leads to activation of the receptor by oligomerisation or dimerisation. This, in turn facilitates autophosphorylation of tyrosine residue that serves as a recruitment site for adaptor proteins and initiates various signalling cascades (Hubbard & Miller, 2007; Schlessinger, 2000). The signal from activated RTKs is strictly regulated through dephosphorylation by protein tyrosine phosphatase and degradation via ubiquitination (Joazeiro et al., 1999).

Despite tight regulation and control of RTK activity, aberrant kinase activity has been reported in various cancer including lung cancers (Blume-Jensen & Hunter, 2001). This can be due to mutation, overexpression, autocrine activation or chromosomal translocation that constitutively activates RTKs resulting in malignant transformation and carcinogenesis. Studies have demonstrated that more than 50% of known RTKs have been implicated in oncogenic malignancies including: EGFR, ALK, insulin growth factor receptor (IGFR), MET, vascular endothelial growth factor receptor (VEGFR), and platelet derived growth factor receptor (PDGFR) (Blume-Jensen & Hunter, 2001).

Identification of oncogenic RTKs has led to the development of small molecule tyrosine kinase inhibitor (TKI) that primarily inhibit the activation of

RTKs and its downstream signalling. Imatinib was the first TKI approved by FDA in 2001 followed by gefitinib, sunitinib, dosatinib, crizotinib, afatinib, erlotinib, ceritinib, alectinib, brigatinib (Jiao et al., 2018).

Table 1.2 Molecular alteration in NSCLC

Gene	Alteration	Frequency (%) AC	Frequency (%) SCC	Potential targeted therapy	Reference
EGFR	Mutation	10-15	2-3	Erlotinib, gefitinib, afatinib	(Paez et al., 2004)
ALK	Fusion	2-7	rare	Crizotinib, ceritinib, alectinib, loratinib	(Lin et al., 2017; Soda et al., 2007)
HER2	Mutation	<5	N/A	Neratinib, afatinib, trastuzumab	(Pao & Girard, 2011)
MET	Mutation	<5	<5	Tivantinib, cabozantinib, onartuzumab	(Pao & Girard, 2011)
BRAF	mutation	1-6	4-5	Vemurafenib, dabrafenib, trametinib	(Paik et al., 2011)
ROS1	Fusion	1-2	N/A	Crizotinib	(Rikova et al., 2007; Takeuchi et al., 2012)
NF1	Mutation	12	10	N/A	(Collisson et al., 2014; Kandoth et al., 2013)
FGR1	Amplification	N/A	20	Dovitinib, ponatinib, AZD4547, BGJ398	(Weiss et al., 2010)
KRAS	Mutation	15-25	1-2	Selumetinib plus docetaxel combination	(Mascaux et al., 2005)
PI3CA	Mutation	5	15	BEZ235, BKM120, GDC0941	(Kawano et al., 2006)
KEAP1	Mutation	17	12	N/A	(Singh et al., 2006)
CDKN2A	Mutation	7	15	N/A	(Lou-Qian et al., 2013)
TP53	Mutation	52	79	N/A	(Mitsudomi et al., 2000)
PTEN	Mutation	2	10	GDC0941, BEZ235, BKM120	(Jin et al., 2010)

Gene	Alteration	Frequency (%) AC	Frequency (%) SCC	Potential targeted therapy	Reference
RET	Fusion	1	N/A	Carbozantinib, vandetanib	(Kohno et al., 2012)
DDR2	Mutation	N/A	2-3	Dasatinib	(Hammerman et al., 2011)

1.3. ALK-positive non-small cell lung cancer

ALK-positive NSCLC is one of the subtypes of NSCLC that is commonly associated with young age patients (Hallberg & Palmer, 2011). Previously, ALK was believed to be mutually exclusive to other oncogenic mutations such as EGFR and KRAS (Gainor et al., 2013; Zhang et al., 2010). The clinical genotyping data from 1,683 NSCLC patients and 34 ALK-positive NSCLC patients progressed on crizotinib showed absence in EGFR or KRAS mutations (Gainor et al., 2013). However, recent studies have demonstrated the concomitant presence of mutations such as EGFR and KRAS in around 0.6 % to 19 %patients with ALK-positive NSCLC (Rossing et al., 2013; Sahnane et al., 2016; Yang et al., 2014). The patients harbouring both ALK rearrangement and EGFR mutations were benefited from crizotinib compared to erlotinib treatment, whereas response to crizotinib in patients with ALK and KRAS was opposite (Sahnane et al., 2016). This shows that different oncogenic driver mutations may co-exist in AC making it genetically heterogeneous and thus integrated therapy could be a better option for these patients (Sahnane et al., 2016).

1.3.1. Anaplastic Lymphoma Kinase (ALK)

ALK, a transmembrane receptor tyrosine kinase (RTK), is a member of the insulin receptor superfamily (Palmer et al., 2009). The ALK gene is located on the short arm of chromosome 2 at position 23 and encodes anaplastic lymphoma kinase receptor tyrosine kinase (ALK RTK). ALK was first identified in 1994 as a fusion partner of nucleophosmin (NPM) in anaplastic large cell lymphoma (ALCL) (Morris et al., 1994). Here, the kinase domain of ALK was fused with the N-terminus of NPM. Subsequently, the full length ALK receptor was identified in 1994 (Iwahara et al., 1997; Morris et al., 1997).

ALK is highly expressed during foetal development and diminishes shortly after the birth (Soda et al., 2007). In adults, expression of ALK is restricted to a subset of neuronal cells, the small intestine, and testes (Morris et al., 1994; Shaw & Engelman, 2013). The role of ALK in human physiology is not clearly understood. However, ALK is believed to play a role in the development and

maintenance of the nervous system (Iwahara et al., 1997). In mice, ALK knockout resulted in a normal lifespan with mild abnormalities in the hippocampus, frontal cortex and hypogonadotropic hypogonadism (Bilsland et al., 2008; Witek et al., 2015). Furthermore, ALK regulates canonical signalling pathways such as mitogen activated protein kinase (MAPK), janus activated kinase-signal transducer and activator of transcription (JAK-STAT), phosphoinositide 3-kinase (PI3K)-protein kinase B (AKT) and phospholipase C gamma (PLCγ) pathways that play a major role in regulation of cellular proliferation and survival (Chiarle et al., 2008; Hallberg & Palmer, 2013) .

1.3.2. ALK structure and ligands

ALK is a highly conserved RTK that has a ligand binding extracellular domain, a hydrophobic putative transmembrane region, and an intracellular tyrosine kinase domain (Figure 1.1B). The extracellular domain consists of a glycine rich domain, low density lipoprotein class A (LDLa) and two meprin A-5 protein and receptor protein tyrosine phosphatase Mu (MAM) domains (Figure 1.1B**)**. The functions of each of these domains are unclear (Iwahara et al., 1997; Loren et al., 2001; Morris et al., 1997; Stoica et al., 2001). However, LDLa is speculated to be involved in ligand binding while MAM domains are believed to be involved in cell-cell interactions (Beckmann & Bork, 1993; Daly et al., 1995; Fass et al., 1997). The transmembrane domains connect the extracellular region with the intracellular kinase domain, which contains small N-terminal and large C-terminal lobes that are linked by a hinge region forming a cleft for ATP or substrate binding. The C-terminal lobe contains an activation loop that comprises of three tyrosine containing motifs (tyrosine 1278, 1282 and 1283) (Bossi et al., 2010; Lee, Jia, et al., 2010). Mouse and human ALK have high similarity (87% at protein level) except one extra tyrosine at position 1604 in human ALK that plays an important role in tumour progression (Bai et al., 1998). Human ALK consists of 1620 amino acids while mouse, *Drosophila and C. elegans* ALK is made up of 1621, 1701 and 1421 amino acids (Bai et al., 1998; Iwahara et al., 1997; Liao et al., 2004; Morris et al., 1997; Reiner et al., 2008). Molecular weight

of human ALK is around 180 kDa. However, ALK in SDS-PAGE is usually detected at 220 kDa due to posttranslational modification such as glycosylation (Morris et al., 1997).

ALK was initially described as an orphan receptor with no known activating ligands. The small heparin-binding growth factors such as midkine (MK) and pleiotrophin (PTN) have been reported as the activating ligands for mammalian ALK (Stoica et al., 2001; Stoica et al., 2002). However, subsequent studies have found contradictory results and are controversial (Dirks et al., 2002; Mathivet et al., 2007; Moog-Lutz et al., 2005; Motegi et al., 2004). PTN failed to phosphorylate and activate ALK in glioblastoma/neuroblastoma cells (Mathivet et al., 2007) and in 293ALK cells (Dirks et al., 2002). Later in 2015, heparin and the novel cytokine augmentor α and β (FAM 150) were reported as a ligand of ALK (Murray et al., 2015; Reshetnyak et al., 2015). Long-chain heparin binds to the extracellular domain of ALK thereby inducing dimerization and activation of ALK in neuroblastoma cells (Murray et al., 2015). Similarly, augmentor α and β bind to ALK resulting in its phosphorylation and activation in NIH/3T3 cells harbouring ALK (Reshetnyak et al., 2015).

1.3.3. ALK rearrangement

Genomic alterations including chromosomal translocation, mutation, and overexpression of ALK is observed in many cancers including NSCLC (Hallberg & Palmer, 2013). The frequency of ALK gene rearrangements is comparatively higher in NSCLC compared to other cancer types such as breast, colorectal, renal cell, ovarian (Lin et al., 2017). The most common rearrangement in NSCLC is echinoderm microtubule-associated protein-like 4 (EML4)-ALK that was first identified by Soda et al. in 2007 (Soda et al., 2007). EML4 is a cytoplasmic protein that has an essential role in the formation of microtubules and microtubule-binding proteins (Houtman et al., 2007). EML4 consists of an amino-terminal coiled-coil (CC) domain, basic domain, hydrophobic echinoderm microtubule associated protein-like protein (HELP) domain and C-terminus with four WD repeats (Figure 1.1B) (Pollmann et al., 2006). ALK and EML4 genes are located

on chromosome 2p23 and 2p21, respectively, and are separated by 12.7 megabases and are oriented in opposite direction. A small inversion within the short arm of chromosome 2 juxtaposes the 5'end of the EML4 gene and the 3' end of the ALK gene leading to the formation of EML4-ALK fusion oncogene (Figure 1.1A). The EML4-ALK fusion oncogene in turn encodes EML4-ALK oncoproteins that consist of the intracellular tyrosine kinase domain of ALK and an amino-terminal portion of EML4 (Figure 1.1B). The EML4 domain mediates constitutive dimerisation and activation of the ALK kinase domain, independent of ligand and thereby induces aberrant activation of ALK downstream signalling (RAS-MAPK, PI3-AKT, JAK-STAT) that promotes cell proliferation and survival (Soda et al., 2007). Multiple chimeric EML4-ALK variants have been identified that contain the same intracellular tyrosine kinase domains of ALK but have a different section of EML4. Out of 15 different variants identified, variant 1 (E13; A20) is the most common found in 33% of NSCLC. This is followed by variant 3a/b (E6a/b;A20) detected in 29% of NSCLC (Sasaki et al., 2010).

Apart from EML4, other fusion partners of ALK are TRK-fused gene (TFG), kinesin family member 5B (KIF5B), kinesin light chain 1 (KLC1), protein tyrosine phosphatase nonreceptor type 3 (PTPN3), translocated promoter region (TPR) and all are detected less frequently in NSCLC (Table 1.3) (Rikova et al., 2007; Takeuchi et al., 2009; Togashi et al., 2012). All fusion partners share some common characteristics: 1) Promoter of partner protein determines the initiation of transcription of the fusion protein. 2) Sub-cellular localisation of the fusion protein is controlled by the partner protein. 3) The partner protein induces the dimerisation or oligomerisation of ALK fusion that facilitates autophosphorylation and activation of the ALK kinase domain.

Table 1.3: ALK fusions in NSCLC

Fusion protein	Chromosomal translocation	Frequency	Reference
EML4-ALK	Inv(2)(p21;p23)	2-7	(Lin et al., 2017; Soda et al., 2007)
TFG-ALK	t(2;3)(p23;q21)	2	(Rikova et al., 2007)
KIF5B-ALK	t(2;10)(p23;p11)	<1	(Takeuchi et al., 2009)
KLC1-ALK	t(2;14)(p23;q32)	<5	(Togashi et al., 2012)
PTPN3-ALK	t(2;9)(p23;q31)	N/A	(Jung et al., 2012)
TPR-ALK	t(1;2)(p23;q31.1)	N/A	(Choi et al., 2014)
DCTN1-ALK	t(2;2)(p13;p23)	N/A	(Iyevleva et al., 2015)
GCC2-ALK	t(2;2)(p23;q12)	N/A	(Jiang et al., 2018)

Abbreviations: ALK, Anaplastic lymphoma kinase; DCTN1, Dynactin subunit 1; EML4, echinoderm microtubule associated protein like 4; GCC2, GRIP and coiled-coil domain-containing protein 2; KIF5B; kinesin family member 5B; KLC1, kinesin light chain 1; PTPN3, protein tyrosine phosphatase nonreceptor type 3; TFG, TRK-fused gene; TPR, translocated promoter region

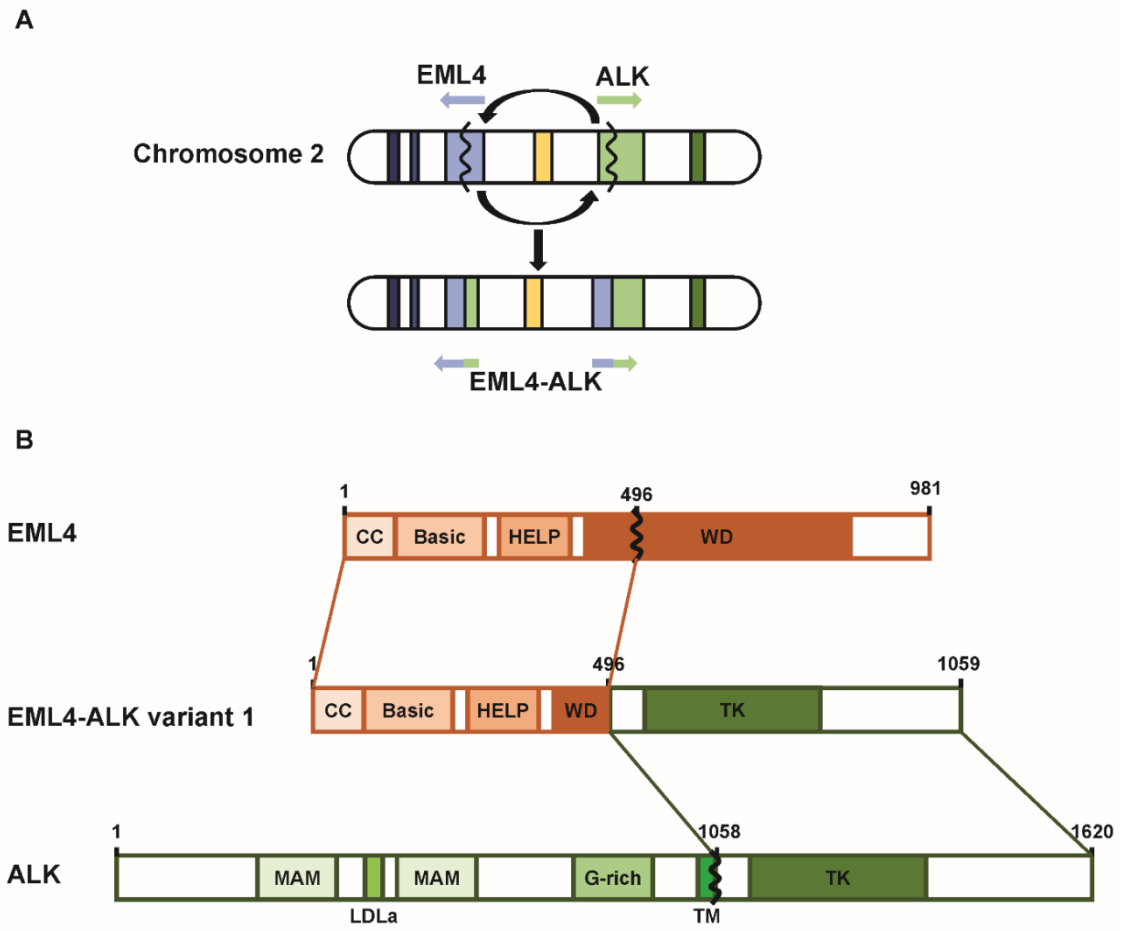

Figure 1.1 EML4-ALK fusion in non-small cell lung cancer. (A) A small inversion on short arm of chromosome 2 causes fusion of exon 13 of EML4 (5′) to exon 20 of ALK (3′) resulting in the formation of EML4-ALK fusion oncogene. (B) General structure of ALK, EML4 and EML4-ALK (variant 1) fusion oncoprotein. Structure of ALK consists of extracellular portion comprised of two MAM domain (amino acids 264-427 and 480-626), an LDL domain (453-471) and glycine rich domain (816-940); transmembrane domain (1039-1059) and intracellular tyrosine kinase domain (1116-1383). EML4 is comprised of N-terminal CC that is separated from C-terminal HELP and WD repeat domain by a basic region.
Adapted from (Bayliss et al., 1209; Gandhi et al., 2015; Roskoski, 2013; Soda et al., 2007).

1.3.4. Clinical detection of ALK

Molecular testing of prognostic biomarkers is crucial for the selection of appropriate therapy in non-small cell lung cancer. The National Comprehensive Cancer Network (NCCN) Clinical Practice Guideline in Oncology and Guideline from the College of American Pathologist (CAP) recommend molecular testing for ALK rearrangements/fusions in patients with metastatic non-squamous or advanced stage adenocarcinoma NSCLC (Lindeman et al., 2013; NCCN Clinical Practice Guidelines in Oncology (NCCN Guidelines®), 2020). Methods to detect ALK rearrangement include fluorescence *in situ* hybridisation (FISH), immunohistochemistry (IHC), next-generation sequencing (NGS) and reverse transcriptase-polymerase chain reaction (RT-PCR) assays. Each method has its own benefits and drawbacks.

1.3.4.1. Fluorescence in situ hybridisation

FISH is the gold standard assay for the detection of ALK rearrangements in NSCLC (Martelli et al., 2009; Perner et al., 2008; Shaw et al., 2009; Tang et al., 2019). The Vysis ALK Break-Apart FISH probe kit (Abbott molecular Inc) has been approved by the food and drug administration (FDA) as a companion diagnostic test prior to administration of ALK tyrosine kinase inhibitors (Tang et al., 2019; Weickhardt et al., 2013). This method uses fluorescently labelled DNA probes that bind to and localise specific genomic region in the nuclei of tumour samples. The Vysis ALK Break-Apart probe kit consists of a 5′ ALK probe of approximately 442 kb labelled with green fluorophores and a 3′ ALK probe of approximately 300 kb labelled with orange fluorophores. In non-rearranged cells, the orange and green probes are closely located resulting in a merged (yellow) signal. Whereas in ALK rearrangement cells, these probes are separated resulting in a split (green and orange) signal. Furthermore, the presence of an isolated red signal without coexistence of a green signal is considered positive. This suggests that ALK rearrangement has occurred with either loss of the 5′ probe binding site or masking within the plane of the section (Tang et al., 2019; Weickhardt et al., 2013).

The FISH assay can detect ALK rearrangement regardless of fusion partner and variant (Weickhardt et al., 2013). However, the major challenge is the interpretation of the results that require technical expertise. It is difficult to identify a split signal in the fusion gene with small physical separation between 5' and 3' ALK sequences such as EML4-ALK that are separated by only 12 Mb (Camidge et al., 2010). Moreover, FISH cannot distinguish between different EML4-ALK fusion variants (Cha et al., 2016). Apart from this, FISH is an expensive, time-consuming assay that requires specialised equipment and laboratory techniques (Kerr, 2014).

1.3.4.2. Immunohistochemistry

IHC is a reliable alternative diagnostic approach for the detection of ALK rearrangements (Conklin et al., 2013; Sun et al., 2012; To et al., 2013). The VENTANA ALK (D5F3) CDx assay (Ventana Medical Systems, Inc) has been approved by the FDA as companion diagnostic test to identify ALK rearrangement (Conde et al., 2016; Marchetti et al., 2016). IHC uses specific monoclonal antibodies that bind to the specific epitope of the ALK fusion protein regardless of variant and fusion partner. Unlike ALCL, NSCLC has a low expression level of ALK fusion protein that decreases the sensitivity of IHC for the detection of ALK rearrangement. The sensitivity and specificity of IHC were improved by using high-affinity antibodies such as D5F3 (Cell Signaling Technology). and 5A4 (Novocastra, Leica Biosystems), and a highly sensitive detection system. Moreover, IHC is cost effective and easier to perform thereby, making it an efficient method for screening ALK rearrangement in NSCLC (Conklin et al., 2013; Minca et al., 2013; Mino-Kenudson et al., 2010; Park et al., 2012).

1.3.4.3. Next generation sequencing

NGS has emerged as reliable alternative diagnostic approach to FISH or IHC (Dacic et al., 2016; Lin et al., 2019). The FoundationOne CDx assay (Foundation Medicine, Inc) has been approved by the FDA as a companion diagnostic test for recognition of ALK rearrangement (U.S. Food and Drug

Administration, 2020b). This method allows simultaneous parallel sequencing of multiple analytes for the detection of potentially targetable genetic alteration such as gene mutation, rearrangement and copy number alterations in a variety of cancers, including ALK, within a single assay (Lin et al., 2019; Vigneswaran et al., 2016; Weickhardt et al., 2013). Comprehensive profiling of genome identified ALK rearrangement in a subset of NSCLC patients who showed negative results in the prior FISH assay. These patients exhibited responses to ALK inhibitors that were similar to the response rate in patients with positive results in FISH assay (Ali et al., 2016; Peled et al., 2012). Furthermore, NGS is cost effective method and can be a suitable option in the cases where the results from FISH or IHC are inconclusive (Lin et al., 2019). NGS can identify different ALK fusion subtypes and concomitant mutation allowing the discovery of new fusions beyond NSCLC (Beadling et al., 2016; Vendrell et al., 2017).

1.3.4.4. Reverse transcriptase-polymerase chain reaction

RT-PCR is a RNA based highly specific diagnostic test for detection of ALK rearrangement (Liu et al., 2016; Soda et al., 2012; Takeuchi et al., 2008). This method was originally used to identify EML4-ALK gene rearrangement in NSCLC (Soda et al., 2007). However, it is not recommended as an alternative to FISH for the detection of ALK prior to the administration of ALK inhibitors (Lindeman et al., 2013). RT-PCR can detect known ALK fusions and variants but may misdiagnose novel ALK fusion partners. The challenge is increasing the number of ALK fusion partners that require a multiplex RT-PCR approach with multiple validated primers. Furthermore, the extraction of RNA and cDNA synthesis from FFPE tumour samples is difficult due to the degradation of messenger RNA making it less feasible (Kerr, 2014; Sanders et al., 2011; Solomon et al., 2009). However, this method can be applied to the cytology specimens such as bronchial lavage fluid, sputum, pleural effusion (Soda et al., 2012; Wang et al., 2016).

1.3.5. Prevalence of ALK positive non-small cell lung cancer

ALK gene rearrangement is found in 2-7% of patient with NSCLC (Koivunen et al., 2008; Perner et al., 2008; Soda et al., 2007; Wong et al., 2009). ALK-positive NSCLC has adenocarcinoma histology and is observed in younger age patients with non-smoking or light smoking history (Shaw et al., 2009; Toyokawa & Seto, 2014b; Wong et al., 2009). In New Zealand, 8.4% of the patients diagnosed with nonsquamous NSCLC tested positive for ALK gene rearrangement (McKeage et al., 2019). Furthermore, ALK-positive NSCLC was more prevalent in younger (13.8%) compared to older (7.1%) patients, non-smokers (22.3%) versus smokers (2.9%) and in Maori (6.9%), Pacific (10.8%) or Asian (22.0%) ethnic groups versus New Zealand Europeans (4.4%) (McKeage et al., 2019).

1.3.6. Treatment approach for ALK-positive NSCLC

The treatment approach for the advanced stage non-squamous NSCLC has evolved and is continuously changing with time (Melosky, 2018). Chemotherapy was the preferred choice of treatment for stage III and IV NSCLC until the discovery of targeted therapy (Dong et al., 2019). Platinum based doublets with third generations chemotherapy drugs were used for the treatment of advanced stage NSCLC. However, chemotherapy drugs exhibit strong treatment related adverse events, thereby limiting their clinical benefits (Nagasaka & Gadgeel, 2018; Schiller et al., 2002). Advances in the understanding of tumour biology have led to the development of small molecule inhibitors that target the specific genomic abnormalities including EGFR, ALK in NSCLC (Dong et al., 2019).

ALK tyrosine kinase inhibitors (TKIs) are the preferred first line therapy for NSCLC patients with advanced ALK rearrangement. The presence of an ALK fusion oncogene should be detected by FISH or IHC prior to the administration of ALK-TKIs (Barrows et al., 2019; Khan et al., 2018; Solomon, Wilner, et al., 2014). However, systemic chemotherapy is indicated if urgent treatment is required before the confirmation of genotype. The treatment plan is reassessed when the test result is available. Since no clinical trials report the optimal timing

for the administration of an ALK inhibitor in patients already on chemotherapy, the patients testing positive for ALK fusion oncogene are switched to ALK inhibitors (Moran & Sequist, 2012; Solomon, 2020).

Alectinib, a second generation ALK TKIs, is currently approved by FDA as a first line treatment for the patients with ALK-positive NSCLC (McCusker et al., 2019; U.S. Food and Drug Administration, 2017a). Second generation ALK TKIs such as ceritinib and brigatinib demonstrate greater potency than crizotinib and may be an alternative to alectinib. However, brigatinib is not yet approved by FDA as first-line treatment (Melosky, 2018; Solomon, 2020). Crizotinib was the first ALK TKI approved by FDA for the treatment of ALK-positive NSCLC (Kazandjian et al., 2014; Solomon, Mok, et al., 2014). Although alectinib is now the preferred first-line treatment, some parts of the world still use crizotinib due to its superiority over standard chemotherapy (McCusker et al., 2019). Moreover, NCCN Clinical Practice Guideline in Oncology has indicated that alectinib, ceritinib, brigatinib and crizotinib are all first line therapies in advanced or metastatic ALK-positive NSCLC (NCCN Clinical Practice Guidelines in Oncology (NCCN Guidelines®), 2020). Prior to the ALK-TKIs, chemotherapy was used for the treatment of these patients. (Barrows et al., 2019). The current treatment approaches for ALK-TKI naïve or resistant ALK-positive NSCLC patients are illustrated in Figure 1.2.

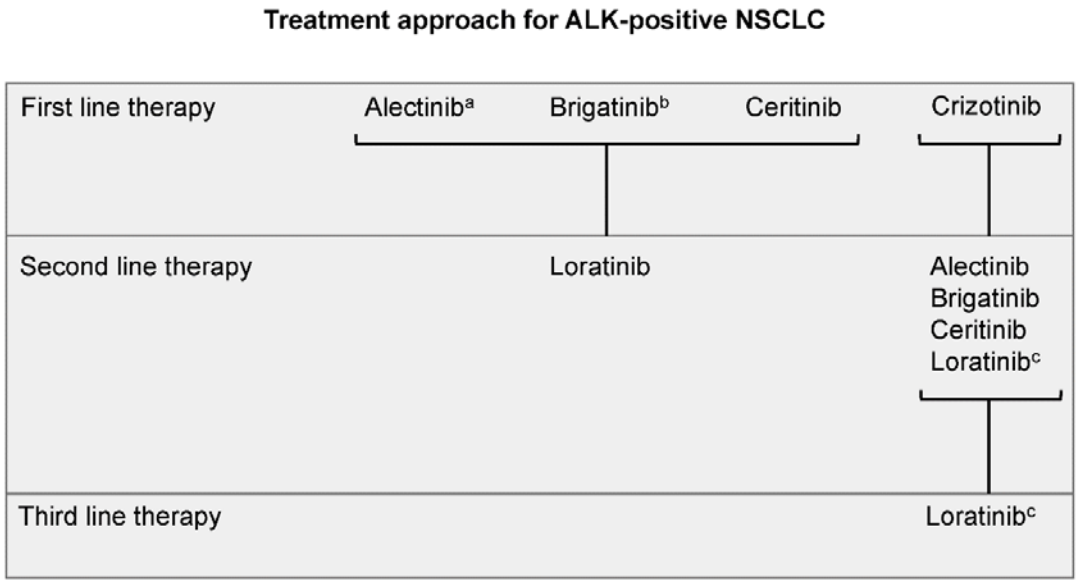

a. Alectinib is the preferred agent for first-line therapy (NCCN clinical practice guideline in oncology, 2020).
b. Brigatinib has not yet approved by FDA as first line therapy (Meloskey et al., 2018; Solomon et al., 2020).
c. Loratinib has been approved by FDA as the second and third line treatment of patients progressed on crizotinib (U.S. Food and Drug Administration., 2018).

Figure 1.2 Schematic diagram showing the proposed treatment algorithm in ALK-positive NSCLC. Adapted from (NCCN Clinical Practice Guidelines in Oncology (NCCN Guidelines®), 2020)

1.4. Crizotinib

Crizotinib is an orally active aminopyridine-based RTK inhibitor described chemically as (R)-3-[l-(2,6-dichloro-3-fluorophenyl)ethoxy]-5-[1-(piperidin-4-yl)-1H-pyrazol-4-yl] pyridin-2-amine4 (Figure 1.3). The molecular formula and molecular weight of crizotinib is $C_{21}H_{22}Cl_2FN_5O$ and 450.34 daltons, respectively.

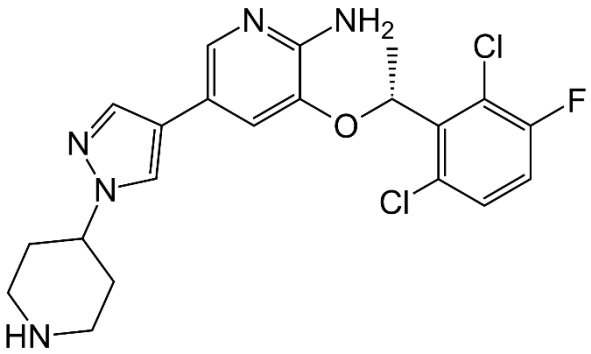

Figure 1.3 Chemical Structure of crizotinib. (Figure is obtained from Wikipedia – in public domain)

Crizotinib is a highly selective ATP competitive small molecule inhibitor of ALK, MET and ROS1 receptor tyrosine kinases and their variants. Crizotinib binds to the ATP binding site of these RTKs and inhibits their autophosphorylation and their subsequent downstream signalling pathways (Bergethon et al., 2012; Cui et al., 2011). Crizotinib has an anti-proliferative activity that is associated with G1-S–phase cell cycle arrest and induction of apoptosis (Christensen et al., 2007; Toyokawa & Seto, 2014a). Initially, it was developed as MET inhibitor. However, higher selectivity and specificity of crizotinib for ALK and better clinical outcome in ALK rearranged lung cancer patients made it the first line therapy for ALK-positive NSCLC. Based on good clinical results from phase I and II clinical trials, the FDA and the European medicines evaluation agency (EMEM) approved crizotinib for treatment of locally advanced or metastatic ALK+ NSCLC in 2011 and 2012, respectively (Kazandjian et al., 2014; Metro et al., 2017).

1.4.1. Pharmacokinetics

A dose escalation phase I trial determined that 250 mg BID is the maximum tolerated dose (MTD) of crizotinib (Kwak et al., 2010; Kwak et al., 2009). After administration of a single oral dose of crizotinib (250 mg), the peak plasma concentration (C_{max}) was reached after approximately 4-6 h with a terminal half-life of 43-51 h. Steady-state concentrations were obtained within 15 days of starting crizotinib treatment (250 mg BID), with a mean plasma trough of 256 ng/ml. This was higher than the efficacious concentration (120 ng/ml) for ALK inihibition found in preclinical models (Hamilton et al., 2015). Administration of crizotinib results in an equal distribution of the drug between blood cells and plasma. More than 90% of crizotinib binds to human plasma protein, and a lesser extent to serum albumin and α-1 acid glycoproteins. Following intravenous (IV) administration of crizotinib, the mean volume of distribution was 1772 L, showing the extensive distribution of crizotinib from plasma into tissues. However, the penetration of crizotinib into cerebrospinal fluid and across blood-brain barrier (BBB) is poor, with cerebrospinal fluid and plasma ratio being 0.0026. The total bioavailability of crizotinib is 43%. Administration of a single dose of crizotinib (250 mg) together with a standard high fat meal did not change the exposure and C_{max} to a clinically relevant level. Thus, crizotinib is recommended to be taken with or without food (Curran, 2012; Frampton, 2013; Hamilton et al., 2015).

Crizotinib is predominantly metabolised in the liver by cytochrome P450 (CYP) 3A4/5 isoenzymes by both *O*-dealkylation, with the subsequent conjugation of the *O*-dealkylated metabolites and oxidation of piperidine ring to crizotinib lactam (active metabolite) (Pfizer Inc., 2019). Co-administration of crizotinib with potent CYP3A inducers and CYP3A inhibitors may alter the plasma concentration of crizotinib (Pfizer Inc., 2019). Furthermore, both *in vitro* and *in vivo* studies showed that crizotinib is a moderate time dependent inhibitor and weak inducer of CYP3A enzymes (Johnson et al., 2015; Mao et al., 2013). Therefore, crizotinib may alter the plasma concentration of CYP3A substrate when given concomitantly (Pfizer Inc., 2019). The potential drug interactions of

crizotinib are presented in Table 1.4. Crizotnib and its metabolites are primarily excreted from faecal route with 63% being eliminated via the faeces (53% as unchanged drug) and then from biliary route where 22% is eliminated in the urine (1.3-2.3% as unchanged drug) (Curran, 2012).

Table 1.4: Potential drug interaction of crizotinib (Pfizer Inc., 2012)

Drugs	Mechanism of interaction	Effect
Ketoconazole, itraconazole, clarithromycin, atazanavir, indinavir, nefazodone	Inhibit CYP3A enzyme	Increase the plasma concentration of crizotinib
Rifampin, phenobarbital, carbamazepine, phenytoin, rifabutin, St. John's Wort.	Induces CYP3A enzyme	Decrease the plasma concentration of crizotinib
Alfentanil, cyclosporin, ergotamine, midazolam	Inhibition of CYP3A enzyme by crizotinib	Increase the plasma concentration of CYP3A substrate

1.4.2. Preclinical Studies

Biochemical and cell-based phosphorylation assays showed the selectivity of crizotinib was around 20-fold higher for ALK and MET compared to over 120 other tyrosine and serine-threonine kinases (Christensen et al., 2007; Zou et al., 2007). Cell viability assays demonstrated that crizotinib inhibited the survival of SU-DHL-1 and Karpas299 cells expressing the NPM-ALK fusion gene with IC_{50} values of 43±2 nmol/L and 32±1 nmol/L, respectively. Christensen et al. also found that the phosphorylation of NPM-ALK in anaplastic large cell lymphoma cell line (SU-DHL-1 and Karpas299) was potently inhibited by crizotinib at mean IC50 value of 24 nmol/L. Also, immunodeficient Beige mice bearing Karpas299 ALCL tumour xenografts were orally administered with crizotinib which led to complete regression of all tumours at a dose of 100 mg/kg within 15 days (Christensen et al., 2007).

Crizotinib potently inhibited the cell viability of the neuroblastoma line NB-1 by suppressing proliferation and ALK mediated signalling. Furthermore, strong inhibition of ERK and AKT signalling was observed in crizotinib treated NB-1 neuroblastoma cells (McDermott et al., 2008). Similarly, cell proliferation of a non-small cell lung cancer cell line, H3122, harbouring the EML4-ALK variant 1 and kelly neuroblastoma with an activating mutation was also suppressed by crizotinib (McDermott et al., 2008). These results from preclinical studies demonstrated that crizotinib could act as a potential therapeutic target in ALK rearranged NSCLC and lead quickly to clinical studies.

1.4.3. Clinical Studies

Based on preclinical results obtained from *in vitro* and *in vivo* animal experiment, clinical studies of crizotinib began in 2006. The clinical efficacy of crizotinib in ALK-positive NSCLC patient with advanced or metastatic tumours has been analysed in phase I (Profile 1001), phase II (Profile1005) and phase III (Profile1007 and Profile1014) clinical trials (Camidge et al., 2012; Kwak et al., 2010).

1.4.3.1. Phase I clinical trial (Profile 1001)

The therapeutic efficacy and toxicity of crizotinib were evaluated in an open-label, noncomparative, multicentre two-part trial Phase I clinical trial (Camidge et al., 2012; Kwak et al., 2010). The first part consisted of standard dose-escalation pharmacokinetic evaluation, where the maximum tolerated dose of crizotinib was determined. Thirty-seven patients with any solid tumour type including pancreatic, colorectal, ALCL and NSCLC were administered crizotinib at doses ranging from 50 mg OD to 300 mg BID on a continuous schedule. Three dose limiting toxicities were observed where one patient receiving 200 mg OD developed grade 3 elevation of alanine aminotransferase (ALT), and the other two patients receiving 300 mg BID had grade 3 level fatigue. Reduction of dose to 250 mg BID was tolerable with mild grade 1 and 2 adverse effect including vomiting, nausea, and diarrhoea. Furthermore, out of 37 patients, 2 patients with

ALK rearrangement showed improved clinical outcome (Kwak et al., 2010; Kwak et al., 2009).

Next, the therapeutic efficacy of crizotinib was evaluated in an expanded cohort of patients harbouring ALK rearrangement. A total of 1500 NSCLC patient were screened for the presence of ALK rearrangement, with only 82 patients testing positive for ALK. Crizotinib (250 mg BID) was orally administered to 82 patients in a 28-day cycle. The objective response rate (ORR) was 57% (i.e., 47 patients out of 82 respond to the treatment). Among these 47 patients, 46 had partial response whereas 1 showed a complete response. The remaining 33% (27 patients) had stable diseases. Mean duration of treatment was 6.4 months where 63 patients (77%) continued to receive crizotinib even after the data cutoff (Kwak et al., 2010).

Furthermore, Camidge et al. have reported updated result from phase I study (Camidge et al., 2012). A total of 149 patients with locally advanced or metastatic ALK-positive NSCLC (stage III or IV) received oral crizotinib 250 mg twice daily in 28-day cycles. Mean duration of treatment was 10.8 months and 55% of patients continued to receive crizotinib after data cutoff point. An objective response (OR) of 60.8% was observed in 87 patients with three patients responding completely and 84 of them partially to crizotinib treatment. Mean progression free survival (PFS) was 9.7 months whereas PFS was longer (median 18.3 months) for patients receiving crizotinib as first line therapy. The estimated overall survival at 6 and 12 months was 87.9% and 74.8%, respectively. The majority of patients (97%) exhibited grade 1 or 2 adverse events including nausea, diarrhoea, vomiting, constipation and peripheral oedema. Severe adverse event (grade 3 or 4) was experienced by a number of patients (36 patients) that included neutropenia, raised ALT, lymphopaenia and pneumonitis (Camidge et al., 2012).

1.4.3.2. Phase II clinical trial (Profile 1005)

Profile 1005 was a single-arm, multicentre, open-label study that evaluated the efficacy and safety of orally administered crizotinib at a dose of 250 mg BID

in a 21-day cycle (Blackhall et al., 2017). Patients with advanced ALK-positive NSCLC whose disease progressed after one or more chemotherapies were included. This study was conducted with 1066 participants that were divided into two groups. First group comprised of 908 patients whose ALK-positive status was determined in a central laboratory and second group comprised of 158 patients whose ALK-positive status was determined locally. An ORR of 54% and 41%, median PFS of 8.4 months and 6.9 months and median OS of 21.8 months and 16.9 months was observed in the first and the second group, respectively. Majority of patients (96%) experienced treatment related adverse events. The most commonly observed adverse events of any grade were visual disorder (58%), nausea (51%), vomiting (47%) and diarrhoea (47%). Grade 3 or 4 neutropenia and elevated transaminases were found in 13% and 8% patients, respectively (Blackhall et al., 2017).

Thus, the results from phase I and II studies demonstrated the potent antitumor activity of crizotinib in patients with advanced ALK-positive NSCLC.

1.4.3.3. Phase III clinical trial (Profile 1007 and 1014)

The therapeutic efficacy of crizotinib was compared with chemotherapy in a randomised, open-labelled phase III (Profile 1007) clinical trial. The study enrolled 347 patients with locally advanced or metastatic ALK-positive NSCLC and with Eastern Cooperative Oncology Group (ECOG) performance status ranging from 0-2 and had received one prior platinum-based chemotherapy regimen. Most patients were younger (<65 years), non-smokers and had adenocarcinoma histology. Of 347 patients, 173 received oral crizotinib at a dose of 250 mg BID while the remaining 174 subjects received intravenous chemotherapy (either pemetrexed 500 mg/m^2 body surface area or docetaxel 75 mg/m^2) every 3 weeks. PFS was the primary end point of the study, whereas secondary end points were OS, response rate that include partial and complete responses, safety, and patient reported outcomes. Crizotinib treatment demonstrated superior therapeutic efficacy with longer median PFS rate of 7.7 months (95% CI, 6.0 to 8.8) and higher ORR of 65% (95%CI, 58 to 72) compared

to chemotherapy (pemetrexed or docetaxel) with only 3 months (95% CI, 2.6 to 4.3) of PFS and 20% (95% CI, 14 to 26) of ORR. However, there was no significant improvement in OS of patients receiving crizotinib (median 20.3 months) compared to chemotherapy (median 22.8 months). Adverse events including visual disorder, gastrointestinal side effects, elevated ALT was common among patients receiving crizotinib, whereas dyspnea, alopecia, and fatigue were common in those treated with chemotherapy (Shaw et al., 2013).

The randomised, multicentre, open labelled Profile 1014 trial compared the clinical efficacy and safety of crizotinib as a first line treatment against standard chemotherapy (pemetrexed plus platinum) in patients with locally advanced and metastatic ALK-positive NSCLC. 343 patients were enrolled in this study where 172 received oral crizotinib (250 mg BID) and the remaining 171 received standard chemotherapy (pemetrexed, 500 mg/m^2 of body surface and either cisplatin, 75 mg/m^2 or carboplatin, target AUC of 5 to 6 mg/ml/min) for 3 weeks for up to 6 cycles. Crizotinib demonstrated superior efficacy compared to pemetrexed plus platinum standard chemotherapy in treatment naïve ALK-positive NSCLC patients. The median PFS was significantly longer in patients assigned to crizotinib (10.9 months, 95% CI, 8.3 to 13.9) compared to those treated with chemotherapy (7.0 months, 95% CI, 6.8 to 8.2). Similarly, patients assigned to crizotinib had significantly higher ORR of 74% (95% CI, 67 to 81) than those receiving chemotherapy (45%, 95% CI, 37 to 53). Both treatment groups experienced grade 1 and 2 adverse events where vision disorder, nausea, vomiting, oedema were common in the crizotinib treatment group and nausea, fatigue, and decreased appetite were mostly observed in the chemotherapy group. Crizotinib led to greater suppression in lung cancer symptoms and improvement in a quality of life (Solomon, Mok, et al., 2014). Overall, both Profile 1007 and profile 1014 demonstrated the superior efficacy of crizotinib over standard chemotherapy in patients previously untreated or treated with one or more platinum-based chemotherapy.

1.5. Limitation of crizotinib

The clinical benefit of crizotinib is highly limited due to relapse of diseases in the central nervous system and development of systemic resistance. Despite the significant response of crizotinib in ALK-positive NSCLC, the majority of patients eventually progress to a diseases of the central nervous system (Kim et al., 2016; Shaw et al., 2011). Retrospective analysis of data from two clinical trials (PROFILE 1005 and PROFILE 1007) found low intracranial ORR to crizotinib in patients with ALK-positive NSCLC and previously treated or untreated brain metastases (Costa et al., 2015). The poor CNS activity may be due to the poor BBB penetration of crizotinib (Costa et al., 2011; Maillet et al., 2013). Costa et al. reported that crizotinib has a low cerebrospinal fluid (CSF) concentration of 0.616 ng/ml compared to its plasma concentration (237 ng/ml) (Costa et al., 2011). Furthermore, the majority of patients treated with tyrosine kinase inhibitors including crizotinib exhibit systemic resistance. Understanding the underlying mechanism of resistance is crucial to select optimal therapy that can combat resistance and improve patient outcome (Camidge & Doebele, 2012; Lin et al., 2017). Both patient-derived and cell-based resistant models of crizotinib have provided a better understanding of underlying molecular mechanism of crizotinib resistance (Crystal et al., 2014). Resistance to crizotinib can be either primary (intrinsic) or secondary (acquired) resistance (Lovly & Shaw, 2014).

1.5.1. Primary resistance

Despite the presence of ALK rearrangement, approximately 40% of patients do not respond to crizotinib (Kwak et al., 2010). The underlying mechanism of primary resistance to crizotinib is not fully understood. One study suggested that the presence of different ALK fusion genes and EML4-ALK variants may contribute to the heterogenous response of ALK-positive tumours to ALK inhibitor. They showed that different ALK fusion genes and EML4-ALK variants (*(v1, v2, v3a* and *v3b*) exhibited different sensitivity to crizotinib. The EML4-ALK variants *v2 and v3a* a showed significant difference in sensitivity to crizotinib with growth inhibitory concentration (GI_{50}) of 150 and 1000 nmol/L, where as

v1 and v3b have GI_{50} values of 470 nmol/L (Heuckmann et al., 2012). Furthermore, some studies suggested that intratumoural heterogeneity may be the underlying reason behind intrinsic resistance to crizotinib. Cai et al. identified intratumoural genetic heterogeneity in ALK-rearranged NSCLC harbouring ALK/EGFR coalteration. The distribution of ALK fusion and EGFR in tumour tissue was very random where some tumour cells had concomitant coexistence of both, and some had either one of them (Cai et al., 2015). Moreover, ALK-positive NSCLC patients harbouring both ALK and KRAS poorly responded to crizotinib (Sahnane et al., 2016). The genetic diversity within the tumour tissue can hinder accurate diagnosis and selection of appropriate treatment that may lead to intrinsic resistance.

1.5.2. Secondary resistance

Despite the initial response to crizotinib, the majority of patients eventually develop acquired resistance within a year of therapy (Choi et al., 2010; Katayama et al., 2011). Resistance mechanisms are further classified into ALK dominant (on-target) mechanism where tumour cells solely depend on ALK signalling and ALK non-dominant (off-target) mechanism where tumour cells rely on different signalling pathways other than ALK (Figure 1.4) (Drizou et al., 2017; Lin et al., 2017).

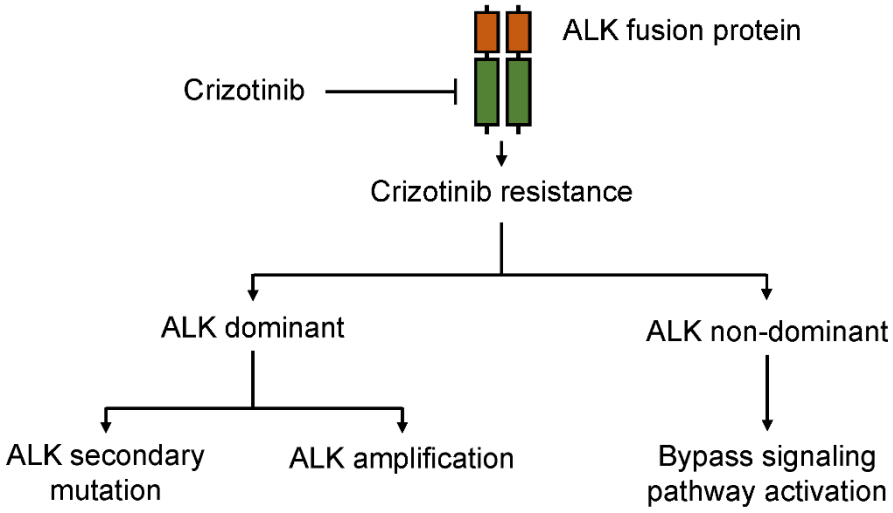

Figure 1.4 Overview of mechanism of acquired resistance to crizotinib. Treatment with crizotinib binds to the ATP binding site and thereby inhibit EML4-ALK activation. However, acquired resistance is developed that is classified into ALK dominant (on target) and ALK non-dominant (off target) resistance. Adapted from (Steuer & Ramalingam, 2014).

1.5.2.1. ALK dominant mechanism

The ALK dominant mechanism includes secondary mutation and amplification (copy number gain) of ALK that re-establish kinase activity and preserve the dominance of ALK signalling (Camidge & Doebele, 2012; Lin et al., 2017). Almost 30% of cases with acquired crizotinib resistance develop secondary mutations in the kinase domain of ALK (Doebele et al., 2012; Katayama et al., 2012). Choi et al. identified two *de novo* mutations, L1196M and C1156Y, through the molecular analyses of sputum and pleural-effusion specimens of crizotinib resistant ALK-positive NSCLC patients. Interestingly, BA/F3 cells harbouring L1196M mutation were more resistant to crizotinib compared to those expressing C1156Y mutations (Choi et al., 2010). The L1196M is a gatekeeper mutation, analogous to T790M in EGFR that alters ATP binding pocket and impairs crizotinib binding through steric interference (Choi et al., 2010; Gainor & Shaw, 2013; Lin et al., 2017; Steuer & Ramalingam, 2014). Similarly, several studies have identified other secondary mutations such as F1174L/C/V, L1152R, I115Tins, G1202R, G1202del, S1206Y/C, G1269A/S, G1123S/D, E1210K, I1171T/N/S, L1198P and D1203N (Doebele et al., 2012; Gainor et al., 2016; Heuckmann et al., 2011; Ignatius Ou et al., 2014; Katayama et

al., 2012; Sasaki et al., 2011; Zhang, Wang, et al., 2011). The G1269A mutation lies within the active site and hinders crizotinib binding (Doebele et al., 2012). While the C1156Y, L1152R and I115Tins affect residues adjacent to the N-terminus and F1174C/L/V mutations affect residues at the C-terminus(Choi et al., 2010; Friboulet et al., 2014; Katayama et al., 2012). Solvent-front mutations (G1202R, G1202del, D1203N, and S1206Y/C) impair crizotinib binding via steric hindrance (Friboulet et al., 2014; Gainor et al., 2016; Ignatius Ou et al., 2014; Katayama et al., 2012), while the I1171T/N/S mutation may hinder ALK-TKI binding by distorting the αC helix of ALK (Katayama et al., 2014; Toyokawa et al., 2014). Furthermore, amplification of ALK alone or in combination with secondary mutations was observed in crizotinib resistant ALK positive NSCLC patients (Doebele et al., 2012; Katayama et al., 2012). Katayama et al. noted the ALK amplification as a potential resistance mechanism in an *in vitro* resistant model of crizotinib that was developed by exposure of ALK-positive NSCLC (H3122) cells to increasing concentration of crizotinib. Cells exposed to an intermediate concentration of crizotinib (0.6 μM) harboured ALK amplification, whereas higher concentration (1 μM) of crizotinib exhibited both ALK amplification and L1196M gatekeeper mutation (Katayama et al., 2011).

1.5.2.2. ALK non-dominant mechanism

The ALK non-dominant mechanism includes activation of alternative signalling pathways (bypass tracks) through genetic alterations (mutations or amplification), dysregulation of feedback mechanism or autocrine signalling, leading to ALK independent growth and survival of tumour cells (Dagogo-Jack & Shaw, 2016; Lin et al., 2017). Approximately 40% of patients who develop resistance to crizotinib do not harbour ALK amplifications or secondary mutations, instead bypass signalling tracks are activated (Katayama et al., 2015). Sasaki et al. was first to identify the activation of EGFR as the possible bypass mechanism in *in vitro* resistant model of crizotinib (Sasaki et al., 2011). This was further supported with clinical analysis of ALK-positive tumour biopsies from patients resistant to crizotinib (Doebele et al., 2012; Katayama et al., 2012). The

possible mechanism of EGFR activation in crizotinib resistant patients includes an increase in EGFR phosphorylation, upregulation of EGFR ligands and mutation or amplification of EGFR (Doebele et al., 2012; Kang et al., 2018; Katayama et al., 2012; Tanizaki, Okamoto, Okabe, et al., 2012). Other potential bypass mechanism include mutations of KRAS, PIK3CA, MET, amplifications (copy number gains) of, cKIT, HGF, and activation of SRC, IGFR, HER2, (Boland et al., 2013; Crystal et al., 2014; Doebele et al., 2012; Kang et al., 2018; Katayama et al., 2012; Lovly et al., 2014; Sasaki et al., 2011; Tanizaki, Okamoto, Okabe, et al., 2012).

1.6. Strategies to overcome crizotinib resistance

Understanding the diverse molecular mechanisms of resistance have provided knowledge for the development of novel therapeutic strategies. These strategies should effectively treat the relapse by overcoming the resistance as well as improve patient outcome by preventing or delaying the emergence of resistance (Dagogo-Jack & Shaw, 2016; Lin et al., 2017; Lovly & Pao, 2012). The selection of appropriate treatment strategies depends on the type of resistance mechanism involved (Lovly & Pao, 2012).

1.6.1. Next generation ALK tyrosine kinase inhibitor

One of the most common strategies to combat resistance is the use of next generation ALK-TKIs. Crizotinib resistant patients who harbour ALK mutation or amplification and are still addicted to ALK signalling are treated with next generation ALK-TKIs (Shaw & Engelman, 2013). In comparison to crizotinib, these TKIs are highly potent and have better penetration of the BBB (Pirker & Filipits, 2019; Shaw & Engelman, 2013). Currently, three second generation ALK-TKIs ceritinib, alectinib and brigatinib have been approved by the FDA as the second line treatment of crizotinib-resistant patients (U.S. Food and Drug Administration, 2017a, 2017b, 2017c). Recently, a third generation ALK-TKI, loratinib, has been approved by the FDA as the second- or third-line treatment of patients who have progressed on crizotinib (U.S. Food and Drug Administration, 2018b). The treatment approach for ALK-positive NSCLC using next generation ALK-TKIs is illustrated in Figure 1.2.

1.6.1.1. Ceritinib

Ceritinib was the first second generation ALK-TKI approved by the FDA in 2014 for the treatment of ALK-positive NSCLC patients resistant to crizotinib (U.S. Food and Drug Administration, 2017c). It is a highly potent (20-fold more potent than crizotinib), ATP competitive, small molecule inhibitor of ALK (Friboulet et al., 2014; Marsilje et al., 2013). In an *in vitro* crizotinib resistant model, ceritinib effectively overcame resistant conferring mutations, L1196M, G1269A, I1171T

and S1206Y, but was ineffective at inhibiting G1202R and F1174C mutations (Friboulet et al., 2014). A phase I (ASCEND-1) trial demonstrated the anti-tumour activity of ceritinib in both crizotinib naïve and crizotinib pretreated ALK-positive NSCLC patients (Kim et al., 2016; Shaw & Engelman, 2014). Similarly, single-arm phase II trials evaluated efficacy and safety of ceritinib in chemotherapy and crizotinib pretreated (ASCEND-2) and ALK-TKI naïve (ASCEND-3) patients. In both studies, ceritinib demonstrated clinically meaningful and improved responses (Crino et al., 2016; Felip et al., 2015). In phase III (ASCEND-4) trial, ceritinib demonstrated superior efficacy compared to platinum-pemetrexed doublet chemotherapy with an ORR (72.5% versus 26.7%) and PFS (16.6 versus 8.1 months) (Soria et al., 2017). Based on results from the ASCEND-4 trials, ceritinib was approved by the FDA in 2017 for the treatment of patients with metastatic ALK-positive NSCLC (U.S. Food and Drug Administration, 2017c). Furthermore, a phase III (ASCEND-5) trial demonstrated that ceritinib was more efficacious over single-agent chemotherapy in patients pretreated with crizotinib and platinum-based doublet chemotherapy (Shaw, Kim, et al., 2017). The most common adverse events associated with ceritinib were diarrhoea, nausea, vomiting, fatigue, rise in ALT and AST (Kim et al., 2016; Shaw, Kim, et al., 2017).

1.6.1.2. Alectinib

Alectinib is an orally available, highly potent and selective small molecule inhibitor of ALK. Preclinical studies have demonstrated that alectinib is active against the crizotinib-resistant ALK mutations including L1196M, F1174L, C1156Y, G1269A, 1151Tins and L1152R, but less potent against G1202R ALK mutation (Kodama et al., 2014; Sakamoto et al., 2011). Alectinib was granted breakthrough therapy designation in 2013 and was finally approved in 2015 by the FDA for the treatment of metastatic ALK-positive NSCLC patients who had progressed on crizotinib (Larkins et al., 2016). In phase I/II trial, alectinib demonstrated promising anti-tumour activity in crizotinib resistant ALK-positive NSCLC patients, including those with CNS metastases. It also

confirmed grade 3 neutropenia and headache as the dose-limiting toxicities and determined 600 mg BID as a recommended dose for phase II trials (Gadgeel et al., 2014). A single-group, multicentre, phase II trial evaluated the efficacy and safety of alectinib in crizotinib resistant ALK-positive NSCLC patients. Alectinib showed promising efficacy and was well tolerated (Shaw, Gandhi, et al., 2016). Furthermore, two phase III trials compared the efficacy of alectinib over crizotinib in treatment naïve ALK-positive NSCLC patients. Both studies demonstrated the superiority of alectinib over crizotinib with improved mPFS (Hida et al., 2017; Peters et al., 2017). These results led to the approval of alectinib by the FDA in 2017 (U.S. Food and Drug Administration, 2017a). The common adverse event associated with alectinib were grade 1-2: constipation, fatigue, myalgia, peripheral oedema and grade 3-4 increase in blood creatine phosphokinase, ALT and AST (Shaw, Gandhi, et al., 2016).

1.6.1.3. Brigatinib

Brigatinib is an orally available, potent multiple tyrosine kinase inhibitors of ALK, ROS1, fms like tyrosine kinase 3 (FLT3) and EGFR (Huang et al., 2016; Zhang et al., 2016). Cell based studies have demonstrated broad spectrum activity of brigatinib against ALK mutations conferring resistance to ALK-TKIs including L1196M, C1156Y, 1151Tins, D1203N, F1174L/V, E1210K, G1269A, V1180L, I1171N but less potency against G1202R mutation (Gainor et al., 2016; Zhang et al., 2016). In a single-arm phase I/II trial, brigatinib demonstrated promising clinical activity with an acceptable safety profile. A dose escalation phase I study established grade 3 increased ALT (240 mg daily) and grade 4 dyspnoea (300 mg daily) as dose limiting toxicities and determined 180 mg daily as the recommended dose for phase II trial. However, due to early pulmonary toxicity at 180 mg, two additional regimens were assessed, 90 mg once daily and 180 mg once daily with a 7-day lead-in at 90 mg daily (Gettinger et al., 2016). In a randomised, multicentre phase II trial, two regimens of brigatinib were evaluated in crizotinib refractory ALK-positive NSCLC patients. Brigatinib demonstrated substantial and better response along with intracranial disease

control (Kim et al., 2017). Furthermore, in phase III (ALTA-1L) trial, brigatinib demonstrated superior efficacy over crizotinib in crizotinib naïve ALK-positive NSCLC patients with a higher rate of PFS at 1 year (67% vs 43%), ORR (71% vs 60%) and intracranial response (78% vs 29%) (Camidge et al., 2018). The most common adverse event associated with brigatinib included grade 1-2 nausea, fatigue, diarrhea and grade 3-4 elevated lipase, dyspnoea, hypertension, elevated CPK and pneumonitis (Camidge et al., 2018; Gettinger et al., 2016).

1.6.1.4. Loratinib

Loratinib is a novel highly potent, selective, ATP competitive small molecule inhibitor of ALK and ROS1. It is effective against all known mutation (L1196M, C1156Y, L1198F, E1210K, L1152R, S1206Y G1269A, 1151Tins, F1174L/C) including the highly resistant G1202R mutation (Gainor et al., 2016; Johnson, Richardson, et al., 2014; Zou et al., 2015). A single-arm phase I trial demonstrated robust systemic and intracranial activity of loratinib in metastatic ALK-positive NSCLC patients, most of whom had brain metastases and had been pre-treated with two or more TKIs. The study selected a phase 2 dose of 100 mg OD but failed to identify MTD (Shaw, Felip, et al., 2017). A phase II trial further confirmed the efficacy of loratinib in both treatment naïve and ALK-TKI pretreated ALK-positive NSCLC patients. Adverse events associated with loratinib were hypercholesterolaemia, hypertriglyceridemia, peripheral neuropathy and oedema (Solomon et al., 2018). A recent study reported greater efficacy of loratinib in patients harbouring ALK mutation compared with patients without ALK mutation. They also suggested that tumour genotyping for ALK mutation may identify patients who are more likely to benefit from loratinib (Shaw et al., 2019). Currently, randomised phase III trial is ongoing, where loratinib is being compared with crizotinib in treatment naïve ALK-positive NSCLC patients (ClinicalTrials.gov National Library of Medicine (US), 2017).

1.6.2. Upfront combination therapy

Although mono or sequential therapy of ALK-TKIs is highly effective in treatment of ALK-TKIs naïve/refractory ALK-positive NSCLC patients, acquired resistance invariably develop (Lin et al., 2017; Metro et al., 2017; Recondo et al., 2020). Combination therapy is another effective strategy that can overcome and delay the emergence of resistance (Bozic et al., 2013; Crystal et al., 2014; Lovly & Pao, 2012; Zhou & Cox, 2015). The combination of two drugs targets key pathways in a synergistic or additive manner that in turn enhances therapeutic efficacy even at lower dose (Bayat Mokhtari et al., 2017; Saputra et al., 2018). This strategy requires an understanding of the most critical signalling event essential for the proliferation and survival of tumour cells (Hrustanovic et al., 2015). In patients with identified bypass tracks, co-targeting primary oncoproteins and critical downstream effectors may be an effective strategy to overcome resistance (Crystal et al., 2014). Furthermore, Bozic et al. found that the combination of two drugs with no cross-resistance may result in long-term disease control in most patients. They also reported that upfront combination of two drugs to be highly effective compared to sequential therapy. They even suggested triple therapy in patients with a large disease burden (Bozic et al., 2013).

Identifying the secondary target for combination therapy requires the understanding of the cellular process and downstream signalling pathway that are critical in the survival of tumour cells. The following sections contain detailed information on molecular mechanism involved in tumour progression and downstream signalling in ALK-positive NSCLC.

1.7. Molecular mechanism involved in regulation of tumour progression

Cancer is an extremely diverse and heterogenous disease with underlying molecular events that drive the transformation of normal cells into malignant cancer cells. The underlying mechanisms that are critical for tumour progression include but is not limited to proliferation, apoptosis, angiogenesis (Evan & Vousden, 2001). Hanahan and Weinberg proposed distinct hallmarks of cancer that include sustained proliferation, resistance to apoptosis, induction of angiogenesis, activation of invasion and metastasis, deregulation of cellular metabolism, evading tumour suppression, and avoiding immune destruction (Hanahan & Weinberg, 2000, 2011). Therapeutic strategies targeting these critical molecular events can causes suppression in tumour growth and survival (Feitelson et al., 2015; Ferrara & Kerbel, 2005; Pfeffer & Singh, 2018; Zhao & Adjei, 2015). The majority of drugs used for the treatment of cancer including ALK-positive NSCLC either induce apoptosis or inhibit proliferation, angiogenesis to suppress cancer proliferation and survival (Christensen et al., 2007; Kaufmann & Earnshaw, 2000; Padma, 2015; Schirrmacher, 2019; Zhou et al., 2016).

1.7.1. Proliferation

Proliferation is a fundamental biological process that is essential for normal growth and development. In normal cells, proliferation is tightly regulated with control being a balance between growth-promoting and growth-inhibiting signals and is responsible for maintenance of tissue homeostasis (Barbarino et al., 2017). Cell proliferation depends on the rate of cell division, the fraction of cell undergoing cell division, and the rate of cell death (Andreeff et al., 2000). However, cancer cells lose their ability of control cell division, disturbing the fine balance between cell gain and cell loss, that causes aberrant cell proliferation and growth (Farber, 1995).

1.7.1.1. Cell cycle

The cell cycle is a series of event that facilitates DNA replication and division of a cell into two daughter cells. It consists of four sequential phases including first gap (G1), synthesis (S), second gap (G2) and the mitotic (M) phases. S and M phase are functional phases where DNA replication occurs during S phase and cell division during M phase. G1 and G2 phase are preparatory phases that precede S and M phases, respectively. G1 and G2 phase are involved in protein synthesis to support the DNA synthesis and cell division in the following phase, respectively. G0 is a quiescent state where the cell has stopped dividing and exited the cell cycle. Cells in G0 phase can remain there or re-enter the cell cycle (Norbury & Nurse, 1992; Schafer, 1998). Cell cycle checkpoints ensure that the events of cell cycle occur in correct order. Two types of cell cycle checkpoints have been elucidated – 1) DNA damage checkpoints in G, S and G2 phases, and 2) spindle assembly checkpoints in the M phase. DNA damage checkpoints ensure that only normal DNA is replicated and passed on to daughter cells. In presence of damaged DNA, these checkpoints arrest the cell cycle that allows time for DNA repair. Spindle assembly checkpoints ensure that a complete set of chromosomes is passed on to daughter cells. In the presence of improper alignment of chromosomes on the mitotic spindle, it arrests the cell cycle at metaphase until accurate chromosome segregation can be guaranteed (Elledge, 1996; Hartwell & Weinert, 1989; Vermeulen et al., 2003).

Cell cycle progression through each phase is regulated by two key regulatory molecules: cyclin dependent kinases (CDKs) and cyclins. CDKs are serine/threonine protein kinase that requires binding of regulatory subunits (cyclins) for their catalytic activity. The activated CDKs-cyclin heterodimer phosphorylates targeted substrate that regulates the transition of cell cycle phases. Association of cyclin D (D1, D2, D3) with CDK4 and CDK6 are essential for G1 progression, complexes of cyclin E (E1 and E2) with CDK2 are required for G1-S transition, complexes of cyclin A (A1 and A2) with CDK2 is required for progression of S phase and functions through G2, complexes of cyclin A with CDK1 promotes entry into M phase and association of cyclin B (B1, B2 and B3)

with CDK1 is required during mitosis (Lees, 1995; Nigg, 1995; Vermeulen et al., 2003).

The activity of cyclin-CDK complexes are regulated by different mechanisms – 1) synthesis and degradation of cyclins at a particular stage of the cell cycle, 2) activation of CDK by phosphorylation of threonine and tyrosine residues by CDK activating kinase (CAK), 3) deactivation of CDK by phosphorylation of its ATP binding site, 4) inactivation of CDKs or cyclin-CDKs complex by cyclin dependent kinase inhibitors (CKIs) (Lees, 1995). Two families of CKIs – INK4 and Cip/Kip regulate the activity of CDKs and cyclin-CDKs complexes. INK4 families include p16INK4A, p15INK4B, p18INK4C, and p19INK4D that specifically bind to and inhibit CDK4 and CDK6. Cip/Kip families include p21CIP1, p27KIP1, and p57KIP2 that inhibit CDK2 and CDK2-cyclin complexes (Lees, 1995; Vermeulen et al., 2003).

1.7.2. Apoptosis

Apoptosis, also known as programmed cell death, is a physiological process that is responsible for balancing proliferation and maintaining tissue homeostasis (Fulda & Debatin, 2006). It also provides a defence mechanism by eliminating damaged, stressed and potentially dangerous cells (Norbury & Hickson, 2001). The term apoptosis was first used by Kerr et al. in 1972 to introduce a morphologically distinct type of cell death (Kerr et al., 1972). A typical morphological and biochemical feature of apoptosis includes membrane blebbing, cell shrinkage and DNA fragmentation (Hengartner, 2000; Kerr et al., 1972). Caspases are the key effectors of apoptosis that are initially expressed as an inactive proenzyme. Based on their activity, caspase can be divided into – 1) initiators (caspase-2,-8,-9,-10), executioners (caspase-3,-6,-7) and inflammatory caspases (caspase-1,-4,-5). In response to cell damage, initiator caspases get activated that in turn activate executioner caspases. This activation initiates a cascade of events leading to apoptosis (Cohen, 1997; Degterev et al., 2003; Shi, 2002).

There are two major types of apoptosis pathways – the extrinsic pathway (the death receptor pathway) and the intrinsic pathway (the mitochondrial pathway) (Figure 1.5) (Igney & Krammer, 2002). Both pathways eventually merge to a common pathway also called as execution pathway. Dysregulation of these pathways can lead to various pathological conditions including cancer (Solary et al., 1996).

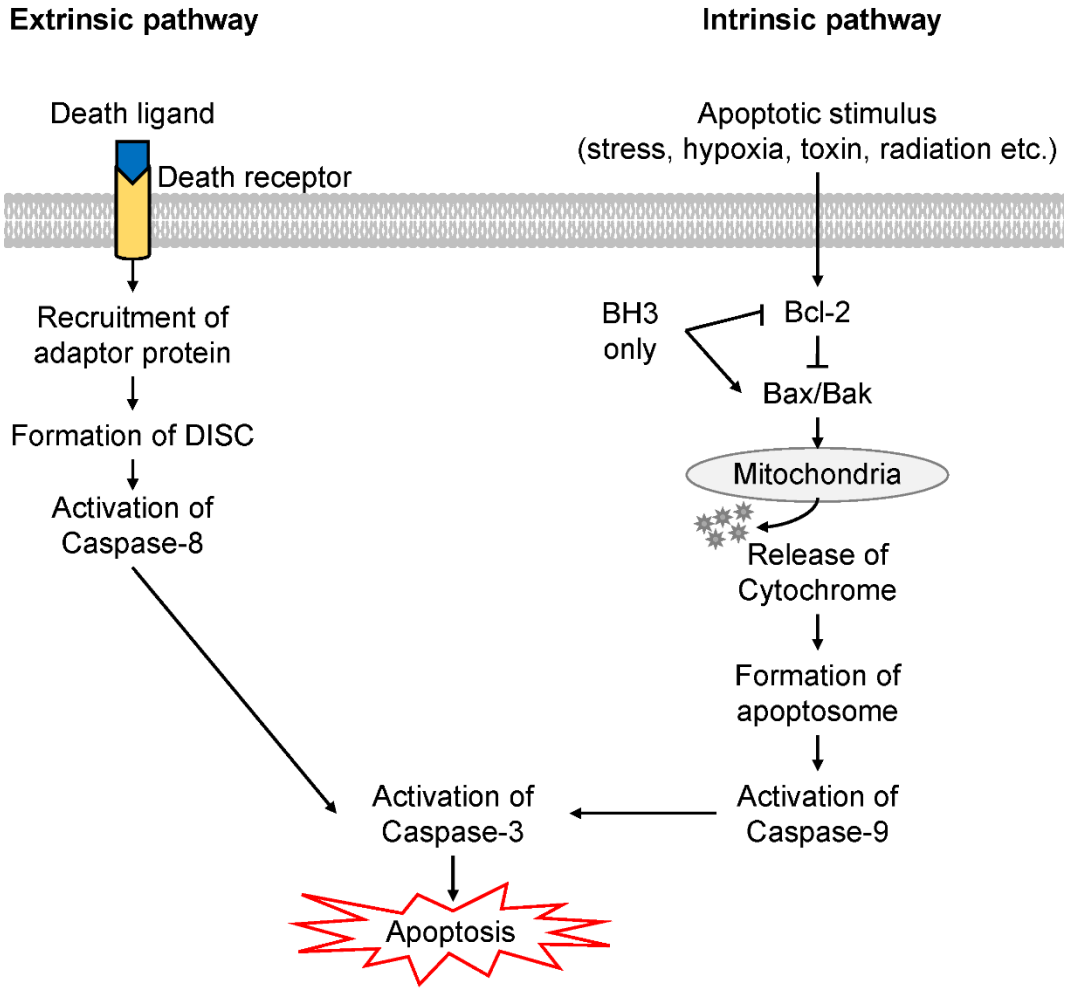

Figure 1.5 Schematic representation of apoptotic pathway. Apoptotic pathway is classified into extrinsic pathway that is mediated by death receptor and intrinsic pathway that is initiated by cell in the response to damage and mediated by mitochondria. Adapted from (Baig et al., 2016; D'Arcy, 2019; Elmore, 2007).

1.7.2.1. Extrinsic pathway

The extrinsic pathway is mediated by death receptors present on the cell surface, such as tumour necrosis factor receptor (TNF), fatty acid synthetase receptor (FasR), TNF-related apoptosis-inducing ligand receptor (TRAIL-R). The death receptor consists of a cysteine rich extracellular domain and intracellular cytoplasmic death domain (Ashkenazi & Dixit, 1998). Binding of death ligands such as fatty acid synthetase ligand (FasL) or tumour necrosis factor alpha (TNFα) induces oligomerisation of the receptor that causes conformational change and activation of death domain. This is followed by the recruitment of the adaptor proteins such as Fas-associated death domain (FADD) and TNF receptor-associated death domain (TRADD) and procaspase-8 that forms death inducing signalling complex (DISC) (Aggarwal, 2003; Hsu et al., 1995; Oberst et al., 2010; Wajant, 2002; Walczak & Sprick, 2001). DISC facilitates dimerisation and auto-catalytic activation of procaspase-8 to caspase 8 (Kischkel et al., 1995; Oberst et al., 2010). The activated caspase-8 then initiates apoptosis by activation of executioner caspase (Jin & El-Deiry, 2005; Kominami et al., 2012).

1.7.2.2. Intrinsic pathway

The intrinsic pathway is mediated by diverse internal stimuli such as genetic damage, hypoxia, radiation, toxins, surplus Ca^{2+}, oxidative stress, viral infections, upregulation of oncogenes and deprivation of growth factors, hormones and cytokines (Elmore, 2007). This pathway is tightly regulated by Bcl-2 family of proteins that are further divided in to anti-apoptotic/ pro-survival (Bcl-2, Bcl-X_L, Bcl-W, Bcl-B, Mcl-1, Bfl-1/A1, Bcl2l 12) or Bcl-2 homology 3 (BH3) only proapoptotic (Bim, Bad, Puma, Bid, Noxa, Bmf, Diva, Bik) or proapoptotic effector (Bak, bax, bok) proteins (Tzifi et al., 2012; Warren et al., 2019). In response to internal stimuli, BH3 only pro-apoptotic proteins are activated which then initiates apoptosis either by direct activation of Bcl-2-associated X protein (Bax) and Bcl-2 antagonist/killer-1 (Bak) at the mitochondrion or neutralisation of anti-apoptotic Bcl-2 family proteins (Chen et al., 2005; Kim et al., 2006; Kuwana et al., 2005; Merino et al., 2009; Willis et al.,

2005). The activated Bax and Bak undergoes homo-oligomerisation that permeabilise the mitochondrial outer membrane (Kuwana et al., 2002; Mikhailov et al., 2003). The mitochondrial outer membrane permeabilisation allows the release of various apoptogenic factors into the cytosol including cytochrome c, second mitochondria-derived activator of caspase/direct inhibitor of apoptosis-binding protein with low pI (Smac/DIABLO), serine proteinase omi/high temperature requirement protein A Omi/HtrA (Du et al., 2000; Garrido et al., 2006; Suzuki et al., 2001; Verhagen et al., 2000). The cytochrome c then binds to apoptosis protease activating factor (Apaf-1) and procaspase-9 to form a complex called as apoptosome (Cain et al., 2002; Riedl & Salvesen, 2007). The apoptosome facilitates the activation of procaspase-9 to caspase-9 that in turn activates the executioner caspases resulting in induction of apoptosis (Brenner & Mak, 2009; Cain et al., 2002; Kroemer et al., 2007; Wang, 2001). On the other hand, Smac/DIABLO and Omi/HtrA promote apoptosis by inhibiting the activity of inhibitors of apoptosis proteins (IAPs) (Du et al., 2000; Yang et al., 2003).

1.7.2.3. Execution pathway

Both the intrinsic and extrinsic pathway of apoptosis converge to the execution pathway where the executioner caspases (capases-3,-6,-7) are cleaved and activated by initiator caspases (Igney & Krammer, 2002). The activated executioner caspases, most importantly caspase-3, mediate apoptosis through the cleavage of multiple cellular proteins including cellular DNA repair proteins, structural proteins, mediators and regulators of apoptosis, and cell cycle related proteins (Degterev et al., 2003). Caspase-3 cleaves the inhibitor of the DNase caspase activated deoxyribonuclease (ICAD) and releases endonuclease, that migrates to nucleus and causes DNA fragmentation. Cleavage of structural proteins such as actin by caspase-3 leads to membrane blebbing and cell fragmentation (Igney & Krammer, 2002). Similarly, capase-3 mediate cleavage of DNA repair proteins such as poly (ADP-ribose) polymerase (PARP). PARP is a nuclear protein that is activated by a breakdown of single or double stranded DNA. PARP facilitates DNA repair by catalysing the attachment of ADP-ribose

polymer to multiple nuclear factor (Degterev et al., 2003; Smulson et al., 2000). These cleavages of cellular proteins by caspase-3 contribute to typical biochemical and morphological changes in apoptotic cells (Igney & Krammer, 2002). The last step of apoptosis is the formation of apoptotic bodies that are recognised by the phagocytes where they are engulfed and eliminated (Elmore, 2007; Jin & El-Deiry, 2005).

1.7.3. Angiogenesis

Angiogenesis is the physiological process that is involved in formation and growth of new capillary blood vessels from pre-existing vessels (Carmeliet, 2000; Hanahan & Folkman, 1996). The process of angiogenesis is complex and consists of multiple-steps: 1) Degradation of basement membrane and extracellular matrix components surrounding the endothelial tube by proteolytic enzymes, 2) activation and migration of endothelial cells, 3) proliferation of endothelial cells, 4) conversion of endothelial cells into tube like structures and formation of capillary tubes (Fan et al., 1995). Angiogenesis generally occurs during embryonic development, wound healing, and female reproductive cycling. In normal conditions, there is a tight balance between inhibitors and inducers of angiogenesis (Folkman & Shing, 1992). However, this process is deregulated in many pathological conditions including cancer (Folkman, 1995; Nishida et al., 2006).

Studies have shown that tumours become dormant with tiny diameters of 2-3 mm in the absence of neovascularisation. During tumour progression, the tumour itself initiates angiogenesis to sustain its growth and survival (Folkman, 1972; Gimbrone et al., 1972; Hanahan & Folkman, 1996). There is activation of the angiogenic switch leading to continuous sprouting of new vessels (Hanahan & Folkman, 1996). Angiogenic switch is initiated by upregulation of pro-angiogenic factors and downregulation of anti-angiogenic factors (Baeriswyl & Christofori, 2009; Bergers & Benjamin, 2003). The vascular endothelial growth factor (VEGF) is a key regulator of tumour angiogenesis (Ferrara et al., 2003; Yancopoulos et al., 2000). In presence of hypoxia, tumours induce the production

of VEGF (Brogi et al., 1994; Shweiki et al., 1992). Binding of VEGF-A to VEGF receptor-2 (VEGFR-2) on endothelial cells causes receptor dimerisation and autophosphorylation that in turn activates several downstream signalling pathways including MAPK/ERK, PI3K/AKT that promotes the formation of new blood vessels (Hofer & Schweighofer, 2007; Munoz-Chapuli et al., 2004). Conversely, VEGF-B and VEGF-C binds to VEGFR-3 on lymphatic endothelial cells and promotes lymph-angiogenesis (Alitalo et al., 2005). Other proangiogenic factors that have a role in tumour angiogenesis include epidermal growth factor (EGF), transforming growth factor (TGF), basic fibroblast growth factor (FGF), platelet-derived growth factor (PDGF) (Li et al., 2018; Nishida et al., 2006)

1.8. Key signalling pathways of ALK

Understanding the downstream signalling of ALK and the mechanism responsible for its deregulation provides information regarding ALK mediated cellular transformation and thus can be a basis for personalised therapy. Studies have reported several ALK downstream signalling that is best characterised from the ALK fusion forms such as ALK-NPM and ALK-EML4. The major signalling pathways downstream of ALK include RAS/MAPK, AKT/mTOR, JAK/STAT, PLCγ pathway (Figure 1.6) (Chiarle et al., 2008; Hallberg & Palmer, 2013).

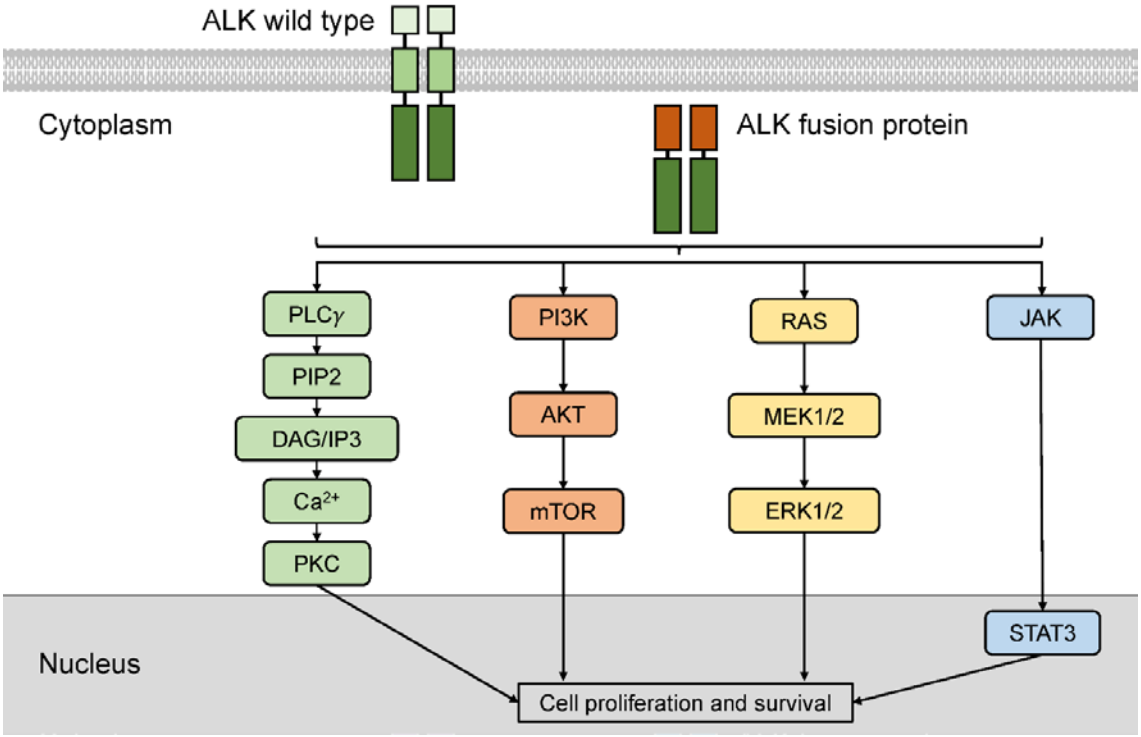

Figure 1.6 Schematic representation of ALK downstream signalling pathway. ALK activation results in upregulation of downstream signalling pathway such as PLCγ, AKT/mTOR, RAS/MAPK and JAK/STAT that promotes cancer cell proliferation and survival. Adapted from (Hallberg & Palmer, 2013; Lin et al., 2017; Shaw & Solomon, 2011; Solomon, Wilner, et al., 2014).

1.8.1. RAS/MAPK pathway

The mitogen-activated protein kinase (MAPK) pathway involve highly conserved kinase modules that transfer extracellular signal to intracellular machinery that controls fundamental cellular processes such as proliferation, growth, differentiation, migration, apoptosis (Molina & Adjei, 2006; Morrison, 2012; Zhang & Liu, 2002). In this pathway, binding of ligand to RTK or genomic alteration such as chromosomal translocation facilitates dimerisation and autophosphorylation of tyrosine kinase residues. Adaptor proteins such as growth factor receptor bound protein 2 (Grb2) contain an SH2 domain that binds to the phosphor-tyrosine residue of activated receptor. Adaptor proteins then recruit guanine nucleotide exchange factors (GEFs) such as SOS that promote the association of Ras with guanosine-5'-triphosphate (GTP). The GTP bound Ras interacts with Raf and increases its activity. The activated Raf phosphorylates downstream MEK, which in turn phosphorylates and activates ERK also known as mitogen-activated protein kinase (MAPK). The ERK then phosphorylates various downstream substrates in cytosol and nucleus including ribosomal S6 kinases (RSKs), SRC-1, Elk-1, c-Fos, c-Myc that are responsible for cellular process (Avruch et al., 1994; Cobb & Goldsmith, 1995; Molina & Adjei, 2006; Roux & Blenis, 2004; Seger & Krebs, 1995).

Dysregulation of this pathway has been reported in one third of cancers including ALK-positive NSCLC (Dhillon et al., 2007; Hilger et al., 2002; Hoshino et al., 1999). Both patient derived tissue samples and cell lines harbouring NPM-ALK fusion showed upregulation of the RAS/MAPK pathway (Marzec, Kasprzycka, Liu, Raghunath, et al., 2007; Staber et al., 2007). Adaptor proteins such as insulin receptor substrate-1 (IRS- 1), src homology 2 containing (Shc) and Grb2 interact with auto phosphorylated tyrosine kinase residues of NPM-ALK that activates RAS/MAPK downstream signalling (Crockett et al., 2004; Fujimoto et al., 1996; Riera et al., 2010). Recently, Marzec et al observed direct activation of MEK by NPM-ALK independent of Raf (Marzec, Kasprzycka, Liu, Raghunath, et al., 2007).

The RAS/MAPK pathway has been reported to be the major downstream signalling pathway in ALK-positive NSCLC harbouring EML4-ALK (Hrustanovic et al., 2015; Zhou & Cox, 2015). EML4-ALK activates all three Ras isoforms (N-Ras, K-Ras, H-Ras) in the lung adenocarcinoma cells leading to upregulation of RAS/MAPK signalling. The HELP domain of EML4 plays an important role in activation of Ras. The hydrophobic residue of HELP domain may mediate the membrane association and access to Ras. However, deletion of the HELP domain impaired the ability of EML4-ALK to activate Ras and its downstream RAS/MAPK signalling (Hrustanovic et al., 2015).

1.8.2. AKT/mTOR pathway

AKT/mTOR pathway is an important signalling network that converts extracellular stimuli into intracellular signals and regulates cellular function such as cell growth, survival, proliferation, and motility (Papadimitrakopoulou, 2012). Phosphatidylinositol 3-kinases (PI3Ks) belongs to the family of lipid kinases that are divided into three classes (Class I, II, III) based on their structure and substrate specificity. Class I PI3Ks are heterodimers composed of catalytic (i.e. p110) and regulatory subunits (i.e. p85). The Class I PI3Ks are further divided into Class IA (PI3Kα, β, and δ), that is activated by receptors with tyrosine kinase activity, and Class IB (PI3Kγ), that is activated by G protein coupled receptors (Fruman et al., 1998). Activation and autophosphorylation of RTKs result in recruitment of PI3K to the plasma membrane by direct binding to phosphorylated tyrosine kinase residue or indirect binding to adaptor proteins via Src-homology 2 (SH2) domain of p85 regulatory subunits. This leads to the activation of a catalytic p110 subunit that in turn phosphorylates phosphatidylinositol-4,5-bisphosphate (PIP2) to generate phosphatidylinositol-3,4,5-trisphosphate (PIP3). PIP3 then binds to AKT (serine/threonine protein kinase B) through its pleckstrin homology (PH) domain allowing the phosphorylation and activation of AKT by phosphoinositide dependent kinase 1 (PDK1) at Thr308 and by the mammalian target of rapamycin complex 2 (mTORC2) at Ser-473 (Porta et al., 2014; Yip, 2015). The activated AKT then

phosphorylates substrates in the nucleus and cytoplasm including inhibitory phosphorylation of glycogen synthase kinase 3 (GSK-3), pro-apoptotic factors such as Bcl-2 associated dead promoter (BAD) and Forkhead box on (FOXO), tuberous sclerosis protein 2 (TSC2) and activation of murine double minute 2 (MDM2) (Porta et al., 2014; Yip, 2015). The inhibition of TSC2 leads to the activation of mammalian target of rapamycin (mTOR) that in turn phosphorylates 4E-binding protein 1 (4EBP1), and ribosomal protein S6 kinase beta-1 70kD (S6K1) resulting in increased protein synthesis (Porta et al., 2014; Yip, 2015).

AKT/mTOR pathway is crucial for transforming the activity of EML4-ALK in ALK-positive NSCLC. Inhibition of this pathway reduced the growth of tumour in both *in vitro* and *in vivo* xenograft model of EML4-ALK-positive NSCLC (Chen et al., 2010; Koivunen et al., 2008). Furthermore, activation of the AKT/mTOR pathway has been reported in cell lines and patients derived tissue samples of NPM-ALK-positive anaplastic large cell lymphoma (ALCL) (Bai et al., 2000; Slupianek et al., 2001). Polgar et al. showed that NPM-ALK interacted with regulatory subunit p85 and activates PI3K and its downstream effector, serine/threonine kinase (Akt) (Polgar et al., 2005). The activated pathway in turn phosphorylated downstream substrates such as mTOR, GSK3, FOXO3 and promoted oncogenesis (Gu et al., 2004; Marzec, Kasprzycka, Liu, El-Salem, et al., 2007; McDonnell et al., 2012).

1.8.3. JAK/STAT pathway

The JAK/STAT pathway communicates information from extracellular stimuli to the cell nucleus and plays an important role in cell proliferation, survival, differentiation and apoptosis (Harrison, 2012). There are four members of the JAK family (JAK1, JAK2, JAK3, TYK2) and seven members of STATs (STAT1, STAT2, STAT3, STAT4, STAT5A, STAT5B, and STAT6) (Aaronson & Horvath, 2002). Dimerisation of receptor brings JAKs into close proximity that allows transphosphorylation and activation of JAKs. The activated JAKs then phosphorylate tyrosine kinase residue of receptors, thereby creating docking

sites for adaptor proteins including STATs. STATs when bound to the receptor become phosphorylated by JAKs. Activated STATs then dissociate, dimerise and translocate to nucleus and regulate transcription of target genes including c-Jun, c-Myc, Bcl-2, Mcl-1, $p21^{waf1}$, and $p27^{kip1}$ (Amin et al., 2003; Kisseleva et al., 2002; Rawlings et al., 2004).

The JAK/STAT pathway is constitutively active in NPM-ALK-positive ALCL. Some studies have reported that JAK3 binding and activation is essential for activation of STAT3 by NPM-ALK. While others have suggested that activation of STAT3 by NPM-ALK is independent of JAK3. The activated STAT3 then regulates the transcription of proteins such as c-Myc, survivin, Bcl-2, cyclin D1 and promotes cell survival of NPM-ALK-positive ALCL (Amin et al., 2003; Chiarle et al., 2005; Marzec et al., 2005; Zamo et al., 2002). Moreover, the JAK/STAT pathway is also important for transforming the activity of EML4-ALK in ALK-positive NSCLC (Roux & Blenis, 2004)

1.8.4. PLCγ pathway

The PLCγ pathway is involved in regulation of cellular process such as cell proliferation, differentiation, survival and migration (Falasca et al., 1998). Two isoforms $PLC\gamma_1$ and $PLC\gamma_2$ have been identified where each isoform has a putative pleckstrin homology (PH) domain, two catalytic domains separated by two SH2 domains, an SH3 domain and a putative split PH domain (Carpenter & Ji, 1999; Falasca et al., 1998). Activation of the receptor facilitates the binding of PLCγ to tyrosine phosphorylation sites of the receptor via the SH2 domain, leading to tyrosine phosphorylation and activation of PLCγ. The activated PLCγ in turn induces the hydrolysis of PIP2 to inositol-1,4,5-triphosphate (IP3) and diacylglycerol (DAG). These two molecules act as the intracellular secondary messengers that mediate the release of calcium from the endoplasmic reticulum into the cytosol as well as activates the serine/threonine, protein kinase C (PKC). The activated PKC then phosphorylates various substrate that are involved in cell cycle progression and proliferation (Berridge, 2009; Falasca et al., 1998; Nishizuka, 1995).

The activation of the PLCγ pathway in NPM-ALK- ALCL was first reported by Bai et al in 1998 (Bai et al., 1998). PLCγ binds to the phosphorylated tyrosine 664 of NPM-ALK via its SH2 domain that in turn causes phosphorylation and activation of PLCγ. They also found that transfection of NPM-ALK^{Y664F}, mutation of Y664 to phenylalnine, in Ba/F3 cells abrogated its transforming ability (Bai et al., 1998).

1.9. MEK inhibitors

MEK inhibitors are the small molecule inhibitor of mitogen activated protein kinase kinase enzymes (MEK1/2) (Cheng & Tian, 2017; Kim & Giaccone, 2018; Wang et al., 2007). They have demonstrated potent anti-tumour activity in both preclinical and clinical study of various cancer including melanoma and NSCLC (Cheng & Tian, 2017; Kim & Giaccone, 2018; Wang et al., 2007). Several MEK inhibitors have been developed till date including trametinib, cobimetinib, binimetinib that are approved by the FDA for the treatment of advance melanoma harboring BRAF mutation (U.S. Food and Drug Administration, 2017d, 2018a, 2020a; Wright & McCormack, 2013). Whereas some are under clinical trials including selumetinib, PD-325901, refametinib (Cheng & Tian, 2017; Kim & Giaccone, 2018; Wang et al., 2007).

1.9.1. Trametinib

Trametinib is the first MEK inhibitor that was approved by the FDA for treatment of advance melanoma (Wright & McCormack, 2013). It is ATP-noncompetitive, highly selective, allosteric inhibitor of MEK 1/2 (Abe et al., 2011; Gilmartin et al., 2011). Preclinical studies demonstrated the potent anti-tumour activity of trametinib resulting in significant tumour suppression in various cancers (Abe et al., 2011; Gilmartin et al., 2011; Yamaguchi et al., 2011). In clinical study trametinib showed the greater efficacy with prolonged PFS and overall survival in BRAF mutant melanoma (Falchook et al., 2012; Flaherty, Infante, et al., 2012; Flaherty, Robert, et al., 2012; Infante et al., 2012; Menzies & Long, 2014). Furthermore, combination of trametinib with BRAF inhibitor, dobrafenib improved OS and prolonged PFS of patients with BRAF mutation melanoma (Flaherty, Infante, et al., 2012; Menzies & Long, 2014). The most common adverse events were rash, diarrhoea, peripheral edema and dermatitis acneiform (Flaherty, Infante, et al., 2012; Flaherty, Robert, et al., 2012).

1.9.2. Cobimetinib

Cobimetinib is selective, ATP-noncompetitive, allosteric inhibitor of MEK 1/2 (Hoeflich et al., 2012; Rice et al., 2012). Preclinical studies in BRAF and KRAS mutant cells showed the broad anti-tumour efficacy of cobimetinib (Choo et al., 2013). A phase I clinical trial investigated the pharmacokinetics, efficacy and safety of cobimetinib in patients with advance solid tumour (Rosen et al., 2016). Cobimetinib demonstrated durable response with tolerable adverse events. The most common adverse events were diarrhoea, rash, fatigue, nausea, vomiting and edema (Rosen et al., 2016). In phase III clinical trial, combination of cobimetinib with vemurafenib showed greater therapeutic efficacy with prolong PFS (12.3 months vs 7.2 months) compared to vemurafenib monotherapy in BRAF mutant melanoma (Ascierto et al., 2016). This has led to the approval of combination treatment of cobimetinib and vemurafenib by FDA in 2015.

1.9.3. Binimetinib

Binimetinib is highly selective, potent, ATP-noncompetitive, allosteric inhibitor of MEK 1/2 (Bendell et al., 2017; Watanabe et al., 2016). Binimetinib alone demonstrated potent anti-tumour activity in preclinical model of various cancer (Lee, Wallace, et al., 2010). A phase II study evaluated the therapeutic efficacy and safety of binimetinib in advanced melanoma patients harbouring NRAS or BRAF mutation (Ascierto et al., 2013). Binimetinib showed anti-tumour activity in patients with NRAS or BRAF mutation. The most frequent adverse events were acneiform dermatitis, rash, facial oedema, diarrhoea (Ascierto et al., 2013). A phase III clinical trial compared the binimetinib monotherapy with dacarbazine. Binimetinib demonstrated greater efficacy with improved PFS compared to dacarbazine (Dummer et al., 2017).

Among various MEK inhibitor available, in this thesis, selumetinib was selected for the combination with crizotinib. The detail information of selumetinib is given in following section 1.10.

1.10.Selumetinib

Selumetinib (AZD6244: ARRY-142866) is chemically described as 6-(4-bromo-2-chloroanilino)-7-fluoro-N-(2-hydroxyethoxy)-3-methylbenzimidazole-5-carboxamide and has the molecular formula $C17H15BrClFN_4O_3$ and molecular weight of 457.681403 g/mol (Figure 1.7). It is an orally available, potent, non-ATP competitive inhibitor of marker extraction kernel 1/2 (MEK 1/2) that can effectively suppress RAS/MAPK pathway. Selumetinib is highly selective for MEK1/2 compared to more than 40 other kinases at a concentration of 10 µmol/L. It inhibits the enzymatic kinase activity of purified constitutively active MEK1 with an IC_{50} of 14 µmol/L. (Yeh et al., 2007). Binding of selumetinib to the allosteric-inhibitor binding site in MEK1/2 induces conformational changes that inhibit the catalytic activity of MEK, resulting in an inhibition of ERK phosphorylation and its downstream signalling (Davies et al., 2007; Yeh et al., 2007).

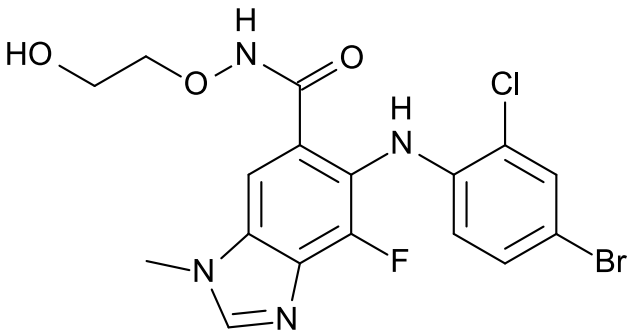

Figure 1.7 Chemical structure of selumetinib. (Figure is obtained from Wikipedia licensed under Creative Commons CC0 1.0 Universal Public Domain Dedication)

1.10.1. Pharmacokinetics

The MTD of selumetinib free base suspension and hydrogen sulphate capsule is 100 mg BID and 75 mg BID, respectively (Adjei et al., 2008; Banerji et al., 2010). After the administration of a single dose of free-base suspension, the median terminal half-life ($t_{1/2}$) was 8 h (Adjei et al., 2008). Similarly, after the administration of a single dose of hydrogen sulphate capsule, the C_{max} was reached after 1-1.6 h with a mean $t_{1/2}$ of 5-8 h. The total body clearance (CL/F)

and volume of distribution at steady state (Vss/F) were consistent across the range of doses, with mean values of 12-23.1 h and 87-126.1 L, respectively. Furthermore, the comparison of pharmacokinetics (PKs) of two formulations demonstrated significantly higher maximum plasma concentration (1316 ng/ml vs. 523 ng/mL) and AUC over 24 h (4454 ng/mL/h vs. 2260 ng/mL/h) of hydrogen sulphate capsule compared to freebase solutions (Banerji et al., 2010). The administration of selumetinib with food decreased the Cmax and AUC by 62% and 19%, respectively, compared with fasting. In the presence of food, the rate of absorption of selumetinib was delayed by approximately 2.5 h. Therefore, selumetinib is recommended to be taken on an empty stomach (Leijen et al., 2011).

In vitro studies showed that selumetinib may be metabolised via CYP enzymes and uridine diphosphate glucuronosyltransferase (UGT) (Dymond et al., 2016; Dymond et al., 2017). Leijen et al. reported that selumetinib is metabolised in the liver through CYP1A2, CYP2C19 and CYP3A4 (Leijen et al., 2011). Thus, coadministration of selumetinib with potent CYP3A4/CYP2C19 inducers or inhibitors may alter the plasma concentration of selumetinib (Dymond et al., 2017). Selumetinib is likely to be eliminated through glucuronidation as the majority of selumetinib metabolites were detected as glucuronide conjugates (Leijen et al., 2011). Selumetinib and its metabolites are predominantly excreted from faeces route (59%) and moderately eliminated in the urine (33%) (Dymond et al., 2016).

1.10.2. Preclinical studies

Selumetinib causes inhibition of cellular growth in various cancer cells including NSCLC, colorectal, pancreatic and melanoma (Davies et al., 2007; Yeh et al., 2007). Yeh et al. reported that selumetinib was highly potent in cell lines harbouring activating RAS and B-Raf mutations. However, it had minimal effect on Malme-3M cell line (control cell line to melanoma), suggesting that inhibition of cell growth is not due to general cytotoxicity (Yeh et al., 2007). Furthermore, selumetinib suppressed tumour growth in an *in vivo* xenograft model of BRAF

and KRAS mutation. It exhibited potent anti-tumour activity through inhibition of cell proliferation and induction of apoptosis (Davies et al., 2007; Meng, Dai, et al., 2010). The activity of selumetinib was highly enhanced when combined with targeted agents such as AKT, mTOR and VEGFR inhibitors, EGFR inhibitors and chemotherapy drugs such as docetexal, temozolomide (Haass et al., 2008; Holt, Logie, Davies, et al., 2012; Holt, Logie, Odedra, et al., 2012; Meng, Dai, et al., 2010; Takahashi et al., 2012). Most of these combinations resulted in synergistic inhibition of tumour growth in preclinical *in vivo* studies.

1.10.3. Clinical Studies

Based on the promising activity of selumetinib in preclinical models, several clinical studies have been performed in patients with advanced cancer to evaluate the efficacy of selumetinib as a monotherapy or in combination with cytotoxic agents such as docetaxel and targeted agents such as VEGFR, EGFR inhibitors.

1.10.3.1. Phase I trials

Two phase I studies were performed to evaluate tolerability, PKs, pharmacodynamics (PDs) of selumetinib (formulated as free base suspension and hydrogen sulphate capsule) in patients with advanced cancer (Adjei et al., 2008; Banerji et al., 2010). The MTD for selumetinib free base suspension was 200 mg BID, but a lower dose level (100 mg BID) was recommended for phase II trials due to the presence of a dose-dependent increase in the frequency and severity of rash. The most frequent and dose-limiting toxicity was rash, occurring in almost 74% of all patients. Other most common adverse events were grade 1-2 diarrhoea, nausea, fatigue and grade 3-4 oedema and elevation of ALT (Adjei et al., 2008). The adverse events were mostly dose dependent and was resolved after dose interruption or reduction (Adjei et al., 2008; Banerji et al., 2010). The MTD for selumetinib formulated as hydrogen sulphate capsule was 75 mg BID. The toxicity profile was similar to that observed with the free-base suspension of

selumetinib. The most common toxicities included fatigue, acneiform, nausea, dermatitis, diarrhoea, peripheral oedema (Banerji et al., 2010).

Phase I trial evaluated the safety, tolerability, PKs and MTD of selumetinib in combination with docetaxel 75 mg/m^2 iv or dacarbazine 1000 mg/m^2 iv administered every 21 days in patients with advanced solid tumours. The MTD of selumetinib in combination with docetaxel or dacarbazine was 75 mg BID. The common adverse events were peripheral oedema, diarrhoea, fatigue, nausea, vomiting (LoRusso et al., 2017). Furthermore, phase I trials investigated the combination of selumetinib with targeted agents such as vandetanib (dual EGFR and VEGFR inhibitor), gefitinib, erlotinib (EGFR inhibitor), temsirolimus (mTOR inhibitor) (ClinicalTrials.gov National Library of Medicine (US), 2012, 2013; Infante et al., 2017). The main aims were to determine the safety, toxicity and PKs profile of these combinations and establish the MTD. The MTD of selumetinib in combination with vandetanib was 100 mg OD or 50 mg BID. (Saka et al., 2015). The MTD of selumetinib recommended in combination with erlotinib 100 mg od was 100 mg and with temsirolimus 25 mg once weekly was 50 mg BID. The combinations had overlapping toxicities, but PK profile was similar to monotherapy (Infante et al., 2017).

1.10.3.2. Phase II trials

In a phase II trial, efficacy of selumetinib was evaluated over pemetrexed as a second- or third-line treatment in patients with advanced NSCLC. 84 patients were randomised to receive selumetinib 100 mg oral free-based suspension BID or pemetrexed 500 mg/m^2 every 3 weeks. This study failed to show the superiority of selumetinib monotherapy over pemetrexed with mPFS of 67 and 90 days, respectively. Disease progressions were observed in 28 (70%) and 26 (59%) patients in the selumetinib and pemetrexed groups, respectively (Hainsworth et al., 2010).

A multicentre phase II trial evaluated the efficacy and safety of selumetinib in combination with docetaxel in previously treated advanced KRAS-mutant NSCLC patients. 87 patients were randomised in 1:1 ratio to receive docetaxel 75

mg/m^2 iv. every 21 days in combination with either selumetinib hydrogen-sulphate capsules 75 mg BID (n=44) or placebo (n=43). The selumetinib treatment group had improvement in median OS (9.4 vs. 5.2 months), mPFS (5.3 vs. 2.1 months), ORR (37% vs. 0%) compared to placebo. The adverse events were more common in the selumetinib group that included grade 3-4 neutropenia, febrile neutropenia and asthenia (Janne et al., 2013).

The clinical efficacy of the combination of selumetinib and erlotinib was investigated in randomised phase II trial. Patients (n=89) were divided into two groups based on the presence of KRAS mutation. The combination failed to show improvement in ORR or PFS compared to selumetinib monotherapy in both groups. Furthermore, combination treatment increased toxicities, thereby suggesting the requirement of dose reduction (Carter et al., 2016).

1.10.3.3. Phase III trials

A randomised, double blinded phase III trial (SELECT-1) was conducted to assess the safety and efficacy of selumetinib plus docetaxel compared with docetaxel alone as a second line treatment in advanced NSCLC bearing KRAS mutation. The primary end point was PFS and secondary end points were ORR, OS, duration of response and safety and tolerability. The combination of selumetinib and docetaxel failed to meet the primary end point with no significant difference in PFS between combination and docetaxel group (3.9 vs. 2.8 months, respectively). The median OS was 8.7 months with the combination and 7.9 months with docetaxel alone. ORR was slightly higher in the combination group (20.1%) compared to docetaxel (13.7%). Furthermore, adverse events of grade 3 or higher were more common with combination (67%) than docetaxel (45%) (Janne et al., 2017).

1.11.Hypothesis and Aims

1.11.1. Hypothesis

1. The combination of crizotinib and selumetinib will produce improved efficacy in both crizotinib naïve and crizotinib resistant ALK-positive NSCLC cells.
2. The combination treatment will suppress the major downstream RAS/MAPK signalling pathway.
3. The combination treatment will reduce tumour growth by induction of apoptosis and inhibition of proliferation.
4. Administration of crizotinib and selumetinib will be safe *in vivo* with no drug interaction.
5. An orthotopic model of lung cancer can be developed via tail vein injection of ALK-positive NSCLC cells (H3122).

1.11.2. Aims

1. To investigate the effect of crizotinib or selumetinib and their combination treatment in crizotinib naïve and crizotinib resistant ALK-positive NSCLC cell lines.
2. To examine potential molecular mechanism behind the synergistic effect of crizotinib and selumetinib combination treatment.
3. To examine the efficacy of crizotinib and selumetinib combination treatment in a xenograft model of ALK-positive NSCLC.
4. To evaluate the preclinical toxicity of crizotinib and selumetinib combination therapy in male Balb/c mice.
5. To establish an orthotopic lung cancer model in male immunocompromised SCID mice.

Chapter 2: Exploring the anti-cancer activity of crizotinib and selumetinib combination treatment and its underlying mechanism of suppression of cell proliferation in ALK-positive NSCLC cells

This chapter is based on the following peer-reviewed publication:

Shrestha N, Nimick M, Dass P, Rosengren R, Ashton J. Mechanisms of suppression of cell growth by dual inhibition of ALK and MEK in ALK-positive non-small cell lung cancer. Scientific Reports 9, 18842 (2019). https://doi.org/10.1038/s41598-019-55376-4

J.A, R.R, N.S contributed on experimental design, N.S carried out experiments and data analysis M.N trained N.S in lab techniques, P.D contributed PCR and DNA sequencing.

2.1. Introduction

Crizotinib is a first generation ALK-TKI that demonstrated superiority over standard chemotherapy, with longer progression free survival and a higher objective response rate (Solomon, Mok, et al., 2014). Crizotinib has been rapidly followed by second and third generation ALK inhibitors such as ceritinib, alectinib, brigatinib and lorlatinib (Lin et al., 2017). Despite the marked anti-tumour activity of crizotinib and other ALK inhibitors, cancer drug resistance develops typically within a few years of treatment.

Mechanisms of resistance to crizotinib involve the alteration of the target gene itself either by mutation or amplification, and activation of bypass signalling pathways (Choi et al., 2010; Doebele et al., 2012; Heuckmann et al., 2011; Hrustanovic et al., 2015; Katayama et al., 2012; Sasaki et al., 2011; Tanizaki, Okamoto, Okabe, et al., 2012; Zhang, Wang, et al., 2011) . Some mediators in these signalling pathways are druggable targets and have been under investigation for combination drug treatment. Upfront combination drug treatment of several targets has been argued as one strategy to delay or overcome drug resistance (Crystal et al., 2014; Zhou & Cox, 2015). Bozic et al. have argued that the probability of a combination being curative increases if the mutation of the locations in the genome that confer resistance to the combination decreases (Bozic & Nowak, 2016; Bozic et al., 2013). Following this, the drug targets was termed "independent" if mutations that provide resistance to drugs against one target in a combination do not necessarily cause resistance to drugs against the other target(s).

ALK overexpression and constitutive activation is unique to ALK-positive NSCLC cells; thus, with a highly specific first target established, the search for secondary targets is facilitated. One strategy to this search is to investigate mediators of bypass signalling pathways as co-targets for combination with ALK inhibitors. These include RTKs such as EGFR, IGFR, HER2 and cKIT, or mutation in EGFR or KRAS. These can regulate downstream signalling independently, promoting the growth and survival of cells irrespective of ALK inhibition

(Hrustanovic et al., 2015; Katayama et al., 2012; Lovly et al., 2014; Sasaki et al., 2011; Tanizaki, Okamoto, Okabe, et al., 2012). Promisingly, Hrustanovic et al. have demonstrated *in vitro* and *in vivo* that targeting MEK together with ALK in cancer cells harbouring EML4-ALK is highly effective at suppressing cell proliferation compared to inhibition of either target alone (Hrustanovic et al., 2015). Upfront combination of ALK and MEK inhibition has improved the response in a preclinical model of EML4-ALK NSCLC, and in a patient-derived acquired resistant cellular model of EML4-ALK (Crystal et al., 2014).

In this study, the dual inhibition of ALK and MEK was further investigated in ALK-positive NSCLC. Selumetinib, a potent, non-ATP competitive inhibitor of marker extraction kernel 1/2 (MEK1/2), was selected as a co-target for the upfront combination. Selumetinib inhibits the phosphorylation of MEK and downregulates the RAS/MAPK signalling pathway (Yeh et al., 2007). It has demonstrated potent anti-tumour activity in preclinical and clinical trials of various cancers including NSCLC (Davies et al., 2007; Garon et al., 2010; Hainsworth et al., 2010).

Furthermore, the ALK-positive NSCLC cell line (H3122) was used in this study to explore the effect of combination and its underlying mechanism of inhibition of cancer cell proliferation. H3122 cells were derived from the pleural fluid of a 54-year-old female patient with stage IV adenocarcinoma (Fujishita et al., 2003). Various ALK-positive NSCLC cell lines such as H3122, STE-1, DFCI032 and H2228 cells are available (Koivunen et al., 2008; Lovly et al., 2014). H3122, DFCI032 and STE-1 cells harbour EML4-ALK E13:A20 (variant 1) resulting from the fusion of exon 13 of EML4 and 20 of ALK. Whereas H2228 cells harbour EML4-ALK E6a/b: A20 (variant 3) resulting from the fusion of exon 6 of EML4 with exon 20 of ALK (Koivunen et al., 2008; Lovly et al., 2014). H3122 cells were chosen in this study as they harbour EML4-ALK variant 1 that is commonly expressed in NSCLC (Cha et al., 2016; Koivunen et al., 2008; Sabir et al., 2017; Yoshida et al., 3383). H3122 cells are highly sensitive to ALK inhibitor (particularly to crizotinib) and are clinically relevant to human treatment (Cha et al., 2016; Sabir et al., 2017; Yoshida et al., 3383).

2.2. Aims and objectives

The aims of this chapter were (1) to explore if the combination of ALK/MEK inhibition is consistent with "independent" drug action as described above, (2) to investigate whether the development of ALK-inhibitor resistance leads to cross-resistance to MEK inhibition, (3) to examine whether the combined drug action was greater than that predicted by a Loewe model – a model for measuring the effect of drug combinations, (4) to explore the molecular mechanism behind the superiority of combination over single-drug treatment.

The specific objectives were: (1) to determine the effect of crizotinib and selumetinib single drug treatment on cell viability of ALK-negative (A549), crizotinib naive (H3122) and crizotinib resistant (CR-H3122) ALK-positive NSCLC cell lines, (2) to examine the combined effect of crizotinib and selumetinib on cell viability of A549, H3122 and CR-H3122 cell lines, (3) to determine the effect of the combination on downstream RAS/MAPK signalling pathway, (4) to evaluate the effect of the combination on cell cycle phases and mode of cell death, (5) to determine the effect of the combination on the endogenous expression of proteins involved in cell cycle and apoptosis.

2.3. Methods and Materials

2.3.1. Materials

2.3.1.1. Chemical reagents

Crizotinib and selumetinib were purchased from LC laboratories (Woburn, MA, USA). Bovine serum albumin (BSA), Foetal bovine serum (FBS), penicillin/streptomycin, Rosswell park memorial institute medium (RPMI), TrypLE Express were purchased from Life Technologies (Auckland, New Zealand). Acrylamide (1:30) and precision plus protein kaleidoscope were obtained from Bio-Rad Laboratories (Hercules, CA, USA). CL-XPosure film, supersignal west pico were obtained from Thermo Fisher Scientific (Auckland, New Zealand). Acetic acid, ammonium persulphate, bicinchoninic acid (BCA) solution, bromophenol blue, citric acid, copper sulphate (CuSO4), Ethylenediaminetetraacetic acid (EDTA), 4-(2-hydroxyethyl)-1-piperazineethanesulfonic acid (HEPES), nonidet P-40 (NP-40), phenylmethanesulfonyl fluoride (PMSF), phosphate buffered saline (PBS), ponceau red stain, propidium iodide (PI), sodium dodecyl sulphate (SDS), sodium bicarbonate (NaHCO3), sodium chloride (NaCl), sodium orthovanadate (Na3VO4), tetrasodium pyrophosphate ($Na_4P_2O_7$), sodium fluoride (NAF), sodium hydroxide (NaOH), sulforhodamine B (SRB), trizma base, trizma hydrochloride (Tris-HCL), triton-x 100, N,N,N,N-tetramethyethylene diamine (TEMED), hydrochloric acid (HCl), dimethyl sulfoxide (DMSO), and Propidium iodide were purchased from Sigma- Aldrich (St Louis, MO, USA). FxCycle PI/RNase was from Life Technologies (Carlsbad, CA, USA). Annexin V-APC and Ac-DEVD-AFC caspase-3 fluorogenic substrate were purchased from BD Biosciences (San Jose, CA, USA). Trichloroacetic acid (TCA) was purchased from Global Science (Auckland, New Zealand). Glycine and polyoxyethylene (20) sorbitan monolaurate were from Calbiochem (San Diego, CA, USA). Polyvinylidene fluoride (PVDF) membrane was purchased from Millipore Corporation (Ramona, CA, USA). Milk powder was purchased from Pam's product limited (Auckland, New Zealand).

2.3.1.2. Antibodies

Antibodies against ALK (D5F3), p-ALK (Tyr1604), p-ERK, Bcl2, Bim, PARP, cleaved PARP, caspase-3, cleaved caspase-3, cyclinD1, P27 were purchased from Cell Signaling Technology (Danvers, MA, USA). Erk1/2, β-tubulin were obtained from Sigma Aldrich (St Louis, MO, USA). HRP-conjugated goat anti-rabbit and HRP-conjugated goat anti-mouse were obtained from Calbiochem (San Diego, CA, US).

2.3.2. Methods

2.3.2.1. Cell culture

The human adenocarcinoma ALK-positive non-small cell lung cancer (H3122) cell line harbouring EML4-ALK variant 1 fusion gene was gifted from Professor Daniel Costa, Harvard University. Human adenocarcinoma non-small cell lung cancer cell line (A549) harbouring K-RAS gene codon 12-point mutation was kindly provided by Dr Gregory Giles, University of Otago. Crizotinib-resistant ALK-positive non-small cell lung cancer (CR-H3122) cells were generated as described in Wilson et al. (Wilson et al., 2017). Briefly, H3122 cells were cultured with increasing concentrations of crizotinib starting from 0.4 μM for 24 h followed by 0.56 μM for the next 24 h. Cells were then maintained in 0.80 μM from the 3rd day to 4 months. The Media was changed every 2-3 days supplemented with crizotinib (0.80 μM), 10% foetal bovine serum (FBS), penicillin (100 U/mL), streptomycin (100 μg/mL). H3122 and A549 cells were maintained in Rosswell Park Memorial Institute medium (RPMI) supplemented with penicillin (100 U/mL), streptomycin (100 μg/mL) and 5% and 2% of FBS, respectively.

Cells were cultured in 75 cm^2 culture flask and incubated at 37° C, 5% CO_2, 95% humidified air. Cells were passaged under the aseptic condition when 90% confluency was reached. Cells were washed with 5 ml of isotonic phosphate buffered saline (1x PBS) solution twice and then incubated with trypsin solution (2.69 mM EDTA, 1g/L trypsin, 0.14 M NaCl, 76.78 mM Tris HCl; pH 8) for 2-3 minutes such that all the cells were detached from the flask. An equal volume of

media was added to the flask and cells were collected and transferred into a 50 ml conical tube. This was followed by centrifugation at 1200 rpm for 3 mins at 4^{o}C. The supernatant was discarded, and cell pellets were suspended in fresh growth media. All the procedures were performed in a biosafety cabinet to prevent any cross-contamination. Cell count was performed under a microscope by using a haemocytometer and the required number of cells was used for respective experiments.

2.3.2.2. Cell viability assay

H3122, A549, CR-H3122 were seeded in triplicate into a 96 well plate at the concentration of 7×10^3, 4×10^3, and 10×10^3 cells per well, respectively, and were incubated at 37^{o}C, 95% humidified and 5% CO_2 for 24 h. Next, cells were treated with a respective concentration of drug solution made in DMSO and was further incubated for 72 h. Vehicle control cells were treated with 0.1-0.5% of DMSO.

To determine the inhibitory effect of crizotinib, selumetinib, and their combination on cell survival, the sulforhodamine B (SRB) colourimetric assay was performed as described by Skehan et al. (Skehan et al., 1990). Briefly, after 72 h of drug treatment, the media was aspirated, and cells were fixed using 0.5 ml of 10% trichloroacetic acid (TCA) solution. The plates were incubated at 4°C for 30 min followed by washing with distilled water (dH_2O) for 3 times. Next, plates were either air-dried overnight at room temperature or dried in a hot air drier for 45 min. Cells were then stained by adding 0.5 mL of SRB (0.4% of SRB made in 1% acetic acid) and incubated for 10 min at room temperature. SRB binds to basic amino acids residues under mild acidic conditions, thereby giving pink staining to the protein. SRB reagent was aspirated off the plate and remaining unbound SRB stain was removed by washing with 1% acetic acid for three times. The plates were dried in a hot air drier for 45 min followed by addition of 0.1 mL of 10 mM Tris base pH 10.5 and incubation for 10 min at room temperature to allow the solubilization of SRB in Tris solution. The absorbance was read at 510 nm using Spectramax Plus plate reader and data was obtained by SoftMax Pro software. The amount of dye extracted from stained cells is

proportional to the cell mass which can be extrapolated to measure cell number (Orellana & Kasinski, 2016; Vichai & Kirtikara, 2006). The standard calibration curve was used to determine the cell number. The concentration of each drug required to reduce the cell viability by 50% (IC_{50}) was determined by nonlinear regression using Graphpad Prism software. Three independent experiments were performed in triplicate.

2.3.2.3. Western blotting

Cell lysate preparation

H3122 and CR-H3122 cells were seeded in Petri dishes at a density of 2.0 × 10^6 cells per dish and incubated in 5% CO_2, 95% humidified air, 37° C for 24 h. H3122 cells were treated with vehicle (DMSO 0.1%), crizotinib (0.25 μM), selumetinib (7.5 μM) and their combination for 24 h and 48 h. CR-H3122 cells were treated with vehicle (DMSO 0.1%), crizotinib (2.5 μM), selumetinib (7.0 μM) and their combination for 24 h. On the following day, cells were washed with 5 ml of ice-cold 1x PBS (isotonic) for two time and lysed with lysis buffer (50 mM Tris base (pH-7.5), 150 mM NaCl, 1 mM EDTA, 1 mM EGTA, 0.5% NP-40, 0.5% SDS, 1 mM sodium orthovanadate, 2.5 mM sodium pyrophosphate, 10 mM sodium fluoride, 1 mM PMSF, complete protease inhibitor cocktail and phosphatase inhibitor). Cells were scraped with a scraper and then collected in a 1.5 mL Eppendorf tube. Cell lysates were sonicated three times for 7 sec each followed by centrifugation at 14000 rpm for 8 min at 4°C. The supernatant was transferred to a new Eppendorf tube before protein concentration was determined.

Bicinchoninic Acid (BCA) assay

The protein concentration of cell lysates was determined by bicinchoninic acid (BCA) assay as described in Smith et al. (Smith et al., 1985). Briefly, bovine serum albumin protein standard 0.5 mg/mL was used to obtain the standard curve. First, 2 μL of cell lysate of each sample was pipetted into 96 well plates in triplicate. BCA solution (50:1) was prepared freshly by adding 50 volumes of

BCA and 1 volume of 4% copper sulphate pentahydrated ($CuSO_4.5H2O$) solution. BCA solution (200 µL) was added to each well and incubated in dark at 37°C. Absorbance was measured at 562 nm using Biorad Benchmark Plus microplate reader and data was obtained from Microplate Manager Software. A standard curve was used to determine the protein concentration of samples and each sample was normalised to obtain 2 µg/ µL of protein. 4x laemmli sample buffer (62.5 mM Tris HCl, 1% SDS, 10% glycerol, 0.005% bromophenol blue, 355 mM β-mercaptoethanol, pH 6.8) was added to each sample and denatured by boiling at 95°C for 5 min. The samples were frozen at -20°C until required.

Gel electrophoresis

Sodium dodecylsulphate-polyacrylamide gel (SDS-PAGE) electrophoresis was used to separate proteins based on their molecular weight (MW) as described in Laemmli, 1970 (Laemmli, 1970). Different percentage of resolving gel ranging from 10% to 12% (30% acrylamide/bisacrylamide (29:1) solution, 1.5 M lower Tris buffer, pH8.8, 50% glycerol, 10% APS, H_2O, TEMED) and a stacking gel (30% acrylamide/bisacrylamide (29:1) solution, 0.5 M upper Tris buffer, 10% of APS, dH_2O, TEMED) was made depending upon the type of proteins of interest. Samples were defrosted and 20 µL of protein was loaded on each well of gels. Molecular weight protein marker was loaded in each gel to identify the respective proteins based on their molecular weight. Gels were run in Bio-Rad Mini-Protean III apparatus at 80 V in SDS-running buffer (25 mM Tris-base, pH 8.3, 0.192 M glycine, 0.1% (w/v) SDS) for approx. for 20 mins until the protein get migrated to the end of stacking gel. Then, the voltage was increased to 120 V until the protein reached to the bottom of resolving gel.

Transfer and Antibody staining

The proteins were transferred to methanol activated PVDF membrane in transfer buffer (25 mM Tris-base, pH 8.3, 0.192 M glycine and 10% methanol) using Bio-Rad wet transfer system at 100 V for 1.5 h. After the completion of the transfer, membranes were washed with TBS (0.025 mM Tris-base, 0.1 M NaCl,

pH 7.4) and stained with ponceau red for 1 min. Next, membranes were washed with TBST (0.025 mM Tris-base, 0.1 M NaCl, pH 7.4 and 0.5% Tween 20) for 3 times and then incubated in blocking buffer (2 % BSA) for 1 h at room temperature. This was followed by washing the membranes with TBS and incubation with respective primary antibody (2% BSA) overnight at 4°C. The dilution of primary antibody used was – Erk ½ (1:5000), pERK ½ (1:1000), ALK (1:1000), pALK (1:1000), BCl2 (1:1000), Bim (1:1000), p27 (1:1000), cyclinD1 (1:1000), total caspase-3 (1:1000), cleaved caspase-3 (1:1000), total PARP (1:1000), cleaved PARP (1:1000), β-tubulin (1: 2000). After this, membranes were washed in TBST (0.05% Tween 20, 0.025 mM Tris-base, 0.1 M NaCl, pH 7.4) for 5 times (5 min each) and incubated with horseradish-peroxidase conjugated goat anti-mouse or goat anti-rabbit secondary antibody (1: 3000 in 5% non-fat milk in TBST) for 1 h at room temperature. Following incubation, membranes were washed with TBST 5 times (5 min each). Proteins bands were visualised using SuperSignal West Pico Chemiluminescent Substrate and developed in x-ray films using 100 plus Automatic X-ray film processor from ALL-Pro Imaging. The images were scanned using Bio-Rad GS-710 densitometer and densities of each band were quantified using Quantity One software (BioRad). The densities of the respective proteins were normalised to β-tubulin. Three independent experiments were performed.

2.3.2.4. Cell cycle assay

The effect of drug treatment on the different phases of the cell cycle was determined by analysing cellular DNA content by flow cytometer. H3122 (300,000 cells/well) and CR-H3122 (350,000 cells/well) cells were seeded into 6 well plates and incubated for 24 h in 5% CO_2, 95% humidified air at 37° C. H3122 cells were treated with vehicle (DMSO 0.1%), crizotinib (0.25 μM), selumetinib (7.5 μM) and their combination for 24 h and 48 h. CR-H3122 cells were treated with vehicle (DMSO 0.1%), crizotinib (2.5 μM), selumetinib (7.0 μM) and their combination for 24 h and 48 h. Following the incubation period, the cells were washed twice with 1 mL of warmed isotonic PBS. Trypsin (200 μL) was added to

each well and were incubated at 37°C for 4 min to allow the detachment of cells from the base of the wells. Cells were then collected in 15 mL falcon tube with 2 mL of warmed RPMI media and were centrifuged at 2000 rpm for 3 min at 4°C. The supernatant was aspirated, and cell pellets were resuspended in 1 mL of isotonic cold PBS (4°C) and were centrifuged again. The supernatant was removed, and cells pellets were resuspended in 300 µL of PBS and were fixed by adding 600 µL of ice-cold 70% ethanol dropwise while vortexing gently to avoid clumping of cells. The tubes were sealed with paraffin and were stored at 4°C.

Next, the cells were centrifuged at 2000 rpm for 3 min at 4°C. The supernatant was aspirated, and the cell pellets were washed and resuspended in 300 µL of ice-cold isotonic PBS (4°C) and centrifuged. Finally, cell pellets were resuspended in 150 µL of FxCycle PI/RNase staining solution and incubated in the dark for 30 min at room temperature. The samples were transferred to FAC tube and analysed by Gallious BD flow cytometer. The Data obtained was analysed using FlowJo version 10 software. Three independent experiments were performed.

2.3.2.5. Apoptosis assay

The effect of drug treatment on the mode of cell death was determined using propidium iodide/ annexin V staining by fluorescence-activated cell sorting (FACS). H3122 (300,000 cells/well) and CR-H3122 (350,000 cells/well) cells were seeded into 6 well plates and incubated in 5% CO2, 95% humidified air for 24 h at 37°C. H3122 cells were treated with vehicle (DMSO 0.1%), crizotinib (0.25 µM), selumetinib (7.5 µM) and their combination for 24 h, 48 h and 72 h. CR-H3122 cells were treated with vehicle (DMSO 0.1%), crizotinib (2.5 µM), selumetinib (7.0 µM) and their combination for 24 h and 48 h. After the incubation period, cells were washed with warm isotonic PBS (37°C) for two times and incubated with 200 µL of trypsin for 4 min at 37°C allowing the cells to detach from the wells. Cells were then collected in a fresh 15 ml tube with 2 ml of warm media and centrifuged at 2000 rpm for 3 min at 4°C. The supernatant was aspirated, and cell pellets were resuspended and washed with ice-cold

isotonic PBS followed by centrifugation. The supernatant was discarded, and cell pellets were resuspended in 100 µL of binding buffer (10 mM HEPES, 140 mM NaCl, 2.5 mM $CaCl_2$) and transferred to FACS tube. Annexin V-APC (5 µL) was added to each tube containing cells and mixed gently followed by incubation for 15 min in the dark at room temperature. Next, 2.5 µL of 50 µg/mL propidium iodide and 200 µL of the binding solution was added to each tube and was further incubated for 15 min in the dark at room temperature. Finally, the samples were analysed on BD Gallios flow cytometer. Data obtained were analysed using Kaluza analysis Software. Three independent experiments were performed.

2.3.2.6. Ac-DEVD-AMC Caspase-3 activity assay

H3122 (3 × 105 cells/well) and CR-H3122 (3.5 × 105 cells/well) cells were seeded in 6-well culture plates and incubated for 24 h. H3122 cells were treated with vehicle (DMSO 0.1%), crizotinib (0.25 µM), selumetinib (7.5 µM) and their combination for 48 h. CR-H3122 cells were treated with vehicle (DMSO 0.1%), crizotinib (2.5 µM), selumetinib (7.0 µM) and their combination for 24 h. H3122 and CRH3122 cells were treated with 5 µM and 100 µM of cisplatin (positive control), respectively. Following incubation, cells were washed with isotonic PBS 2 times and treated with trypsin for 2-3 mins allowing the cells to detached from the wells. Cells were then collected, washed with isotonic 0.01 M PBS and centrifuged for 5 min at 5000 rpm. The supernatant was discarded, and cell pellets were suspended in 100 µL buffer (100 mM HEPES pH 7.5, 10% sucrose, 0.1% CHAPS and 0.0001%NP-40) supplemented with 1 M dithiothreitol (DTT) and caspase-3 substrate. The mixture was further incubated for 30 min at 37°C. The samples were diluted to 1:5 in a buffer (100 mM HEPES pH 7.5, 10% sucrose, 0.1% CHAPS and 0.0001%NP-40) and the intensity emitted by the Ac-DEVD-AMC caspase-3 fluorogenic substrate was examined using Cary Eclipse fluorescence spectrofluorometer with an excitation wavelength of 380 and emission wavelength range of 400- 500 nm. The assay buffer supplied with DTT was used as the blank. Three independent experiments were performed.

2.3.2.7. Data analysis

Cell viability data were normalised to control and analysed by nonlinear regression model using Graphpad Prism V7 software. Cell cycle and apoptosis data were analysed using a two-way ANOVA coupled with Bonferroni post-hoc test. All other data that did not involve time were analysed using a one-way ANOVA coupled with Bonferroni post-hoc test. All data are presented as the mean ± SEM. $P < 0.05$ was the minimal requirement for a statistically significant difference.

To determine if crizotinib and selumetinib suppress cell proliferation in a manner consistent with independent drug action in both H3122 and CR-H3122 cells, combination treatment data was modelled by calculating the combination index (CI) described by Chou and Talalay using CompuSyn software (Chou & Talalay, 1983). The Chou Talalay CI was calculated using the equation 2.1. CI >1, =1, <1 indicate antagonistic, additive, or synergistic interaction respectively. Commonly used in the study of drug synergy (positive interaction), this approach is derived from the zero-interaction (additivity) model of Loewe. This model is based on the assumption of a shared target for two drugs. Therefore, an effect greater than predicted by Loewe additivity (Chou-Talaly CI < 1) means that the central assumption of the Loewe model is falsified; thus, that the drugs act on separate drug targets.

$$\mathbf{CI} = \frac{\boldsymbol{d_1}}{\boldsymbol{D_1}} + \frac{\boldsymbol{d_2}}{\boldsymbol{D_2}}$$

Equation 2.1 Chou Talalay combination index equation

where, d_1 and d_2 are the concentration of drug 1 and drug 2 that in combination give same response as drug 1 alone (D_1) and drug 2 alone (D_2).

Determining whether drugs that act on separate targets have a positive interaction (synergy) requires a different zero-interaction model (the Bliss model) (Goldoni & Johansson, 2007). The Bliss model assumed that the two or more drugs in the combination will have independent target. Bliss model CI is calculated using equation 2.2. CI >1, =1, <1 indicate antagonistic, additive, or synergistic interaction respectively. This analysis was not carried out since the

aim of this study was to test the synergistic interaction rather than independent drug action.

$$\mathbf{CI} = \frac{\boldsymbol{E_1} + \boldsymbol{E_2} - \boldsymbol{E_1} \cdot \boldsymbol{E_2}}{\boldsymbol{E_{12}}}$$

Equation 2.2 Bliss model combination index equation

where, E_1 is the degree of effect produced by drug 1, E_2 is the degree of effect produced by drug 2, E_{12} is the degree of effect produced by the combination of drug 1 and 2.

2.4. Results

2.4.1. Mechanism of suppression of cell proliferation by the combination treatment in H3122 cell line

2.4.1.1. IC_{50} values following crizotinib and selumetinib single drug treatment

The relative potency of crizotinib and selumetinib single drug treatment was initially examined in H3122 and A549 non-small cell lung cancer cells. Both cell lines were treated with a range of drug concentrations (0.001- 40 μM) for 72 h. H3122 cells were highly sensitive to crizotinib compared to selumetinib, with IC_{50} values of 0.1 ± 0.07 and 3.1 ± 0.65 μM, respectively (Figure 2.1A). Sensitivity to crizotinib by ALK-negative A549 cells was markedly less than for ALK-positive cells with an IC_{50} value of 0.8 ± 0.07μM (Figure 2.1B). IC_{50} value for selumetinib was similar in A549 cells as in H1322 cells, with IC_{50} values of 2.0 ± 0.14 (Figure 2.1B).

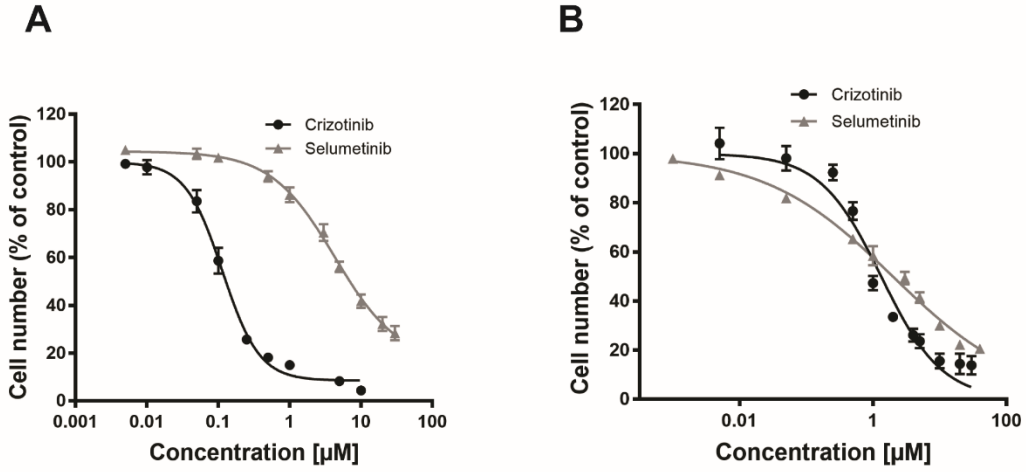

Figure 2.1 Cytotoxicity of crizotinib and selumetinib in non-small cell lung cancer cells. (A) H3122 cells were seeded in 96 wells plates at 7 ×10^3 cells per well and treated with crizotinib (0.001 – 10 μM), selumetinib (0.001 – 30 μM) or vehicle control (0.1% DMSO) for 72 h. (B) A549 cells were seeded in 96 wells plates at 4 ×10^3 cells per wells and treated with crizotinib (0.001 – 30 μM), selumetinib (0.001 – 40 μM) or control (0.1% DMSO) for 72 h. SRB assay was performed. All data are presented as mean ± SEM. Three independent experiments were performed in triplicate. IC_{50} values were determined by non-linear regression analysis.

Table 2.1 Summary of IC_{50} values of crizotinib and selumetinib

Drug	Cell line	IC_{50} (μM) [a]
Crizotinib	H3122	0.1 ± 0.07
Selumetinib	H3122	3.1 ± 0.65
Crizotinib	A549	0.8 ± 0.07
Selumetinib	A549	2.0 ± 0.14

[a] Values are the mean ± SEM

2.4.1.2. The combined effect of crizotinib and selumetinib treatment on cell viability

The effect of crizotinib and selumetinib combination treatment was then investigated in H3122 and A549 cells. Six different combinations were selected using equivalent potencies relative to each drug's IC_{50} value. For each concentration, the two drugs alone were compared with the combination of the two. Chou-Talalay analysis was performed to determine if the two drugs acted with greater than Loewe additivity (Chou & Talalay, 1983). The results showed that 3 out of 6 drug combinations elicited a significant reduction in cell viability compared to both single drug treatments ($p < 0.05$, one-way ANOVA) (Figure 2.2A). Interestingly, all drug combinations showed greater than Loewe additivity (Chou-Talalay Combination index < 1) (Figure 2.2B). Contrary to H3122 cells, the combined effect of crizotinib and selumetinib was solely driven by selumetinib in A549 cells (Figure 2.2C). Only one of the combinations showed a significant decrease in cell viability compared to either single drug treatment ($p < 0.05$, one-way ANOVA) (Figure 2.2C). Furthermore, combination indices showed that all combinations except the higher concentrations were mutually antagonistic (CI > 1) (Figure 2.2D).

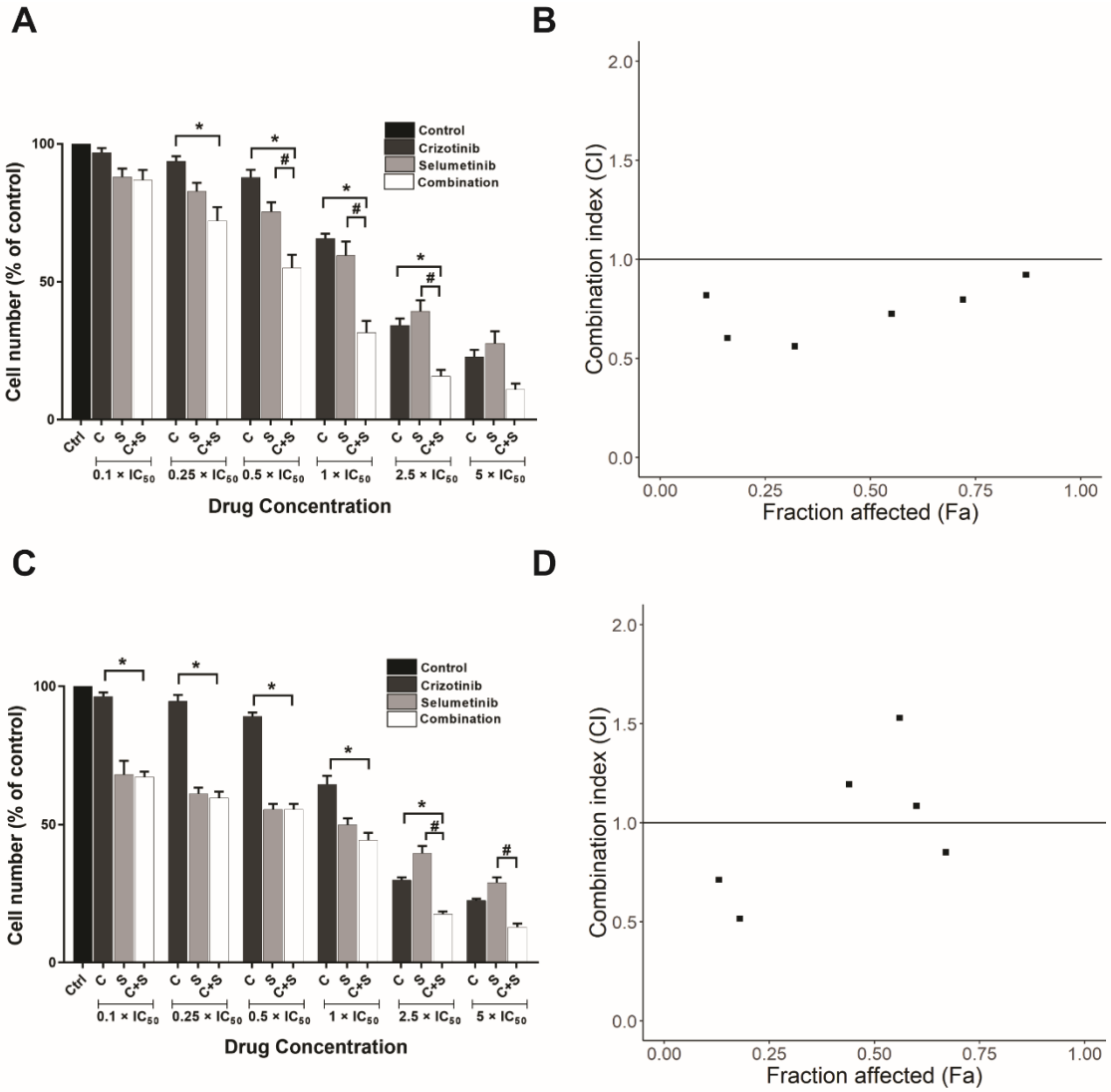

Figure 2.2 Effect of crizotinib, selumetinib and their combination treatment in non-small cell lung cancer. (A) H3122 cells were seeded in 96 well plates at 7 ×10^3 cells per well and (C) A549 cells 4 ×10^3 cells per well and then treated with the indicated concentration of crizotinib, selumetinib and their combinations for 72 h. SRB assay was performed. Bar denotes; ■ DMSO control, ■ crizotinib, ■ selumetinib and □ combination of both. Combination index plot for drug combination in (B) H3122 and (D) A549 cells. The horizontal line represents Loewe additivity. CI > 1, = 1, < 1 indicate antagonistic, additive or synergistic interaction respectively. Bars represent the mean ± SEM. Significance was determined by one-way-ANOVA with a Bonferroni post-hoc test. Three independent experiments were performed in triplicate. *$p < 0.05$ for crizotinib vs. combination and #$p < 0.05$ for selumetinib vs. combination.

2.4.1.3. Effect of combination treatment on downstream signalling pathway

To investigate the mechanisms involved in the suppression of cell proliferation by the combination treatment, key proteins downstream of the RAS/MAPK signalling pathway were examined. Western blotting was performed to determine the activation of ALK and MEK, by measuring the expression of ALK, phosphorylated-ALK (p-ALK), ERK and phosphorylated-ERK (p-ERK). H3122 cells were treated with vehicle control (DMSO 0.1%), crizotinib (0.25 μM), selumetinib (7.5 μM) and their combination for 24 h. After 24 h, p-ALK/ALK was decreased 90% by both crizotinib alone and the combination of crizotinib and selumetinib, whereas there was no change following selumetinib (Figure 2.2B). Additionally, p-ERK/ERK was reduced 64% by crizotinib, 95% by selumetinib, and 99% by the drugs in combination ($p < 0.05$, one-way ANOVA) (Figure 2.3C).

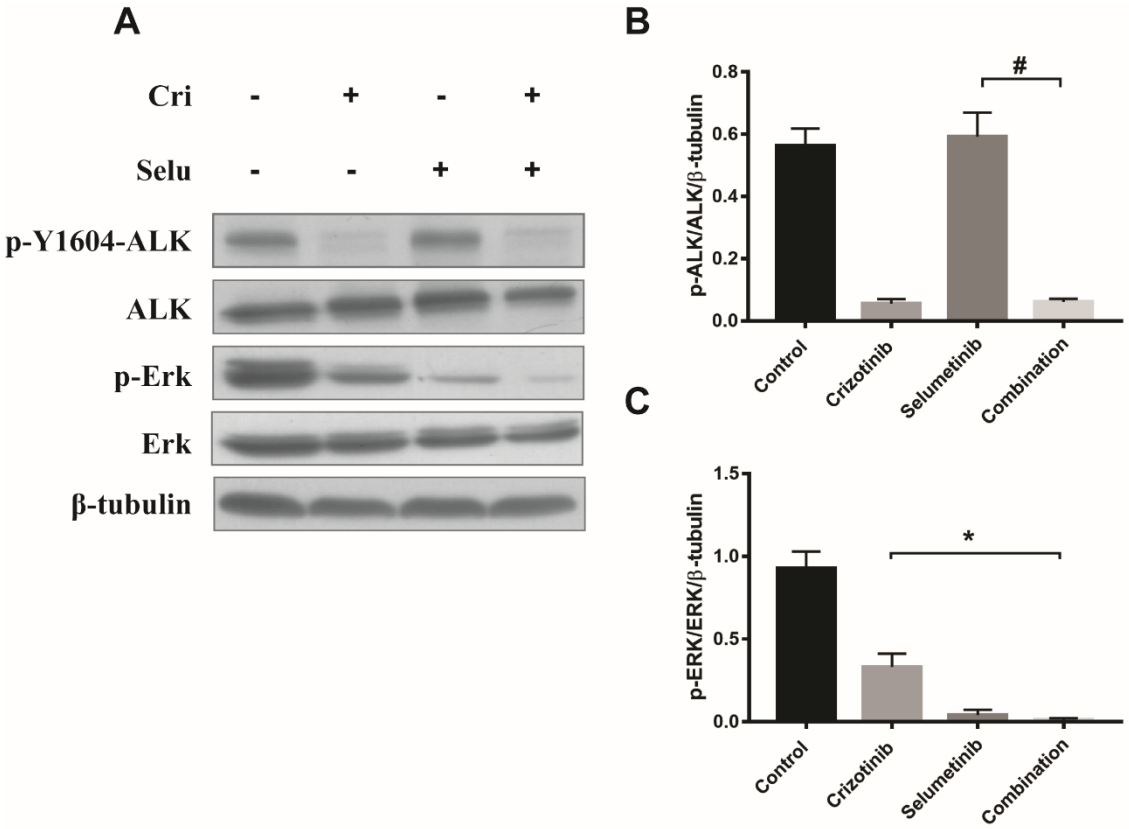

Figure 2.3 Effect of crizotinib, selumetinib and their combination on downstream RAS/MAPK signalling pathways in H3122 cells. (A) Representative Western blots of ALK, p-ALK, ERK, p-ERK. Cells were treated with vehicle control (0.1%DMSO), crizotinib (0.25 μM), selumetinib (7.5 μM) and their combinations for 24 h. Cell lysates were subjected to SDS-PAGE and probed with specific antibodies. Densitometry of Western blots of (B) p-ALK/ALK and (C) p-ERK/ERK. All data are presented as mean ± SEM. Significance was determined by one-way-ANOVA with Bonferroni post-hoc test. Three independent experiments were performed in triplicate. * $p < 0.05$ for crizotinib vs. combination and #$p < 0.05$ for selumetinib vs. combination.

2.4.1.4. Effect of combination on cell cycle progression and cell cycle markers

The impact of combination treatment on cell cycle progression was investigated in H3122 cells. Cells were treated with vehicle control (DMSO 0.1%), crizotinib (0.25 μM), selumetinib (7.5 μM) and their combination for 24 h and 48 h and analysed by flow cytometry with PI staining.

Cell cycle analysis showed that both crizotinib and selumetinib as single drug treatments significantly increased the accumulation of cells in the G1 phase by 10% and 17%, respectively, compared to the control after 24 h ($p < 0.05$, two-way ANOVA), (Figure 2.4A). After 48 h of drug treatment, selumetinib significantly increased the accumulation of cells in the G1 phase compared to the control by 5.5% ($p < 0.05$, two-way ANOVA), while that for crizotinib decreased by 2%. Furthermore, the combination of the two drugs significantly increased the percentage of cells in the G1 phase by 16% and 8%, respectively, compared to crizotinib and selumetinib single drug treatment after 24 h ($p < 0.05$, two-way ANOVA). Following 48 h, the combination significantly increased the percentage of cells in G1 phase compared to crizotinib by 6%, whereas that for the combination treatment decreased by 2% compared to selumetinib.

In contrast, both the crizotinib and selumetinib single drug treatment decreased the percentage of cells in S phase by 3% and 5 %, respectively after 24 h and 0.5% and 3%, respectively after 48 h compared to the control. Moreover, the combination treatment further decreased the percentage of cells in S phase by 5% and 2% after 24 h compared to crizotinib and selumetinib, respectively. While after 48 h, the combination treatment decreased the percentage of cells in S phase by 2% compared to crizotinib only.

Next, the endogenous expression of proteins involved in the G1 to S phase transition such as cyclin D1 and the cyclin dependent kinase inhibitor, p27, were examined using Western blotting. H3122 cells were treated with vehicle control (DMSO 0.1%), crizotinib (0.25 μM), selumetinib (7.5 μM) and their combination for 24 h and the respective proteins were probed using specific antibodies. The expression of cyclin D1 was significantly decreased following crizotinib (62%) and selumetinib (76%) compared to the control ($p < 0.05$, one-way ANOVA).

Furthermore, combination drug treatment significantly decreased the protein expression of cyclin D1 (> 80%) compared to both the single drug treatments ($p < 0.05$, one-way ANOVA) (Figure 2.4C). Furthermore, crizotinib and selumetinib single drug treatment significantly increased the endogenous expression of p27 by 1.1-fold and 3.4-fold, respectively, compared to the control ($p < 0.05$, one-way ANOVA). Similarly, the expression level of p27 was significantly increased by 4.0- and 1.3-fold following combination treatment compared to crizotinib or selumetinib alone ($p < 0.05$, one-way ANOVA) (Figure 2.4E). Hence, selumetinib enhanced the anti-proliferative effect of crizotinib by increasing G1 phase arrest, which resulted from a decrease in cyclin D1 and an increase in p27 expression.

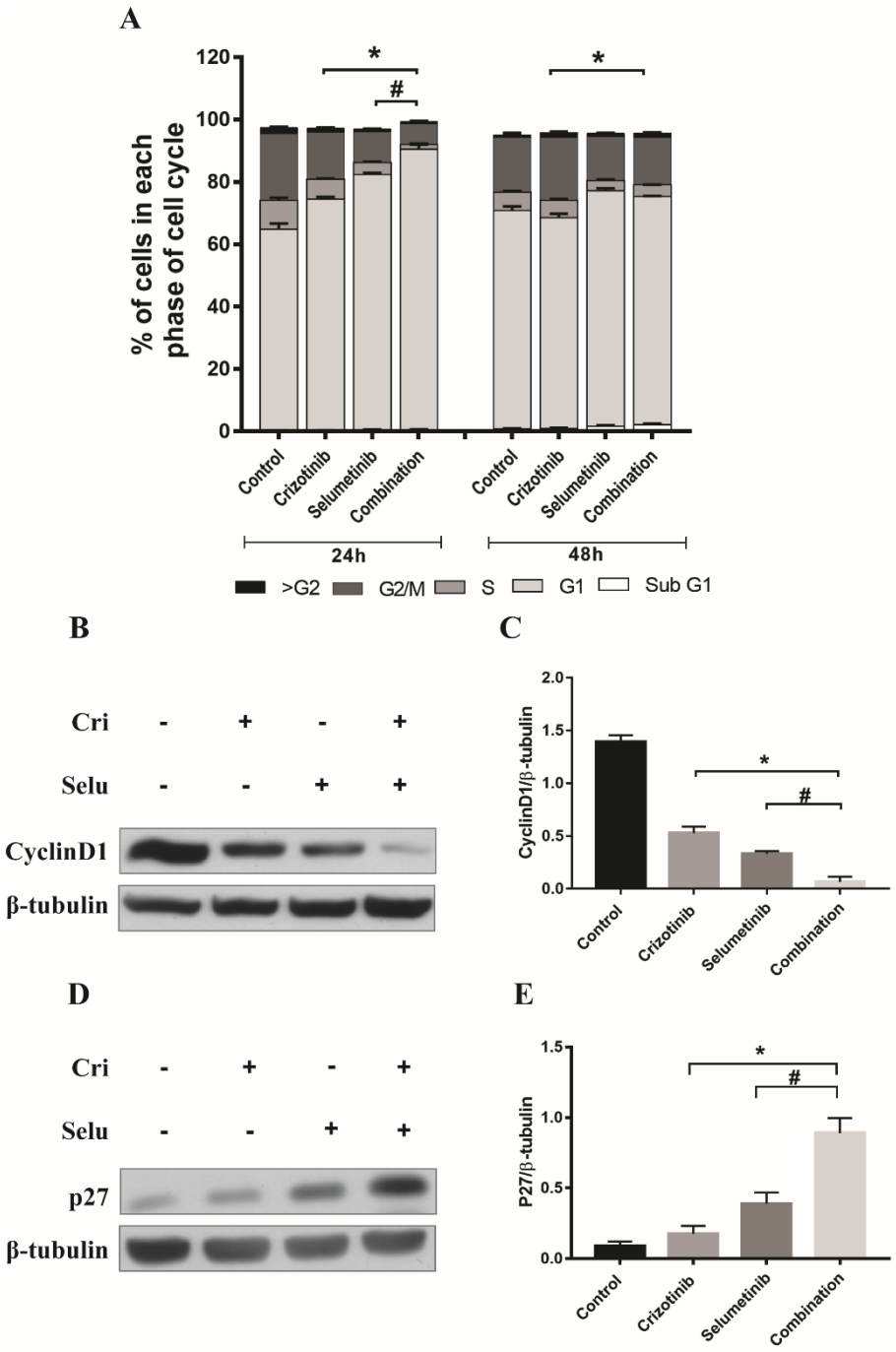

Figure 2.4 Effect of crizotinib, selumetinib and their combination on cell cycle progression and cell cycle markers in H3122 cells. (A) cell cycle progression. Cells were treated with vehicle control (DMSO 0.1%), crizotinib (0.25 μM), selumetinib (7.5 μM) and their combination for 24 h and 48 h. Propidium iodide staining and flow cytometry was used to determine the proportion of cells in different cell cycle phases. Bar denotes; ■ > G2, ■ G2/M, ■ S, ■ G1, □ sub G1. Significance was determined by two-way-ANOVA with Bonferroni post-hoc test. Representative Western blots of (B) cyclinD1 and (D) p27 after 24 h exposure of drugs treatment. Cell lysate were subjected to SDS-PAGE and probed with specific antibodies. Densitometry of Western blots of (C) cyclinD1 and (E) p27. Significance was determined by one-way-ANOVA with Bonferroni post-hoc test. All data are presented as mean ± SEM. Three independent experiments were performed. *$p < 0.05$ for crizotinib vs. combination and #$p < 0.05$ for selumetinib vs. combination.

2.4.1.5. Effect of combination treatment on the induction of apoptosis and apoptotic markers

Crizotinib also exhibits anti-tumour activity via induction of apoptosis (Christensen et al., 2007). Similarly, selumetinib, a potent MEK1/2 inhibitor, downregulates the RAS/MAPK signalling pathway leading to activation of downstream apoptotic signalling (Holt, Logie, Odedra, et al., 2012). Therefore, whether the combination of crizotinib with selumetinib could enhance the induction of apoptosis in H3122 cells was investigated. Cells were treated with vehicle control (DMSO 0.1%), crizotinib (0.25 μM), selumetinib (7.5 μM) and their combination for 24 h, 48 h and 72 h and analysed by flow cytometry with PI and Annexin V staining.

Following drug treatment, apoptosis was initiated at 24 h, reached maximum at 48 h and entered late apoptotic phase at 72 h (Figure 2.5). The percentage of early apoptotic cells was slightly higher with crizotinib and selumetinib single drug treatment (4% and 5 %, respectively, after 24 h), (4% and 7%, respectively, after 48 h) than the control (2% after 24 h and 48 h). Whereas the combination treatment resulted in a significantly higher percentage of early apoptotic cells (9% and 17% after 24 h and 48 h, respectively) compared to either of the single drug treatments ($p < 0.05$, two-way ANOVA) (Figure 2.5).

To determine the drivers of apoptosis, the endogenous expression of key regulators of intrinsic apoptosis such as Bcl2, Bim, caspase-3, cleaved caspase-3, were examined by Western blotting. Cells were treated with vehicle control (DMSO 0.1%), crizotinib (0.25 μM), selumetinib (7.5 μM) and their combination for 24 h and 48 h and the respective proteins were probed using specific antibodies.

There was no change in the endogenous expression of Bcl2 with crizotinib, selumetinib and their combination treatment for 24 h (Figure 2.6B). On the other hand, the endogenous expression of Bim was increased by both crizotinib and selumetinib single-drug treatment compared to the control after 24 h and 48 h (Figure 2.6D). Furthermore, combination treatment significantly increased the endogenous expression of Bim after 24 h and 48 h by 1.5-fold and 3.0-fold,

respectively, compared to crizotinib ($p < 0.05$, one-way ANOVA), whereas there was slight increase (0.3-fold) compared to selumetinib ($p > 0.05$, one-way ANOVA) (Figure 2.6D).

After 24 h of drug treatment, cleaved caspase-3 expression was negligible but was significantly increased after 48 h of combination treatment (Figure 2.7B). This observation is consistent with results from apoptosis assay suggesting that induction of apoptosis was maximal after 48 h of treatment. There was more than 7-fold increase in expression of cleaved caspase-3 following crizotinib and selumetinib single-drug treatment compared to the control. Similarly, combination treatment significantly increased cleaved caspase-3 expression by 3 to 7-fold compared to either drug alone (Figure 2.7B) ($p < 0.05$, one-way ANOVA). To confirm this, caspase-3 activity was determined where a sharp increase was seen after 48 h of treatment with the combination (Figure 2.7C) ($p < 0.05$, one-way ANOVA). This was consistent with the results from Western blotting.

Next, to determine whether the caspase-3 mediate cleavage of PARP, the endogenous expression of PARP and cleaved PARP was examined. Crizotinib and selumetinib alone increased the expression of cleaved PARP by more than 12-fold compared to the control. Moreover, the expression of cleaved PARP was markedly increased by 8 to 26-fold following combination treatment compared to either drug alone ($p < 0.05$, one-way ANOVA) (Figure 2.8B). These results showed that the combination of crizotinib and selumetinib significantly increased apoptosis by increasing the expression of Bim, cleaved caspase-3 and cleaved PARP to a degree that was not reached by crizotinib alone.

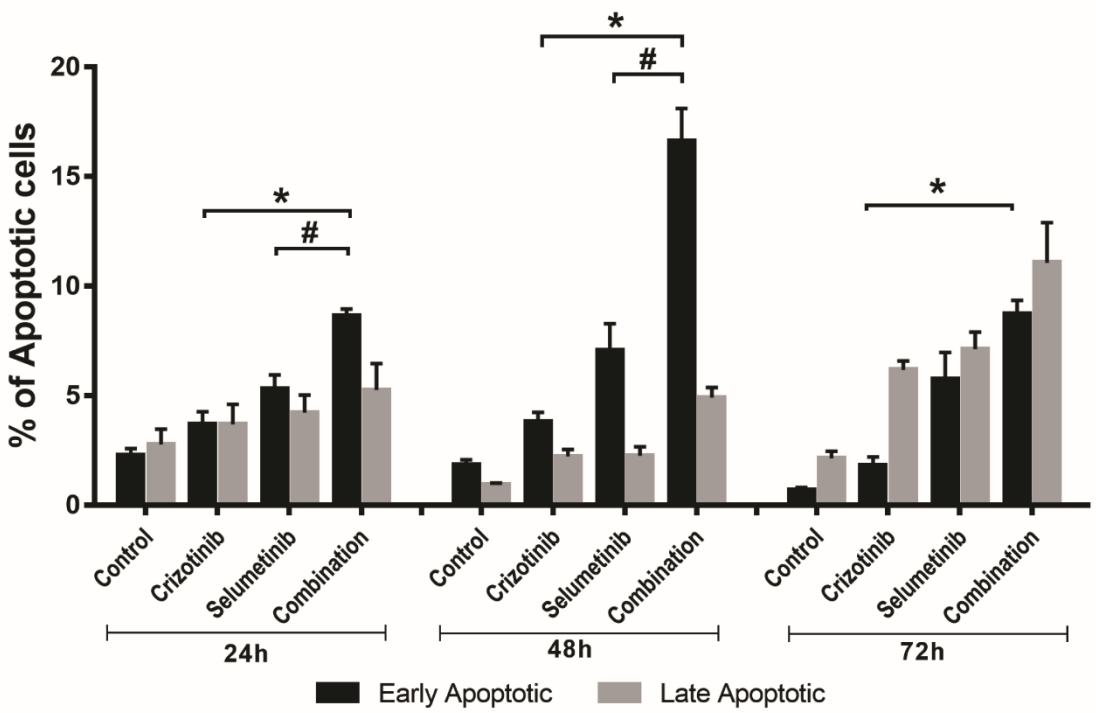

Figure 2.5 Mode of cell death following crizotinib, selumetinib and their combination in H3122 cells. Cells were treated with vehicle control (DMSO 0.1%), crizotinib (0.25 μM), selumetinib (7.5 μM) and their combination for 24 h, 48 h and 72 h. Cells were stained with propidium iodide and Annexin V. The flow cytometry was used to determine the proportion of apoptotic cells. Bar denotes; ■ Early apoptotic, ■ late apoptotic Significance was determined by two-way-ANOVA with Bonferroni post-hoc test. All data are presented as mean ± SEM. Three independent experiments were performed. *$p < 0.05$ for crizotinib vs. combination and #$p < 0.05$ for selumetinib vs. combination.

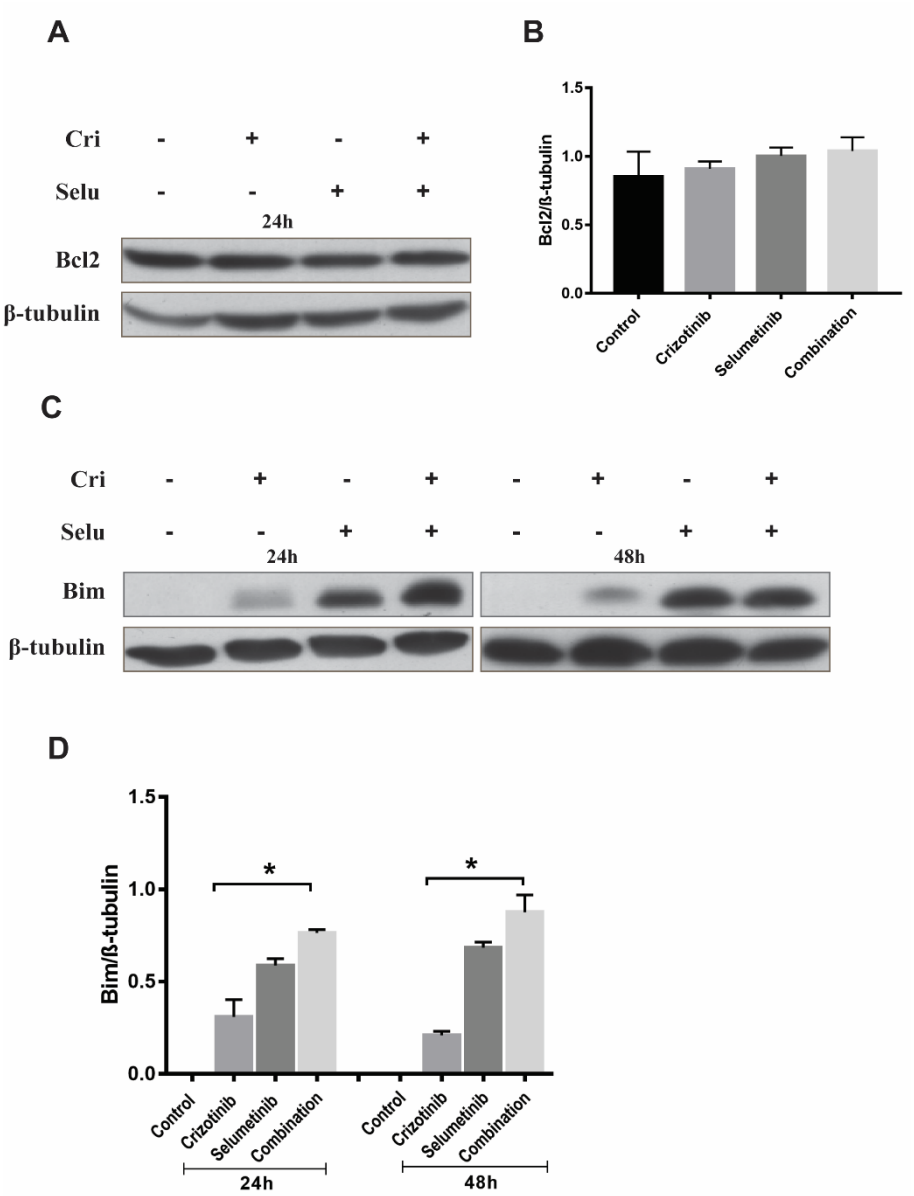

Figure 2.6 Expression of Bcl2 and Bim following treatment with crizotinib, selumetinib and their combinations in H3122 cells. Representative Western blots of (A) Bcl2 and (C) Bim, respectively. Cells were treated with vehicle control (DMSO 0.1%), crizotinib (0.25 μM), selumetinib (7.5 μM) and their combination for the indicated time. Cell lysates were subjected to SDS-PAGE and probed with specific antibodies. Densitometry of Western blots of (B) Bcl2 and (D) Bim. Significance was determined by one-way-ANOVA with Bonferroni post-hoc test. All data are presented as mean ± SEM. Three independent experiments were performed. *$p < 0.05$ for crizotinib vs. combination and #$p < 0.05$ for selumetinib vs. combination.

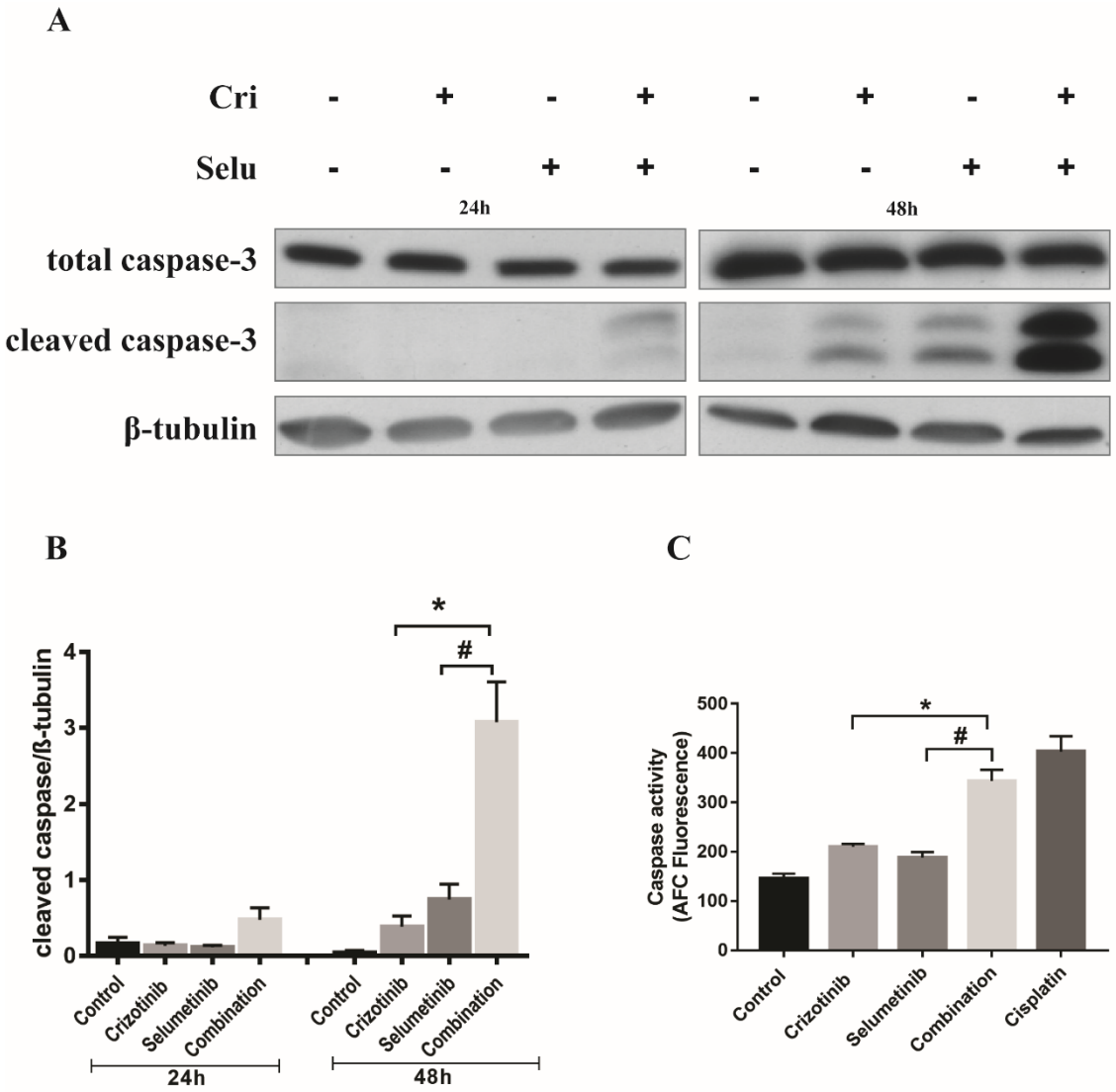

Figure 2.7 Effect of crizotinib, selumetinib and their combination on cleaved caspase-3 in H3122 cells. (A) Representative Western blots total caspase-3 and cleaved caspase-3. Cells were treated with vehicle control (DMSO 0.1%), crizotinib (0.25 μM), selumetinib (7.5 μM) and their combination for 24 h and 48 h. Cell lysates were subjected to SDS-PAGE and probed with specific antibodies. (B) Densitometry of Western blots of cleaved caspase-3. (C) Caspase-3 activity after treatment with the indicated concentration of crizotinib, selumetinib, their combination and cisplatin (positive control) for 48 h. Significance was determined by one-way-ANOVA with Bonferroni post-hoc test. All data are presented as mean ± SEM. Three independent experiments were performed. *$p < 0.05$ for crizotinib vs. combination and #$p < 0.05$ for selumetinib vs. combination

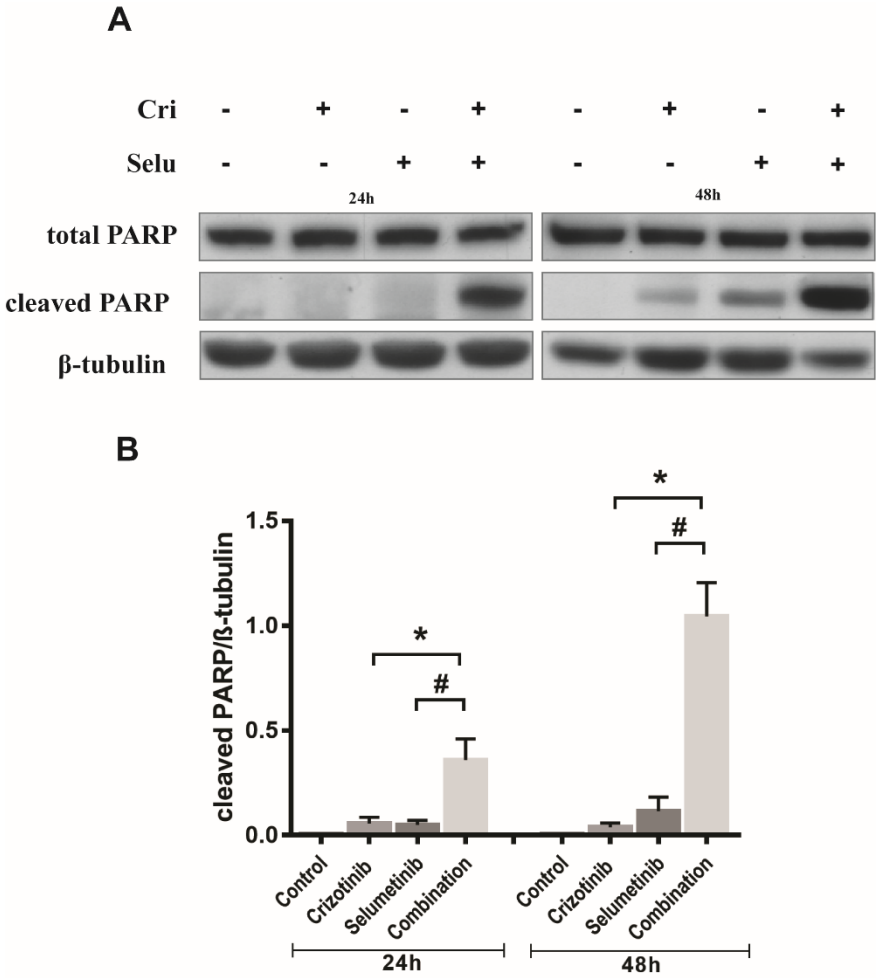

Figure 2.8 Expression of cleaved PARP following treatment with crizotinib, selumetinib and their combination H3122 cells. (A) Representative Western blots total PARP and cleaved PARP. Cells were treated with vehicle control (DMSO 0.1%), crizotinib (0.25 μM), selumetinib (7.5 μM) and their combination for 24 h and 48 h. Cell lysates were subjected to SDS-PAGE and probed with specific antibodies. (B) Densitometry of Western blots of cleaved PARP. Significance was determined by one-way-ANOVA with Bonferroni post-hoc test. All data are presented as mean ± SEM. Three independent experiments were performed. *$p < 0.05$ for crizotinib vs. combination and #$p < 0.05$ for selumetinib vs. combination**.**

2.4.2. Mechanism of suppression of cell proliferation by the combination treatment in CR-H3122 cell line

2.4.2.1. Effect of crizotinib, selumetinib and their combination treatment on cell viability

The anti-proliferative effect of crizotinib and selumetinib single drug treatment was examined in crizotinib resistant ALK-positive NSCLC cells (CR-H3122). CR-H3122 cells were treated with crizotinib (0.005- 40 μM) and selumetinib (0.001- 150 μM) for 72 h. The sensitivity of CR-H3122 cells to crizotinib was highly reduced compared to H3122 cells, with an IC_{50} value of 2.3 ± 0.5 μM (22-fold over the parental H3122 cells). The IC_{50} value for selumetinib was elevated in CR-H1322 cells to 11.1 ± 2.12 μM, a 3-fold increase compared to H3122 (Figure 2.9A). Interestingly, all of the various concentrations of the two drugs in combination significantly suppressed the cell proliferation of CR-H3122 cells compared to single drug treatment ($p < 0.05$, one-way ANOVA) (Figure 2.9B). Interestingly, the combination of crizotinib with selumetinib was highly potent in the resistant cells compared to the parental H3122 cells (Chou-Talalay Combination Indices < 0.3) (Figure 2.9C)

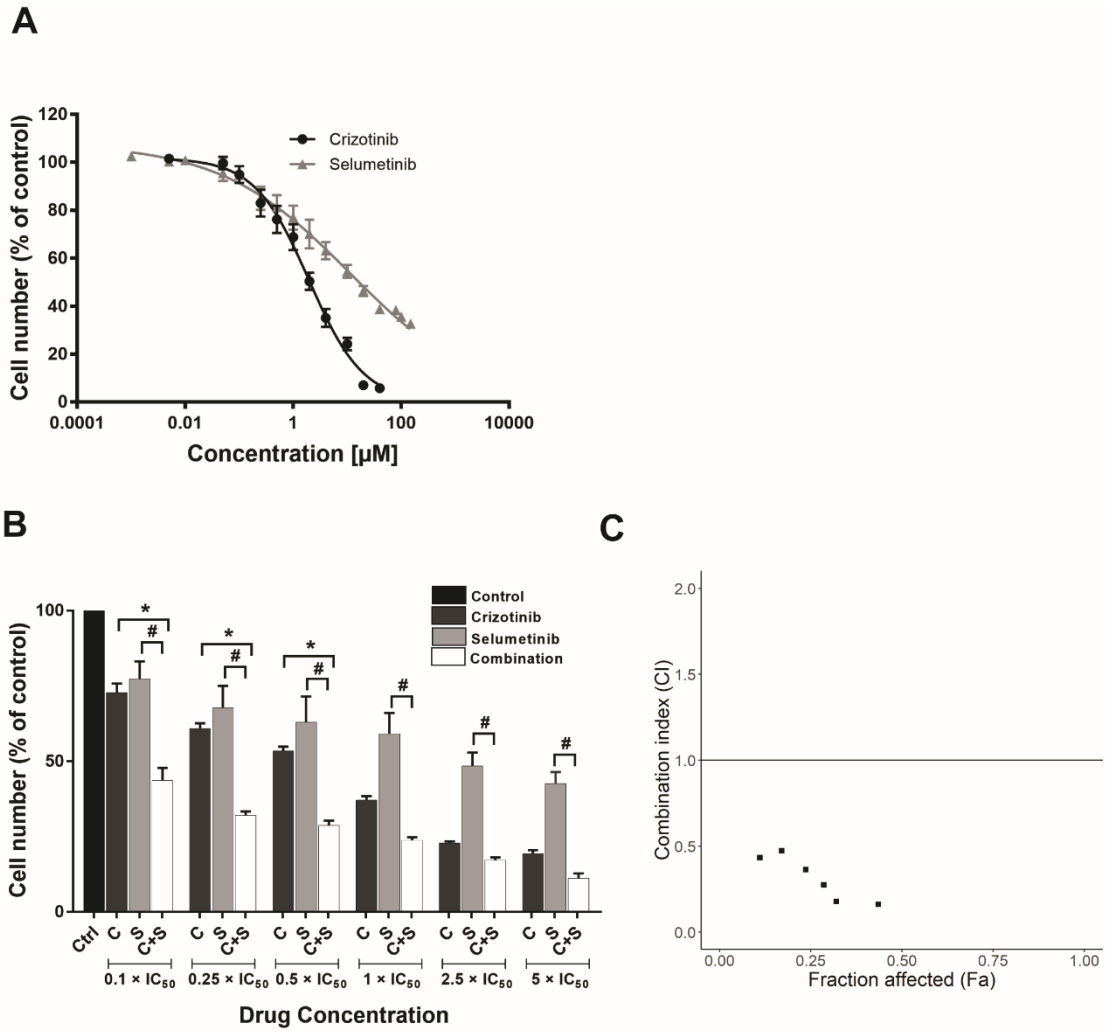

Figure 2.9 Effect of crizotinib, selumetinib and their combination on cell viability of CR-H3122 cells. (A) Crizotinib and selumetinib single drug treatment (B) Combination treatment. Cells were seeded in 96 wells plate at 10 ×10^3 cells per well and treated with the indicated concentration of crizotinib, selumetinib and their combinations for 72 h. SRB assay was performed**.** Bar denotes: ■ DMSO control, ■ crizotinib, ■ selumetinib and □ combination of both. Significance was determined by one-way-ANOVA with Bonferroni post-hoc test. (C) Combination index plot for drug combination of crizotinib and selumetinib. The horizontal line represents Loewe additivity. CI >1, =1, <1 indicate antagonistic, additive or synergistic interaction respectively. All data are presented as mean ± SEM. Three independent experiments were performed in triplicate. *p < 0.05 for crizotinib vs. combination and #p < 0.05 for selumetinib vs. combination.

Table 2.2 IC_{50} values of crizotinib and selumetinib in CR-H3122 cell lines

Drug	Cell line	IC_{50} (μM)[a]
Crizotinib	CR-H3122	2.3 ± 0.5
Selumetinib	CR-H3122	11.1 ± 2.12

[a] Values are the mean ± SEM

2.4.2.2. Effect of combination treatment on downstream signalling pathways

To further evaluate the mechanisms for the drug combination's effects on crizotinib resistant cells, proteins downstream of the RAS/MAPK signalling pathway were examined. CR-H3122 cells were treated with vehicle control (DMSO 0.1%), crizotinib (2.5 μM), selumetinib (7.0 μM) and their combination for 24 h. Crizotinib alone had almost no effect on the phosphorylation of ALK and ERK in CR-H1322 cells, consistent with ALK inhibitor resistance. Nor was there any significant reduction of ALK phosphorylation by the combination (< 43%) compared to either of the single drug treatment ($p > 0.05$, one-way ANOVA) (Figure 2.10B). However, the cells remained sensitive to ERK phosphorylation by selumetinib, with a 93% decrease in pERK/ERK protein expression after 24 h. Moreover, the combination of crizotinib and selumetinib significantly decreased the protein expression of pERK/ERK by 99% ($p < 0.05$, one-way ANOVA).

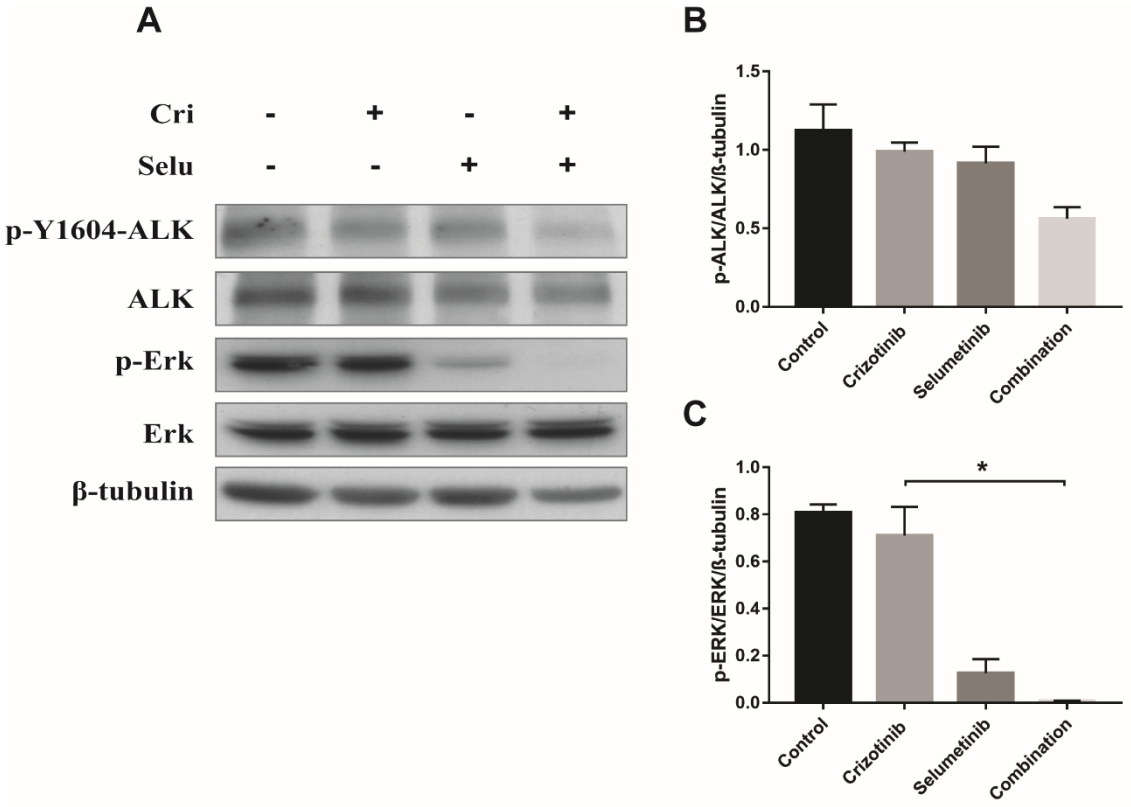

Figure 2.10 Effect of crizotinib, selumetinib and their combination on downstream RAS/MAPK signalling pathways in CR-H3122 cells. (A) Representative Western blots of ALK, p-ALK, ERK, p-ERK. Cells were treated with vehicle control (0.1%DMSO), crizotinib (2.5 μM), selumetinib (7.0 μM) and their combinations for 24 h. Cell lysates were subjected to SDS-PAGE and probed with specific antibodies. Densitometry of Western blots of (B) p-ALK/ALK and (C) p-ERK/ERK. All data are presented as mean ± SEM. Significance was determined by one-way-ANOVA with Bonferroni post-hoc test. Three independent experiments were performed in triplicate. * $p < 0.05$ for crizotinib vs. combination and #$p < 0.05$ for selumetinib vs. combination.

2.4.2.3. Effect of the combination treatment on cell cycle progression and cell cycle markers

To determine the effect of crizotinib, selumetinib and their combination treatment on cell cycle progression of crizotinib resistant cells, cell cycle assay was performed. CR-H3122 cells were treated with vehicle control (DMSO 0.1%), crizotinib (2.5 μM), selumetinib (7.0 μM) and their combination for 24 h and then analysed by flowcytometry with PI staining. Cell cycle analysis showed that after 24 h and 48 h both crizotinib and selumetinib single drug treatment increased the percentage of cells arrested in the G1 phase by more than 4% compared to the control. Furthermore, the combination treatment significantly increased the percentage of cells in G1 phase after 24 h and 48 h by more than 16% compared to crizotinib ($p < 0.05$, two-way ANOVA) (Figure 2.11A). In contrast, the percentage of cells in G1 phase slightly decreased (1.3%) after 24 h followed by a marked increase (6 %) after 48 h with the combination compared to selumetinib (Figure 2.11A). However, both single and combination treatment of crizotinib and selumetinib decreased the percentage of cells arrested in the S phase by more than 2% compared to the control and either of the single drug treatment, respectively (Figure 2.11A).

Next, the expression of cyclin D1 and P27 involved in the transition from G1 to S phase was examined using Western blotting. CR-H3122 cells were treated with vehicle control (DMSO 0.1%), crizotinib (2.5 μM), selumetinib (7.0 μM) and their combination for 24 h and the respective proteins were probed using specific antibodies. The expression of cyclin D1 was decreased with crizotinib (42%) and selumetinib (80%) compared to the control. Moreover, the drug combination decreased cyclin D1 expression by more than 97% compared to either single drug treatment (Figure 2.11C). The single drug treatment of crizotinib and selumetinib significantly increased the expression of p27 by 2.0- and 3.2-fold, respectively, compared to the control. ($p < 0.05$, one-way ANOVA). Similarly, the expression level of p27 was significantly increased by 1.8- and 1.2-fold with the combination treatment compared to crizotinib or selumetinib alone ($p < 0.05$, one-way ANOVA) (Figure 2.11E)

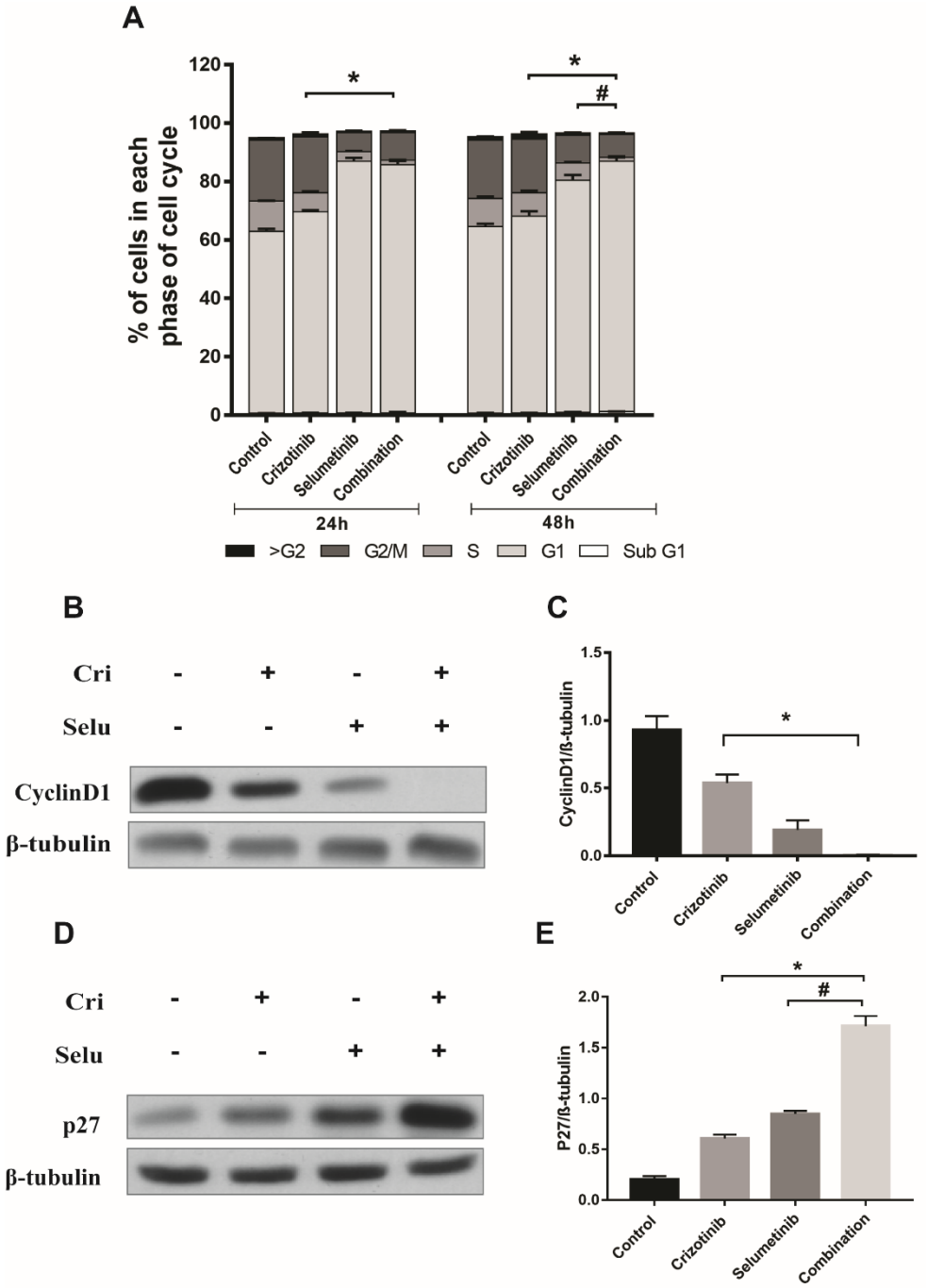

Figure 2.11 Effect of crizotinib, selumetinib and their combination on cell cycle progression and cell cycle markers in CR-H3122 cells. (A) cell cycle progression. Cells were treated with vehicle control (DMSO 0.1%), crizotinib (2.5 μM), selumetinib (7.0 μM) and their combination for 24 h and 48 h. Propidium iodide staining and flow cytometry was used to determine the proportion of cells in different cell cycle phases. Bar denotes; ■ > G2, ■ G2/M, ■ S, ■ G1, □ sub G1. Significance was determined by two-way-ANOVA with Bonferroni post-hoc test. Representative Western blots of (B) cyclinD1 and (D) p27 after 24 h exposure to drugs treatment. Cell lysates were subjected to SDS-PAGE and probed with specific antibodies. Densitometry of Western blots of (C) cyclinD1 and (E) p27. Significance was determined by one-way-ANOVA with Bonferroni post-hoc test. All data are presented as mean ± SEM. Three independent experiments were performed. *$p < 0.05$ for crizotinib vs. combination and #$p < 0.05$ for selumetinib vs. combination.

2.4.2.4. Effect of combination treatment on the induction of apoptosis and apoptotic markers in CR-H3122 cells

To determine the effect of crizotinib, selumetinib and their combination on the mode of cell death in CR-H3122 cells, apoptotic assay was performed. Cells were treated with vehicle control (DMSO 0.1%), crizotinib (2.5 μM), selumetinib (7.0 μM) and their combination for 24 h and 48 h and analysed by flow cytometry with PI and Annexin V staining. Following drug treatment, apoptosis was maximum at 24 h and entered late apoptotic phase at 48 h. After 24 h, the percentage of early apoptotic cells was slightly higher with crizotinib and selumetinib single drug treatment (8% and 5%, respectively), whereas the combination treatment resulted in a significantly higher percentage of early apoptotic cells (18%) ($p < 0.05$, two-way ANOVA) (Figure 2.12A).

Western blotting was performed to determine the expression of apoptotic markers such as Bim, Bcl2, total caspase-3, cleaved caspase-3, PARP, and cleaved PARP. CR-H3122 cells were treated with vehicle control (DMSO 0.1%), crizotinib (2.5 μM), selumetinib (7.0 μM) and their combination for 24 h and 48 h. Similar to what was observed in H3122 cells, there was no change in expression of Bcl2 with crizotinib, selumetinib and their combination (Figure 2.12C). On the other hand, combination treatment increased the expression of Bim by 12-fold ($p < 0.05$, one-way ANOVA) and 0.26-fold ($p > 0.05$, one-way ANOVA) compared to crizotinib and selumetinib, respectively (Figure 2.12E).

Furthermore, combination treatment significantly increased the expression of cleaved caspase-3 by 0.3- and 5.3-fold compared to crizotinib and selumetinib, respectively ($p < 0.05$, one-way ANOVA) (Figure 2.13B). This was further confirmed by performing a caspase-3 assay. Here, the combination treatment increased caspase-3 activity by 0.24- and 1.1-fold compared to crizotinib and selumetinib, respectively (Figure 2.13C) that was consistent with the result from Western blotting. Similarly, the expression of cleaved PARP was significantly increased with combination treatment by 0.9- and 3.2-fold compared to crizotinib and selumetinib, respectively ($p < 0.05$, one-way ANOVA) (Figure 2.13E).

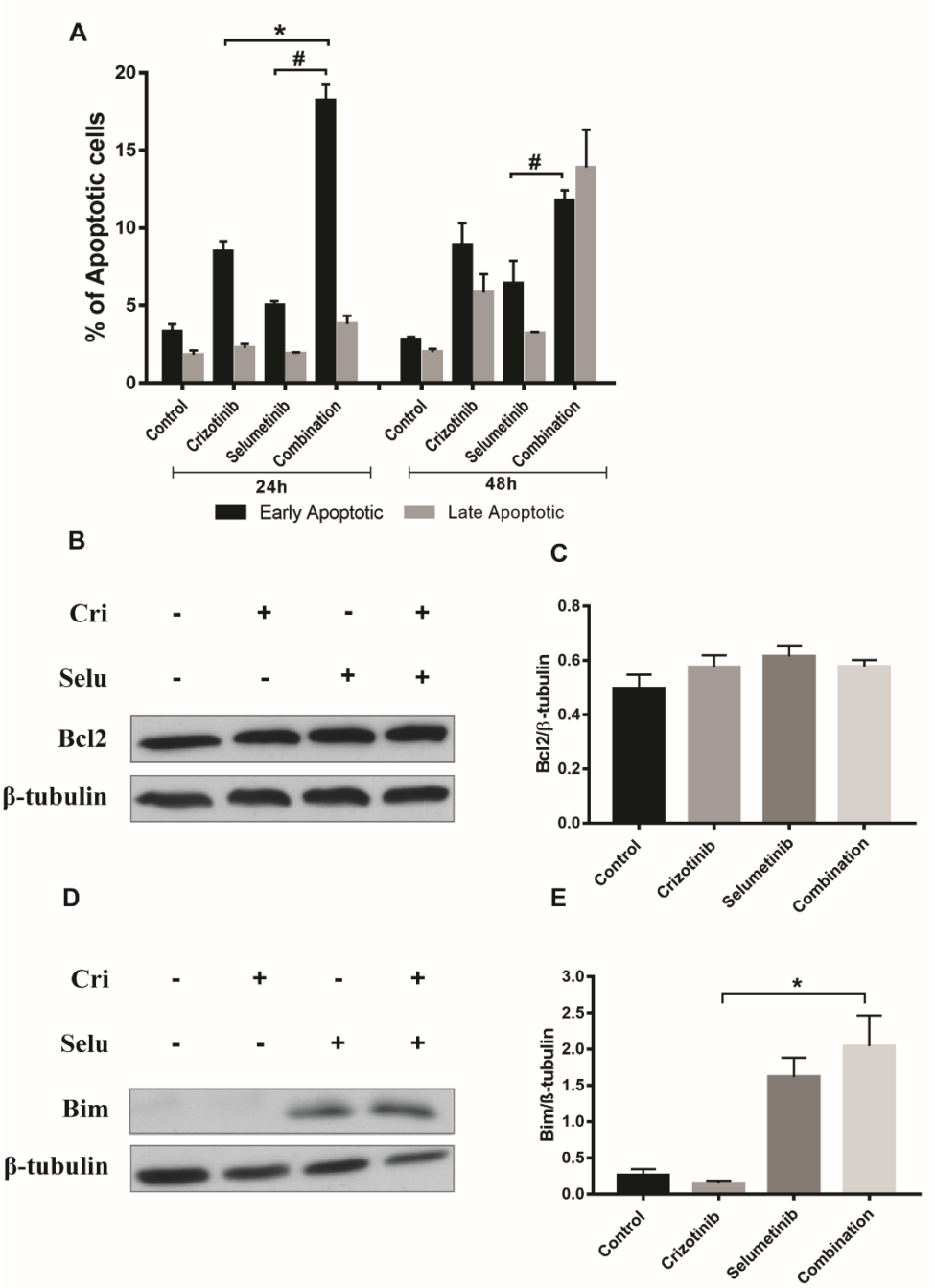

Figure 2.12 Effect of crizotinib, selumetinib and their combination on the mode of cell death and apoptotic marker in CR-H3122 cells. (A) Percentage of apoptotic cells after treatment with vehicle control (DMSO 0.1%), crizotinib (2.5 μM), selumetinib (7.0 μM) and their combination for 24 h and 48. This was followed by staining with propidium iodide and Annexin V and analysing by flow cytometry. Bar denotes; ■ Early apoptotic, ■ late apoptotic. Significance was determined by two-way-ANOVA with Bonferroni post-hoc test. Representative Western blots of (B) Bcl2 and (D) Bim. Cells were treated with vehicle control (DMSO 0.1%), crizotinib (0.25 μM), selumetinib (7.5 μM) and their combination for 24 h. Cell lysates were subjected to SDS-PAGE and probed with specific antibodies. Densitometry of Western blots of (C) Bcl2 and (E) Bim. Significance was determined by one-way-ANOVA with Bonferroni post-hoc test. All data are presented as mean ± SEM. Three independent experiments were performed. *$p < 0.05$ for crizotinib vs. combination and #$p < 0.05$ for selumetinib vs. combination.

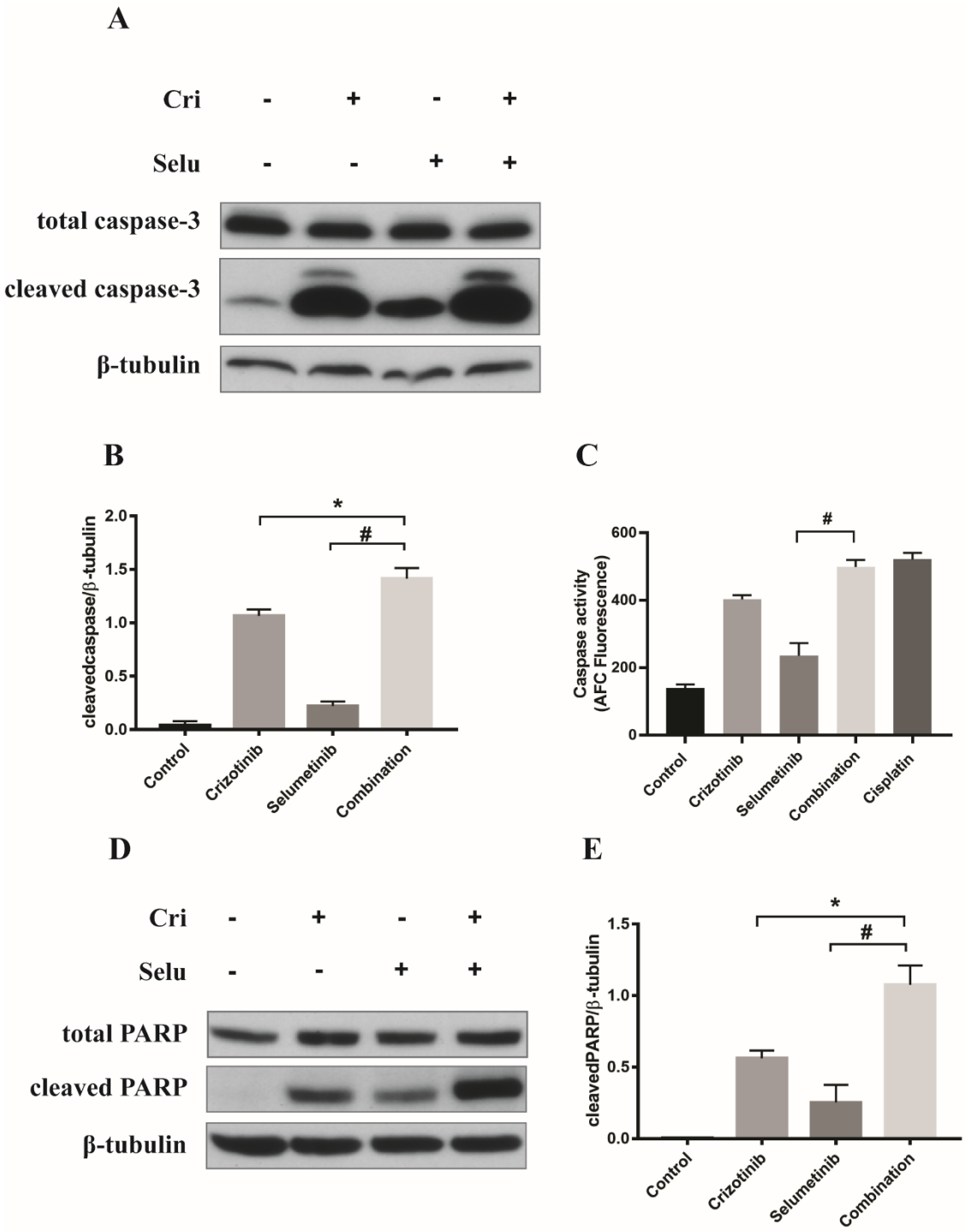

Figure 2.13 Effect of crizotinib, selumetinib and their combination on cleaved caspase-3 and cleaved PARP in CR-H3122 cells. Representative Western blots (A) cleaved caspase-3 and (D) cleaved PARP. Cells were treated with vehicle control (DMSO 0.1%), crizotinib (2.5 μM), selumetinib (7.0 μM) and their combination for 24 h. Cell lysates were subjected to SDS-PAGE and probed with specific antibodies. Densitometry of Western blots of (B) cleaved caspase-3 and (E) cleaved PARP. (C) Caspase-3 activity after treatment with the indicated concentration of crizotinib, selumetinib, their combination and cisplatin (positive control) for 24 h. Significance was determined by one-way-ANOVA with Bonferroni post-hoc test. All data are presented as mean ± SEM. Three independent experiments were performed. *$p < 0.05$ for crizotinib vs. combination and #$p < 0.05$ for selumetinib vs. combination.

2.5. Discussion

The combined effect of crizotinib and selumetinib was investigated in both crizotinib naïve and crizotinib resistant ALK-positive NSCLC cells. Furthermore, the molecular mechanism behind the synergistic effect of combination treatment was explored. The combination treatment showed superiority over either of the single drug treatments by downregulating the major RAS/MAPK signalling pathway that in turn inhibits proliferation and induces apoptosis.

The cell viability assay showed that H3122 cells were highly sensitive to crizotinib compared to selumetinib. Whereas the sensitivity to crizotinib was decreased in A549 cells suggesting that crizotinib is highly specific to EML4-ALK harbouring cell line. Furthermore, the development of crizotinib resistance did not cause appreciable cross-resistance to selumetinib in EML4-ALK- positive cells (IC_{50} values of crizotinib and selumetinib were increased by 22- and 3-fold, respectively, compared to parental H3122 cells). Combination of crizotinib and selumetinib inhibited cell viability in H3122 cells to a greater extent than predicted by Loewe additivity (CI < 1) (Chou & Talalay, 1983). Interestingly, this effect was found to an even greater degree in CR-H1322 cells (Chou-Talaly Combination Indices < 0.3) (Chou & Talalay, 1983). This is in contrast to a previous study on the combination of ALK/IGF-1R inhibition by Wilson et al., where the drug combination was effective against H3122 cells, but failed against CR-H1322 cells (Wilson et al., 2017).Together these results suggest that the development of resistance to crizotinib in our experiments did not involve mutations at points in the genome that confer resistance to both targets.

The investigation of underlying mechanisms showed that the drug combination leads to a strong downregulation of the RAS/MAPK signalling pathway that in turn promotes both cell cycle arrest and apoptosis. In both H3122 and CR-H3122 cells, combination treatment significantly decreased the protein phosphorylation of pERK/ERK compared to crizotinib as a single drug treatment. Both crizotinib and selumetinib are known to exhibit anti-tumour activity via G1 cell cycle arrest and induction of apoptosis in various cancers including NSCLC (Christensen et al., 2007; Sale & Cook, 2013; Zhou et al., 2016).

As expected, crizotinib and selumetinib single drug treatment increased the accumulation of cells in the G1 phase compared to the control. And interestingly, their combination further increased this G1 phase arrest and suppressed the S phase. This may be due to a decrease in the activity of ERK following the combination treatment. The RAS/MAPK pathway is involved in the regulation of G1 cell cycle proteins. Phosphorylation of ERK leads to migration to the nucleus and activation of cyclin D1 and downregulation of p27. Thus, ERK plays an important role for entry into the S phase of the cell cycle (Bhatt et al., 2005).

Combination treatment also significantly increased apoptosis compared to individual drugs in both crizotinib naïve and crizotinib resistant ALK-positive NSCLC cells. Specifically, cleaved caspase-3 and cleaved PARP were markedly increased following combination treatment, which was mediated by Bim, a pro-apoptotic protein in the Bcl2 family (though Bcl2 itself was not changed). Both crizotinib and selumetinib individually increased the expression of Bim which is consistent with other studies in B-cell lymphoma and NSCLC cells (Bhalla et al., 2011; Tanizaki et al., 2011). The mechanism behind the increase in expression of Bim is associated with a decrease in the phosphorylation of ERK, as it is well known that the RAS/MAPK signalling pathway phosphorylates Bim and promotes its proteasomal degradation thereby suppressing apoptosis (Ley et al., 2003).

Similarly, a significant increase in cleaved caspase-3 and cleaved PARP was observed in CR-H3122 cells following combination treatment. This effect was driven mostly by crizotinib where the contribution of selumetinib was minimal. Following selumetinib treatment, apoptosis was a Bim-dependent process, but apoptosis induced by crizotinib was independent of Bim. This may be because crizotinib can inhibit the RAS/MAPK pathway along with other ALK downstream pathways such as AKT/mTOR or JAK/STAT that may contribute to apoptosis with the involvement of other pro- or anti-apoptotic proteins (Hamedani et al., 2014; Zheng et al., 2013). Future studies will be required to determine the mechanism(s) involved in crizotinib resistant cell lines.

Notably, Bim, PARP and CDK, mediate complementary aspects of tumour cell suppression, namely cell death and proliferation, respectively. They are druggable targets, Bim by BH3 analogues, PARP by PARP inhibitors and CDK by specific inhibitors. Hence the results suggest that triple or even quadruple drug treatments should be screened (i.e., ALK, MEK, Bim, and PARP targeting) in the quest for even greater and longer-term cancer suppression.

Chapter 3: Toxicity and efficacy of crizotinib and selumetinib combination treatment in a mouse model of ALK-positive NSCLC

This chapter is based on the following peer-reviewed publication:

Shrestha N, Bland AR, Bower RL, Rosengren R, Ashton J. Inhibition of MEK alone and in combination with ALK inhibition suppresses tumor growth in a mouse model of ALK-positive lung cancer. Journal of Pharmacology and Experimental Therapeutics, jpet.120.266049

J.A, R.R, N.S contributed on experimental design, J.A and N.S performed data analysis, N.S carried out experiments, N.S, A.B and R.B contributed on xenograft development, oral dosing and necropsy.

3.1. Introduction

In **Chapter 2**, it was demonstrated in *in vitro* studies that the combination of crizotinib and selumetinib strongly inhibited the proliferation of ALK-positive NSCLC cells. This resulted from a reduction in MAPK signalling that in-turn decreased cell proliferation and increased apoptosis via increased expression of apoptotic markers BIM, cleaved caspase-3, cleaved PARP and the cyclin dependent kinase inhibitor, p27 and decreased expression of the cell proliferation marker, cyclin D1. However, *in vitro* efficacy does not necessarily translate into *in vivo* efficacy. Therefore, this chapter reports the results of the singular and combined effect of crizotinib and selumetinib in a xenograft model of ALK-positive NSCLC.

Efficacy is only one element of the usefulness of a therapeutic strategy. Equally important is potential toxicity. When crizotinib was approved for the treatment of ALK-positive NSCLC (Camidge et al., 2012; Kazandjian et al., 2014; Kwak et al., 2010) based on a Phase I dose escalation study, the maximum tolerated dose (MTD) for crizotinib in humans was calculated as 250 mg p.o. twice daily (Kwak et al., 2010; Kwak et al., 2009). Treatment related adverse events were mostly grade 1-2 such as gastrointestinal upset, visual disturbances, and peripheral oedema. Grade 3-4 adverse events including neutropenia, raised alanine aminotransferase (ALT) enzymes, lymphopenia and pneumonitis were observed in a minority of patients (Camidge et al., 2012). Similarly, MTD of selumetinib formulated as hydrogen sulphate was 75 mg p.o. twice daily (Banerji et al., 2010). The common adverse events were grade 1-2 diarrhoea, nausea, fatigue and grade 3-4 oedema, elevation of ALT, acneiform dermatitis, pleural effusion (Adjei et al., 2008; Banerji et al., 2010). The risk of toxicity, either additive or synergistic is increased when two drugs are given in combination (Farr & Bacon, 1995). Thus, it is important to investigate the potential toxicity of the combination of crizotinib and selumetinib.

Investigation of drug-drug interaction for the combination of an anti-cancer drug is also crucial to assess its efficacy and toxicity (Scripture & Figg, 2006).

Crizotinib is predominantly metabolised by the cytochrome P450 isoform CYP3A and was reported to be both a time-dependent moderate inhibitor and weak inducer of CYP3A (Johnson et al., 2015; Mao et al., 2013). Similarly, CYP3A is the major enzyme responsible for the oxidative metabolism of selumetinib (Dymond et al., 2016). Therefore, it is crucial to investigate whether the two drugs potentially inhibit each other's metabolism.

Although ALK-positive NSCLC patients were highly responsive to crizotinib, the majority of patients developed resistance typically within a year of therapy (Solomon, Wilner, et al., 2014). This suggests the need for new therapeutic strategies such as combination therapy to overcome the resistance and improve the survival of patients.

3.2. Aims and Objectives

The aims of this chapter were (1) to investigate the efficacy of the combination treatment in a xenograft model of ALK-positive NSCLC, (2) to explore the underlying mechanism of tumour suppression by crizotinib, selumetinib and their combination treatment, (3) to evaluate the safety of single and combined treatment of crizotinib and selumetinib in male Balb/c mice and, (4) to examine whether the combination of crizotinib and selumetinib modulate CYP3A activity.

The specific objectives were (1) to generate a xenograft model of ALK-positive NSCLC, (2) to examine the singular and combined effect of crizotinib and selumetinib on suppression of tumour growth in the xenograft model , (3) to examine the effect of crizotinib and selumetinib singular and combination treatment on proliferation, apoptosis and angiogenesis of tumour cells, (4) to determine the adverse effect of the drugs treatment on kidney and liver function and, (5) to perform CYP3A activity assay and western blot to examine the activity and polypeptide level of CYP3A.

3.3. Methods and Materials

3.3.1. Materials

3.3.1.1. Chemical reagents

Selumetinib and crizotinib were purchased from LC laboratories (Woburn, MA, USA). RPMI, BSA, FBS, penicillin/streptomycin were purchased from Life Technologies (Auckland, New Zealand). 3, 3'-diamino benzadine (DAB) substrate kit and streptavidin-horseradish peroxidase were purchased from BD Biosciences (San Diego, CA, USA). Haematoxylin quick stain (QS) (modified Mayer's formula), avidin–biotin blocking kit were purchased from Vector Laboratories (Burlingame, CA, USA). Acrylamide (1:30) and precision plus protein kaleidoscope were obtained from Bio-Rad Laboratories (Hercules, CA, USA). Acetone, acetylacetone, hydrogen peroxide (30%) and methanol were obtained from Merck (Billerica, MA, USA). ALT assay kit, bicinchoninic acid assay kit, CL-XPosure film, cryomatrix, NADPH and supersignal west pico were purchased from Thermo Fisher Scientific (Waltham, MA, USA). Creatinine colourimetric assay kit was purchased from Cayman Chemical Company (Ann Arbor, MI, USA). Ammonium acetate, barium hydroxide, butylated hydroxytoluene (BHT), citric acid, DMSO, dithiothreitol (DTT), ethylenediaminetetraacetic acid (EDTA) eosin Y solution alcohol, glycerol matrigel, PBS, poly-L-lysine, potassium chloride (KCL), potassium pyrophosphate, trizma hydrochloride (Tris-HCL), xylene (DPX) mounting medium and zinc sulphate were purchased from Sigma Aldrich (St Louis, MO, USA). Xylene was purchased from Bio-lab (Auckland, New Zealand). Dako pen was purchased from Dako (Glostrup, Denmark).

3.3.1.2. Antibodies

Ki67 was purchased from Abcam (Cambridge, UK). CD105 was obtained from Antibodies- online.com (Limerick, USA). ApopTag peroxidase in situ apoptosis detection kit was obtained from Merck (Billerica, MA, USA). Antibodies against CYP3A and GAPDH antibody were purchased from Thermo

Fisher Scientific (Waltham, MA, USA). Polyclonal goat anti-rabbit immunoglobulin/biotinylated were purchased from Dako (Glostrup, Denmark). HRP-conjugated goat anti-rabbit and HRP-conjugated goat anti-mouse were obtained from Calbiochem (San Diego, CA, US).

3.3.2. Methods

3.3.2.1. Animal housing and care

Male nude (Nu/J) were purchased from the Animal Resource Centre (Canning Vale, Australia). Male Balb/c mice were purchased from the Hercus-Taieri Resource Unit (University of Otago, Dunedin, New Zealand). Mice were housed in the pathogen-free condition supplied with free access to sterile water and food (Reliance rodent diet). The room was maintained at a temperature of 21-24^{o}C with relative humidity at 30 ± 5% on a scheduled 12 h light/dark cycle and mice were acclimatised for 4 days prior to the experiment. All animal experiments were approved by the University of Otago Animal Ethics Committee (AEC Approval No. 18-21 and 18-82).

3.3.2.2. Drug efficacy in a xenograft model of ALK-positive non-small cell lung cancer

An ALK-positive NSCLC xenograft model was established by subcutaneous injection of H3122 cells (2 × 10^6 cells in 50 µL Matrigel and 50 uL of media) in the flank region of Nu/J mice. Once the tumour volume had reached ~100 mm^3, the mice were randomised into four groups (n=7). Each group received either vehicle (25% DMSO/75% olive oil, 5 ml/kg), crizotinib 25 mg/kg, selumetinib 25 mg/kg or their combination p.o once daily for 14 days. Animal equivalent dose was calculated from the equation as described in Nair et al. (Nair et al., 2018).The animal doses were chosen on the basis that it is lower or equivalent to a well-tolerated human dose (Banerji et al., 2010; Kwak et al., 2010; Nair et al., 2018; Nencioni et al., 2014; Zhou et al., 2012). Body weight and tumour volume were measured daily. Tumour volume (mm^3) was calculated by multiplying the length (L) x height (H) x width (W). At the end of treatment,

mice were euthanised by carbon dioxide inhalation. Mice were perfused with isotonic PBS and major organs including liver, kidney, spleen. heart, lung, testes were removed and weighed. Tumours were removed, weighed, and fixed in 4% paraformaldehyde for 24 h followed by 30% cold sucrose for 24 h at 4^{o}C. Tumours were embedded in optimal cutting temperature compound (OCT) solution and frozen immediately in liquid nitrogen. The frozen tumours were stored at -20^{o}C until further required.

3.3.2.3. Immunohistochemistry of tumour sections

Ki67

Cell proliferation in tumour sections was estimated by using Ki67 antibody. The tumours were sliced at a thickness of 10 µm and stored in -20^{o}C. The sections were thawed at room temperature for 30 min and washed with isotonic PBS two times for 5 min each. Excess of PBS was aspirated, and the sections were fixed with 4% ice-cold acetone for 10 min at room temperature. Slides were then air-dried and Dako pen was used to draw a circle around each section. Endogenous peroxidase activity was blocked with hydrogen peroxide (3% in methanol) for 20 min at room temperature. The sections were washed with isotonic PBS three times for 5 min each. Heat mediated antigen retrieval was performed by incubating sections in 0.01 M citrate buffer with 0.05% Tween 20, pH 6.8 for 10 min at 95^{o}C. The sections were then incubated with blocking buffer (2% normal goat serum, 1% BSA, 4 drop/1 ml of avidin) for 1 h at room temperature in a humidified chamber. This was followed by overnight incubation with Ki67 antibody (1:100 in 0.2% BSA with 4 drop/1 ml of biotin) at 4^{o}C in a humidified chamber. For negative controls, the antibody was replaced with PBS. Next, the sections were washed with isotonic PBS two times for 5 min each and then incubated with biotinylated secondary antibody (1:500 in 0.2% BSA) for 30 min at room temperature. The streptavidin was applied for 30 min at room temperature and a signal was detected using DAB (5 min). The sections were counterstained with haematoxylin QS and dehydrated with increasing concentrations of ethanol (70%, 95%, 100%) for 2 min each. Lastly, the sections

were soaked in xylene two times for 5 min each and then mounted using DPX mounting solution. The slides were scanned with the Aperio Image ScanScope System (Leica, Chicago, IL, USA) and were analysed blinded to the treatment group. The nuclear image analysis algorithm was used to quantify Ki67 stained (proliferative) cells.

TUNEL assay

The TUNEL assay was performed to visualise apoptotic cells using the ApopTag *in situ* detection kit as per the manufacture's instruction. Briefly, sections were washed in isotonic PBS two times. The sections were then fixed in ethanol-acetic acid solution (2:1) and incubated with 3% hydrogen peroxide (5 min) to block endogenous peroxidases. The sections were incubated with an equilibrating buffer for 5 min followed by terminal deoxynucleotidyl transferase (TdT) enzyme for 1 h in a humidified chamber. For negative control, the TdT enzyme was replaced with PBS. The reaction was stopped using stop/wash buffer (10 min) and washed with isotonic PBS three times. This was followed by the incubation of the section with anti-digoxigenin peroxidase for 30 min at room temperature. Finally, the sections were stained with DAB, counterstained with haematoxylin QS, dehydrated and mounted. Slides were then scanned with the Aperio Image ScanScope System (Leica, Chicago, IL, USA) and were analysed blinded to the treatment group. The nuclear image analysis algorithm was used to quantify TUNEL stained (apoptotic) cells.

CD105

CD105, an indicator of microvessel density (MVD), is highly expressed in endothelial cells of tumour blood vessels. The tumours were sectioned (10 μm) and were fixed in acetone for 10 min. Endogenous peroxidase activity was blocked with 3% hydrogen peroxide and was incubated with blocking buffer in a humidified chamber for 1 h at room temperature. This was followed by overnight incubation with CD105 antibody (1:100 with biotin) in a humidified chamber at 4^{o}C. For negative controls, the antibody was replaced with PBS. The

sections were incubated with biotinylated secondary antibody (1:100) for 30 min. The streptavidin was applied for 30 min at room temperature and a signal was detected using DAB. The sections were counterstained with haematoxylin QS, dehydrated and mounted. Slides were then scanned with the Aperio Image ScanScope System (Leica, Chicago, IL, USA). The microvessel analysis algorithm was used to quantify the MVD at a dark- and light-staining threshold of 180 and 210, respectively

3.3.2.4. *In vivo* toxicity studies

Male Balb/c mice were divided into 2 groups. Group 1 (n=6) received either vehicle (10% DMSO/ 90% olive oil), crizotinib 5 mg/kg, selumetinib 25 mg/kg or their combination p.o once daily for 14 days. Similarly, group 2 (n=6) received either vehicle (25% DMSO/ 75% olive oil 5mL/kg), crizotinib 25 mg/kg and a combination of crizotinib 25 mg/kg and selumetinib 25 mg/kg p.o once daily for 14 days. As a positive control for CYP3A induction, mice (n=5) were orally administered daily with dexamethasone (50 mg/kg) for 4 days (McCune et al., 2000; Valentine et al., 2006; Xu, Zhang, et al., 2018). At the end of treatment, mice were euthanised by carbon dioxide inhalation Blood was collected from the posterior vena cava using a heparinised syringe. The plasma was separated by centrifugation at 5000 rpm for 10 min at 4°C and stored at -20°C. Mice were perfused with isotonic PBS and major organs including liver, kidney, spleen. heart, lung, testes were removed, weighed, and washed with isotonic ice-cold PBS. The organs were then submerged in 10% formalin for 48 h followed by 30% starch solution for 24 h in a cold room (4°C). Finally, the organs were embedded in OCT solution and were frozen immediately in liquid nitrogen. The frozen organs were stored in -20°C until further required. The organ weight was determined and expressed as a percentage of total body weight.

3.3.2.5. Alanine Transaminase activity

Alanine transaminase (ALT), an indicator of hepatotoxicity, was determined using the commercially available Infinity ALT colourimetric assay kit. The assay was performed according to the manufacturer's instruction.

Briefly, 10 µL of plasma was transferred to cuvette which was then diluted to 100 µL with milli-Q water. This was followed by the addition of 1000 µL of warm ALT reagent (37°C). Absorbance was measured on a visible spectrophotometer at a wavelength of 340 nm for 0 to 3 min. ALT activity, expressed in international unit per litre (U/L), was determined from the following equations.

$$\boldsymbol{ALT\ activity\ in\ Units\ per\ litre}\ (\boldsymbol{U/L}) = \boldsymbol{\Delta\ Abs/min} \times \boldsymbol{factor}$$

Equation 3.1 Calculation of alanine transaminase activity

where, $\boldsymbol{\Delta\ Abs}$ is absorbance (0min)- absorbance (3min) and the factor was calculated as below:

$$\boldsymbol{Factor} = \boldsymbol{TV} \times \mathbf{1000/6.3} \times \boldsymbol{SV} \times \boldsymbol{P}$$

Equation 3.2 Calculation of factor for alanine transaminase activity

where, $\boldsymbol{TV}$ is total reaction volume in ml (1 ml), $\boldsymbol{SV}$ is Sample volume in ml (0.1 ml), $\mathbf{6.3}$ is millimolar absorption coefficient of NADH at 340 nm, $\boldsymbol{P}$ is cuvette pathlength in cm (1 cm).

3.3.2.6. Creatinine assay

Creatinine, an indicator of renal function, was determined using a commercially available creatinine colourimetric assay kit from Cayman chemical company. The assay was performed according to the manufacturer's instructions. Briefly, all the reagents were equilibrated to room temperature. Creatinine reaction buffer was prepared by mixing creatinine sodium borate, creatinine surfactant and creatinine 1 M sodium hydroxide in 1:3:2 ratio. Creatinine standard (0-5.0 mg/dL) was prepared as per the manufacturer's protocol. 15 µL of standard and sample (plasma) in duplicate was added to a 96 well plate. This was followed by the addition of 100 µL of creatinine reaction buffer. Next, 100 µL of creatinine colour reagent was added to each. The absorbance was measured on a microplate spectrophotometer at a wavelength of 490 nm at 1 min and 7 min, respectively. The change in optimal density (Δ OD) was calculated from equation 3.3. Adjusted Δ O.D. was obtained by subtracting the average of Δ OD of control (zero concentration (0 mg/dL) of

creatinine standard) from the standards and test samples. The creatinine concentration in mg/dL was calculated from equation 3.4

$$\Delta\ OD\ =\ A_{490}\ (7min)\ -\ A_{490}\ (1min)$$

Equation 3.3 Calculation of change in optimal density

where, $\Delta\ OD$ is change in optimal density, A is absorbance.

$$\boldsymbol{Cr = \frac{Adjusted\ sample\ \Delta\ OD - (y - intercept)}{slope} \times sample\ dilution}$$

Equation 3.4 Calculation of serum creatinine

where, Cr is creatinine in mg/dL.

3.3.2.7. Histology

Histology was performed to investigate cellular change in the liver of mice that exhibited increased ALT activity. The frozen livers were sliced at a thickness of 15 μm using a cryostat microtome (CM 1959, LEICA Biosystems) maintained at -20°C. The liver sections were placed on poly-L-lysine-coated microscope slides and then dried under a fan overnight. The dried sections were then stored at -20°C until required. The sections were thawed for 30 min at room temperature and washed in isotonic PBS two times for 5 min each. This was followed by rinsing of sections with distilled water for 10 sec and staining with heamotoxylin QS (H-3404) for 10 sec. Next, the sections were rinsed in tap water until a blueish colour was obtained. The sections were washed in dH_2O and rinsed in 95% ethanol for 10 sec. The sections were then counterstained with eosin for 15 sec. The excess of eosin was removed by rinsing in 95% ethanol. Next, the sections were dehydrated in increasing concentration of ethanol (70%, 95%, 100%) for 2 min. Lastly, the sections were soaked in xylene two times for 5 min each and mounted in DPX mounting solution. Finally, the sections were examined, and representative pictures were captured using the Nikon RM229 microscope.

3.3.2.8. Microsome preparation

Hepatic microsomes were prepared from treated mice as previously described by Guengerich (Guengerich, 2014). Briefly, the liver was removed and placed in individual beakers containing 1.15% potassium chloride (KCl) on ice. The liver was washed with 1.15% KCl, trimmed and debris was removed. This was followed by homogenisation of the liver with 2 mL of buffer A pH 7.4 (0.1 M Tris, 0.1 M KCl, 1 mM EDTA, 20 µM BHT). Homogenisation was carried out with a Teflon-glass homogeniser using 5-6 vertical passes. The homogenate was then centrifuged at 10,000 rpm for 20 min. The supernatant was transferred into new tubes and was centrifuged at 35,000 rpm for 1 h. The supernatant obtained was discarded and an equal volume of buffer B pH 7.4 (0.1 M potassium pyrophosphate, 1 mM EDTA, 20 µM BHT) was added into the same centrifuge tube containing pellets. The pellets were dislodged with the use of a pipette and then homogenised with 4 passes of the Teflon-glass homogeniser. The homogenate was centrifuged at 35,000 rpm for 1 h. Again, the supernatant was discarded and 1 mL of buffer C pH 7.4 (10 mM Tris-HCl, 1 mM EDTA, 20% glycerol) was added to the pellet and again homogenised. Note that dithiothreitol (DTT) was added to each buffer (Buffer A, B, C) before use. The final homogenate was transferred to Eppendorf tubes and was stored in -80^{o}C. The BCA assay was performed as described in **Section 2.3.2.3** of **Chapter 2** to determine the protein concentration of the microsomes.

3.3.2.9. Erythromycin N-demethylation

Erythromycin N-demethylation assay was performed to determine the catalytic activity of CYP3A as described by Kitada et al. (Kitada et al., 1988). The reaction mixture containing 1 mg of microsomal protein and 0.45 ml of erythromycin buffer (0.1 M phosphate buffer pH 7.4, 0.1 mM EDTA and 0.4 mM erythromycin) was prepared and incubated for 2 min at 37^{o}C in a shaking water bath. The reaction was initiated by addition of 0.05 mL of 50 mM NADPH. After 30 min, 0.33 mL of 15% zinc sulphate was added and was incubated for 5 min at room temperature. Next, 0.33 mL of saturated barium hydroxide was added to

each sample, mixed gently, and was further incubated for 5 min. The samples were then centrifuged for 10 min at 2000 rpm. 0.83 ml of supernatant was pipetted into new glass test tubes followed by addition of 0.33 mL of Nash reagent (30% ammonium acetate and 0.4% acetylacetone). The samples were then incubated for 30 min at 60^{o}C, centrifuged and absorbance of the supernatant was measured on a visible spectrophotometer at the wavelength of 415 nm. The catalytic activity of CYP3A was expressed as nmol/mg/min.

3.3.2.10. Western blotting

Western blotting was performed as described in the **Section 2.3.2.3** of **Chapter 2**. Briefly, 1 µg/ µL of proteins sample were prepared and heated in 4×-Laemmli sample buffer at 95^{o}C for 5 min. 10 µL was then subjected to SDS-PAGE and analysed by Western blotting. The concentration of the primary antibody used was - CYP3A (1: 1000) and GAPDH (1: 3000).

3.3.2.11. Statistical analysis

Tumour volume was analysed using a two-way ANOVA mixed effect coupled with a Tukey post-hoc test, with day of treatment as a repeated-measures factor and drug treatment as an independent factor. All other data that were independent of the time were analysed using a one-way ANOVA coupled with Bonferroni post-hoc test. Data are presented as the mean ± SEM. $p < 0.05$ was the minimal requirement for a statistically significant difference. Data were tested for normality using the Kolmogorov-Smirnov test, and non-normal data was log-transformed before further analysis using Graphpad prism V8.

3.4. Results

3.4.1. Efficacy of the combination treatment in xenograft model of ALK-positive non-small cell lung cancer

In a previous study, the combination of crizotinib and selumetinib significantly decreased the proliferation of ALK-positive NSCLC cells. To determine whether the *in vitro* efficacy is translated to *in vivo*, the efficacy of the crizotinib, selumetinib and their combination was further investigated in a xenograft model of ALK-positive NSCLC. Nu/J mice bearing H3122 xenografts were treated with crizotinib (25 mg/kg), selumetinib (25 mg/kg) and their combination orally once daily for 14 days. Mice were monitored daily for their weight loss and survival. There were slight decreases in the bodyweight of the mice in all four groups (Table 3.1), but no statistically significant difference in body weight between the treatment groups and the vehicle control was observed ($p > 0.05$, one-way ANOVA). Similarly, there were no significant differences in organ weight (expressed as % of body weight) among the treatment groups compared to the vehicle control ($p > 0.05$, one-way ANOVA) (Table 3.1)

Crizotinib, selumetinib and their combination treatment significantly decreased tumour volume by 52%, 59% and 76% compared to the vehicle control. Furthermore, combination treatment significantly decreased tumour volume by 50% and 42%, respectively, compared to the crizotinib ($p < 0.05$, two-way ANOVA) and the selumetinib ($p < 0.05$, two-way ANOVA) single drug treatments. Of particular note, unexpectedly mice treated with selumetinib alone decreased tumour growth greater than crizotinib alone (although statistically not significant) (Figure 3.1A). However, there was no significant difference in tumour weight among the treatment groups (Figure 3.1B). Moreover, the correlation between tumour volume and tumour weight was examined. high correlation ($r = 0.9903$) was found, suggesting unbiased measurement (Figure 3.1C).

Table 3.1 Body weight and organ weight of Nu/J mice

	Vehicle	Crizotinib 25 mg/kg	Selumetinib 25 mg/kg	Combination
Body weight change (g)	-0.2 ± 0.29	-0.45 ± 0.38	-0.4 ± 0.34	-0.03 ± 0.47
Organ Weight (% of Body Weight)				
Liver	6.05 ± 0.41	5.8 ± 0.21	6.2 ± 0.3	6.5 ± 0.14
Spleen	0.41 ± 0.07	0.49 ± 0.03	0.47 ± 0.03	0.49 ± 0.02
Lungs	1.09 ± 0.09	1.17 ± 0.05	1.16 ± 0.07	1.12 ± 0.07
Heart	0.49 ± 0.08	0.57 ± 0.02	0.57 ± 0.02	0.6 ± 0.01
Kidneys	1.73 ± 0.3	1.97 ± 0.03	2.07 ± 0.05	2.05 ± 0.07
Testes	0.8 ± 0.13	0.89 ± 0.05	0.9 ± 0.07	0.85 ± 0.04
Brain	1.19 ± 0.06	1.23 ± 0.06	1.18 ± 0.07	1.26 ± 0.1

Statistical significance was determined by one-way ANOVA with Bonferroni post-hoc test. All data are presented as mean ± SEM from n = 7. Multiple comparisons among treatment groups and vehicle did not show a significant difference in both body and organ weight ($p > 0.05$, one-way ANOVA)

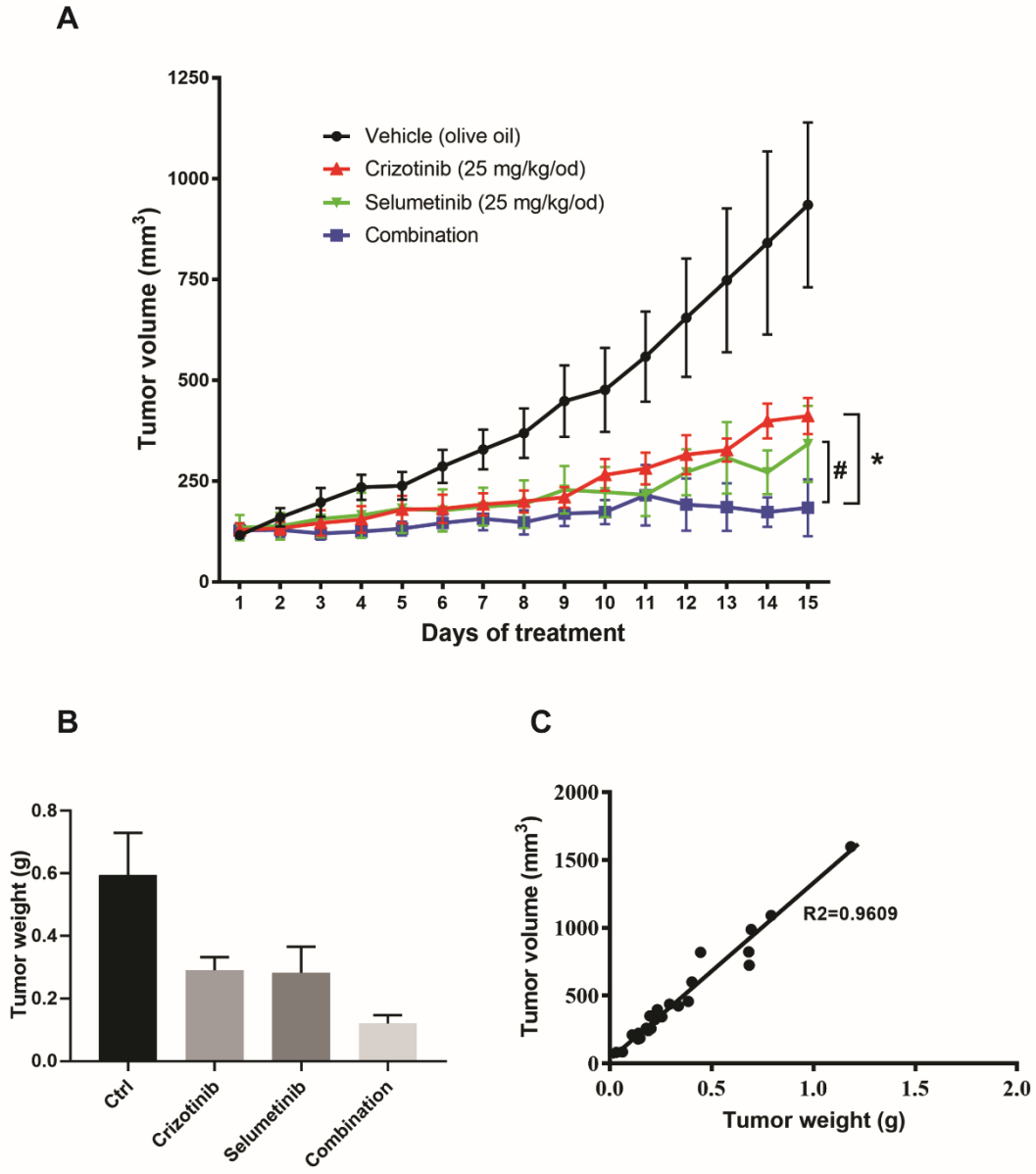

Figure 3.1 Effect of crizotinib, selumetinib and their combination on tumour growth in a xenograft model of ALK-positive NSCLC. (A) Tumour volume (mm^3) of male Nu/J mice bearing H3122 xenograft during treatment with a vehicle (olive oil), crizotinib (25 mg/kg), selumetinib (25 mg/kg) and their combination orally once daily for 14 days. Significance was determined by mixed-model two-way ANOVA with Tukey post-hoc tests. Data are presented as mean ± SEM, from n=7. Statistical differences between the growth curves as a whole are indicated as *$p<0.05$ for crizotinib vs. combination and, #$p < 0.05$ for selumetinib vs. combination, (B) Tumour weight in grams. Significance was determined by one-way ANOVA with Bonferroni post-hoc test. Data are presented as mean ± SEM from n=7. (C) Correlation between tumour volume and tumour weight.

3.4.2. Effect of the crizotinib, selumetinib and their combination on proliferation, apoptosis, and angiogenesis.

To determine the mechanism of tumour growth suppression by crizotinib, selumetinib and their combination, immunohistochemistry of tumour sections was performed. Nu/J mice bearing H3122 xenografts were treated with crizotinib (25 mg/kg), selumetinib (25 mg/kg) and their combination orally once daily for 14 days. Tumours were excised, sectioned and immunolabelling with respective antibodies was performed. Ki67 is a marker of proliferating cells, and 60-70% of cells in tumours from all treatment groups were Ki67 positive with no significant difference among the treatment groups and vehicle control (Fig. 3.2B, $p > 0.05$, one-way ANOVA). Because selumetinib alone suppressed tumour growth more than the ALK inhibitor crizotinib, it was hypothesised that a possible mechanism that could explain this could be inhibition of angiogenesis by interference with ERK signalling (Murphy et al., 2006). Immunohistochemistry for CD105, an endothelial cell marker was carried out. However, all tumours from all treatment groups were well vascularised as visualised with CD105 staining, with no statistically significant difference in MVD among the treatment groups and vehicle control (Fig. 3.3B, $p > 0.05$, one-way ANOVA).

It was then hypothesised that the frequency of apoptotic cells would be greatest in the treatment groups with the greatest tumour suppression (i.e., selumetinib alone and crizotinib plus selumetinib combination). However, histological staining for apoptosis using TUNEL unexpectedly revealed that the highest frequency of apoptotic cells was in tumours from crizotinib treated mice. By contrast, tumours from mice treated for 14 days with selumetinib either alone or in combination with crizotinib did not show a significantly different frequency of apoptotic cells compared with the vehicle control mice (Fig. 3.4B, $p > 0.05$, one-way ANOVA).

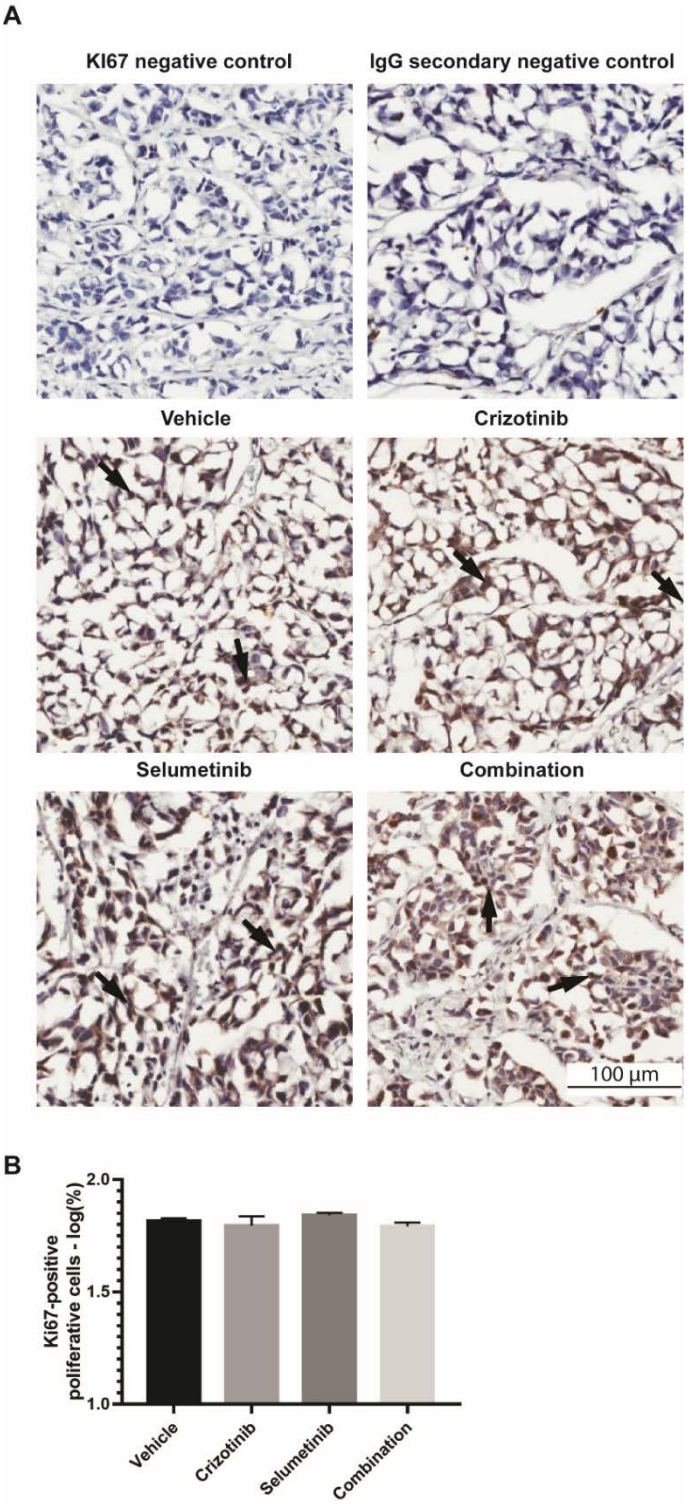

Figure 3.2 Effect of crizotinib, selumetinib and their combination on markers of cell proliferation. (A) Representative IHC staining of Ki67, (B) Quantification of Ki67 positive using nuclear image algorithm. The H3122 xenograft mice were orally gavaged daily with vehicle (25%DMSO/olive oil), crizotinib (25 mg/kg), selumetinib (25 mg/kg) and their combination for 14 days. Tumours were resected and analysed by IHC. Significance was determined by one-way ANOVA with Bonferroni post-hoc tests. All data are presented as mean ± SEM from n=5. Multiple comparisons among the treatment groups and vehicle did not show a significant difference in Ki67 staining ($p > 0.05$). Scale bar: 100 µm.

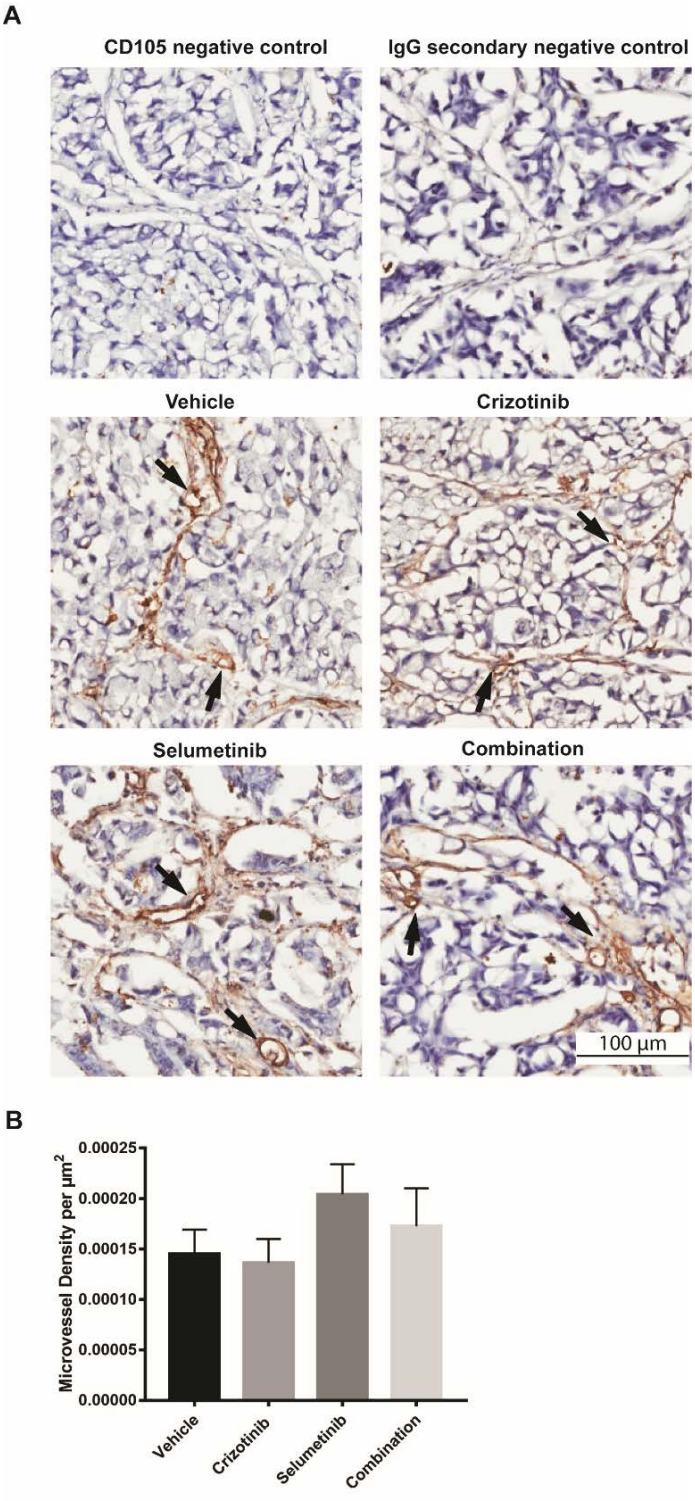

Figure 3.3 Effect of crizotinib, selumetinib and their combination on the marker of angiogenesis. (A) Representative IHC staining of CD105, (B) Quantification of CD105 positive endothelial cells using microvessel algorithm. The H3122 xenograft mice were orally gavaged daily with vehicle (25%DMSO/olive oil), crizotinib (25 mg/kg), selumetinib (25 mg/kg) and their combination for 14 days. Tumours were resected and analysed by IHC. Significance was determined by one-way ANOVA with Bonferroni post-hoc tests. All data are presented as mean ± SEM from n=5. Multiple comparisons among the treatment groups and vehicle did not show a significant difference in CD105 staining ($p > 0.05$). Scale bar: 100 µm.

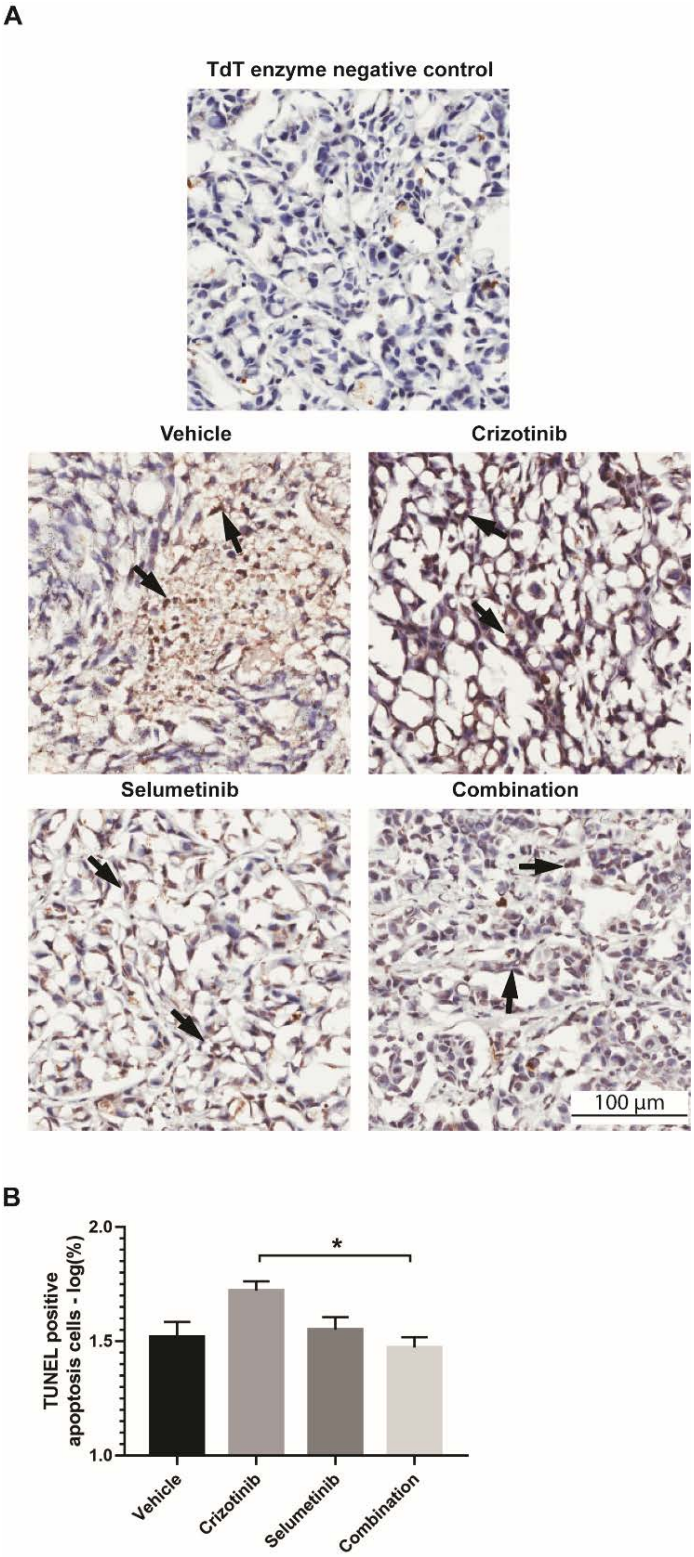

Figure 3.4 Effect of crizotinib, selumetinib and their combination on markers of apoptosis. (A) Representative IHC staining of TUNEL, (B) Quantification of TUNEL positive cells using IHC nuclear image algorithm. The H3122 xenograft mice were orally gavaged daily with vehicle (25%DMSO/olive oil), crizotinib (25 mg/kg), selumetinib (25 mg/kg) and their combination for 14 days. Tumours were resected and analysed by IHC. Significance was determined by one-way ANOVA with Bonferroni post-hoc tests. All data are presented as mean ± SEM from n=5. *$p<0.05$ for crizotinib vs. combination Scale bar: 100 µm.

3.4.3. Pre-clinical toxicity of the combination of crizotinib and selumetinib.

To ensure that the crizotinib, selumetinib, and their combination are safe, Balb/c mice were treated with vehicle (DMSO/olive oil), crizotinib (5 mg/kg or 25 mg/kg), selumetinib (25 mg/kg) and their respective combination orally once daily for 14 days. Mice were monitored daily for weight loss and survival. Change in body weight was not significantly different between the treatment groups ($p > 0.05$, one-way ANOVA) (Table 3.2 and Table 3.3). Furthermore, there was no significant difference in organ weight (expressed as % of body weight) between the treatment groups and vehicle control for all major organs (Table 3.2 and Table 3.3).

Next, to determine the effect of drugs on kidney and liver function, ALT activity and creatinine levels were examined. ALT activity in all treatment groups was not significantly different from vehicle control ($p > 0.05$, one-way ANOVA). However, in group 1, one mouse each from the vehicle, crizotinib, and combination groups had ALT activity greater than 80 U/L (i.e., 122, 296, and 104 U/L, respectively, Figure 3.5A). Similarly, in group 2, one mouse each from the vehicle and crizotinib treated groups had ALT activity values greater than 80 U/L (i.e., 126 and 89 U/L, respectively, Figure 3.5B). Therefore, the histopathology of the liver section was explored by performing H and E staining. No histopathological differences in liver sections between treatment groups and vehicle control were observed. Necrotic cells or lesions were not found in the liver section from the vehicle or drug treatment groups (Figure 3.6). Moreover, there was no significant difference in creatinine level (a kidney function marker) between any of the treatment groups, as all mice had plasma creatinine values in the normal range (< 2 mg/dl) (Figure 3.7).

Table 3.2 Body weight and organ weight of Balb/c mice (Group 1)

	Vehicle	Crizotinib 5 mg/kg	Selumetinib 25 mg/kg	Combination
Body weight change (g)	0.37 ± 0.65	0.03 ± 0.93	0.55 ± 0.73	0.1 ± 0.65
Organ Weight (% of Body Weight)				
Liver	5.26 ± 0.84	5.58 ± 1.01	4.92 ± 0.76	5.16 ± 0.97
Spleen	0.32 ± 0.06	0.39 ± 0.12	0.28 ± 0.02	0.26 ± 0.03
Lungs	0.87 ± 0.20	1.41 ± 0.55	0.87 ± 0.32	0.98 ± 0.25
Heart	0.58 ± 0.11	0.71 ± 0.13	0.55 ± 0.04	0.52 ± 0.05
Kidneys	1.96 ± 0.16	1.94 ± 0.25	1.89 ± 0.09	1.86 ± 0.15
Testes	0.755 ± 0.13	0.73 ± 0.07	0.93 ± 0.25	0.69 ± 0.04

Statistical significance was determined by one-way ANOVA with Bonferroni post-hoc test. All data are presented as mean ± SEM from n = 7. Multiple comparisons among treatment groups and vehicle did not show a significant difference in both body and organ weight ($p > 0.05$, one-way ANOVA**)**

Table 3.3 Body weight and organ weight of Balb/c mice (Group2)

	Vehicle	Crizotinib 25 mg/kg	Selumetinib 25 mg/kg	Combination
Body weight change (g)	-1.23 ± 0.35	-0.28 ± 0.41	0.55 ± 0.73	0.8 ± 0.23
Organ Weight (% of Body Weight)				
Liver	5.60 ± 0.22	5.22 ± 0.22	4.92 ± 0.76	5.33 ± 0.20
Spleen	0.27 ± 0.01	0.28 ± 0.02	0.28 ± 0.02	0.29 ± 0.01
Lungs	1.15 ± 0.14	0.99 ± 0.15	0.87 ± 0.32	0.89 ± 0.08
Heart	0.61 ± 0.08	0.57 ± 0.06	0.55 ± 0.04	0.55 ± 0.03
Kidneys	2.02 ± 0.04	2.02 ± 0.09	1.89 ± 0.09	1.92 ± 0.03
Testes	0.70 ± 0.14	0.65 ± 0.05	0.93 ± 0.25	0.69 ± 0.01

Statistical significance was determined by one-way ANOVA with Bonferroni post-hoc test. All data are presented as mean ± SEM from n = 7. Multiple comparisons among treatment groups and vehicle did not show a significant difference in both body and organ weight ($p > 0.05$, one-way ANOVA*)*

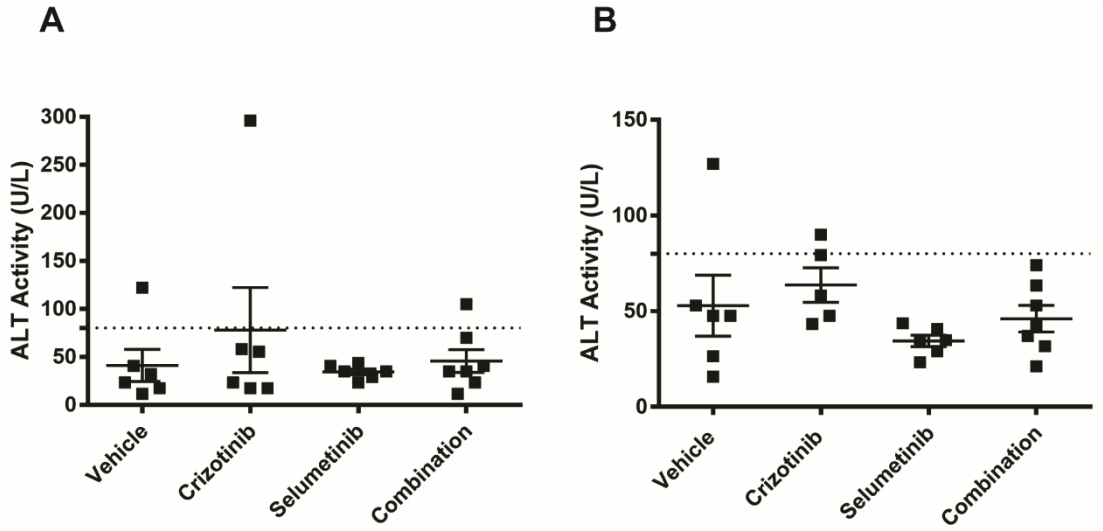

Figure 3.5 Effect of crizotinib, selumetinib, and their combination on liver function in Balb/c mice. Mice were treated with the (A) vehicle (10%DMSO/ 90%olive oil), crizotinib (5 mg/kg), selumetinib (25 mg/kg) and their combination, (B) vehicle (25%DMSO/ 75%olive oil), crizotinib (25 mg/kg), selumetinib (25 mg/kg) and their combination, orally once daily for 14 days. Plasma was separated and ALT assay was performed. Significance was determined by one-way-ANOVA with Bonferroni post-hoc test. All data are presented as mean ± SEM, n=6. None were significantly different.

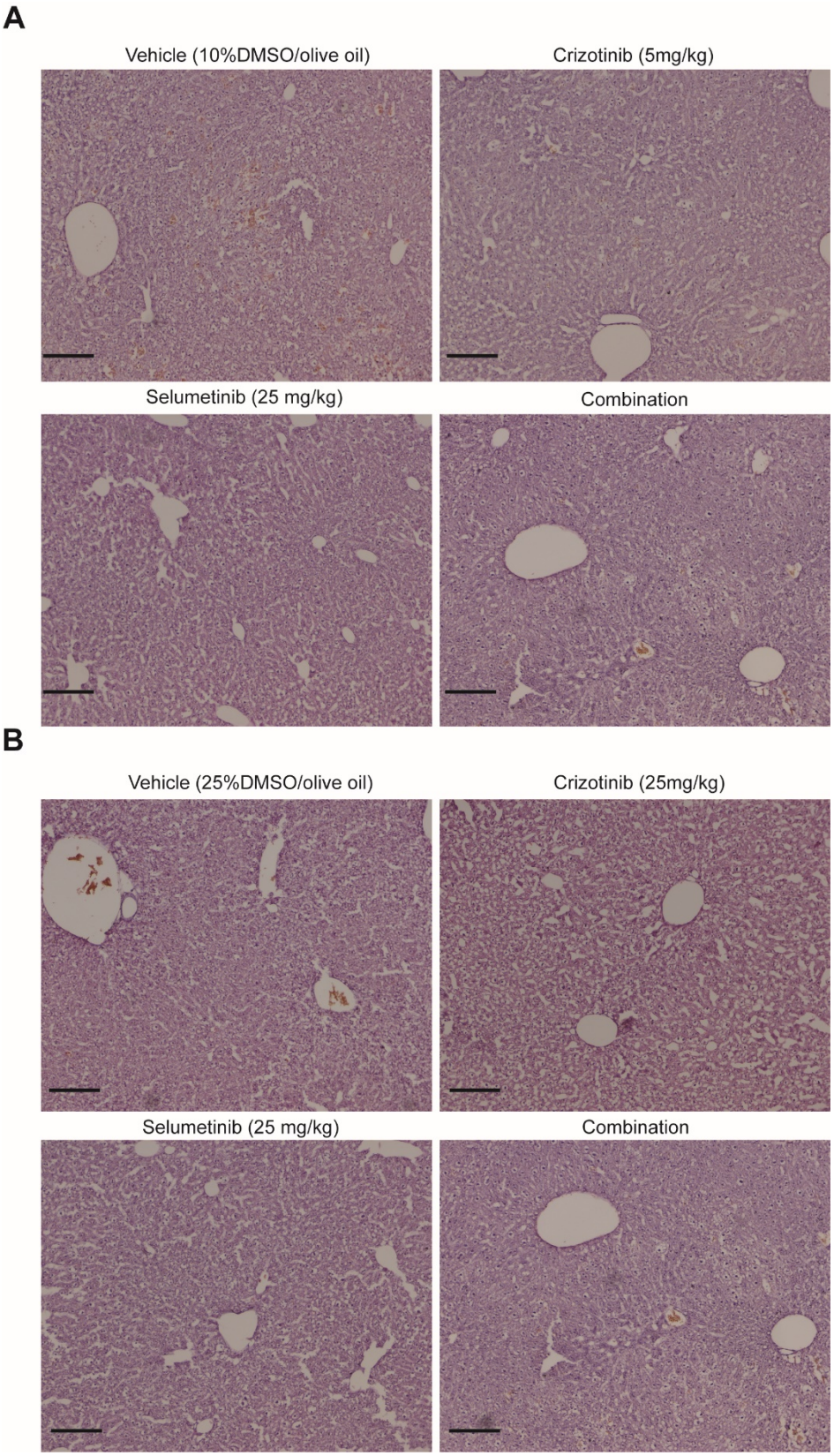

Figure 3.6 Histology of Liver sections. Mice were treated with the (A) vehicle (10%DMSO/ 90%olive oil), crizotinib (5 mg/kg), selumetinib (25 mg/kg) and their combination, (B) vehicle (25%DMSO/ 75%olive oil), crizotinib (25 mg/kg), selumetinib (25 mg/kg) and their combination, orally once daily for 14 days. The liver was excised, and H and E staining was performed. Morphological change in livers sections with elevated ALT was analysed. The picture was taken at 10×. Scale bar: 100 µm**.**

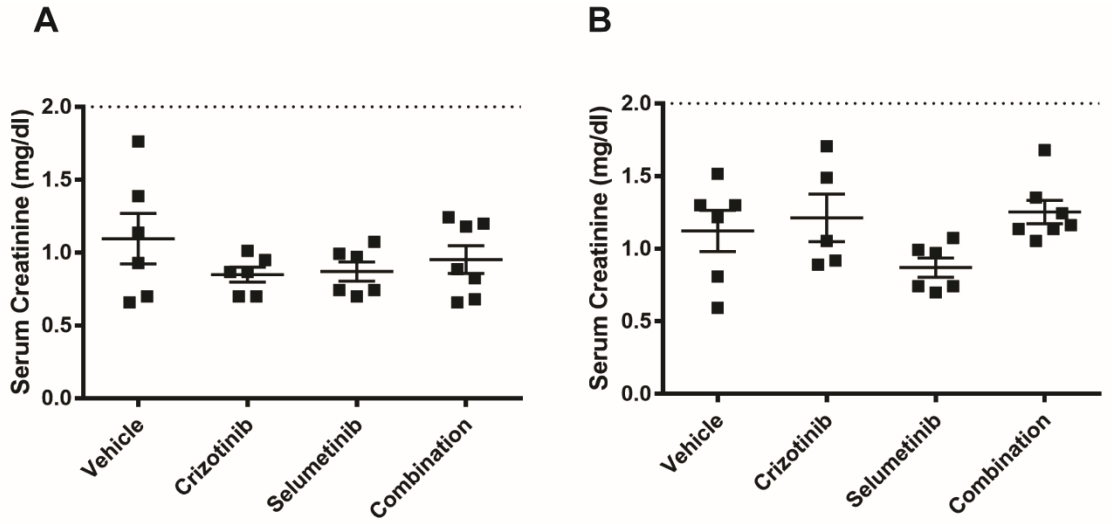

Figure 3.7 Effect of crizotinib, selumetinib, and their combination on kidney function in Balb/c mice. Mice were treated with the (A) vehicle (10%DMSO/ 90%olive oil), crizotinib (5 mg/kg), selumetinib (25 mg/kg) and their combination, (B) vehicle (25%DMSO/ 75%olive oil), crizotinib (25 mg/kg), selumetinib (25 mg/kg) and their combination, orally once daily for 14 days. Plasma was separated and creatinine assay was performed. Significance was determined by one-way-ANOVA with Bonferroni post-hoc test. All data are presented as mean ± SEM, n=6. None were significantly different

3.4.4. Effect of the combination treatment on CYP3A activity

To determine whether crizotinib and selumetinib alone or in combination could alter the activity of their major metabolising enzyme CYP3A was investigated. Balb/c mice were treated with the vehicle (DMSO/olive oil), crizotinib (5 mg/kg or 25 mg/kg), selumetinib (25 mg/kg), and their respective combination orally once daily for 14 days. The liver was excised, microsomes were prepared, and the CYP3A assay was performed. There was no significant change in CYP3A catalytic activity in single or combination treatment of crizotinib and selumetinib compared to the vehicle control. Used as a positive control to check on assay validity, dexamethasone, a CYP3A inducer, significantly increased CYP3A catalytic activity compared to the vehicle control ($p < 0.05$, one-way ANOVA) (Figure 3.8A and 3.8D). Furthermore, Western blotting of microsomal protein showed no change in polypeptide levels of hepatic CYP3A by crizotinib, selumetinib and their combination (Figure 3.8C and 3.8F). Again, a significant increase in CYP3A protein by dexamethasone compared to vehicle control was observed (Figure 3.8C and 3.8F) ($p < 0.05$, one-way ANOVA). These results suggest that neither crizotinib (5 mg/kg or 25 mg/kg) nor selumetinib (25 mg/kg) nor a combination of the two alter the metabolism of either drug.

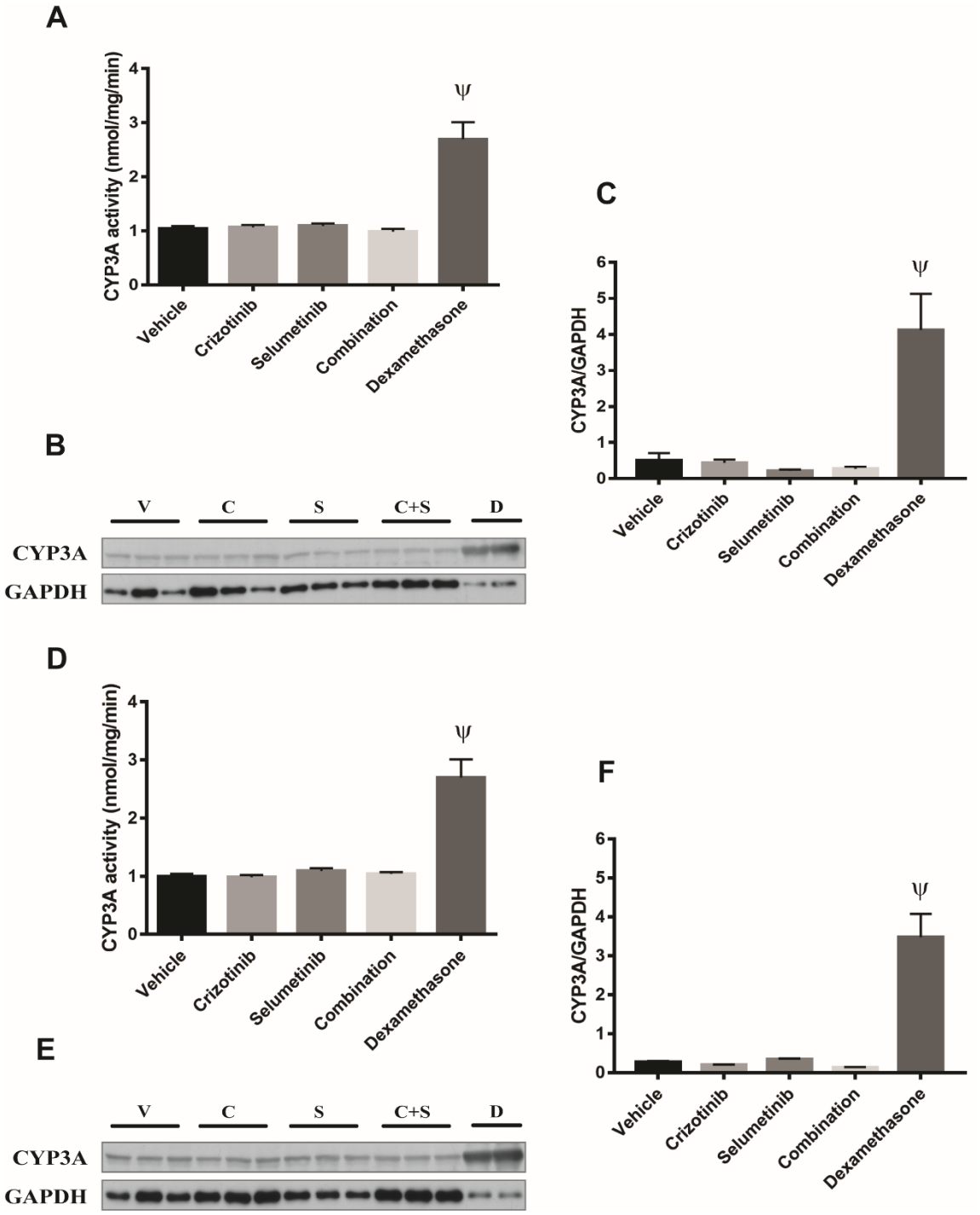

Figure 3.8 Effect of crizotinib, selumetinib and their combination on CYP3A enzyme. (A) CYP3A catalytic activity, (B) Representative Western blots of CYP3A, (C) Densitometry of Western blots of CYP3A of Balb/c mice orally gavaged with vehicle (10%DMSO/olive oil), crizotinib (5 mg/kg), selumetinib (25 mg/kg) and their combination once daily for 14 days. (D) CYP3A catalytic activity, (E) Representative Western blots of CYP3A, (F) Densitometry of Western blots of CYP3A of Balb/c mice orally gavaged with vehicle (25% DMSO/olive oil), crizotinib (25 mg/kg), selumetinib (25 mg/kg) and their combination once daily for 14 days. The liver was harvested and microsomes were prepared. V: vehicle, C: crizotinib, S: selumetinib, C+S: combination, D: dexamethasone. Significance was determined by one-way-ANOVA with Bonferroni post-hoc test. All data are presented as mean ± SEM. Ψ $p < 0.05$ significantly different compared to vehicle control, crizotinib, selumetinib and the combination.

3.5. Discussion

The efficacy of crizotinib and selumetinib combination treatment and their underlying molecular mechanism of tumour suppression was investigated in a xenograft model of ALK-positive NSCLC. Furthermore, the toxicity of both the singular and combination treatment was examined. Lastly, the effect of crizotinib, selumetinib and their combination on the catalytic activity of hepatic CYP3A was determined. The combination showed superior efficacy with substantial tumour suppression compared to single drug treatment, but unexpectedly, selumetinib alone was almost as effective as the two drugs combined. Both the singular and combination treatment elicited no significant toxicity. Moreover, the two drugs had no effect on CYP3A activity and thus were unlikely to alter each other's metabolism.

The combination treatment significantly reduced tumour volume compared to all other treatments. This finding was consistent with the effect of drugs in *in vitro* study, where the combination of crizotinib and selumetinib synergistically inhibit the proliferation of ALK-positive NSCLC cells. The combination almost abolished the RAS/MAPK signalling resulting in a marked decrease in cell proliferation and increase in apoptosis compared to the single drug treatment. Interestingly, selumetinib alone reduced tumour growth to almost the same degree as the drug combination. Nevertheless, the unexpected efficacy of selumetinib as a monotherapy *in vivo* does not support the hypothesis that dual MEK/ALK inhibition in ALK-positive cancer would add benefit beyond what could be achieved by a sufficient dose of a MEK inhibitor alone. This conclusion is supported by toxicology results where 25 mg/kg/day selumetinib did not elevate any of the measures of toxicity. Thus, results comparable to combination drug treatment may be achieved by a MEK inhibitor alone at a tolerable dose.

The results here are in contrast to *in vitro* experiments using H3122 cells, where selumetinib alone was 30-fold less potent at reducing cell viability than crizotinib alone. The reasons for the difference between these *in vitro* and *in vivo* results are unclear. The bioavailability of crizotinib (43%) (Kwon & Meagher,

2012) is only slightly less than that of selumetinib (62%) (Dymond et al., 2016); an insufficient difference to explain the contrast between the results obtained in *in vitro* previously and *in vivo*. The possible differences in drug metabolism may explain the difference in the results. Crizotinib is a primary substrate of CYP3A, and according to *in vitro* studies causes moderate CYP3A protein inhibition and induces mRNA expression (Johnson et al., 2015; Mao et al., 2013; Tan et al., 2010). CYP3A is also the major enzyme responsible for selumetinib metabolism (Dymond et al., 2016). It was hypothesised that CYP3A activity could be greater in mice treated with crizotinib, reducing crizotinib exposure compared to selumetinib administered alone. Nevertheless, no differences were detected in hepatic CYP3A activity and their polypeptide levels among crizotinib, selumetinib, and their combination compared to the vehicle control.

Furthermore, immunohistochemistry was performed in attempts to determine the reasons for the unexpected efficacy of selumetinib as a monotherapy in this study. Both selumetinib and crizotinib are known to have anti-tumour activity by increasing apoptosis and decreasing cell proliferation and angiogenesis (Cozzo et al., 2016; Dai et al., 2017; Takahashi et al., 2012). It was first hypothesised that selumetinib may have had an anti-angiogenic effect through suppression of ERK activation (Murphy et al., 2006). Contrary to this hypothesis, both single and combination treatments did not reduce MVD in tumours taken from mice at day 14 compared to the vehicle control as measured by CD105 immunolabelling (Figure 3.3B). It was then hypothesised that the selumetinib treated tumours would show an increased frequency of apoptosis. Contrary to this hypothesis apoptosis was upregulated only in the crizotinib group compared to the vehicle control (Fig. 3.4B). Finally, it was hypothesised that tumour suppression was due to a cytostatic effect of selumetinib, but in contradiction to this, there were no differences in proliferating cell frequency as measured by Ki67 immunolabelling (Fig. 3.2B).

In vitro study had demonstrated that crizotinib, selumetinib and their combination significantly increased G1 phase arrest using flow cytometry. However, Ki67 is present in G1, S, G2 and the mitotic phase, and only absent in

the G0 phase of the cell cycle (Bruno & Darzynkiewicz, 1992; Guillaud et al., 1989). Therefore, Ki67 labelling may not accurately reflect the response to treatment, as it would not differentiate between cells in G1 arrest and other cells. Moreover, the predictive value of Ki67 labelling index for response to chemotherapy remain controversial. In breast cancer clinical trials, the Ki67 labelling was reported to be an independent prognostic factor but it was not related to improved treatment response (International Breast Cancer Study, 2002; Viale et al., 2008; Yerushalmi et al., 2010). Additionally, in an animal study using a triple negative breast cancer xenograft model, an univariate statistical analysis showed that Ki67 labelling in tumour sections from control and treated mice were comparable, where significant tumour suppression was achieved (Martey et al., 2017). However, a multivariate analysis showed that Ki67 played an important role as a component of a biological network of 16 molecular targets that as a whole predicted treatment outcome with a 95% success rate (Martey et al., 2019). Thus, it is likely that Ki67 also plays a crucial role as a part of a larger protein network in the suppression of H3122 xenograft tumours. Multivariate analysis of different molecular targets of the combination treatment can help to identify the biological networks and interaction between signalling proteins that are crucial in suppression of tumour growth.

Furthermore, suppression of ERK activation is also known to stimulate T-cells activation in some cancers (Ebert et al., 2016). It is highly unlikely that this could account for the results, as the xenograft model employed athymic mice. Further studies are needed to ascertain the translatability of these findings to humans.

Chapter 4: Development of an orthotopic lung cancer model

This chapter is based on the following publication:

Shrestha N, Lateef Z, Martey O, Bland A, Nimick M, Rosengren R, Ashton J. Does the mouse tail vein injection method provide a good model of lung cancer? [version 1; peer review: 2 approved]. F1000Research 2019, **8**:190

J.S, R.R contributed on experimental design, N.S carried out experiments and data analysis, Z.L contributed in tail vein injection, M.N, A.B, O.M provided technical assistance

4.1. Introduction

The development of an appropriate animal model is crucial for translational cancer research to be successful. Mouse models of cancer not only provide an opportunity to learn about cancer molecular biology in the dynamic physiological system, but also facilitates the investigation of novel anti-cancer therapy (Cheon & Orsulic, 2011; Zhang, Moore, et al., 2011). Prior to clinical trials, extensive preclinical studies are conducted to examine the preliminary pharmacokinetics, toxicity and efficacy of anti-cancer drugs (Mak et al., 2014). It is the purpose of this chapter to report on attempts to develop a new and improved mouse model of ALK positive lung cancer.

4.1.1. Mouse models in cancer research

Mouse models in cancer research can be categorised into xenograft, genetically engineered, syngeneic, and chemical induced model (Cekanova & Rathore, 2014; Cook et al., 2012; Kellar et al., 2015). Each model has its own advantages and limitations.

4.1.1.1. Xenograft models

In xenograft cancer models, cancer cells of either human or animal origin are transplanted either subcutaneously under the flank (ectopic) or directly into the organ of tumour origin (orthotopically) in immunocompromised athymic nude mice or severely compromised immunodeficient SCID mice (Bibby, 2004; Liu et al., 2012; Morton & Houghton, 2007; Ruggeri et al., 2014). Athymic nude mice are deficient in T lymphocytes whereas, SCIDs mice are deficient in both B and T lymphocytes making them a suitable host for transplantation of human cancer cells (Bosma & Carroll, 1991; Flanagan, 1966). On the other hand, in immunocompetent mice the human cancer cells are likely to be rejected by the host immune system (Kellar et al., 2015). The use of human cancer cells in xenograft models facilitate the accurate representation of the complexities of human tumour (Kellar et al., 2015). Moreover, orthotopic cancer models closely mimic the microenvironment of human tumours and thus, provide a clinically

relevant system for evaluating novel drug therapies (Kellar et al., 2015; Onn et al., 2003). The main drawback of xenograft cancer models is the use of immunocompromised mice that may not represent natural responses of cancers in humans (Cekanova & Rathore, 2014).

4.1.1.2. Genetically engineered mouse models

Genetically engineered mouse (GEM) models are generated by the manipulation of the mouse germline. They are developed either by activating oncogenes or suppressing tumour suppressor genes via different approaches such as transgenic, gene-targeting such as knockouts, knockins, conditional and inducible, RNA interference or chromosomal engineering (Cheon & Orsulic, 2011; Zhang, Moore, et al., 2011). Transgenic mice are generated by microinjection of DNA into the pronuclei of fertilised zygotes where the transgene sequences are integrated into the mouse genome (Cekanova & Rathore, 2014). This model can be applied to study the role of genetic abnormalities in tumour initiation and progression (Kellar et al., 2015). The major limitation of transgenic models is the inability to control the level and pattern of transgene expression (Cheon & Orsulic, 2011).

4.1.1.3. Syngeneic mouse models

Syngeneic mouse model is developed by injecting immunologically compatible cancer cells into immunocompetent mice. The Lewis lung carcinoma (LCC) model is currently the only reproducible syngeneic model for lung cancer. As these models are fully immunocompetent, they provide actual immune and toxicity responses to cancer therapy and tumour growth (Kellar et al., 2015; Olson et al., 2018). However, the main limitation of the syngeneic model is that its therapeutic efficacy is poorly translated in humans. This is most likely due to inherent differences in human and mouse cancer biology (Cook et al., 2012; Kellar et al., 2015).

4.1.1.4. Chemically induced mouse models

Chemically induced mouse models are generated by exposure to carcinogens such as N-ethyl-N-nitrosourea, N-butyl-N-(4-hydroxybutyl) nitrosamine, N-ethyl-N-nitrosourea, azoxymethane, benzopyrene, urethane 31 and asbestos fibres (Cekanova & Rathore, 2014). This method uses the inbred mouse strains such as A/J or SWR that are susceptible to tumorigenesis (Kellar et al., 2015).

4.1.2. Mouse models in lung cancer

Lung cancer is the leading cause of cancer death worldwide (Ferlay et al., 2015). This gives rise to the need for the development of a clinically relevant animal model of lung cancer that can facilitate the development of novel therapeutic strategies. Different mouse models of lung cancer have been developed using different technique (Kellar et al., 2015).

The mouse model of lung cancer is developed by grafting the lung cancer cells of mouse origin onto a host mouse or induced in tissue by genetic modification or exposure of carcinogens (Henry et al., 1981; Kellar et al., 2015; Soda et al., 2008). The major disadvantages of these models are that they produce tumours of mouse origin that do not recapitulates human cancer (Kellar et al., 2015). On the other hand, the human lung cancer cells are grafted either in the flank (ectopic) or directly into the lungs (orthotopic) of immunocompromised mice, such as SCID or nude mice (Kellar et al., 2015). The ectopic xenograft model of lung cancer is convenient to develop and has been extensively used, but the model does not mimic the organ environment in which the tumour naturally grows (Liu et al., 2012; Richmond & Su, 2008). However, the orthotopic model of lung cancer closely mimic the tumour microenvironment and are clinically relevant (Kang et al., 2006; Liu et al., 2012; Onn et al., 2003).

Orthotopic lung cancer models can be developed by several different methods. The cells may be directly injected into the lung either by intrathoracic implantation via puncture (Liu et al., 2012) or the cells may be introduced into the airways by intratracheal (Kang et al., 2006) or intrabronchial injection (McLemore et al., 1987; Nakajima et al., 2014). Intrathoracic implantation, by

direct puncturing through the intercostal space to lung parenchyma, avoids thoracotomy or intubation, but increases the risk of intrathoracic haemorrhage and haemoptysis (Liu et al., 2012). The intrapulmonary implantation of lung cancer cells generates a site-specific tumour. However, the disadvantages of this method are the requirement of endotracheal intubation and thoracotomy (McLemore et al., 1987; Wang et al., 1997). Nonsurgical bronchial implantation enables the development of a tumour in a lung without causing pneumothorax, bleeding, pleural dissemination, or effusion, but the risk of death during cancer cell inoculation was increased (Nakajima et al., 2014).

Due to the various problems in existing lung cancer models, an orthotopic model of lung cancer was attempted by engraftment via vascular delivery and pulmonary entrapment. This method has been successfully used to create lung tumour nodules in the lungs of immunocompetent mice using Lewis lung carcinoma cells (Zhao et al., 2012) and breast cancer lung metastasis (Rashid et al., 2013) but has not been used to study non-small cell lung cancer using human lung adenocarcinoma cells in immunocompromised mice.

4.2. Aim and objectives

The aim was to establish an orthotopic lung cancer model via tail vein injection of human lung adenocarcinoma cells. The specific objectives were (1) to characterise the tumour nodules from an orthotopic lung cancer model, (2) to detect the human cancer cells in the lung sections from the orthotopic lung cancer mouse model and, (3) to determine the presence of EML4-ALK fusion in the lung sections of mice injected with H3122 cells

4.3. Methods and Materials

4.3.1. Materials

4.3.1.1. Chemical reagents

Crizotinib and selumetinib were purchased from LC laboratories (Woburn, MA, USA). RPMI, BSA, FBS, and penicillin/streptomycin were purchased from Life Technologies (Auckland, New Zealand). 3, 3'-diamino benzadine (DAB) substrate kit and streptavidin-horseradish peroxidase were purchased from BD Biosciences (San Diego, CA, USA). Haematoxylin quick stain (QS) (modified Mayer's formula), avidin-biotin blocking kit were purchased from Vector Laboratories (Burlingame, CA, USA). Acetone, acetylacetone, hydrogen peroxide (30%) and methanol were obtained from Merck (Billerica, MA, USA). Citric acid, DMSO, ethylenediaminetetraacetic acid (EDTA), eosin Y solution alcohol, glycerol, PBS, poly-L-lysine, trizma hydrochloride (Tris-HCL), and xylene (DPX) mounting medium were purchased from Sigma Aldrich (St Louis, MO, USA). Xylene was purchased from Bio-lab (Auckland, New Zealand). Dako pen was purchased from Dako (Glostrup, Denmark)

4.3.1.2. Antibodies

Antibodies against ALK, p-ALK were purchased from Cell Signaling Technology (Danvers, MA, USA). Ki67 antibody was obtained from Abcam (Cambridge, UK). Polyclonal goat anti-rabbit immunoglobulin/biotinylated were purchased from Dako (Glostrup, Denmark). HRP-conjugated goat anti-rabbit was obtained from Calbiochem (San Diego, CA, US).

4.3.2. Methods

4.3.2.1. Cell culture

Cell culture was carried out as described in **Section 2.3.2.1** of **Chapter 2.** Briefly, A549 cells and H3122 cells were maintained in RPMI supplemented with penicillin (100 U/mL), streptomycin (100 µg/mL) and 2% and 5% of FBS,

respectively. Cells were grown in a humidified incubator at 37°C, 5% CO_2 and 95% O_2.

4.3.2.2. Animal housing and care

Male immunocompromised SCID mice were purchased from Animal Resources Centre, Australia (Canning Vale, Australia). SCID mice were housed in pathogen-free condition with sterile woodchip bedding supplied with sterile food (Reliance rodent diet, Dunedin, NZ) and water. Mice were kept in a room maintained at a temperature of 21-24°C with relative humidity at 30 ± 5% on a scheduled 12 h light/dark cycle. All the animal experiments were performed after approval by University of Otago (AEC #9/17).

4.3.2.3. Tail vein injection

Immunocompromised male SCID mice (n=48) weighing 20-30 g were divided into two identical experiments that comprised of 24 mice each. In each experiment, cell suspension of H3122 cell (1×10^6 cells/ml) and A549 cell (1×10^6 cells/ml) in isotonic PBS was prepared. Mice were restrained, the tail was warmed for 3-5 min to dilate the veins, and then 100 µL of cell suspension containing either 1×10^5 H3122 cells or 1×10^5 A549 cells was injected into the lateral vein of the tail by the use of insulin syringes (needle bevel up) (12.7mm × 29G needle). Mice were weighed daily and monitored for respiratory distress, mobility, and signs of pain daily for up to 8 weeks. A weight loss of more than 20% was considered to be unacceptable and would lead to early euthanisation of the mouse. At the end of 3rd, 5th, and 8th week in each experiment, 4 mice from each group (i.e., 8 mice across the two repeats of the experiment) were euthanised by CO_2 inhalation and perfused with isotonic PBS followed by 10% formalin. Major organs such as lungs, liver, kidney, spleen, brain, heart, testes were excised, weighed, and washed with isotonic PBS. The organs were then kept in 10% formalin for 48 hours at 4°C. On the following day, the organs were washed with isotonic PBS and were kept in 30% starch solution for 24 hours at 4°C. Finally, organs were embedded in OCT and were frozen immediately in liquid nitrogen. The frozen organs were stored in -20°C. Lungs were quickly

photographed prior to fixation and compared with the lungs taken from SCID mice that were not injected with lung cancer cells, from another experiment.

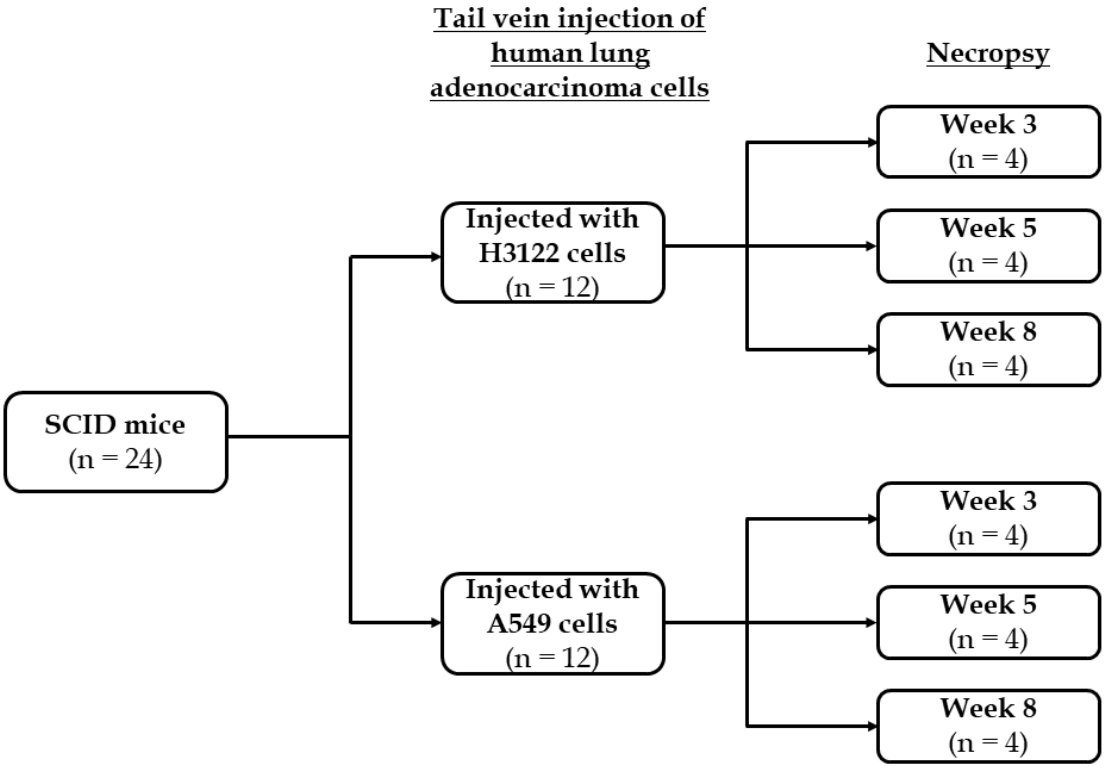

Figure 4.1 Schematic diagram of the study design of development of orthotopic lung cancer mouse model. Two identical experiments with total of (n = 48) mice was carried out as described in the **Section 4.3.2.3**

4.3.2.4. Histology

The frozen lungs were sliced at a thickness of 6-µm using cryostat maintained at -20°C. The lung sections were placed on poly-L-lysine-coated microscope slides and then air-dried overnight. The sections were then stored at -20°C until required.

Lung sections were thawed for 30 min at room temperature followed by washing in isotonic PBS two times for 5 min each. Next, sections were fixed by incubating in the mixture of an equal volume of acetone and methanol for 10 min at room temperature. This was followed by washing the section in distilled water (dH_2O) for 10 sec. Heamotoxylin QS (H-3404) was added to each section and incubated for 25 sec. Then, the sections were rinsed in tap water until the blueish colour was obtained. The sections were washed in dH_2O and dipped in 95%

ethanol for 15 sec. Eosin was then added and incubated for 45 sec. The excess of eosin was removed by rinsing in 95% of ethanol. Next, the sections were dehydrated in increasing concentration of ethanol (70%, 95% and 100%ethanol) for 2 min each. Lastly, the sections were soaked in xylene for 5 min for two times and mountant in DPX mounting solution. Coverslip mounted sections were then examined by two examiners blinded to the treatment groups using a Nikon RM229 microscope.

4.3.2.5. Immunohistochemistry

Ki67

Lung sections of 6-µm thickness were sliced. The sections were thawed for 30 min at room temperature and washed in isotonic PBS for two times 5 min each. Then, the sections were fixed in acetone for 10 min at room temperature. The excess of acetone was aspirated and then treated with 0.3 % H_2O_2 in methanol for 20 min. The sections were air-dried, and the circle was drawn around the section with DAKO pen. Sections were washed with isotonic PBS three times for 2 min each. Antigen retrieval was performed by boiling (at 95^{o}C in water bath) the section in a citrated buffer (10mM citric acid, 0.05% Tween-20) pH 6 for 20-30 min followed by cooling in the same solution for 30 min. Then, the sections were washed with isotonic PBS two times for 5 min each and incubated in range of blocking solution (1.5%-5% goat serum, 0.2%-5% BSA) for 1 h at room temperature in a humidified chamber. Avidin-biotin blocking was performed for the sections treated with biotinylated secondary antibodies. The sections were rinsed with isotonic PBS for 5 min and incubated in primary antibody (Monoclonal mouse anti-human antigen Ki67) at a 1:100 dilution in 0.2% BSA for overnight in a humidified chamber at 4^{o}C.

On the following day, the primary antibody was aspirated, and sections were washed with isotonic PBS four times for 5 min each. The sections were then incubated for up to 2 h with either HRP-conjugated secondary anti-rabbit secondary antibody or up to 45 min with biotinylated secondary antibody (1:100 dilution in 0.2% BSA) was added at room temperature. The streptavidin was

applied for 30 min at room temperature (only for sections incubated with biotinylated secondary antibody). and a signal was detected using DAB. The sections were counterstained with haematoxylin QS. The sections were dehydrated in increasing concentration of ethanol (70%, 95% and 100%) for 2 min each, soaked in xylene and then mountant with DPX mounting solution. Finally, the sections were examined using the Nikon RM229 microscope.

p-ALK

Frozen sections sliced at a thickness of 6-µm were thawed for 30 min followed by washing in isotonic PBS twice for 5 min each. The sections were then fixed in acetone for 10 min and incubated with 3% H_2O_2 in methanol for 20 min. Antigen retrieval was carried out by boiling (at 95^{o}C in water bath) in EDTA buffer (1mM EDTA and 0.05% Tween 20) pH 9 for 30 min and then cooling the sections in same buffer solution for 30 min at room temperature. The sections were incubated in range of blocking solution (1.5%-5% goat serum, 0.2%-1% BSA) for 1 h in a humidified chamber at room temperature. Avidin-biotin blocking was performed for the sections treated with biotinylated secondary antibodies. This was followed by incubation with p-ALK antibody (1:100 in 0.2% of BSA) for 48 hrs in a humidified chamber at 4^{o}C.

Next, the sections were washed with isotonic PBS four times for 5 min and were incubated for up to 2 h with either HRP-conjugated secondary anti-rabbit secondary antibodies or up to 45 min with biotinylated secondary antibody (1:100 dilution in 0.2% BSA) was added at room temperature. The streptavidin was applied for 30 min at room temperature (only for sections incubated with biotinylated secondary antibody) and a signal was detected using DAB. The sections were counterstained with haematoxylin QS, dehydrated and mounted. Finally, the sections were examined using the Nikon RM229 microscope.

4.3.2.6. Statistical analysis

Comparison of weight gain over time between H3122 and A549 cells injected mice was analysed using linear regression. Comparison of body weight

change within a group (3rd, 5th, and 8th week) of mice injected with H3122 and A549 was analysed using one-way ANOVA with Bonferroni post-hoc test. Organ weight at necropsy was analysed using one-way ANOVA with Bonferroni post-hoc test. GraphPad prism V7 was used to carry out all statistical analyses.

4.4. Results

4.4.1. Body weight and Organ weight

Mice were weighed daily and monitored for mobility, respiratory distress, and signs of pain to determine whether the tail vein injection of human lung adenocarcinoma cells affected mouse health. Mice injected with H3122 cells had slightly higher baseline body weight compared to those injected with A549 cells by 1.8 g (Figure 4.2, F value = 884.5, degree of freedom in the numerator (DFn) = 1, degree of freedom in the denominator (DFd) = 111, $p < 0.0001$, linear regression). This difference in weight was maintained throughout the study and there was no significant difference in the rate of weight gained between them (Figure 4.2, 0.068 g/day for mice injected with A549 cells and 0.075g/day for mice injected with H3122 cells, F value = 2.549, DFn = 1, DFd = 110, $p = 0.1133$, linear regression). After 50 days of injecting the cells, mice started to show signs of distress evident as hunched posture, immobility, rough coats, and laboured breathing. At this point mice injected with A549 cells began to lose weight at the rate of 0.08 g/day. However, this was not significant (F value = 1.52. DFn = 1, DFd = 6, $p = 0.2638$, linear regression). On the 8th week, one of the mice had protruding eyes and was euthanised. Following this, remaining mice were also euthanised within a day.

The change in body weight after the 3rd, 5th and 8th week of mice injected with H3122 and A549 cells are presented in Table 4.1 and Table 4.2, respectively. In H3122 injected mice, the change in body weight was significantly higher in mice euthanised at 8th week compared to those in 3rd week. However, in A549 injected mice, the change in body weight was significantly higher in mice euthanised at 8th week compared to those in both 3rd and 5th week.

Furthermore, there were no significant differences in organ weight (expressed as % of body weight) between any of the groups (3rd, 5th and 8th week) ($p > 0.05$, one-way ANOVA) as shown in Table 4.1 and Table 4.2. On visual examination of the lungs, indistinguishable or minimally apparent white patches were observed after 3rd weeks necropsy mice. By the 5th week, numerous

superficial white patches started to appear that further spread widely by week 8 (Figure 4.3 and Figure 4.4). However, no abnormalities were observed in lungs of SCID mice from another experiment that was not injected with lung cancer cells.

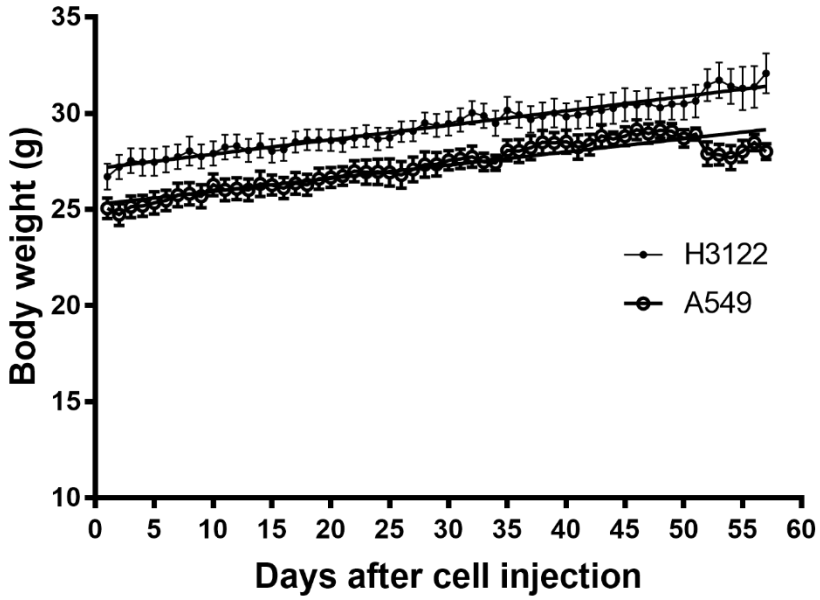

Figure 4.2 Body weight of SCIDS mice injected with H3122 or A549 cells over 8 weeks. SCIDS mice were injected with cell suspension containing either 1 ×10^5 H3122 cells or 1 ×10^5 A549 cells in the lateral vein of the tail. Mice were then euthanised at 3rd, 5th, and 8th week. All data are presented as mean ± SEM. Significance was determined by linear regression analysis**.**

Table 4.1 Body weight and organ weight of SCID mice injected with H3122 cells

	3rd week	5th week	8th week
Body weight change (g)	1.54 ± 0.51	3.01 ± 0.53	3.40 ± 0.58*
Organ weight (% of body weight)			
Liver	7.32 ± 0.52	7.67 ± 0.53	7.46 ± 0.35
Spleen	0.19 ± 0.02	0.19 ± 0.01	0.23 ± 0.01
Lungs	1.33 ± 0.09	1.61 ± 0.09	1.47 ± 0.12
Heart	0.74 ± 0.03	0.90 ± 0.04	0.81 ± 0.03
Kidneys	2.36 ± 0.12	2.44 ± 0.16	2.36 ± 0.07
Testes	0.62 ± 0.03	0.61 ± 0.03	0.57 ± 0.02
Brain	1.41 ± 0.06	1.23 ± 0.05	1.21 ± 0.04

Statistical significance was determined by one-way ANOVA with Bonferroni post-hoc test. All data are presented as mean ± SEM from n = 8. * Significantly increase compared to body weight change in 3rd week

Table 4.2 Body weight and organ weight of SCID mice injected with A549 cells

	3rd week	5th week	8th week
Body weight change (g)	2.34 ± 0.23	2.07 ± 0.41	3.75 ± 0.28*
Organ weight (% of body weight)			
Liver	6.79 ± 0.49	7.40± 0.47	8.30 ± 0.18
Spleen	0.20 ± 0.01	0.22 ± 0.04	0.22 ± 0.01
Lungs	1.18 ± 0.09	1.56 ± 0.09	1.46 ± 0.07
Heart	0.71 ± 0.02	0.88 ± 0.03	0.74 ± 0.02
Kidneys	2.26 ± 0.10	2.39 ± 0.11	2.48 ± 0.09
Testes	0.52 ± 0.04	0.64 ± 0.02	0.60 ± 0.03
Brain	1.29 ± 0.06	1.33 ± 0.06	1.27 ± 0.05

Statistical significance was determined by one-way ANOVA with Bonferroni post-hoc test. All data are presented as mean ± SEM from n = 8. * Significantly increase compared to body weight change in 3rd week and 5th week.

4.4.2. Histology and immunohistochemistry of lung sections

To characterise the tumour nodules in the lungs of mice injected with H3122 and A549 human lung adenocarcinoma cells, H and E staining was performed. Histology of the lungs did not show tumour cell nodules with distinct edges (Figure 4.3 and Figure 4.4). At the 3rd week, lung sections of mice injected with H3122 and A549 cells showed a sparse network of bronchioles, alveolar ducts, and sacs with infrequent areas where cells were aggregated in the parenchyma (Figure 4.3A and Figure 4.4A). By week 5, these areas spread widely and further spread through by week 8. A larger size of Figure 4.3 and Figure 4.4 are given in Appendix 1.3. and Appendix 1.4., respectively.

Immunohistochemistry was performed to examine the presence of cancer cells in the lung sections of H3122 and A549 cells injected mice. However, the areas of cellular density found in the lung sections could not be confirmed as cancer cells as no positive staining for tumour cell markers was observed. The primary antibody for human specific cell marker (Ki67) staining was not distinguishable from that for non-specific labelling in lung sections of mice injected with either cell line. Furthermore, no specific staining with either ALK or p-ALK antibodies was observed in mice injected with H3122 cells. Here, the section incubated with secondary antibody showed high amounts of non-

specific staining. Despite the use of a range of antigen retrieval techniques and different secondary antibodies (both directly conjugated to HRP, and biotinylated), specific labelling of the primary antibody was not detected in lung sections of mice injected with lung cancer cells compared to those not injected with lung cancer cells.

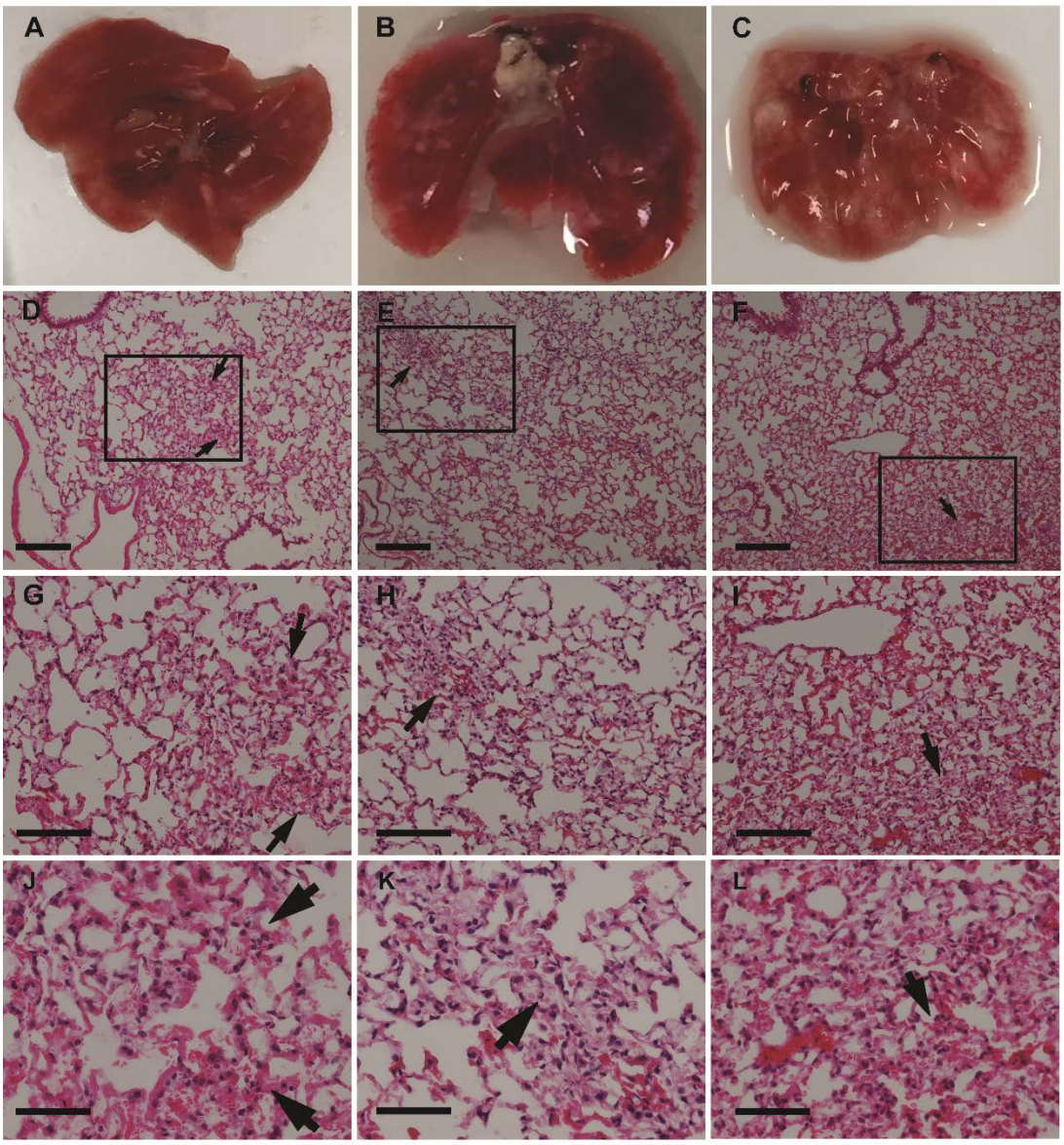

Figure 4.3 Gross appearance and histology of lungs of SCID mice after 3rd , 5th and 8th week of injection with H3122 cells via the tail vein. Mice were injected with 1×10^5 H3122 cells into lateral vein of the tail. Mice were then euthanised after 3rd, 5th and 8th week of injection. Lungs were excised, sectioned and H and E staining was performed. Lungs of mice at (A) 3rd, (B) 5th, (C) 8th weeks after cell injection. White patches on lungs appeared by week 5. H and E staining of lung sections of mice at (D) 3rd, (E) 5th, (F) 8th week after cells injection using a 10× objective. Squares and arrow indicate areas of high cell density. (G-I) Area shown in insets from panel (D-F) respectively, using 20× objective. (J-L) Area shown in insets from images (D-F), respectively, using 40× objective. Scale bars: D-I 100 µM and J-L 50 µM.

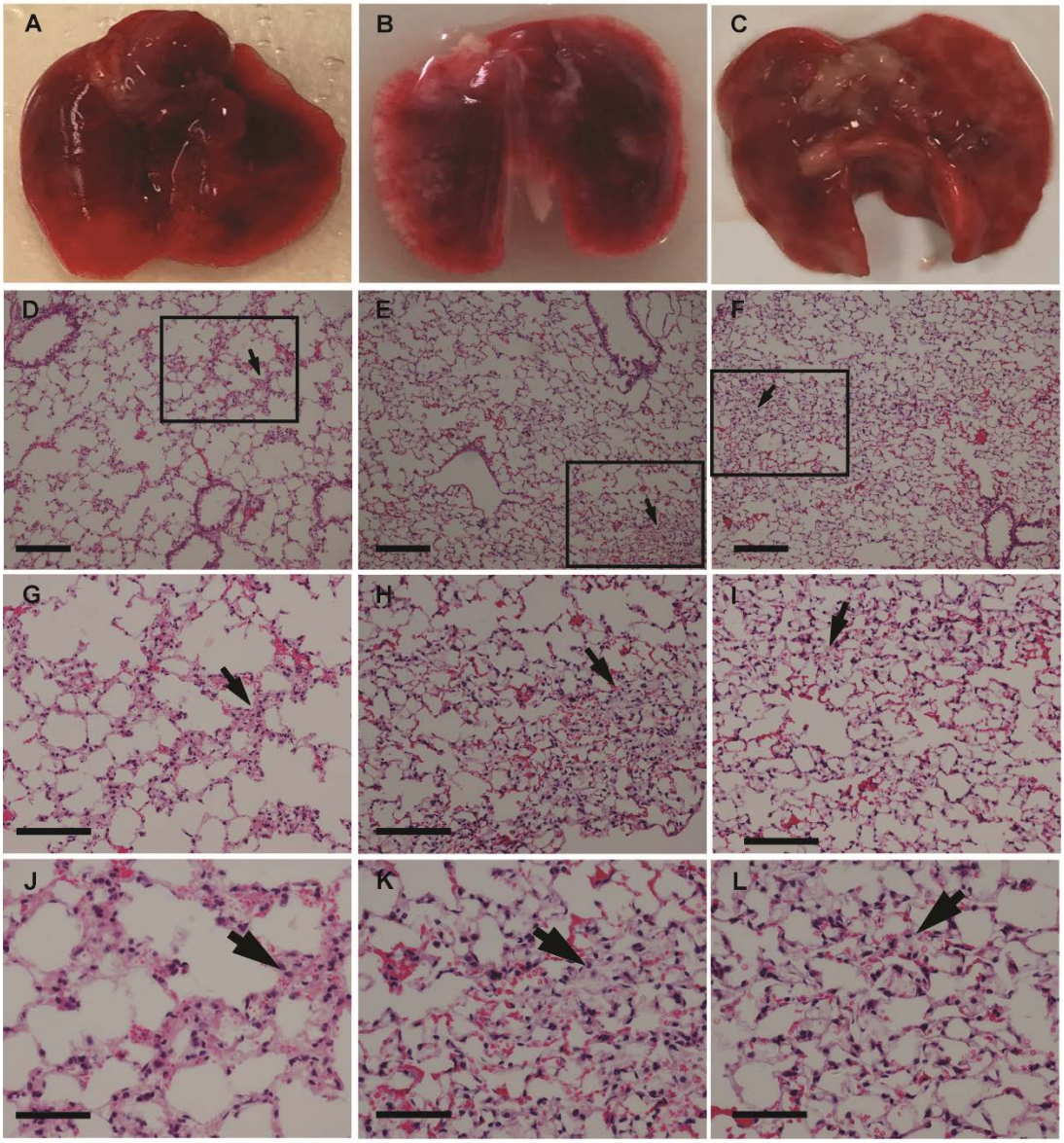

Figure 4.4 Gross appearance and histology of lungs of SCID mice after 3rd, 5th and 8th week of injection with A549 cells via the tail vein. Mice were injected with 1×10^5 A549 cells into the lateral vein of the tail. Mice were then euthanised after 3rd, 5th and 8th week of injection. Lungs were excised, sectioned and H and E staining was performed. Lungs of mice at (A) 3rd, (B) 5th, (C) 8th weeks after cell injection. White patches on lungs appeared by week 5. H and E staining of lung sections of mice at (D) 3rd, (E) 5th, (F) 8th week after cells injection using a 10× objective. Squares and arrow indicate areas of high cell density. (G-I) Area shown in insets from panel (D-F) respectively, using 20× objective. (J-L) Area shown in insets from images (D-F), respectively, using 40× objective. Scale bars: D-I 100 μM and J-L 50 μM.

4.5. Discussion

While it was intended to establish an orthotopic model of lung cancer via tail vein injection of human lung adenocarcinoma cells (H3122 and A549), the development of an orthotopic lung cancer model was not successful. Though some aggregation of cells were observed, discrete tumour nodules were not detected in the histology of the lung sections. Furthermore, no specific positive staining to human cancer markers such as Ki67 and ALK/p-ALK were detected in the lung sections.

The mice injected with human lung adenocarcinoma cells gained body weight during the period of the experiment compared to the baseline body weight though poor animal condition was observed 7-8 week following injection. At each necropsy, no gross physical changes were observed in the major organs. This was evident from no marked differences in their weight. Furthermore, there was a lack of visually identifiable abnormalities on the major organs, except on the lungs. However, further studies are warranted to confirm the infiltration of cancer cells into the major organs.

By the 5th week of necropsy, gross appearance of lungs showed the presence of numerous superficial white spots. Although, histological differences were observed, individual cancer cells could not be identified using immunohistochemistry. There may be two possible reasons for this. First, cancer cells may have been present but not detected by immunolabelling methods. This could potentially be due to over-fixation of lungs with formalin. Testing this hypothesis would require a repeat of the experiment, testing a range of fixation methods or other visualisation methods (such as fluorescently labelling cells). The second possible reason may be that the cancer cells have failed to engraft in the lung parenchyma, such that cellular aggregations in haematoxylin and eosin stained sections were either artefacts or pathological features secondary to embolism. However, this is difficult to reconcile with the time-dependent appearance of superficial lesions on the lungs, loss of body condition, and

increasing density of cells in lung histology, most apparent 8 weeks after injection of human lung adenocarcinoma cells.

Tail vein injection method for the development of animal cancer model is known to cause thromboembolism (Rashid et al., 2013) that can in turn cause localised ischaemia and tissue hypoxia (Evans et al., 2017). Thromboembolism is a significant cause of death in human lung cancer, following the development of tumour nodules (Chew et al., 2008). In the Chew et al. study, a sign of ischaemia was observed in mouse lungs at the beginning of week 5 after injection followed by a sudden decline in the health of the mice at 7-8 weeks. However, the use of tail vein injection method for the development of orthotopic lung cancer model did not result in visible tumour nodules. Additionally, cancer cells could not be detected. Therefore, the lung cancer model described here requires further development before it could be reliably used in preclinical drug development studies.

Chapter 5: Discussion

5.1. Synopsis of thesis

ALK-positive NSCLC most commonly expresses the EML4-ALK fusion protein and it is associated with patients of relatively young age and with a non-smoking history (Hallberg & Palmer, 2011; Shaw et al., 2009; Soda et al., 2007; Toyokawa & Seto, 2014b). Crizotinib is the first generation ALK-TKI with proven superiority over standard platinum-based chemotherapy (Solomon, Mok, et al., 2014). Despite impressive initial responses to crizotinib in over 60% of patients, resistance inevitably develops within a year or two of therapy (Choi et al., 2010; Solomon, Mok, et al., 2014). The aim of this thesis was to develop combination therapy that targets the primary oncoprotein and its major effector aimed at overcoming existing resistance and ultimately at delaying the emergence of resistance. The results of the experiments described in this thesis showed that the combination of the ALK inhibitor crizotinib with MEK inhibitor selumetinib significantly improved efficacy in both *in vitro* and *in vivo* studies. Unexpectedly however, selumetinib alone reduced tumour growth to almost the same degree as the combination treatment in xenograft model of ALK-positive NSCLC. Moreover, both the singular and combination of crizotinib and selumetinib was safe and elicited no alteration in each other's primary metabolizing enzyme, CYP3A. These findings support the clinical investigation of crizotinib and selumtinib combination therapy, but also suggest that much of the benefit of the combination may potentially be achieved using MEK inhibitor as a monotherapy.

5.2. Key findings of thesis

5.2.1. Combination treatment in ALK-positive NSCLC

The identification of an ALK-rearrangement oncogene as a therapeutic target and the development of potent ALK tyrosine kinase inhibitors (TKIs) has revolutionised treatment for ALK-positive patients (Camidge & Doebele, 2012). But despite initial responses, complete and lasting response to ALK-TKI monotherapy is rare to non-existent, as patients typically relapse within a year

of therapy (Sullivan & Planchard, 2015; Ziogas et al., 2018). This has been extended by sequential treatment with second or third generation ALK inhibitors such as ceritinib, alectinib or loratinib but only by several years (Gadgeel et al., 2014; Lin et al., 2017; Shaw, Friboulet, et al., 2016; Shaw et al., 2019; Ziogas et al., 2018). The median OS for ALK-positive NSCLC patients receiving crizotinib followed by a next generation ALK TKIs is 7 years (Pacheco et al., 2019). Therefore, overcoming ALK inhibitor resistance is an area of major research effort. Another promising strategy that can overcome and delay the emergence of resistance is combination therapy (Bozic et al., 2013; Crystal et al., 2014; Lovly & Pao, 2012; Zhou & Cox, 2015). Bozic et al. have concluded on theoretical grounds that the upfront combination of two drugs may be highly effective compared to sequential therapy in delaying the onset of drug resistance (Bozic et al., 2013). Their model predicted that failure of sequential treatment is high even in the absence of cross-resistance mutations, while simultaneous combination therapy has a potential to cure even in the presence of cross-resistance mutations (Bozic et al., 2013). This is because tumours are genetically diverse and are thus likely to contain a small population of cells that may confer resistant to any given drug. Therefore, the use of a single drug is highly unlikely to eradicate a tumour as these cells will survive and multiply resulting in treatment failure. Therefore, combining two or more drugs may increase the chance of improving survival and potentially even cure (Bozic et al., 2013).

Several potential combinations of ALK-TKIs with secondary TKIs for EGFR, IGFR, MEK1/2, STAT3 and SRC, HSP90 inhibitor, and immunotherapy have been investigated in a preclinical model and clinical trial of ALK-positive NSCLC (ClinicalTrials.gov National Library of Medicine (US), 2019a, 2019b; Courtin et al., 2016; Crystal et al., 2014; Cuyas et al., 2016; Hrustanovic et al., 2015; Lovly et al., 2014; Tanizaki, Okamoto, Takezawa, et al., 2012; Yamaguchi et al., 2014). Clinical studies are recruiting to test the efficacy of the combination of ceritinib with trametinib (ClinicalTrials.gov National Library of Medicine (US), 2019b) and alectinib with bevacizumab (ClinicalTrials.gov National Library of Medicine (US), 2019a) in ALK-positive NSCLC patients. Furthermore, Crystal et

al. (Crystal et al., 2014) reported that the combination of ceritinib and MEK inhibitor synergistically inhibit the proliferation of tumour cells in ALK-driven patient-derived *in vitro* and *in vivo* resistant model of ceritinib. They also demonstrated that a combination of crizotinib and SRC inhibitor effectively inhibited the proliferation of tumour cells in patient-derived *in vitro* and *in vivo* resistant models of crizotinib (Crystal et al., 2014). Similarly, combination of crizotinib with either EGFR or IGFR inhibitors showed synergistic inhibition in cell viability of ALK-positive NSCLC cells (Lovly et al., 2014; Wilson et al., 2017; Yamaguchi et al., 2014).

Hrustanovic et al. have identified RAS/MAPK pathway as a major downstream effector of EML4-ALK harbouring lung adenocarcinoma (Hrustanovic et al., 2015). Moreover, they showed that upfront dual inhibition of ALK and MEK enhanced the magnitude and duration of initial response in both *in vitro* and *in vivo* models of ALK-positive NSCLC (Hrustanovic et al., 2015). Building on the work of Hrustanovic et al. this thesis focused on MAPK pathway, targeting MEK, which is an early mediator upstream of ERK but downstream of ALK and other RTKs such as EGFR, IGFR, MET, KIT. Here, the combination of ALK inhibitor, crizotinib, and MEK inhibitor, selumetinib, significantly suppressed the proliferation of tumour cells in *in vitro* and *in vivo* model of ALK-positive NSCLC that complements and corroborates the finding of Hrustanovic et al.

However, there are some important differences between the result from this thesis and those of Hrustanovic et al. This can be explained firstly by a dose of trametinib and selumetinib used in an efficacy study of the combination treatment in xenograft model of ALK-positive NSCLC. Both trametinib and selumetinib are potent as MEK inhibitors (Wu & Park, 2015). Hrustanovic et al. have used the submaximal dose (1 mg/kg/day) of trametinib (Hrustanovic et al., 2015) whereas, in this study maximal dose (25 mg/kg/day) of selumetinib was used. Interestingly, selumetinib alone demonstrated unexpected efficacy in tumour suppression, unlike trametinib that had no marked effect as monotherapy in a xenograft model of H3122 cells.

Next, the combined effect of crizotinib and selumetinib was even greater in crizotinib resistant ALK-positive NSCLC cells, where even a low concentration of both drugs was sufficient to cause the significant suppression of cell proliferation. Clinical studies have suggested that targeting the resistance mechanism after the emergence of resistance may not be optimally efficacious (Johnson, Flaherty, et al., 2014). Johnson et al. showed that a combination of BRAF and MEK inhibitor after the emergence of resistance to BRAF inhibitor added no marked benefit to the patient with BRAF inhibitor-resistant melanoma (Johnson, Flaherty, et al., 2014). However, the dual inhibition of BRAF and MEK in the first line setting had a higher response rate and overall survival compared to BRAF inhibitors in patients with metastatic melanoma (Robert et al., 2015). Unlike for these results, the combination of crizotinib and selumetinib was highly effective in both crizotinib naïve and crizotinib resistant H3122 cells. Thus, the combination is likely to be beneficial even to patients with acquired resistance to crizotinib. However, specific studies are needed to ascertain the translation of these findings to human.

The precise mechanism of resistance in CR-H3122 cells has not been determined. In a previous study, Wilson et al. showed the upregulation of phosphorylation of SRC and ALK in CR-H3122 cells (Wilson et al., 2017). In a separate study, the sequencing of the ALK kinase domain in both H3122 and CR-H3122 did not reveal any differences (Appendix 1, Table A1.1). Thus, it was hypothesised that either ALK copy number is increased or ALK activation is dysregulated. Further studies are needed to understand the mechanism of resistance in CR-H3122 cells.

Taken together, the results presented in this thesis are consistent with the work of Bozic et al. (Bozic & Nowak, 2016; Bozic et al., 2013) who concluded that simultaneous combination therapy can be more effective than sequential combination therapy in delaying the emergence of mutations or combinations of mutations that confer resistance to both drugs (Bozic et al., 2013). Thus, an upfront combination of the two drugs could suppress the accumulation of mutations and ultimately extend the time to relapse.

5.2.2. Mechanism of tumour suppression

5.2.2.1. Effect on apoptosis

Apoptosis plays a vital role in maintaining tissue homeostasis and is responsible for eliminating unwanted, damaged cells (Baig et al., 2016; Hassan et al., 2014; Jin & El-Deiry, 2005). Dysregulation of the apoptotic pathway is a key characteristic of cancer that not only facilitates tumour growth and survival but also renders resistance to therapy (Hassan et al., 2014; Igney & Krammer, 2002). Thus, a key strategy for the treatment of cancer is the use of a drug that can induce apoptosis in cancer cells. Here, it was hypothesised that the combination of crizotinib and selumetinib would combine to increase apoptosis in crizotinib naïve and crizotinib resistant ALK-positive NSCLC cells.

Crizotinib has been reported to exhibit anti-tumour activity by induction of apoptosis in concentration dependent manner in both Karpas299 and SU-DHL-1 ALCL cells (Christensen et al., 2007). The authors reported a 3 to 4-fold increase in the number of apoptotic cells after treatment with 100 nmol/L crizotinib for 24 h (Christensen et al., 2007). Moreover, crizotinib was found to increase the percentage of apoptotic cells in dose dependent manner in both ovarian cancer cells (A2780 and SKOV3) (Huang et al., 2017) and pancreatic cancer cells (PANC-1) (Yan et al., 2014). Similarly, treatment with selumetinib resulted in concentration dependent apoptosis in diffuse large B-cell lymphoma (SUDHL4, SUDHL6 and OCI-LY19) cells (Bhalla et al., 2011). Selumetinib induced > 70% apoptosis in SUDHL4 and > 40% apoptosis in SUDHL6 cells with 200 nM for 48 h, whereas approximately 60% apoptosis in OCI-LY19 cells with 300 nM for 48 h (Bhalla et al., 2011). In breast cancer (MDA-MB-231 and HCC-1937) cells, selumetinib was found to increase the number of apoptotic cells in a concentration dependent manner (Zhou et al., 2016). In the present study, as hypothesised, the combination of crizotinib and selumetinib increased apoptosis compared to either of single drug treatment in both crizotinib naïve and crizotinib resistant ALK-positive NSCLC cells. This was mediated by upregulation of Bim, followed by an increase in the level of cleaved caspase-3 and cleaved PARP.

Bim is a BH3 only proapoptotic protein, belongs to the B-cell lymphoma 2 (Bcl-2) family. In response to cell stress, Bim binds to the anti-apoptotic/pro-survival Bcl-2 proteins through its BH3 domain, sequestering them or directly activating proapoptotic effectors BAX and BAK that in turn trigger permeabilisation of mitochondria. Apoptogenic factors such as cytochrome c get released from mitochondria which then activate the caspases. The activated caspase causes cleavage of multiple cellular proteins such as PARP which induce apoptosis (Bouillet & Strasser, 2002; Campbell & Tait, 2018; Chen et al., 2005; Degterev et al., 2003; O'Connor et al., 1998; Sionov et al., 2015; Strasser et al., 2000). Both crizotinib and selumetinib single drug treatment have been reported to induce apoptosis by upregulating the expression of Bim in various cancer cells including NSCLC cells (Bhalla et al., 2011; Tanizaki et al., 2011). In MET amplification-positive NSCLC (EBC-1 and H1993) cells, crizotinib was found to elicit apoptosis by increasing the expression of Bim. Transfection with siRNA specific to Bim mRNA was found to markedly suppress the upregulation of Bim by crizotinib that in turn resulted in a reduction of crizotinib induced apoptosis (Tanizaki et al., 2011). Crizotinib was also reported to upregulate Bim expression and induce apoptosis in FIG-ROS1-positive glioblastoma (U118) cells (Das et al., 2015). Furthermore, a clinical study by Zhang et al. has shown that the Bim deletion polymorphism in ALK-positive NSCLC patients was related with poor clinical response to crizotinib with shorter PFS (182 days vs. 377 days) and poor ORR (44.4% vs. 81.7%) compared to those without it (Zhang et al., 2017). Similarly, selumetinib was reported to induce apoptosis by upregulating the expression of Bim in NSCLC (Calu-6, H2347 and H3122) cells. Knockdown of Bim by SiRNA was found to markedly decrease the overexpression of Bim by selumetinib that in turn inhibited selumetinib induced apoptosis (Meng, Fang, et al., 2010). In B-cell lymphoma cells, treatment with selumetinib increased the expression of Bim (Bhalla et al., 2011). Thus, Bim is the critical effector for both crizotinib and selumetinib single drug treatment.

Furthermore, the apoptotic effect of crizotinib, selumetinib and their combination was further examined in this project using a xenograft model of

ALK-positive NSCLC. The TUNEL assays were performed to detect apoptotic cells in tumour sections. This assay is based on labelling of DNA breaks where terminal deoxynucleotidyl transferase (TdT) catalyse the attachment of deoxy-nucleotide binds to 3'-OH ends of DNA double stranded break (Gavrieli et al., 1992). Unexpectedly, apoptosis was upregulated only in the crizotinib treated group compared to vehicle control (although the difference was not significant). Neither selumetinib nor the combination exhibited greater apoptotic effect compared to crizotinib alone or vehicle control. These findings are in contrast to *in vitro* results where crizotinib and selumetinib individually elicited apoptosis and their combination synergistically increased apoptosis in H3122 and CR-H3122 cells. This may be explained in part by the cytostatic effect of selumetinib. Some investigators have reported that MEK inhibitors - including selumetinib - have had a mainly cytostatic effect in a preclinical model of acute myelogenous leukaemia. Inhibition of MEK alone was not sufficient to trigger cell death in these cell lines (Zhang et al., 2014). Moreover, selumetinib was found to have a cytostatic effect in *in vitro* and *in vivo* model of melanoma. Selumetinib alone (10 or 30 mg/kg BID) significantly suppressed the tumour growth by decreasing proliferation but did not induce apoptosis in *in vivo* model of melanoma. However, a combination of selumetinib (30 mg/kg) with docetaxel (15 mg/kg) increased its cytotoxic effects that resulted in tumour regression (Haass et al., 2008).

5.2.2.2. Effect on proliferation

The fundamental characteristic of cancer cells is their ability to proliferate uncontrollably (Hanahan & Weinberg, 2000, 2011). Unlike normal cells, cancer cells lose their ability to control cell division leading to aberrant cell proliferation and growth (Farber, 1995; Feitelson et al., 2015; Golias et al., 2004). This is manifested by alteration in activity or expression of proteins involved in cell cycle progression (Feitelson et al., 2015). Since cell proliferation depends on the rate of cell division and the fraction of cells undergoing cell division (Andreeff

et al., 2000), it is crucial to investigate the effect of an anti-cancer drug on the cell cycle progression.

In this study, crizotinib, selumetinib and their combination resulted in G1 cell cycle arrest in both crizotinib naïve and crizotinib resistant ALK-positive NSCLC cells. Interestingly, the combination treatment compared to selumetinib significantly induced G1 phase arrest only at 24 h in crizotinib naïve H3122 cells and at 48 h in crizotinib resistant CR-H3122 cells. The G1 phase arrest was mediated by downregulation of cyclin D1 expression and overexpression of p27 protein that in turn prevent the transition of G1 to S phase. In relation to this, cyclin D1-CDK4/6 and cyclin E-CDK2 complexes have been reported to be essential for G1 progression and G1/S phase transition, respectively. Additionally, p27 - a cyclin dependent kinase inhibitor – has been found to inhibit the activity of CDK2 and CDK2-cyclin complexes (Lees, 1995; Nigg, 1995; Vermeulen et al., 2003). In these studies, the combination of crizotinib and selumetinib synergistically enhanced p27 and reduced cyclin D1 expression that further increased G1 phase arrest and suppressed the S phase. These findings were consistent with the previous studies where both crizotinib and selumetinib single drug treatment resulted in G1 cell cycle arrest. Crizotinib has also been previously found to increase the number of cells in G1 phase and decrease the number of cells in S phase in concentration dependent manner in Karpas299 and SU-DHL-1 ALCL cells (Christensen et al., 2007). A similar result was demonstrated by Xu et al. where the treatment of 40 nM crizotinib for 72 h significantly increased the percentage of cells at G1 phase by 30% and 8% in both Karpas299 and SU-DHL-1 cells, respectively (Xu, Kim, et al., 2018). In pleural mesothelioma (H2593) cells, treatment of 1 μM crizotinib for 48 h increased the proportion of cells in G1 phase compared to control (Kanteti et al., 2016). Similarly, selumetinib was reported to significantly increase the percentage of cells in G1 phase and decrease the percentage of cells in S phase in concentration dependent manner in breast cancer (MDA-MB-231 and HCC-1937) cells (Zhou et al., 2016). In colorectal cancer (COLO205, HCT116, HT-29) and melanoma

(A375 and MelJuso) cells, treatment with 1 μM selumetinib for 48 h resulted in G1 cell cycle arrest (Sale & Cook, 2013).

Furthermore, the observed anti-proliferative effect of single and combined treatment with crizotinib and selumetinib in the *in vitro* study in this project was further explored in an *in vivo* study. Here, Ki67, a nuclear protein associated with cell proliferation (Gerdes et al., 1983), was measured in order to evaluate the anti-proliferative effect of crizotinib, selumetinib and their combination treatment on ALK-positive NSCLC xenografts. Unexpectedly, no change in Ki67 staining was found among treatment groups compared to vehicle control. This finding was in contrast with the finding of *in vitro* studies using H3122 and CR-H3122 cells. Though Ki67 is generally used as a cell proliferation marker to predict the effectiveness of anti-cancer therapy in the suppression of tumour growth, it is crucial to note that the predictive value of Ki67 as an indicator of benefit of chemotherapy remains controversial. In the IBCSG VIII study, premenopausal patients were randomly allocated to receive either six 28-day courses of a combination of chemotherapy (cyclophosphamide, methotrexate, and 5-fluorouracil (CMF)) alone or 24 monthly subcutaneous implants of goserelin alone or sequential treatment of six 28 days of CMF followed by 18 monthly goserelin implants. The sequential treatment of CMF and goserelin improved disease-free survival (DFS) (5-year DFS 88% vs. 84% vs. 73%) compared to CMF or goserelin alone (International Breast Cancer Study et al., 2003). In IBCSG IX study, postmenopausal patients were randomly allocated to receive either three 28 days course of CMF followed by tamoxifen orally for 57 months or tamoxifen alone for 60 months. The sequential treatment of CMF and tamoxifen significantly improved DFS (5 years DFS 84% vs. 69%) and overall survival (89% vs 81%) compared to tamoxifen alone (International Breast Cancer Study, 2002). However, in both clinical trials, no significant interaction between Ki67 labelling and DFS was found (Viale et al., 2008; Yerushalmi et al., 2010). Therefore, Ki67 labelling was not predictive of a better response to chemotherapy in these clinical studies.

5.2.2.3. Effect on angiogenesis

Angiogenesis, a physiological process of formation of new blood vessels from pre-existing vessels, plays an important role in cancer progression and metastasis (Hanahan & Weinberg, 2011; Lugano et al., 2020; Nishida et al., 2006; Tonini et al., 2003; Weis & Cheresh, 2011). Neovasculature formed by the process of angiogenesis is required for proper nourishment (i.e., oxygen and nutrient supply) and elimination of metabolic waste from tumour sites (Hanahan & Weinberg, 2011). Thus, inhibiting the tumour related angiogenesis has become a key tactic to suppress tumour progression in cancer therapy. Both crizotinib and selumetinib individually have been reported to exhibit their anti-tumour activity by inhibiting angiogenesis in various cancers (Cozzo et al., 2016; Takahashi et al., 2012; Yan et al., 2014; Zou et al., 2007). Thus, in this study it was hypothesised that the singular and combined treatment of crizotinib and selumetinib would reduce the angiogenesis in a xenograft model of ALK-positive NSCLC. The level of angiogenesis in tumour section was quantified by MVD was measured by immunolabelling of CD105. CD105, an auxiliary receptor of transforming factor beta (TGF-β) - predominately upregulated in proliferating endothelial cells (Burrows et al., 1995; Nassiri et al., 2011). It is highly specific to tumour neovascularisation (Miyata et al., 2013; Nassiri et al., 2011) compared to other pan-endothelial markers such as CD31 and CD34 that is expressed in pre-existing vasculature, macrophages and, lymphatic endothelial cell (Fina et al., 1990; Lindenmayer & Miettinen, 1995; Miyata et al., 2013). In this study, contrary to the hypothesis, no change in MVD was found in both single and combination treatment group compared to vehicle control. There are at least three possible reasons that may explain this finding. First possible reason may be deregulation of coordination of angiogenesis with continued tumour cell proliferation that causes hypoxia (Tonini et al., 2003). Since there was a rapid increase in tumour size in the vehicle control group (117 mm^3 to 944 mm^3 in 14 days), the rapidly proliferating tumour cells may outgrow the capacity of the host vasculature (Tonini et al., 2003) and decreases neovascularisation. This ultimately reduces the CD105 expression. Second reason may be overexpression of CD105 may not

always represent an increase in rate of angiogenesis (Ollauri-Ibanez et al., 2020). The persistent high level of CD105 did not enhance angiogenesis by stimulating sprouting or vascularisation but rather caused alteration in structure of vasculature that prevented blood vessels from maturing and stabilising. That in turn facilitated invasion and metastasis of tumour cells (Ollauri-Ibanez et al., 2020). Third reason may be that the singular and combination of crizotinib and selumetinib may not have any effect on angiogenesis in ALK-positive NSCLC. Furthermore, in a clinical study involving cervical squamous cell cancer patients treated with radical radiotherapy with/without chemotherapy, no correlation was found between the tumour CD105 expression and survival among the patients. This indicates that the CD105 may have poor predictive value as an indicator of treatment outcome (Metcalfe et al., 2018). Further studies are warranted to confirm this result.

5.2.2.4. Effect on signalling pathways downstream of ALK

Studies have shown that RAS/MAPK, AKT/mTOR and, JAK/STAT pathways are key pathways downstream of ALK that are responsible for the cancer cell survival and proliferation (Chiarle et al., 2008; Hallberg & Palmer, 2013; Lin et al., 2017; Palmer et al., 2009; Solomon, Wilner, et al., 2014). Among these three pathways, RAS/MAPK pathway has been reported to be a major effector of EML4-ALK that is responsible for tumour survival (Hrustanovic et al., 2015). Hrustanovic et al. demonstrated that HELP domain of EML4 drives the activation of RAS/MAPK by engaging all three major RAS isoforms. Resistance to ALK inhibition was observed when MAPK pathway was reactivated either by downregulation of phosphatase DUSP6 or genomic amplification of KRAS-wildtype (Hrustanovic et al., 2015). Thus, in this study, it was hypothesised that the combination treatment targeting primary oncoprotein, ALK and its critical effector, RAS/MAPK pathway would combat resistance, potentially improving therapeutic efficacy.

Crizotinib inhibits the activity of ALK in various cancers expressing ALK fusion oncoproteins (Christensen et al., 2007; Hrustanovic et al., 2015;

McDermott et al., 2008; Yan et al., 2014; Zou et al., 2007). Christensen et al. showed that crizotinib strongly inhibited tyrosine phosphorylation of NPM-ALK which in turn inhibited the phosphorylation of PLCγ, STAT3, AKT and ERK in dose dependent manner, in both *in vitro* and *in vivo* models of anaplastic large cell lymphoma (ALCL) (Christensen et al., 2007). Similarly, crizotinib was reported to potently suppress AKT and ERK signalling in anaplastic large cell lymphoma (SU-DHL-1 and Karpas-299), neuroblastoma (NB-1) and in the H3122 cell line (McDermott et al., 2008). On the other hand, selumetinib, a MEK inhibitor, has been reported to suppress tumour growth by predominantly inhibiting the phosphorylation of ERK in various cancers, including NSCLC (Adjei et al., 2008; Davies et al., 2007; Garon et al., 2010; Holt, Logie, Odedra, et al., 2012; Huynh et al., 2007; Meng, Dai, et al., 2010; Yeh et al., 2007). Screening of tumour cell lines has demonstrated that cells harbouring RAS or RAF mutations with predominantly activated RAS/MAPK signalling pathway have increased sensitivity to selumetinib (Davies et al., 2007; Garon et al., 2010; Haass et al., 2008). In this study, the combination of ALK inhibitor, crizotinib, and MEK inhibitor, selumetinib, demonstrated superior anti-tumour activity by synergistic inhibition of the major downstream RAS/MAPK signalling in both crizotinib naïve and crizotinib resistant ALK-positive NSCLC cells.

5.2.2.5. Role of RAS/MAPK pathway

RAS/MAPK signalling pathway plays a key role in regulating physiological process such as cell proliferation, apoptosis and, angiogenesis (Lu & Xu, 2006; Molina & Adjei, 2006; Morrison, 2012; Zhang & Liu, 2002). Upregulation of RAS/MAPK pathway promotes proliferation and angiogenesis as well as inhibiting apoptosis in various types of cancer (Dhillon et al., 2007; Guo et al., 2020; Lu & Xu, 2006). Various studies have shown the involvement of RAS/MAPK pathway in regulation of G1 cell cycle proteins and progression of cell cycle (Bhatt et al., 2005; Chambard et al., 2007; Terada et al., 1999; Villanueva et al., 2007; Weber et al., 1997). Phosphorylation and activation of ERK facilitates the migration of ERK to the nucleus where it phosphorylates transcription

factors such that in turn upregulates cyclin D1 and downregulates p27 (Bhatt et al., 2005; Chambard et al., 2007; Lavoie et al., 1996; Torii et al., 2006). In this study, the synergistic downregulation of ERK phosphorylation by combination treatment of crizotinib and selumetinib led to G1 phase arrest through overexpression of p27 and suppression of cyclin D1 expression. Thus, RAS/MAPK signalling is crucial for G1 phase progression and entry to the S phase of cell cycle in both H3122 and CR-H3122 cell line.

Furthermore, the RAS/MAPK pathway has been reported to regulate apoptosis by downregulation of the proapoptotic protein Bim (Ewings et al., 2007; Gillings et al., 2009). ERK activation downregulates Bim by both transcriptional and posttranslational modification (Gillings et al., 2009). ERK phosphorylates FOXO3A and promotes the proteasomal degradation of FOXO3A (Yang et al., 2008) that is involved in transcription of Bim (Gilley et al., 2003). On the other hand, ERK directly phosphorylates Bim and facilitates its proteasomal degradation (Ley et al., 2003; Luciano et al., 2003; Marani et al., 2004). This decreases the expression of Bim protein and thereby inhibits apoptosis. In this study, the combination of crizotinib and selumetinib markedly reduced the phosphorylation of ERK that in turn increased the expression of Bim, resulting in increased apoptosis. Other studies have shown that AKT/mTOR pathway is also involved in the regulation of Bim via sequestering the activity of FOX3A (Fu & Tindall, 2008). However, Bland et al. have shown that the crizotinib (0.25 μM) had no effect on the AKT/mTOR pathway as no change in phosphorylation of mTOR was observed in H3122 cells (Bland et al., 2019). These finding further suggests that the upregulation of Bim by the combination treatment in this project may be solely due to the decrease in phosphorylation of ERK.

5.2.3. Safety profile and drug interaction

Drug safety is one of the key elements in the development of new therapy (Alshammari, 2016), so prior investigation of safety profile is important from an early stage of drug development. Other studies have shown that both crizotinib

and selumetinib single drug treatments induce adverse events that range from grade 1-2 to grade 3-4 (Adjei et al., 2008; Banerji et al., 2010; Camidge et al., 2012; Catalanotti et al., 2013). Crizotinib has been reported to cause adverse events such as gastrointestinal upset, visual disturbance, elevation in ALT and AST level, neutropenia (Camidge et al., 2012). On the other hand, selumetinib is known to cause side effects that includes diarrhoea, nausea, acneiform, pleural effusion (Adjei et al., 2008; Banerji et al., 2010; Catalanotti et al., 2013). Thus, in the present study, the possibility of synergistic toxicity that may be induced by the combination of crizotinib with selumetinib was investigated. Combination of crizotinib (5 mg/kg and 25 mg/kg) and selumetinib (25 mg/kg) was well tolerated in mice, with insignificant weight loss and no adverse effect on kidney and liver function. Though some mice from the vehicle control and crizotinib groups showed higher values of ALT (> 80 U/L), there was no histopathological differences in liver morphology with other mice. These findings suggest that oral administration of crizotinib and selumetinib at the dose of 25 mg/kg once daily for 14 days is nontoxic in mice and may increase the quality of life by maintaining efficacy with less risk of adverse events. Further studies are warranted to translate this finding to humans- (Nair et al., 2018).

The narrow therapeutic index and the inherent toxicity of anticancer drugs raise the importance of drug interaction in cancer treatment (Scripture & Figg, 2006). Drug interactions can change the pharmacokinetics or pharmacodynamics of given treatment altering its efficacy and toxicity. Co-administration of drugs that inhibit or induce CYP enzymes or that compete for metabolism by same CYP enzyme have a greater chance of interaction (Scripture & Figg, 2006). It has been reported that crizotinib, a primary substrate of CYP3A, is a moderate inhibitor and weak inducer of CYP3A (Johnson et al., 2015; Mao et al., 2013; Tan et al., 2010). Co-administration of crizotinib (250 mg BID for 28 days) with midazolam (2 mg OD) increased midazolam area under the plasma concentration-time curve by 3.7-fold confirming crizotinib to be a moderate CYP3A inhibitor (Tan et al., 2010). On the other hand, Mao et al. evaluated crizotinib CYP3A4 induction potency in cryopreserved human hepatocytes and found that crizotinib induced

CYP3A4 mRNA expression in a concentration dependent manner (Mao et al., 2013). Similarly, CYP3A4 is the major enzyme responsible for selumetinib oxidative metabolism (Dymond et al., 2016). Selumetinib AUC was increased with co-administration of a CYP3A4 inhibitor such as itraconazole while the AUC was decreased with a CYP3A4 inducer such as rifampicin (Dymond et al., 2017). In this study, the effect of single and combination treatment of crizotinib and selumetinib on catalytic activity of CYP3A enzyme was investigated. Contrary to previous studies, oral administration of either 5 mg/kg or 25 mg/kg crizotinib once daily for 14 days did not alter liver CYP3A activity compared to the vehicle control. These findings suggest that crizotinib at the given dose regimen neither inhibited nor induced the CYP3A enzyme in mice. Moreover, the combination of crizotinib (5 mg/kg and 25 mg/kg) and selumetinib (25 mg/kg) had no effect on CYP3A catalytic activity and thus were unlikely to alter each other's metabolism.

5.2.4. Orthotopic lung cancer model

Development of an appropriate mouse model is crucial for screening new drug candidates for the treatment of lung cancer. Therefore, the development of a mouse model is an indispensable part of the lung cancer drug development process. The goal of this investigation was to develop an orthotopic lung cancer model via tail vein injection of two human lung adenocarcinoma (A549, H3122) cell lines that could recapitulate human lung cancer for preclinical assessment of novel anti-cancer drugs. Tail vein injection techniques have been successfully used previously in the development of breast cancer lung metastasis model (Rashid et al., 2013) and other lung cancer models (Zhao et al., 2012). Rashid et al. injected breast cancer (4T1-luc2) cell line (1×10^6 cells in 100 µL PBS) into the median tail vein of Balb/c mice that instantly generated diffusely distributed cell implantation throughout the lungs (Rashid et al., 2013). Also, tail vein injection of red fluorescent protein (RFP)- labelled Lewis lung carcinoma cells (2×10^6 cells in 100 µL PBS) in female C57 immunocompetent mice resulted in tumour colonies in the lung by day 5 (Zhao et al., 2012). In this study, the tail vein

injection of H3122 and A549 cells in SCID mice resulted in some aggregation of cells with no discrete tumour nodules, consistent with the dispersed cancer cell pattern obtained by Rashid et al. (Rashid et al., 2013). However, immunolabeling of human cancer marker failed to detect any cancer cells in the lung sections.

The pathological changes in the lungs of mice after tail vein injection of tumour cells were consistent with thromboembolism. Area of white patches was observed on the lungs that correspond to areas of hypoxia prominent at the beginning 5 weeks after injection. Studies have shown that tail vein injection may lead to sudden death following thromboembolic event (Rashid et al., 2013). In addition to this, tail vein injection has been criticised for lack of more steady progression of tumour burden in a breast cancer lung metastasis model (Rashid et al., 2013). Therefore, an attempt to establish orthotopic lung cancer model in this study remains inconclusive and requires further studies to confirm the presence of human lung adenocarcinoma cells in the lungs of the mice.

5.3. Clinical implications

NSCLC patients harbouring ALK rearrangement are highly sensitive to ALK-TKIs and thus are the preferred choice of therapy in these patients (Lin et al., 2017; Ziogas et al., 2018). In clinical settings, despite great initial response, patients on ALK-TKI monotherapy or sequential treatment with next generation ALK-TKIs unavoidably develop resistance within several years of therapy (Choi et al., 2010; Lin et al., 2017; Ziogas et al., 2018). Thus, complete, and lasting response to ALK-TKIs is extremely rare. Upfront combination treatment could be a promising alternative strategy that can improve initial response as well as overcome resistance resulting in long-term disease control.

In this study, the combination of ALK inhibitor, crizotinib and MEK inhibitor, selumetinib significantly decreased the growth of tumour in both *in vitro* and *in vivo* model of ALK-positive NSCLC compared to monotherapy. This finding indicates that the combination of crizotinib and selumetinib has the potential to prevent the emergence of resistance with a higher and more robust

response in ALK-positive NSCLC patients and thereby could improve the ORR, OS and PFS.

Interestingly, inhibition of MEK alone was almost as effective as the combination treatment to suppress the tumour growth in xenograft model of ALK-positive NSCLC. Therefore, MEK inhibitor as a monotherapy can also be a prospective candidate for treatment of ALK-positive NSCLC. Furthermore, the combination showed a greater effect in reducing cell viability of crizotinib resistant ALK-positive NSCLC cells even at the low dose of individual drugs. So, the combination treatment could effectively overcome the acquired crizotinib resistance even at the lower doses of the two drugs and thus could be a potential alternative treatment for patients progressed on crizotinib.

Moreover, the combination of crizotinib and selumetinib, each at the dose of 25 mg/kg, did not show any interactions and was safe. Thus, the combination treatment is likely to attain optimum efficacy while exhibiting no or minor treatment related adverse event. This could ultimately improve the quality of life. Currently, several clinical trials of combination therapy using ALK inhibitors with other drugs such as MEK inhibitors, angiogenesis inhibitors etc. are being conducted (ClinicalTrials.gov National Library of Medicine (US), 2019a, 2019b, 2020). The outcome from these studies may inform further about the safety and efficacy of the combination therapy in clinical scenarios.

5.4. Limitations and future studies

This study evaluated the effect of crizotinib and selumetinib combination treatment using only one ALK-positive (H3122) cell line harbouring variant 1. Though H3122 cells are the most commonly used cell line and are clinically relevant to human treatment (Cha et al., 2016; Sabir et al., 2017; Yoshida et al., 3383) this study has not explored, compared and confirmed the effect of the combination treatment on other ALK-positive cell lines such as STE-1 cells – also harbouring variant 1 - and H2228 cells harbouring variant 3. Secondly, the CR-H3122 cell line was generated in the Ashton lab by addition of increasing concentrations of crizotinib in H3122 cells and was maintained in 0.8 μM of

crizotinib prior to experiment. Though the CR-H3122 cells were highly resistant to crizotinib, the precise mechanism of resistance in CR-H3122 cells is still unclear. Thus, future studies need to explore the mechanism of CR-H3122 cells by carrying out whole genome sequencing as well as genome microarray analyses to detect the expression of other genes that could be altered by a bypass mechanism. Thirdly, immunolabelling was performed to determine the mechanism of tumour suppression by crizotinib, selumetinib and their combination. However, it was not possible to draw any specific conclusion from the data obtained. Here, only one tumour marker was used to examine the effect of treatment on proliferation or apoptosis or angiogenesis. The use of at least two different methods would be helpful to confirm the result. For example Flow cytometry or IHC of bromodeoxyuridine (BrdU) that measures the fraction of cells involved in chromosomal DNA synthesis (Barnes & Gillett, 1995; Beresford et al., 2006) could be used together with Ki67 immunolabeling, IHC of VEGF (Maae et al., 2011), a potent angiogenic factor, could be used together with CD105 and analysis of cleaved caspase-3 (western blotting or IHC or flow cytometry) (Crowley & Waterhouse, 2016; Martey et al., 2017) together with the TUNEL assays.

Although tail vein injection of H3122 and A549 cells into SCID mice was carried out to develop an orthotopic lung cancer model, IHC for Ki67 or ALK was unable to detect human cancer cells in the lung section of the mice. One possible explanation for this as that fixation of lungs by formalin may have masked antigen exposure. This problem might be overcome in future by the use of fluorescently tagged human adenocarcinoma cell line (Zhao et al., 2012) or overexpression of luciferase gene (Rashid et al., 2013) that will facilitate the detection of cancer cells either by live imaging via *in vivo* imaging technology or fluorescence microscopy and flow cytometry of lung samples. Also, the confirmation of the white patches resembling hypoxia in the lung of mice as the hypoxic lesion was not made. Thus, in future studies, the hypoxic lesions could be confirmed using tetrazolium chloride (Linsell & Ashton, 2014) staining in fresh lung sections.

In vitro derived resistant cells are established by exposing specific targeted therapy to sensitive cells until resistance emerges. Though these cell lines may give an idea regarding potential resistance mechanism, they could never be applied for treatment decisions for individual patients (Crystal et al., 2014). On the contrary, resistant cells obtained directly from patients progressed on specific targeted therapy can provide information on genetic alteration occurred clinically resulting in the drug resistance. This could be helpful in choosing appropriate therapy to combat resistance (Crystal et al., 2014). Therefore, in future studies, the effect of crizotinib and selumetinib should be explored in both *in vitro* and *in vivo* patient derived resistant model of ALK-positive NSCLC.

Lastly, this study identifies, Bim, PARP and CDK as druggable target and thus showed the possibility of triple drug therapy. Bozic et al. have reported that the triple therapy is essential for those patients with large tumour burden (Bozic et al., 2013). Therefore, the use of BH3 mimetic Bcl2 inhibitor or PARP inhibitor or CDK inhibitor together with crizotinib and selumetinib may be even more effective in suppressing ALK+ tumour growth.

5.5. Conclusion

In this study, the combination of crizotinib and selumetinib synergistically inhibited the cell viability of both crizotinib naïve and crizotinib resistant ALK-positive NSCLC cells. The suppression of cell proliferation was mediated by downregulation of RAS/MAPK signalling pathway that led to a decrease in cell cycle progression and increase in apoptosis. The combination treatment synergistically increased the expression of cyclin D1 and downregulated p27 expression resulting in G1 cell cycle arrest. Furthermore, the upregulation of Bim facilitated the increase in intrinsic apoptosis of H3122 and CR-H3122 cells. Moreover, the *in vitro* effect of the combination treatment was successfully translated in a xenograft model of ALK-positive NSCLC where the combination showed significant suppression of tumour growth. Unexpectedly, selumetinib alone markedly suppressed tumour growth raising the possibility that MEK inhibitor alone may be almost as effective as the combination therapy. Both

singular and combination of crizotinib and selumetinib were non-toxic and did not interact with each other's major metabolizing enzyme, CYP3A. Thus, these findings led support to the clinical investigation of dual ALK/MEK inhibition therapy as a strategy to delay or overcome drug resistance in ALK-positive NSCLC and suggest the possibility of drug therapies with three or more targets.

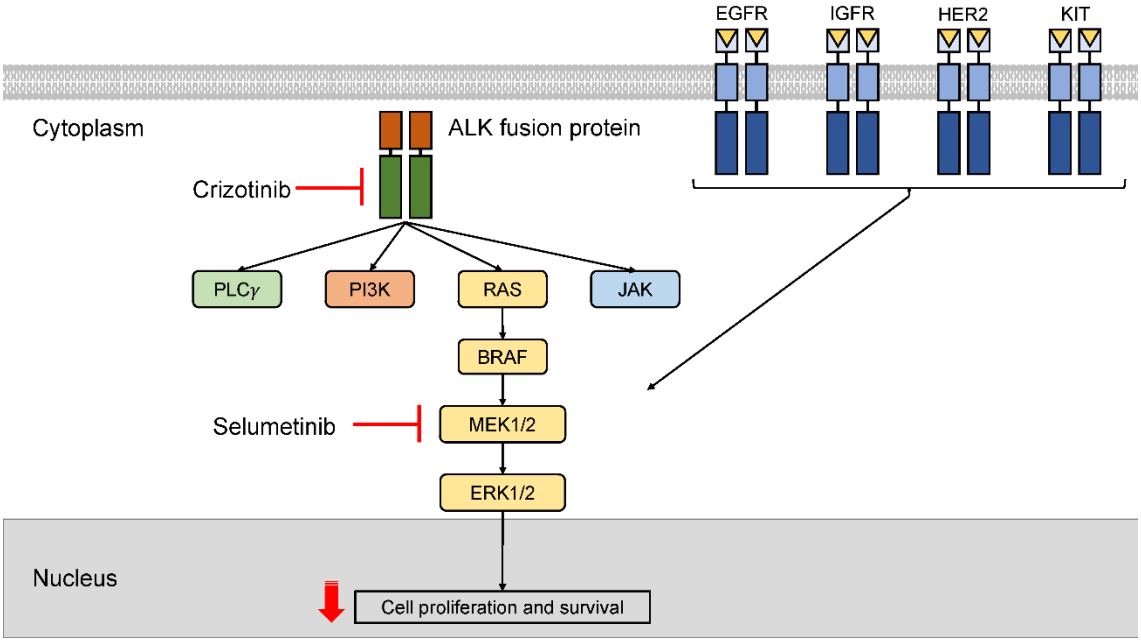

Figure 5.1 Schematic diagram illustrating the mechanism behind marked inhibition of tumour cell proliferation in ALK-positive NSCLC by the combination of crizotinib and selumetinib.

Appendix 1: Appendices

A1.1. ALK kinase domain sequences of crizotinib naïve and crizotinib resistant ALK-positive NSCLC

Table A1.1 ALK kinase domain sequences of H3122 and CR-H3122 cell lines. The kinase domain of ALK was amplified from H3122 and CR-H3122 cDNA using PCR primers (Table A1.2). After gel purification the PCR products were sequenced using Sanger sequencing. The sequences of exons 22-25 (NM_004304), corresponding to the kinase domain are indicated in bold.

Cell line	ALK domain sequence (forward strand, 5′ to 3′)
H3122	CCTCATTCGGGGTCTGGGCCATGGCGCCTTTGGGGAGGTGTAT GAAGGCCAGGTGTCCGGAATGCCCAACGACCCAAGCCCCCTG CAAGTGGCTGTGAAGACGCTGCCTGAAGTGTGCTCTGAACAG GACGAACTGGATTTCCTCATGGAAGCCCTGATCATCAGC**AAA TTCAACCACCAGAACATTGTTCGCTGCATTGGGGTGAGCCT GCAATCCCTGCCCCGGTTCATCCTGCTGGAGCTCATGGCGG GGGGAGACCTCAAGTCCTTCCTCCGAGAGACCCGCCCTCG CCCGAGCCAGCCCTCCTCCCTGGCCATGCTGGACCTTCTGC ACGTGGCTCGGGACATTGCCTGTGGCTGTCAGTATTTGGA GGAAAACCACTTCATCCACCGAGACATTGCTGCCAGAAACT GCCTCTTG**ACCTGTCCAGGCCCTGGAAGAGTGGCCAAGATTG GAGACTTCGGGATGGCCCGAGACATCTACAGGGCGAGCTACT ATAGAAAGG
CR-H3122	CTCATTCGGGGTCTGGGCCATGGCGCCTTTGGGGAGGTGTATG AAGGCCAGGTGTCCGGAATGCCCAACGACCCAAGCCCCCTGC AAGTGGCTGTGAAGACGCTGCCTGAAGTGTGCTCTGAACAGG ACGAACTGGATTTCCTCATGGAAGCCCTGATCATCAGC**AAAT TCAACCACCAGAACATTGTTCGCTGCATTGGGGTGAGCCTG CAATCCCTGCCCCGGTTCATCCTGCTGGAGCTCATGGCGGG GGGAGACCTCAAGTCCTTCCTCCGAGAGACCCGCCCTCGCC CGAGCCAGCCCTCCTCCCTGGCCATGCTGGACCTTCTGCAC GTGGCTCGGGACATTGCCTGTGGCTGTCAGTATTTGGAGG AAAACCACTTCATCCACCGAGACATTGCTGCCAGAAACTGC CTCTTG**ACCTGTCCAGGCCCTGGAAGAGTGGCCAAGATTGGA GACTTCGGGATGGCCCGAGACATCTACAGGGCGAGCTACTAT AGAAAGG

Table A1.2 Primer sequences used for amplification and sequencing of ALK kinase domain.

Primer	**Sequence (5′ to 3′)**
ALK_3_F (forward)	CCATCAGTGACCTGAAGGAGG
ALK_3_R (reverse)	TGGCACAGCCTCCCTTTCTAC

A1.2. Raw image of full blots used for western blots

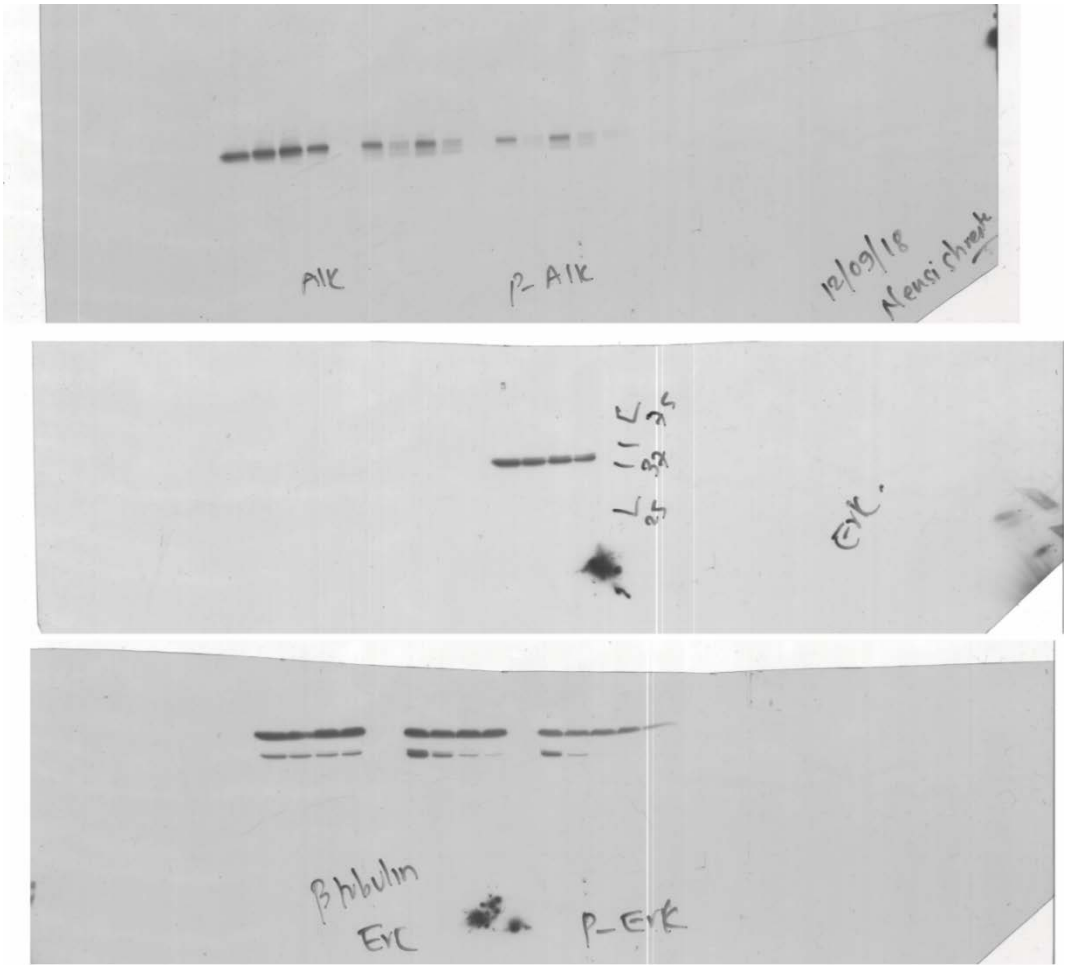

Figure A1.1 Raw image of Western blots for ALK, pALK, ERK, pERK and β-tubulin in H3122 cells

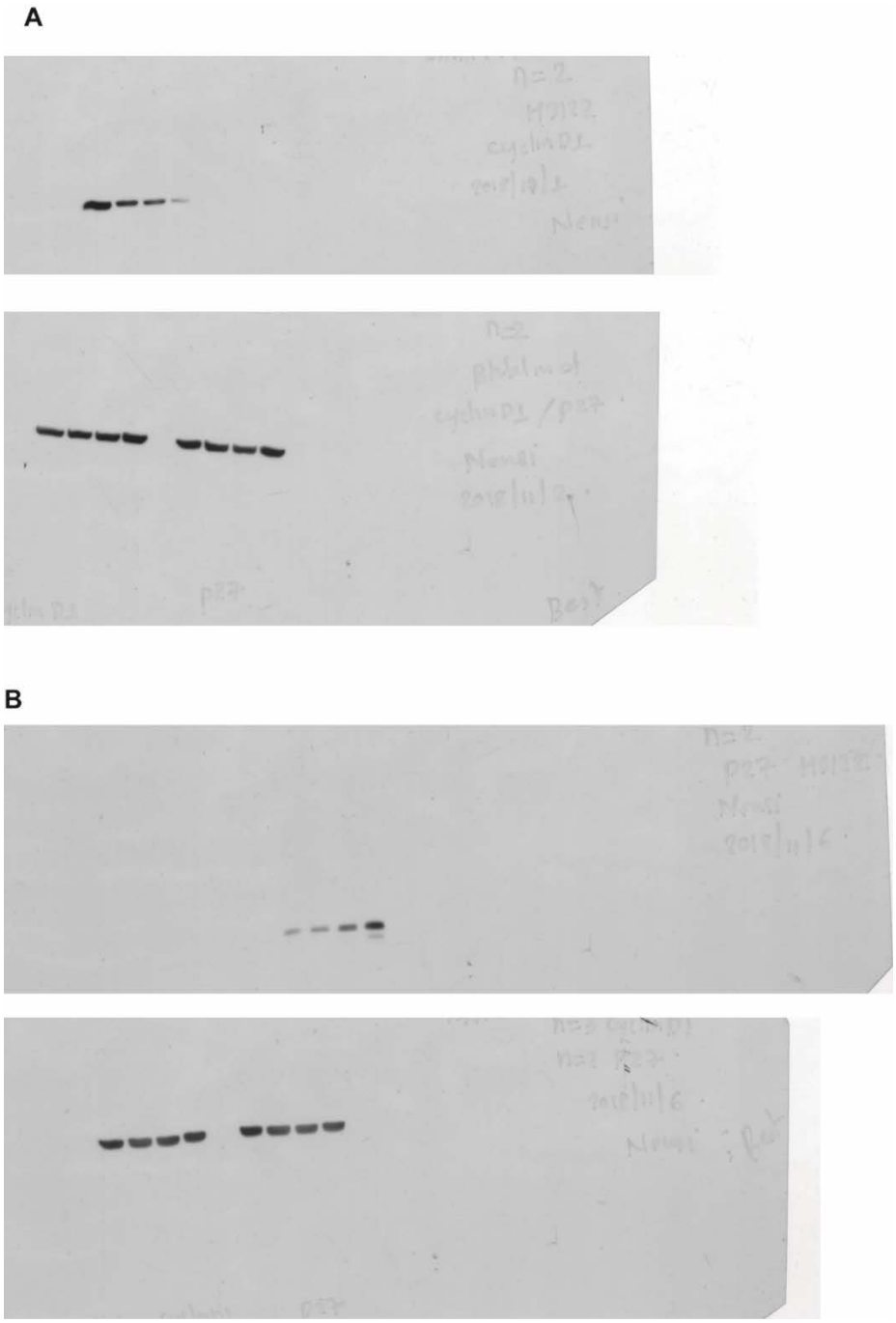

Figure A1.2 Raw image of Western blots for CyclinD1, p27 and β-tubulin in H3122 cells

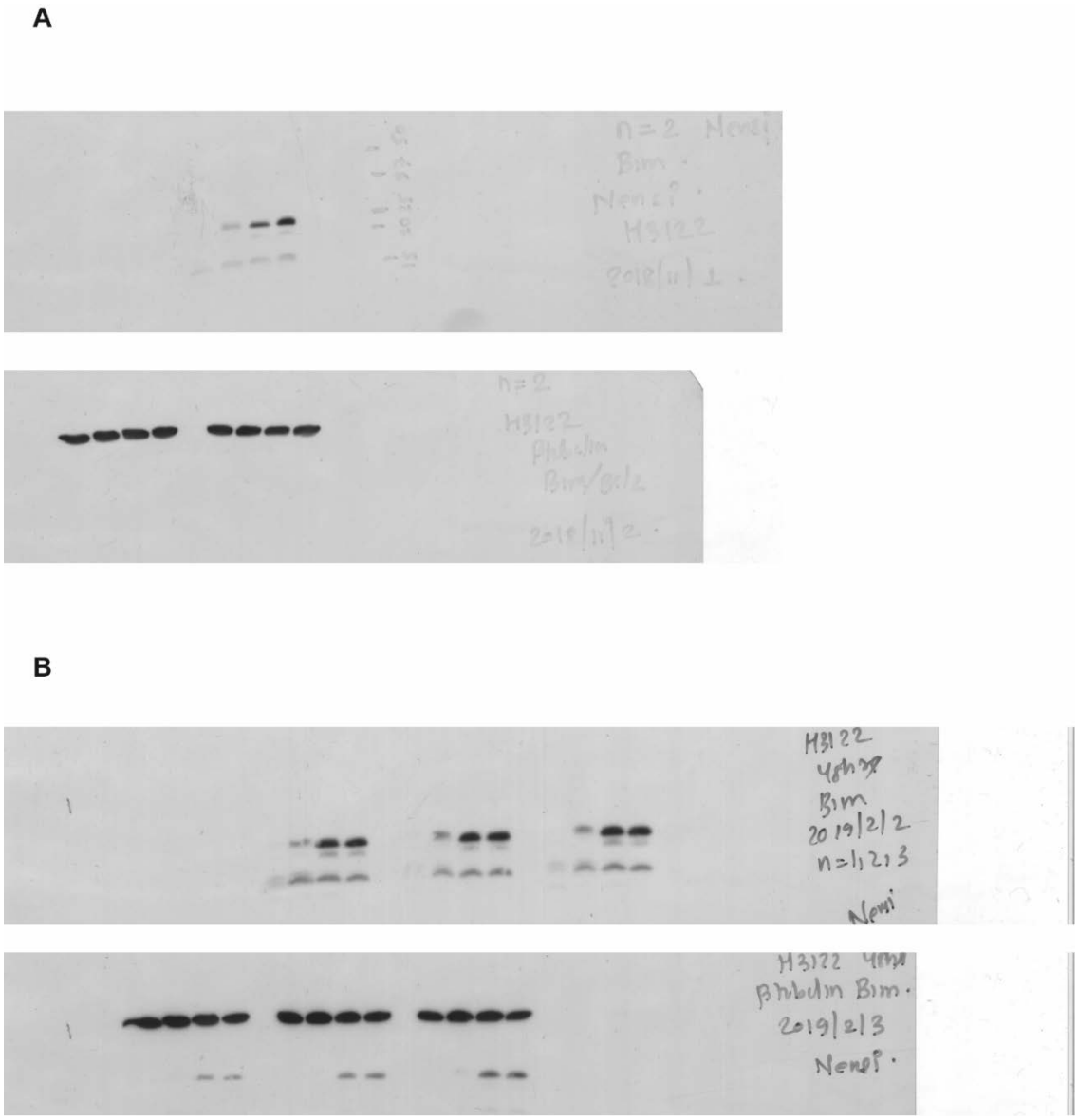

Figure A1.3 : Raw image of Western blots for Bim after 24 and 48 h of drug treatment in H3122 cells

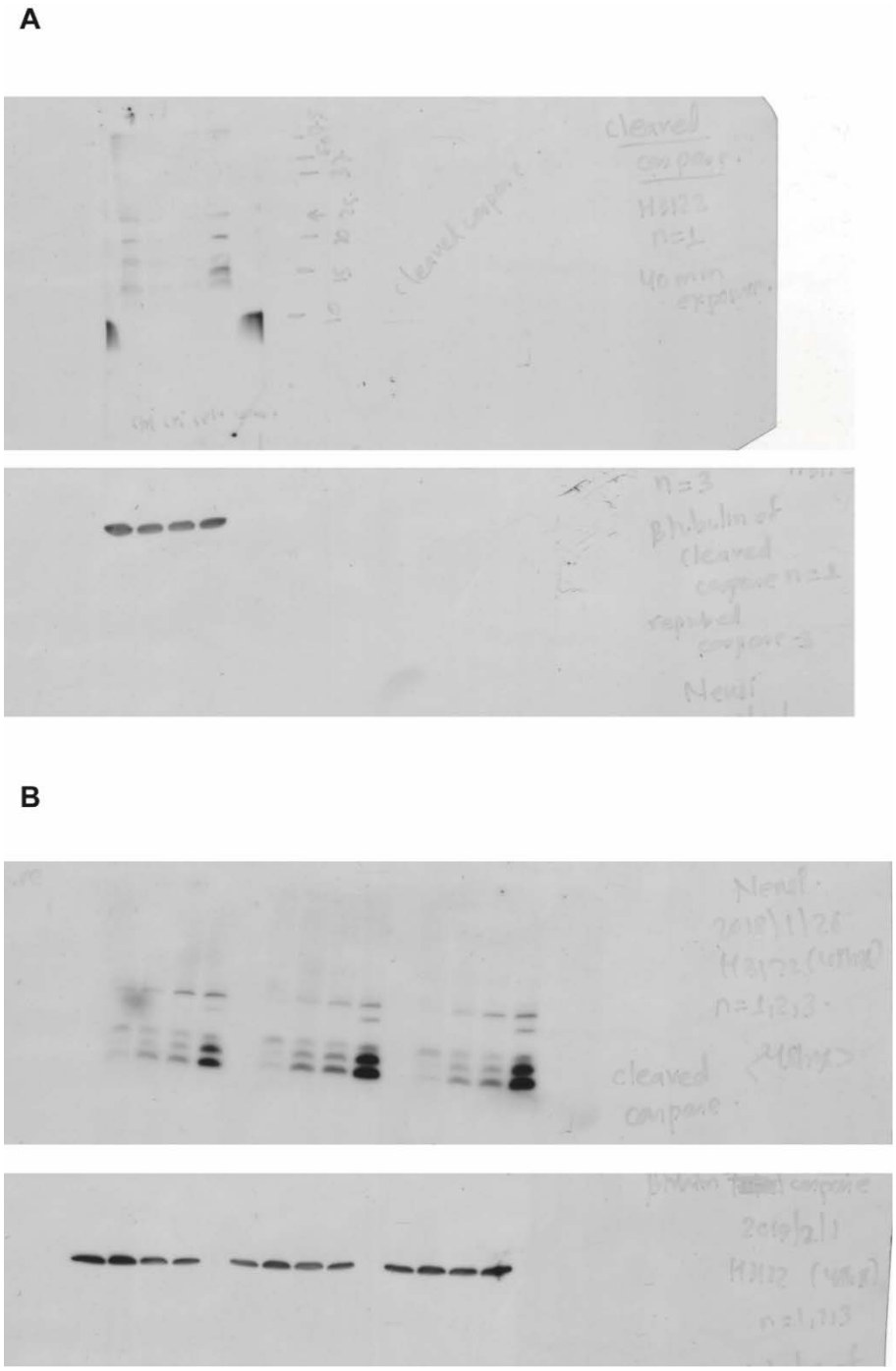

Figure A1.4 Raw image of Western blots for cleaved Caspase-3 after 24 and 48 h of drug treatment in H3122 cells

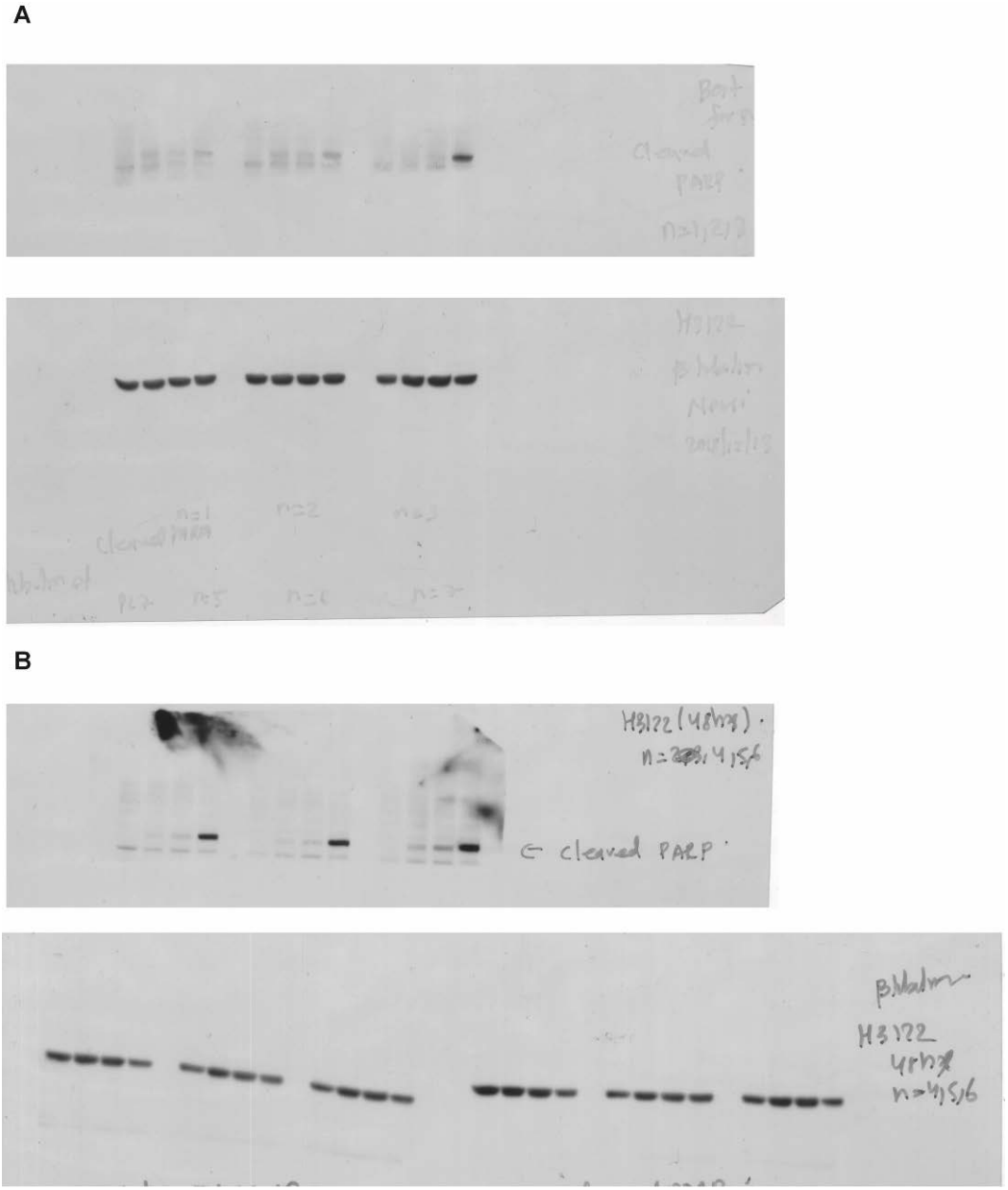

Figure A1.5 Raw image of Western blots for cleaved PARP after 24 and 48 h of drug treatment in H3122 cells

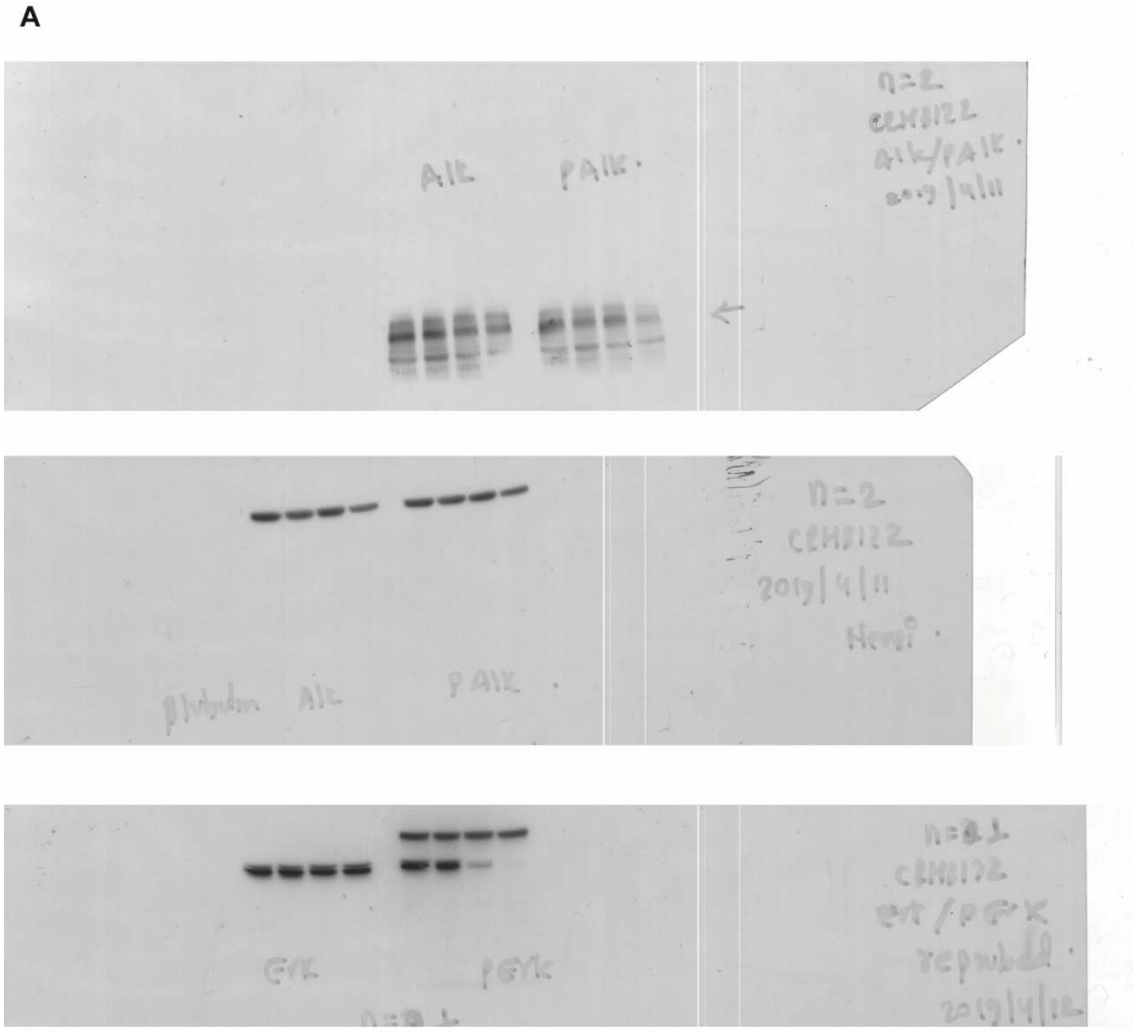

Figure A1.6 Raw image of Western blots for ALK, pALK, ERK, pERK and β-tubulin in CRH3122 cells

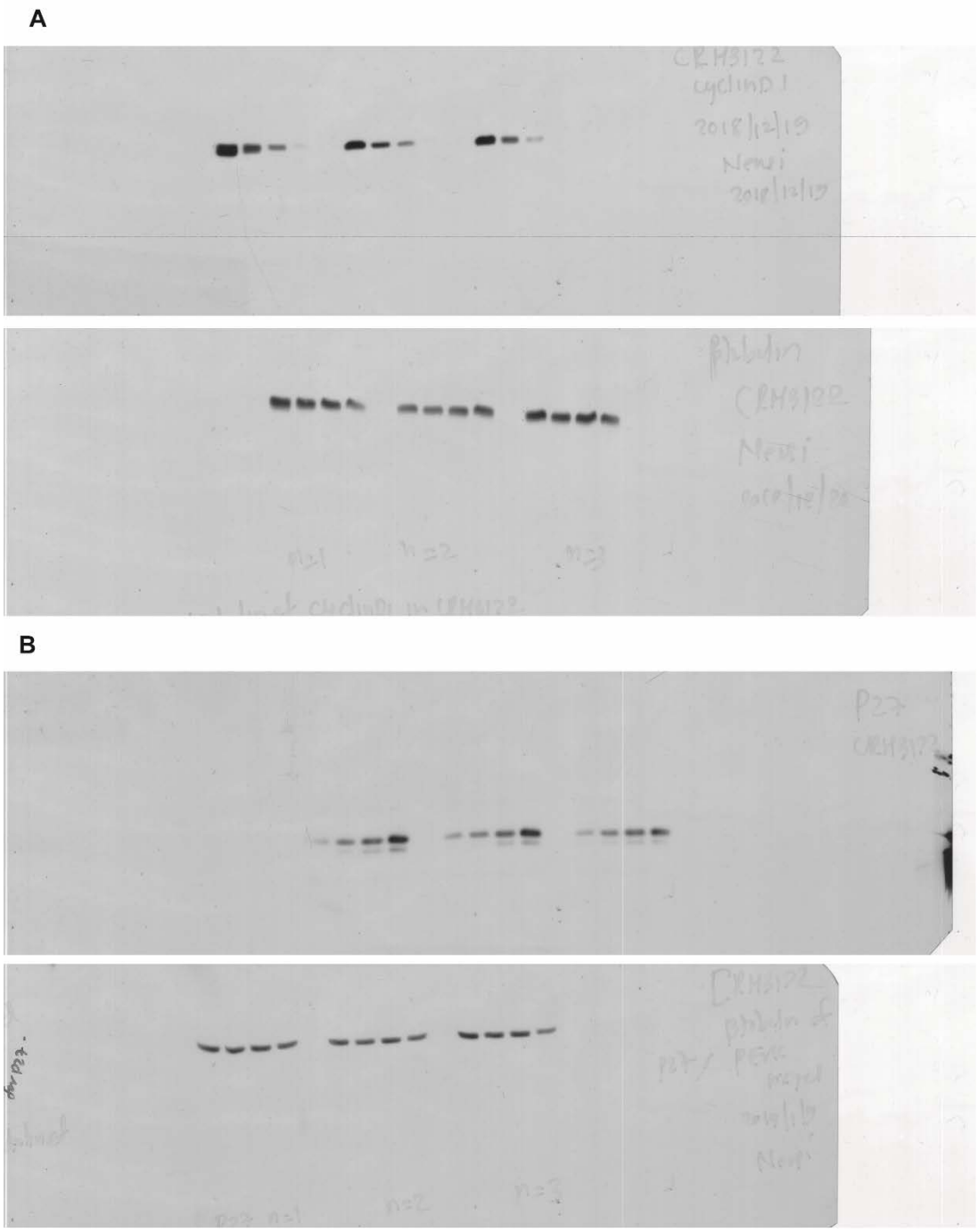

Figure A1.7 Raw image of Western blots for CyclinD1, p27 and β-tubulin in CRH3122 cells

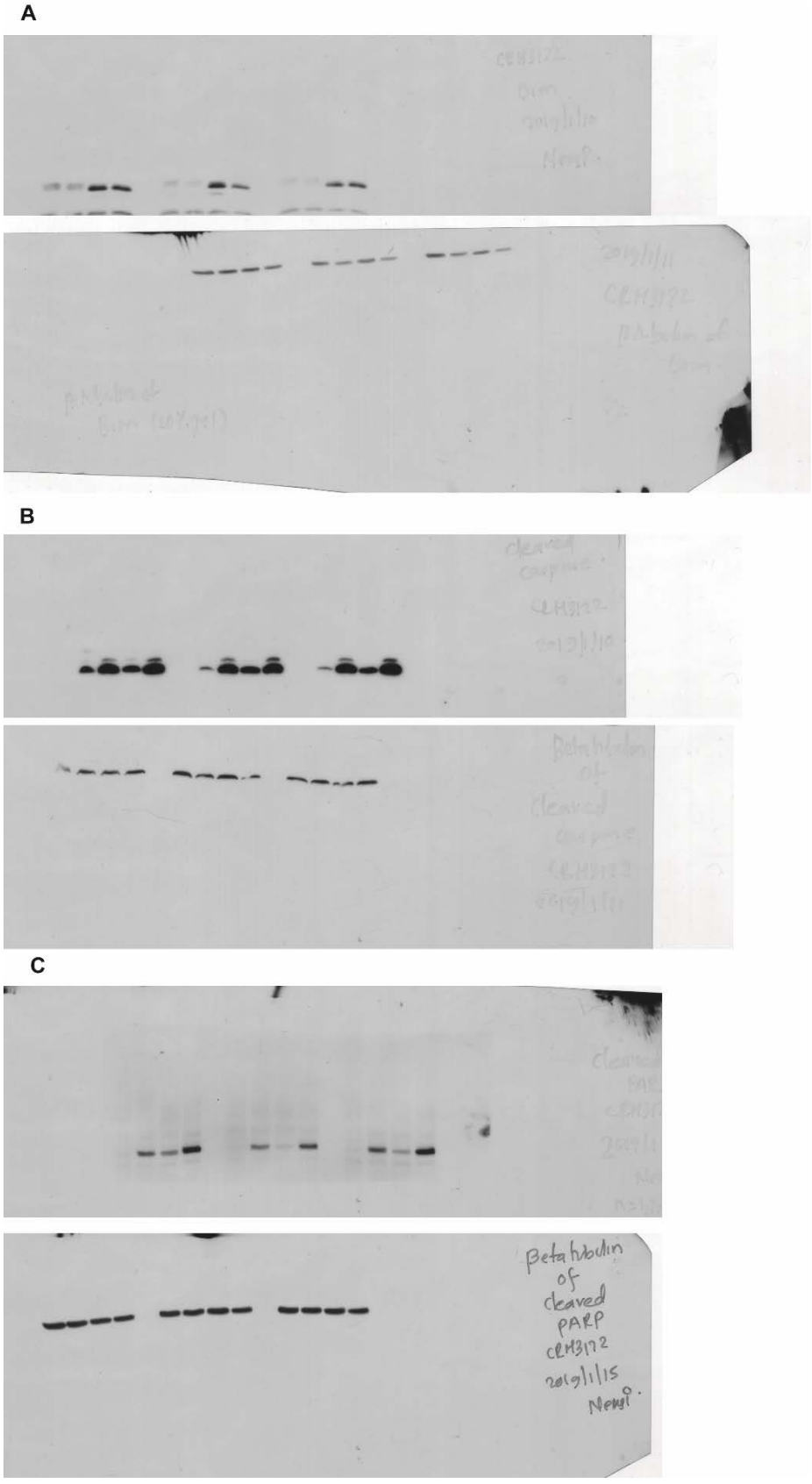

Figure A1.8 Raw image of Western blots for Bim, cleaved Caspase-3, cleaved PARP and β-tubulin after 24 h of drug treatment in CRH3122 cells

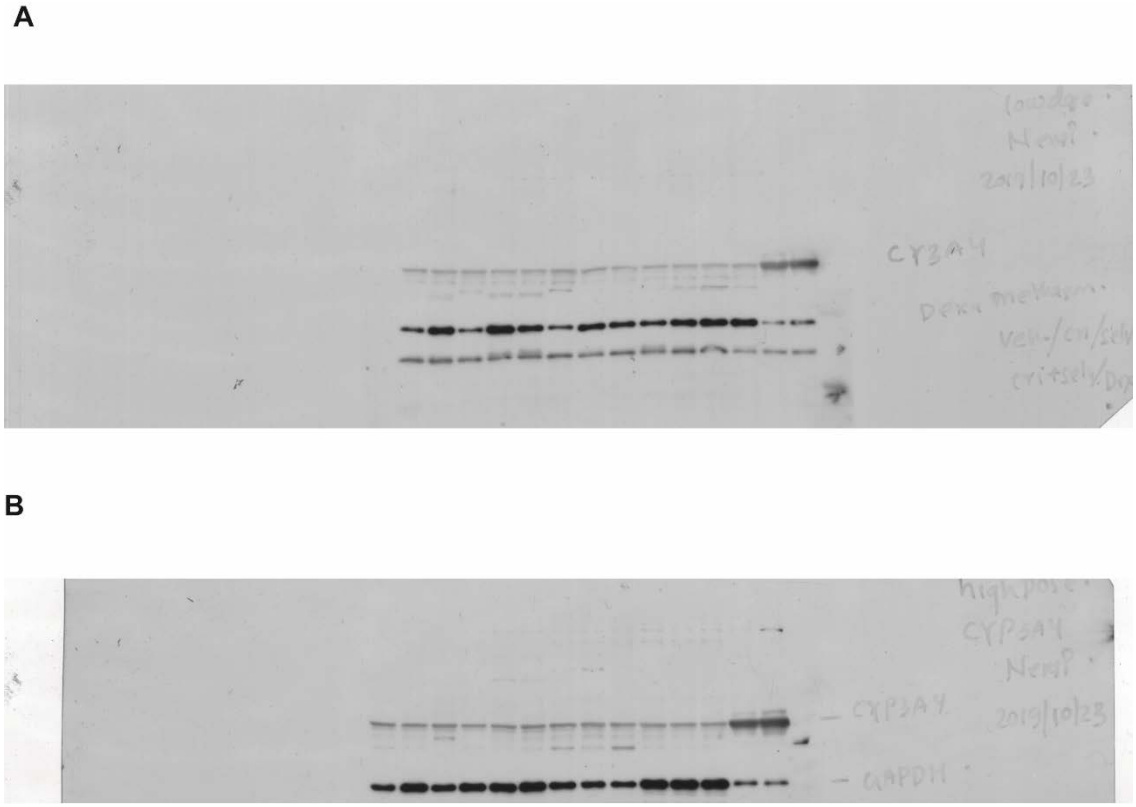

Figure A1.9 Raw image of western blotting for CYP3A and GAPDH.

A1.3. Histology of lung section injected with H3122 cells

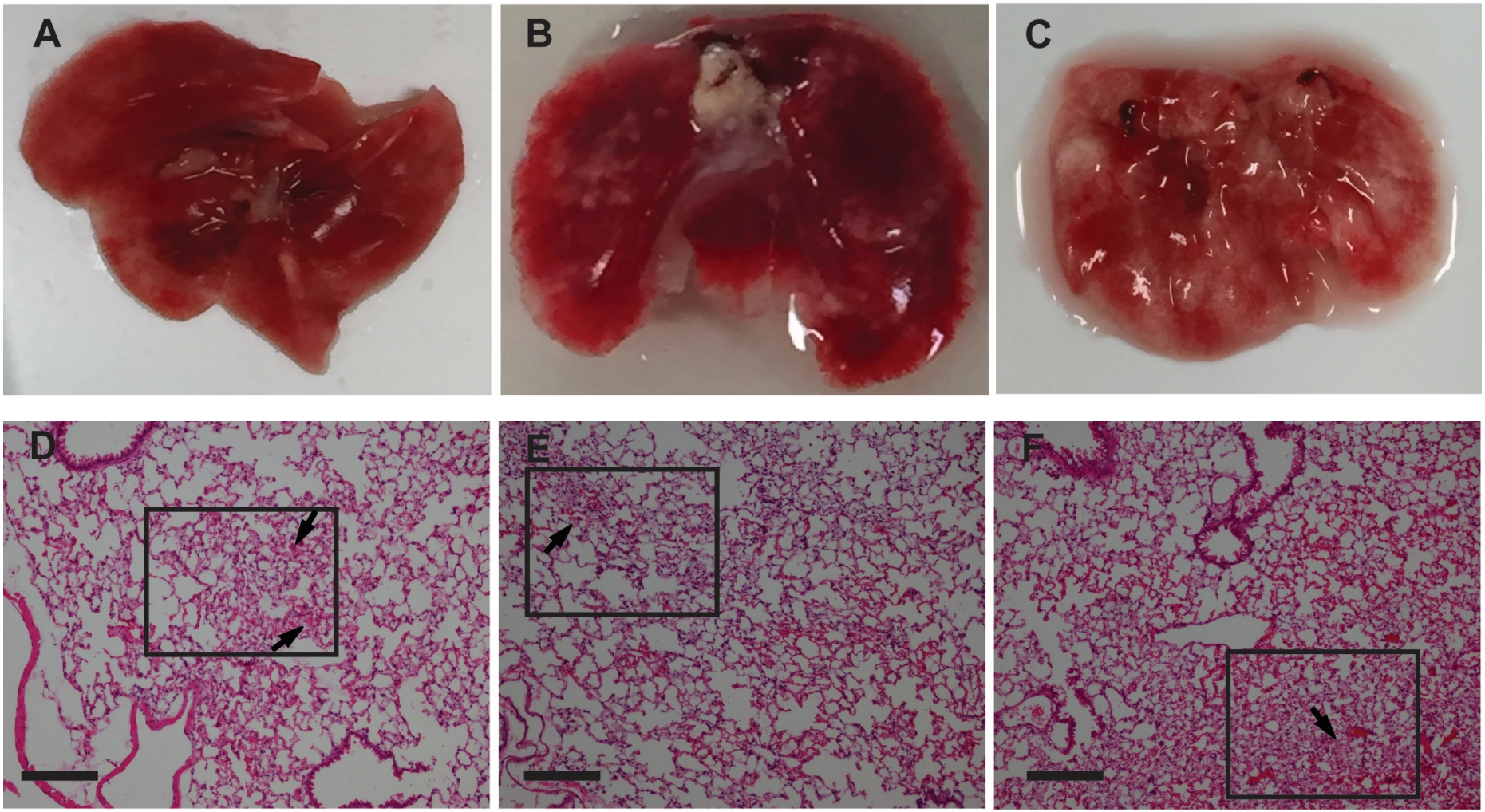

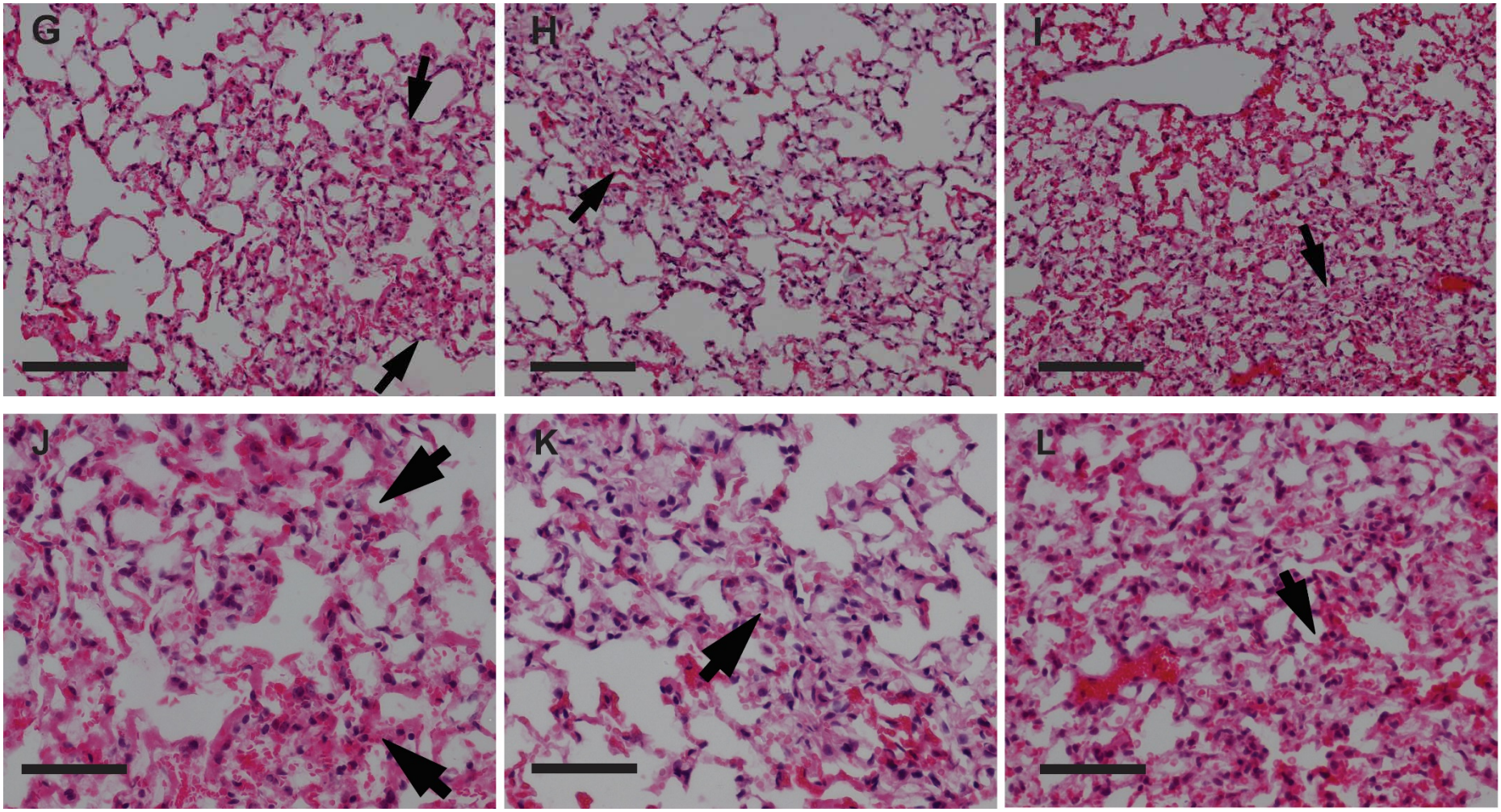

Figure A1.10 Gross appearance and histology of lungs of SCID mice after 3rd , 5th and 8th week of injection with H3122 cells via the tail vein. Mice were injected with 1×10^5 H3122 cells into lateral vein of the tail. Mice were then euthanised after 3rd, 5th and 8th week of injection. Lungs

were excised, sectioned and H and E staining was performed. Lungs of mice at (A) 3rd, (B) 5th, (C) 8th weeks after cell injection. White patches on lungs appeared by week 5. H and E staining of lung sections of mice at (D) 3rd, (E) 5th, (F) 8th week after cells injection using a 10× objective. Squares and arrow indicate areas of high cell density. (G-I) Area shown in insets from panel (D-F) respectively, using 20× objective. (J-L) Area shown in insets from images (D-F), respectively, using 40× objective. Scale bars: D-I 100 μM and J-L 50 μM.

A1.4. Histology of lung section of A549 injected mice

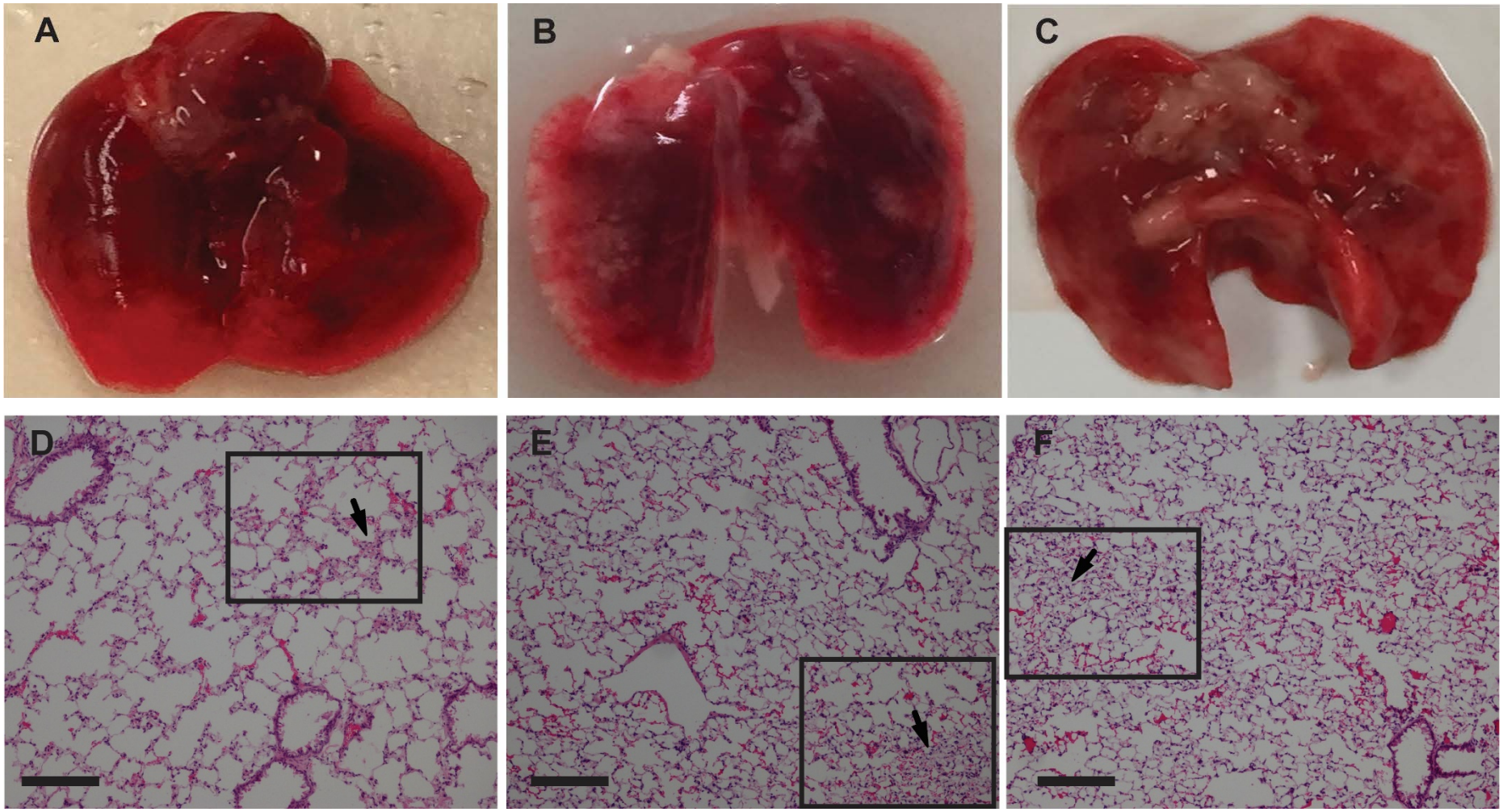

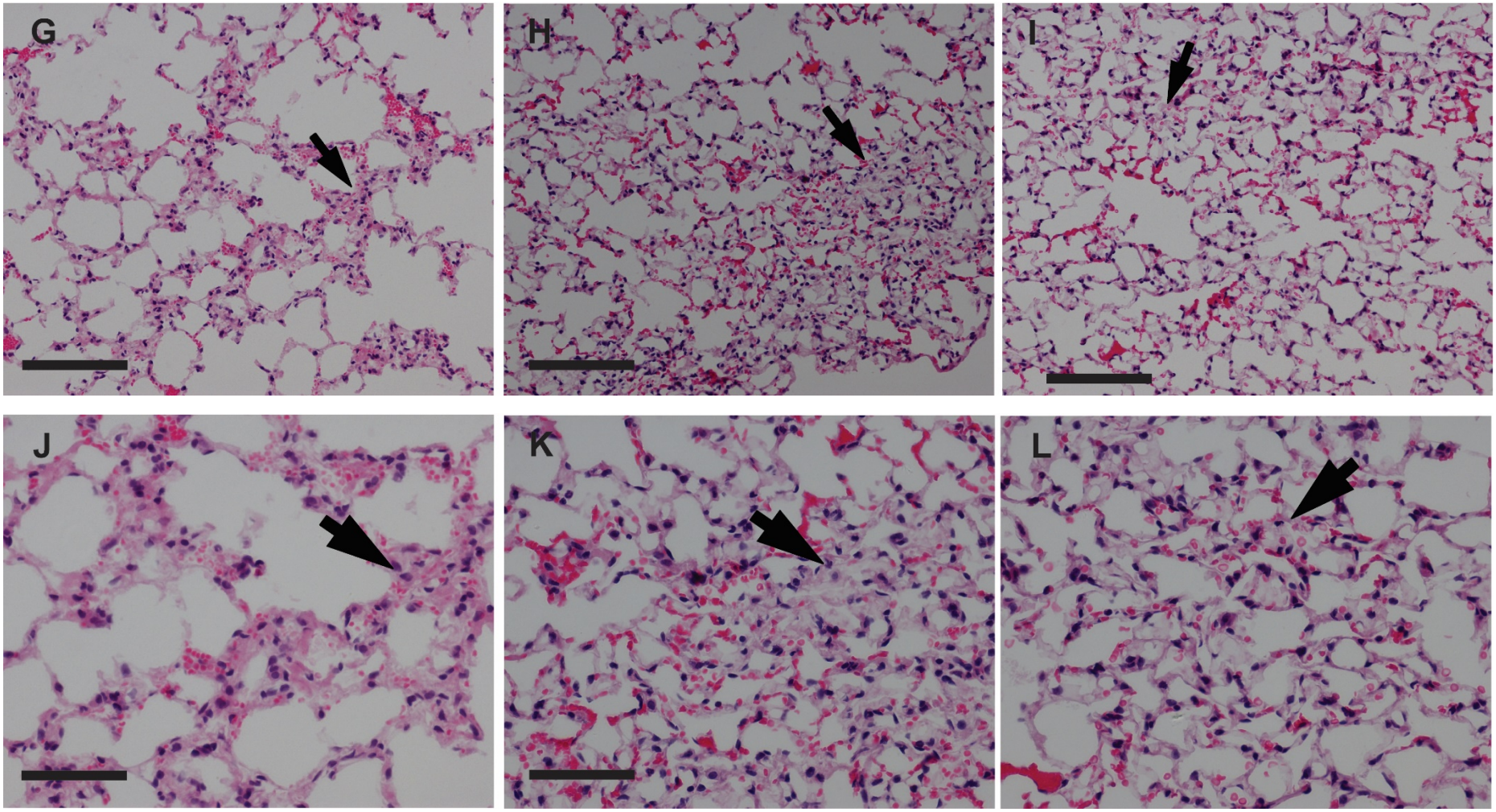

Figure A1.11 Gross appearance and histology of lungs of SCID mice after 3rd, 5th and 8th week of injection with A549 cells via the tail vein. Mice were injected with 1×10^5 A549 cells into the lateral vein of the tail. Mice were then euthanised after 3rd, 5th and 8th week of injection. Lungs

were excised, sectioned and H and E staining was performed. Lungs of mice at (A) 3rd, (B) 5th, (C) 8th weeks after cell injection. White patches on lungs appeared by week 5. H and E staining of lung sections of mice at (D) 3rd, (E) 5th, (F) 8th week after cells injection using a 10× objective. Squares and arrow indicate areas of high cell density. (G-I) Area shown in insets from panel (D-F) respectively, using 20× objective. (J-L) Area shown in insets from images (D-F), respectively, using 40× objective. Scale bars: D-I 100 μM and J-L 50 μM.

A1.5. Relevant permissions

ELSEVIER LICENSE
TERMS AND CONDITIONS

Nov 11, 2020

This Agreement between Ms. Nensi Shrestha ("You") and Elsevier ("Elsevier") consists of your license details and the terms and conditions provided by Elsevier and Copyright Clearance Center.

License Number	4946190659352
License date	Nov 11, 2020
Licensed Content Publisher	Elsevier
Licensed Content Publication	Journal of Thoracic Oncology
Licensed Content Title	The IASLC Lung Cancer Staging Project: Proposals for Revision of the TNM Stage Groupings in the Forthcoming (Eighth) Edition of the TNM Classification for Lung Cancer
Licensed Content Author	Peter Goldstraw,Kari Chansky,John Crowley,Ramon Rami-Porta,Hisao Asamura,Wilfried E.E. Eberhardt,Andrew G. Nicholson,Patti Groome,Alan Mitchell,Vanessa Bolejack,Peter Goldstraw,Ramón Rami-Porta,Hisao Asamura,David Ball,David G. Beer,Ricardo Beyruti et al.
Licensed Content Date	Jan 1, 2016
Licensed Content Volume	11
Licensed Content Issue	1
Licensed Content Pages	13
Start Page	39
End Page	51

Type of Use	reuse in a thesis/dissertation
Portion	figures/tables/illustrations
Number of figures/tables/illustrations	1
Format	both print and electronic
Are you the author of this Elsevier article?	No
Will you be translating?	No
Title	Combination of ALK and MEK inhibitors for the treatment of ALK-positive non-small cell lung cancer
Institution name	University of Otago
Expected presentation date	Nov 2020
Portions	Table 5 on page 44
Requestor Location	Ms. Nensi Shrestha 18 Frederick Street Dunedin, Otago 9016 New Zealand Attn: Ms. Nensi Shrestha
Publisher Tax ID	GB 494 6272 12
Total	0.00 USD
Terms and Conditions	

INTRODUCTION

1. The publisher for this copyrighted material is Elsevier. By clicking "accept" in connection with completing this licensing transaction, you agree that the following terms and conditions

References

Aaronson, D. S., & Horvath, C. M. (2002). A road map for those who don't know JAK-STAT. *Science, 296*(5573), 1653-1655. doi:10.1126/science.1071545

Abe, H., Kikuchi, S., Hayakawa, K., Iida, T., Nagahashi, N., Maeda, K., Sakamoto, J., Matsumoto, N., Miura, T., Matsumura, K., Seki, N., Inaba, T., Kawasaki, H., Yamaguchi, T., Kakefuda, R., Nanayama, T., Kurachi, H., Hori, Y., Yoshida, T., Kakegawa, J., Watanabe, Y., Gilmartin, A. G., Richter, M. C., Moss, K. G., & Laquerre, S. G. (2011). Discovery of a Highly Potent and Selective MEK Inhibitor: GSK1120212 (JTP-74057 DMSO Solvate). *ACS Med Chem Lett, 2*(4), 320-324. doi:10.1021/ml200004g

Adjei, A. A., Cohen, R. B., Franklin, W., Morris, C., Wilson, D., Molina, J. R., Hanson, L. J., Gore, L., Chow, L., Leong, S., Maloney, L., Gordon, G., Simmons, H., Marlow, A., Litwiler, K., Brown, S., Poch, G., Kane, K., Haney, J., & Eckhardt, S. G. (2008). Phase I pharmacokinetic and pharmacodynamic study of the oral, small-molecule mitogen-activated protein kinase kinase 1/2 inhibitor AZD6244 (ARRY-142886) in patients with advanced cancers. *J Clin Oncol, 26*(13), 2139-2146. doi:10.1200/JCO.2007.14.4956

Aggarwal, B. B. (2003). Signalling pathways of the TNF superfamily: a double-edged sword. *Nat Rev Immunol, 3*(9), 745-756. doi:10.1038/nri1184

Alberg, A. J., Yung, R. C., Strickland, P., & Nelson, J. (2002). Respiratory cancer and exposure to arsenic, chromium, nickel, and polycyclic aromatic hydrocarbons. *Clinics in Occupational and Environmental Medicine, 2*, 779-801. doi:10.1016/S1526-0046(02)00056-0

Alder, I. (1912). Primary malignant growths of the lungs and bronchi; a pathological and clinical study. *London : Longmans*.

Ali, S. M., Hensing, T., Schrock, A. B., Allen, J., Sanford, E., Gowen, K., Kulkarni, A., He, J., Suh, J. H., Lipson, D., Elvin, J. A., Yelensky, R., Chalmers, Z., Chmielecki, J., Peled, N., Klempner, S. J., Firozvi, K., Frampton, G. M., Molina, J. R., Menon, S., Brahmer, J. R., MacMahon, H., Nowak, J., Ou, S. H., Zauderer, M., Ladanyi, M., Zakowski, M., Fischbach, N., Ross, J. S., Stephens, P. J., Miller, V. A., Wakelee, H., Ganesan, S., & Salgia, R. (2016). Comprehensive Genomic Profiling Identifies a Subset of Crizotinib-Responsive ALK-Rearranged Non-Small Cell Lung Cancer Not Detected by Fluorescence In Situ Hybridization. *Oncologist, 21*(6), 762-770. doi:10.1634/theoncologist.2015-0497

Alitalo, K., Tammela, T., & Petrova, T. V. (2005). Lymphangiogenesis in development and human disease. *Nature, 438*(7070), 946-953. doi:10.1038/nature04480

Alshammari, T. M. (2016). Drug safety: The concept, inception and its importance in patients' health. *Saudi Pharm J, 24*(4), 405-412. doi:10.1016/j.jsps.2014.04.008

Amin, H. M., Medeiros, L. J., Ma, Y., Feretzaki, M., Das, P., Leventaki, V., Rassidakis, G. Z., O'Connor, S. L., McDonnell, T. J., & Lai, R. (2003). Inhibition of JAK3 induces apoptosis and decreases anaplastic lymphoma kinase activity in anaplastic large cell lymphoma. *Oncogene, 22*(35), 5399-5407. doi:10.1038/sj.onc.1206849

Andreeff, M., Goodrich, D. W., & Pardee, A. B. (2000). Cell Proliferation, Differentiation, and Apoptosis. In R. C. Blast, D. W. Kufe, R. E. Pollock, R. R. Weichselbaum, J. F. Holland, & E. Frei (Eds.), *Cancer Medicine* (pp. 17-32): B.C. Decker Inc.

Ascierto, P. A., McArthur, G. A., Dreno, B., Atkinson, V., Liszkay, G., Di Giacomo, A. M., Mandala, M., Demidov, L., Stroyakovskiy, D., Thomas, L., de la Cruz-Merino, L., Dutriaux, C., Garbe, C., Yan, Y., Wongchenko, M., Chang, I., Hsu, J. J., Koralek, D. O., Rooney, I., Ribas, A., & Larkin, J. (2016). Cobimetinib

combined with vemurafenib in advanced BRAF(V600)-mutant melanoma (coBRIM): updated efficacy results from a randomised, double-blind, phase 3 trial. *Lancet Oncol, 17*(9), 1248-1260. doi:10.1016/S1470-2045(16)30122-X

Ascierto, P. A., Schadendorf, D., Berking, C., Agarwala, S. S., van Herpen, C. M., Queirolo, P., Blank, C. U., Hauschild, A., Beck, J. T., St-Pierre, A., Niazi, F., Wandel, S., Peters, M., Zubel, A., & Dummer, R. (2013). MEK162 for patients with advanced melanoma harbouring NRAS or Val600 BRAF mutations: a non-randomised, open-label phase 2 study. *Lancet Oncol, 14*(3), 249-256. doi:10.1016/S1470-2045(13)70024-X

Ashkenazi, A., & Dixit, V. M. (1998). Death receptors: signaling and modulation. *Science, 281*(5381), 1305-1308. doi:10.1126/science.281.5381.1305

Avruch, J., Zhang, X. F., & Kyriakis, J. M. (1994). Raf meets Ras: completing the framework of a signal transduction pathway. *Trends Biochem Sci, 19*(7), 279-283. doi:10.1016/0968-0004(94)90005-1

Baeriswyl, V., & Christofori, G. (2009). The angiogenic switch in carcinogenesis. *Semin Cancer Biol, 19*(5), 329-337. doi:10.1016/j.semcancer.2009.05.003

Bai, R. Y., Dieter, P., Peschel, C., Morris, S. W., & Duyster, J. (1998). Nucleophosmin-anaplastic lymphoma kinase of large-cell anaplastic lymphoma is a constitutively active tyrosine kinase that utilizes phospholipase C-gamma to mediate its mitogenicity. *Mol Cell Biol, 18*(12), 6951-6961. doi:10.1128/mcb.18.12.6951

Bai, R. Y., Ouyang, T., Miething, C., Morris, S. W., Peschel, C., & Duyster, J. (2000). Nucleophosmin-anaplastic lymphoma kinase associated with anaplastic large-cell lymphoma activates the phosphatidylinositol 3-kinase/Akt antiapoptotic signaling pathway. *Blood, 96*(13), 4319-4327.

Baig, S., Seevasant, I., Mohamad, J., Mukheem, A., Huri, H. Z., & Kamarul, T. (2016). Potential of apoptotic pathway-targeted cancer therapeutic research: Where do we stand? *Cell Death Dis, 7*, e2058. doi:10.1038/cddis.2015.275

Banerji, U., Camidge, D. R., Verheul, H. M., Agarwal, R., Sarker, D., Kaye, S. B., Desar, I. M., Timmer-Bonte, J. N., Eckhardt, S. G., Lewis, K. D., Brown, K. H., Cantarini, M. V., Morris, C., George, S. M., Smith, P. D., & van Herpen, C. M. (2010). The first-in-human study of the hydrogen sulfate (Hyd-sulfate) capsule of the MEK1/2 inhibitor AZD6244 (ARRY-142886): a phase I open-label multicenter trial in patients with advanced cancer. *Clin Cancer Res, 16*(5), 1613-1623. doi:10.1158/1078-0432.CCR-09-2483

Barbarino, M., D'Angelo, B., Pentimalli, F., & Giordano, A. (2017). Molecular Mechanisms of Cancer Progression: The Central Role of the Retinoblastoma Family Members. *Reviews in Cell Biology and Molecular Medicine, 3*, 72-108. doi:10.1002/3527600906.mcb.201700004

Barnes, D. M., & Gillett, C. E. (1995). Determination of cell proliferation. *Clin Mol Pathol, 48*(1), M2-5. doi:10.1136/mp.48.1.m2

Barrows, S. M., Wright, K., Copley-Merriman, C., Kaye, J. A., Chioda, M., Wiltshire, R., Torgersen, K. M., & Masters, E. T. (2019). Systematic review of sequencing of ALK inhibitors in ALK-positive non-small-cell lung cancer. *Lung Cancer (Auckl), 10*, 11-20. doi:10.2147/LCTT.S179349

Bayat Mokhtari, R., Homayouni, T. S., Baluch, N., Morgatskaya, E., Kumar, S., Das, B., & Yeger, H. (2017). Combination therapy in combating cancer. *Oncotarget, 8*(23), 38022-38043. doi:10.18632/oncotarget.16723

Bayliss, R., Choi, J., Fennell, D. A., Fry, A. M., & Richards, M. W. (1209). Molecular mechanisms that underpin EML4-ALK driven cancers and their response to

targeted drugs. *Cellular and Molecular Life Sciences, 73*(6), 1209-1224. doi:http://dx.doi.org/10.1007/s00018-015-2117-6

Beadling, C., Wald, A. I., Warrick, A., Neff, T. L., Zhong, S., Nikiforov, Y. E., Corless, C. L., & Nikiforova, M. N. (2016). A Multiplexed Amplicon Approach for Detecting Gene Fusions by Next-Generation Sequencing. *J Mol Diagn, 18*(2), 165-175. doi:10.1016/j.jmoldx.2015.10.002

Beckmann, G., & Bork, P. (1993). An adhesive domain detected in functionally diverse receptors. *Trends Biochem Sci, 18*(2), 40-41. doi:10.1016/0968-0004(93)90049-s

Bell, D. W., Gore, I., Okimoto, R. A., Godin-Heymann, N., Sordella, R., Mulloy, R., Sharma, S. V., Brannigan, B. W., Mohapatra, G., Settleman, J., & Haber, D. A. (2005). Inherited susceptibility to lung cancer may be associated with the T790M drug resistance mutation in EGFR. *Nature Genetics, 37*(12), 1315-1316. doi:10.1038/ng1671

Bendell, J. C., Javle, M., Bekaii-Saab, T. S., Finn, R. S., Wainberg, Z. A., Laheru, D. A., Weekes, C. D., Tan, B. R., Khan, G. N., Zalupski, M. M., Infante, J. R., Jones, S., Papadopoulos, K. P., Tolcher, A. W., Chavira, R. E., Christy-Bittel, J. L., Barrett, E., & Patnaik, A. (2017). A phase 1 dose-escalation and expansion study of binimetinib (MEK162), a potent and selective oral MEK1/2 inhibitor. *Br J Cancer, 116*(5), 575-583. doi:10.1038/bjc.2017.10

Beresford, M. J., Wilson, G. D., & Makris, A. (2006). Measuring proliferation in breast cancer: practicalities and applications. *Breast Cancer Res, 8*(6), 216. doi:10.1186/bcr1618

Bergers, G., & Benjamin, L. E. (2003). Tumorigenesis and the angiogenic switch. *Nat Rev Cancer, 3*(6), 401-410. doi:10.1038/nrc1093

Bergethon, K., Shaw, A. T., Ignatius Ou, S.-H., Katayama, R., Lovly, C. M., McDonald, N. T., Massion, P. P., Siwak-Tapp, C., Gonzalez, A., & Fang, R. (2012). ROS1 rearrangements define a unique molecular class of lung cancers. *Journal of Clinical Oncology, 30*(8), 863-870.

Berridge, M. J. (2009). Inositol trisphosphate and calcium signalling mechanisms. *Biochim Biophys Acta, 1793*(6), 933-940. doi:10.1016/j.bbamcr.2008.10.005

Bhalla, S., Evens, A. M., Dai, B., Prachand, S., Gordon, L. I., & Gartenhaus, R. B. (2011). The novel anti-MEK small molecule AZD6244 induces BIM-dependent and AKT-independent apoptosis in diffuse large B-cell lymphoma. *Blood, 118*(4), 1052-1061. doi:10.1182/blood-2011-03-340109

Bhatt, K. V., Spofford, L. S., Aram, G., McMullen, M., Pumiglia, K., & Aplin, A. E. (2005). Adhesion control of cyclin D1 and p27Kip1 levels is deregulated in melanoma cells through BRAF-MEK-ERK signaling. *Oncogene, 24*(21), 3459-3471. doi:10.1038/sj.onc.1208544

Bibby, M. C. (2004). Orthotopic models of cancer for preclinical drug evaluation: advantages and disadvantages. *Eur J Cancer, 40*(6), 852-857. doi:10.1016/j.ejca.2003.11.021

Bilsland, J. G., Wheeldon, A., Mead, A., Znamenskiy, P., Almond, S., Waters, K. A., Thakur, M., Beaumont, V., Bonnert, T. P., Heavens, R., Whiting, P., McAllister, G., & Munoz-Sanjuan, I. (2008). Behavioral and neurochemical alterations in mice deficient in anaplastic lymphoma kinase suggest therapeutic potential for psychiatric indications. *Neuropsychopharmacology, 33*(3), 685-700. doi:10.1038/sj.npp.1301446

Blackhall, F., Ross Camidge, D., Shaw, A. T., Soria, J. C., Solomon, B. J., Mok, T., Hirsh, V., Janne, P. A., Shi, Y., Yang, P. C., Pas, T., Hida, T., Carpeno, J. C.,

Lanzalone, S., Polli, A., Iyer, S., Reisman, A., Wilner, K. D., & Kim, D. W. (2017). Final results of the large-scale multinational trial PROFILE 1005: efficacy and safety of crizotinib in previously treated patients with advanced/metastatic ALK-positive non-small-cell lung cancer. *ESMO Open, 2*(3), e000219. doi:10.1136/esmoopen-2017-000219

Bland, A. R., Bower, R. L., Nimick, M., Hawkins, B. C., Rosengren, R. J., & Ashton, J. C. (2019). Cytotoxicity of curcumin derivatives in ALK positive non-small cell lung cancer. *Eur J Pharmacol, 865*, 172749. doi:10.1016/j.ejphar.2019.172749

Blume-Jensen, P., & Hunter, T. (2001). Oncogenic kinase signalling. *Nature, 411*(6835), 355-365. doi:10.1038/35077225

Boland, J. M., Jang, J. S., Li, J., Lee, A. M., Wampfler, J. A., Erickson-Johnson, M. R., Soares, I., Yang, P., Jen, J., Oliveira, A. M., & Yi, E. S. (2013). MET and EGFR mutations identified in ALK-rearranged pulmonary adenocarcinoma: molecular analysis of 25 ALK-positive cases. *J Thorac Oncol, 8*(5), 574-581. doi:10.1097/JTO.0b013e318287c395

Bosma, M. J., & Carroll, A. M. (1991). The SCID mouse mutant: definition, characterization, and potential uses. *Annu Rev Immunol, 9*, 323-350. doi:10.1146/annurev.iy.09.040191.001543

Bossi, R. T., Saccardo, M. B., Ardini, E., Menichincheri, M., Rusconi, L., Magnaghi, P., Orsini, P., Avanzi, N., Borgia, A. L., Nesi, M., Bandiera, T., Fogliatto, G., & Bertrand, J. A. (2010). Crystal structures of anaplastic lymphoma kinase in complex with ATP competitive inhibitors. *Biochemistry, 49*(32), 6813-6825. doi:10.1021/bi1005514

Bouillet, P., & Strasser, A. (2002). BH3-only proteins - evolutionarily conserved proapoptotic Bcl-2 family members essential for initiating programmed cell death. *J Cell Sci, 115*(Pt 8), 1567-1574.

Bozic, A., & Nowak, A. K. (2016). Resisting Resistance. *Annual Review of Cancer Biology, 1*, 203-221.

Bozic, I., Reiter, J. G., Allen, B., Antal, T., Chatterjee, K., Shah, P., Moon, Y. S., Yaqubie, A., Kelly, N., Le, D. T., Lipson, E. J., Chapman, P. B., Diaz, L. A., Jr., Vogelstein, B., & Nowak, M. A. (2013). Evolutionary dynamics of cancer in response to targeted combination therapy. *Elife, 2*, e00747. doi:10.7554/eLife.00747

Brenner, D., & Mak, T. W. (2009). Mitochondrial cell death effectors. *Curr Opin Cell Biol, 21*(6), 871-877. doi:10.1016/j.ceb.2009.09.004

Brenner, D. R., McLaughlin, J. R., & Hung, R. J. (2011). Previous lung diseases and lung cancer risk: a systematic review and meta-analysis. *PLoS ONE, 6*(3), e17479. doi:10.1371/journal.pone.0017479

Brogi, E., Wu, T., Namiki, A., & Isner, J. M. (1994). Indirect angiogenic cytokines upregulate VEGF and bFGF gene expression in vascular smooth muscle cells, whereas hypoxia upregulates VEGF expression only. *Circulation, 90*(2), 649-652. doi:10.1161/01.cir.90.2.649

Bruno, S., & Darzynkiewicz, Z. (1992). Cell cycle dependent expression and stability of the nuclear protein detected by Ki-67 antibody in HL-60 cells. *Cell Prolif, 25*(1), 31-40. doi:10.1111/j.1365-2184.1992.tb01435.x

Bunn, P. A., Jr., Minna, J. D., Augustyn, A., Gazdar, A. F., Ouadah, Y., Krasnow, M. A., Berns, A., Brambilla, E., Rekhtman, N., Massion, P. P., Niederst, M., Peifer, M., Yokota, J., Govindan, R., Poirier, J. T., Byers, L. A., Wynes, M. W., McFadden, D. G., MacPherson, D., Hann, C. L., Farago, A. F., Dive, C., Teicher, B. A., Peacock, C. D., Johnson, J. E., Cobb, M. H., Wendel, H. G., Spigel, D., Sage, J.,

Yang, P., Pietanza, M. C., Krug, L. M., Heymach, J., Ujhazy, P., Zhou, C., Goto, K., Dowlati, A., Christensen, C. L., Park, K., Einhorn, L. H., Edelman, M. J., Giaccone, G., Gerber, D. E., Salgia, R., Owonikoko, T., Malik, S., Karachaliou, N., Gandara, D. R., Slotman, B. J., Blackhall, F., Goss, G., Thomas, R., Rudin, C. M., & Hirsch, F. R. (2016). Small Cell Lung Cancer: Can Recent Advances in Biology and Molecular Biology Be Translated into Improved Outcomes? *J Thorac Oncol, 11*(4), 453-474. doi:10.1016/j.jtho.2016.01.012

Burrows, F. J., Derbyshire, E. J., Tazzari, P. L., Amlot, P., Gazdar, A. F., King, S. W., Letarte, M., Vitetta, E. S., & Thorpe, P. E. (1995). Up-regulation of endoglin on vascular endothelial cells in human solid tumors: implications for diagnosis and therapy. *Clin Cancer Res, 1*(12), 1623-1634.

Cai, W., Lin, D., Wu, C., Li, X., Zhao, C., Zheng, L., Chuai, S., Fei, K., Zhou, C., & Hirsch, F. R. (2015). Intratumoral Heterogeneity of ALK-Rearranged and ALK/EGFR Coaltered Lung Adenocarcinoma. *J Clin Oncol, 33*(32), 3701-3709. doi:10.1200/JCO.2014.58.8293

Cain, K., Bratton, S. B., & Cohen, G. M. (2002). The Apaf-1 apoptosome: a large caspase-activating complex. *Biochimie, 84*(2-3), 203-214. doi:10.1016/s0300-9084(02)01376-7

Camidge, D. R., Bang, Y. J., Kwak, E. L., Iafrate, A. J., Varella-Garcia, M., Fox, S. B., Riely, G. J., Solomon, B., Ou, S. H. I., Kim, D. W., Salgia, R., Fidias, P., Engelman, J. A., Gandhi, L., Jänne, P. A., Costa, D. B., Shapiro, G. I., LoRusso, P., Ruffner, K., Stephenson, P., Tang, Y., Wilner, K., Clark, J. W., & Shaw, A. T. (2012). Activity and safety of crizotinib in patients with ALK-positive non-small-cell lung cancer: Updated results from a phase 1 study. *The Lancet Oncology, 13*(10), 1011-1019. doi:10.1016/S1470-2045(12)70344-3

Camidge, D. R., & Doebele, R. C. (2012). Treating ALK-positive lung cancer—early successes and future challenges. *Nature Reviews Clinical Oncology, 9*(5), 268-277. doi:10.1038/nrclinonc.2012.43

Camidge, D. R., Kim, H. R., Ahn, M. J., Yang, J. C., Han, J. Y., Lee, J. S., Hochmair, M. J., Li, J. Y., Chang, G. C., Lee, K. H., Gridelli, C., Delmonte, A., Garcia Campelo, R., Kim, D. W., Bearz, A., Griesinger, F., Morabito, A., Felip, E., Califano, R., Ghosh, S., Spira, A., Gettinger, S. N., Tiseo, M., Gupta, N., Haney, J., Kerstein, D., & Popat, S. (2018). Brigatinib versus Crizotinib in ALK-Positive Non-Small-Cell Lung Cancer. *N Engl J Med, 379*(21), 2027-2039. doi:10.1056/NEJMoa1810171

Camidge, D. R., Kono, S. A., Flacco, A., Tan, A. C., Doebele, R. C., Zhou, Q., Crino, L., Franklin, W. A., & Varella-Garcia, M. (2010). Optimizing the detection of lung cancer patients harboring anaplastic lymphoma kinase (ALK) gene rearrangements potentially suitable for ALK inhibitor treatment. *Clin Cancer Res, 16*(22), 5581-5590. doi:10.1158/1078-0432.CCR-10-0851

Campbell, K. J., & Tait, S. W. G. (2018). Targeting BCL-2 regulated apoptosis in cancer. *Open Biol, 8*(5). doi:10.1098/rsob.180002

Carmeliet, P. (2000). Mechanisms of angiogenesis and arteriogenesis. *Nat Med, 6*(4), 389-395. doi:10.1038/74651

Carpenter, G., & Ji, Q. (1999). Phospholipase C-gamma as a signal-transducing element. *Exp Cell Res, 253*(1), 15-24. doi:10.1006/excr.1999.4671

Carter, C. A., Rajan, A., Keen, C., Szabo, E., Khozin, S., Thomas, A., Brzezniak, C., Guha, U., Doyle, L. A., Steinberg, S. M., Xi, L., Raffeld, M., Tomita, Y., Lee, M. J., Lee, S., Trepel, J. B., Reckamp, K. L., Koehler, S., Gitlitz, B., Salgia, R., Gandara, D., Vokes, E., & Giaccone, G. (2016). Selumetinib with and without

erlotinib in KRAS mutant and KRAS wild-type advanced nonsmall-cell lung cancer. *Ann Oncol, 27*(4), 693-699. doi:10.1093/annonc/mdw008

Catalanotti, F., Solit, D. B., Pulitzer, M. P., Berger, M. F., Scott, S. N., Iyriboz, T., Lacouture, M. E., Panageas, K. S., Wolchok, J. D., Carvajal, R. D., Schwartz, G. K., Rosen, N., & Chapman, P. B. (2013). Phase II trial of MEK inhibitor selumetinib (AZD6244, ARRY-142886) in patients with BRAFV600E/K-mutated melanoma. *Clinical Cancer Research, 19*(8), 2257-2264. doi:10.1158/1078-0432.CCR-12-3476

Cekanova, M., & Rathore, K. (2014). Animal models and therapeutic molecular targets of cancer: utility and limitations. *Drug Des Devel Ther, 8*, 1911-1921. doi:10.2147/DDDT.S49584

Cha, Y. J., Kim, H. R., & Shim, H. S. (2016). Clinical outcomes in ALK-rearranged lung adenocarcinomas according to ALK fusion variants. *J Transl Med, 14*(1), 296. doi:10.1186/s12967-016-1061-z

Chambard, J. C., Lefloch, R., Pouyssegur, J., & Lenormand, P. (2007). ERK implication in cell cycle regulation. *Biochim Biophys Acta, 1773*(8), 1299-1310. doi:10.1016/j.bbamcr.2006.11.010

Chen, L., Willis, S. N., Wei, A., Smith, B. J., Fletcher, J. I., Hinds, M. G., Colman, P. M., Day, C. L., Adams, J. M., & Huang, D. C. (2005). Differential targeting of prosurvival Bcl-2 proteins by their BH3-only ligands allows complementary apoptotic function. *Mol Cell, 17*(3), 393-403. doi:10.1016/j.molcel.2004.12.030

Chen, Z., Fillmore, C. M., Hammerman, P. S., Kim, C. F., & Wong, K. K. (2014). Non-small-cell lung cancers: a heterogeneous set of diseases. *Nat Rev Cancer, 14*(8), 535-546. doi:10.1038/nrc3775

Chen, Z., Sasaki, T., Tan, X., Carretero, J., Shimamura, T., Li, D., Xu, C., Wang, Y., Adelmant, G. O., Capelletti, M., Lee, H. J., Rodig, S. J., Borgman, C., Park, S. I., Kim, H. R., Padera, R., Marto, J. A., Gray, N. S., Kung, A. L., Shapiro, G. I., Janne, P. A., & Wong, K. K. (2010). Inhibition of ALK, PI3K/MEK, and HSP90 in murine lung adenocarcinoma induced by EML4-ALK fusion oncogene. *Cancer Res, 70*(23), 9827-9836. doi:10.1158/0008-5472.CAN-10-1671

Cheng, Y., & Tian, H. (2017). Current Development Status of MEK Inhibitors. *Molecules, 22*(10). doi:10.3390/molecules22101551

Cheon, D. J., & Orsulic, S. (2011). Mouse models of cancer. *Annu Rev Pathol, 6*, 95-119. doi:10.1146/annurev.pathol.3.121806.154244

Chew, H. K., Davies, A. M., Wun, T., Harvey, D., Zhou, H., & White, R. H. (2008). The incidence of venous thromboembolism among patients with primary lung cancer. *J Thromb Haemost, 6*(4), 601-608. doi:10.1111/j.1538-7836.2008.02908.x

Chiarle, R., Simmons, W. J., Cai, H., Dhall, G., Zamo, A., Raz, R., Karras, J. G., Levy, D. E., & Inghirami, G. (2005). Stat3 is required for ALK-mediated lymphomagenesis and provides a possible therapeutic target. *Nat Med, 11*(6), 623-629. doi:10.1038/nm1249

Chiarle, R., Voena, C., Ambrogio, C., Piva, R., & Inghirami, G. (2008). The anaplastic lymphoma kinase in the pathogenesis of cancer. *Nat Rev Cancer, 8*(1), 11-23. doi:10.1038/nrc2291

Choi, Y. L., Lira, M. E., Hong, M., Kim, R. N., Choi, S. J., Song, J. Y., Pandy, K., Mann, D. L., Stahl, J. A., Peckham, H. E., Zheng, Z., Han, J., Mao, M., & Kim, J. (2014). A novel fusion of TPR and ALK in lung adenocarcinoma. *J Thorac Oncol, 9*(4), 563-566. doi:10.1097/JTO.0000000000000093

Choi, Y. L., Soda, M., Yamashita, Y., Ueno, T., Takashima, J., Nakajima, T., Yatabe, Y., Takeuchi, K., Hamada, T., Haruta, H., Ishikawa, Y., Kimura, H., Mitsudomi,

T., Tanio, Y., Mano, H., & Group, A. L. K. L. C. S. (2010). EML4-ALK mutations in lung cancer that confer resistance to ALK inhibitors. *N Engl J Med, 363*(18), 1734-1739. doi:10.1056/NEJMoa1007478

Choo, E. F., Ng, C. M., Berry, L., Belvin, M., Lewin-Koh, N., Merchant, M., & Salphati, L. (2013). PK-PD modeling of combination efficacy effect from administration of the MEK inhibitor GDC-0973 and PI3K inhibitor GDC-0941 in A2058 xenografts. *Cancer Chemother Pharmacol, 71*(1), 133-143. doi:10.1007/s00280-012-1988-6

Chou, T.-C., & Talalay, P. (1983). Analysis of combined drug effects: a new look at a very old problem. *Trends in Pharmacological Sciences, 4*, 450-454. doi:https://doi.org/10.1016/0165-6147(83)90490-X

Christensen, J. G., Zou, H. Y., Arango, M. E., Li, Q., Lee, J. H., McDonnell, S. R., Yamazaki, S., Alton, G. R., Mroczkowski, B., & Los, G. (2007). Cytoreductive antitumor activity of PF-2341066, a novel inhibitor of anaplastic lymphoma kinase and c-Met, in experimental models of anaplastic large-cell lymphoma. *Molecular Cancer Therapeutics, 6*(12), 3314-3322.

ClinicalTrials.gov National Library of Medicine (US). (2012, Sep 9, 2019). Identifier: NCT01586624 A Phase I Trial of Vandetanib (ZD6474) and Selumetinib (AZD6244)for Solid Tumours Including Non Small Cell Lung Cancer (VanSel-1). Retrieved from https://clinicaltrials.gov/ct2/show/NCT01586624

ClinicalTrials.gov National Library of Medicine (US). (2013, July 10, 2018). Identifier: NCT02025114 Selumetinib in Combination With Gefitinib in NSCLC Patients. Retrieved from https://clinicaltrials.gov/ct2/show/study/NCT02025114

ClinicalTrials.gov National Library of Medicine (US). (2017, Nov 19, 2019). Identifier: NCT03052608, A Study Of Lorlatinib Versus Crizotinib In First Line Treatment Of Patients With ALK-Positive NSCLC. Retrieved from https://clinicaltrials.gov/ct2/show/NCT03052608#contactlocation

ClinicalTrials.gov National Library of Medicine (US). (2019a, November 26, 2019). Alectinib in Combination With Bevacizumab in ALK Positive NSCLC. Retrieved from https://clinicaltrials.gov/ct2/show/NCT03779191

ClinicalTrials.gov National Library of Medicine (US). (2019b, Nov 14, 2019). Ceritinib + Trametinib in Patients With Advanced ALK-Positive Non-Small Cell Lung Cancer (NSCLC). Retrieved from https://clinicaltrials.gov/ct2/show/NCT03087448

ClinicalTrials.gov National Library of Medicine (US). (2020, January 6, 2020). Study of Safety and Efficacy of Ceritinib in Combination With Nivolumab in Patients With ALK-positive Non-small Cell Lung Cancer. Retrieved from https://clinicaltrials.gov/ct2/show/NCT02393625

Cobb, M. H., & Goldsmith, E. J. (1995). How MAP kinases are regulated. *J Biol Chem, 270*(25), 14843-14846. doi:10.1074/jbc.270.25.14843

Cohen, G. M. (1997). Caspases: the executioners of apoptosis. *Biochem J, 326 (Pt 1)*, 1-16. doi:10.1042/bj3260001

Collisson, E. A., Campbell, J. D., Brooks, A. N., Berger, A. H., Lee, W., Chmielecki, J., Beer, D. G., Cope, L., Creighton, C. J., Danilova, L., Ding, L., Getz, G., Hammerman, P. S., Neil Hayes, D., Hernandez, B., Herman, J. G., Heymach, J. V., Jurisica, I., Kucherlapati, R., Kwiatkowski, D., Ladanyi, M., Robertson, G., Schultz, N., Shen, R., Sinha, R., Sougnez, C., Tsao, M.-S., Travis, W. D., Weinstein, J. N., Wigle, D. A., Wilkerson, M. D., Chu, A., Cherniack, A. D., Hadjipanayis, A., Rosenberg, M., Weisenberger, D. J., Laird, P. W., Radenbaugh, A., Ma, S., Stuart, J. M., Averett Byers, L., Baylin, S. B., Govindan, R.,

Meyerson, M., Rosenberg, M., Gabriel, S. B., Cibulskis, K., Sougnez, C., Kim, J., Stewart, C., Lichtenstein, L., Lander, E. S., Lawrence, M. S., Getz, G., Kandoth, C., Fulton, R., Fulton, L. L., McLellan, M. D., Wilson, R. K., Ye, K., Fronick, C. C., Maher, C. A., Miller, C. A., Wendl, M. C., Cabanski, C., Ding, L., Mardis, E., Govindan, R., Creighton, C. J., Wheeler, D., Balasundaram, M., Butterfield, Y. S. N., Carlsen, R., Chu, A., Chuah, E., Dhalla, N., Guin, R., Hirst, C., Lee, D., Li, H. I., Mayo, M., Moore, R. A., Mungall, A. J., Schein, J. E., Sipahimalani, P., Tam, A., Varhol, R., Gordon Robertson, A., Wye, N., Thiessen, N., Holt, R. A., Jones, S. J. M., Marra, M. A., Campbell, J. D., Brooks, A. N., Chmielecki, J., Imielinski, M., Onofrio, R. C., Hodis, E., Zack, T., Sougnez, C., Helman, E., Sekhar Pedamallu, C., Mesirov, J., Cherniack, A. D., Saksena, G., Schumacher, S. E., Carter, S. L., Hernandez, B., Garraway, L., Beroukhim, R., Gabriel, S. B., Getz, G., Meyerson, M., Hadjipanayis, A., Lee, S., Mahadeshwar, H. S., Pantazi, A., Protopopov, A., Ren, X., Seth, S., Song, X., Tang, J., Yang, L., Zhang, J., Chen, P.-C., Parfenov, M., Wei Xu, A., Santoso, N., Chin, L., Park, P. J., Kucherlapati, R., Hoadley, K. A., Todd Auman, J., Meng, S., Shi, Y., Buda, E., Waring, S., Veluvolu, U., Tan, D., Mieczkowski, P. A., Jones, C. D., Simons, J. V., Soloway, M. G., Bodenheimer, T., Jefferys, S. R., Roach, J., Hoyle, A. P., Wu, J., Balu, S., Singh, D., Prins, J. F., Marron, J. S., Parker, J. S., Neil Hayes, D., Perou, C. M., Liu, J., Cope, L., Danilova, L., Weisenberger, D. J., Maglinte, D. T., Lai, P. H., Bootwalla, M. S., Van Den Berg, D. J., Triche Jr, T., Baylin, S. B., Laird, P. W., Rosenberg, M., Chin, L., Zhang, J., Cho, J., DiCara, D., Heiman, D., Lin, P., Mallard, W., Voet, D., Zhang, H., Zou, L., Noble, M. S., Lawrence, M. S., Saksena, G., Gehlenborg, N., Thorvaldsdottir, H., Mesirov, J., Nazaire, M.-D., Robinson, J., Getz, G., Lee, W., Arman Aksoy, B., Ciriello, G., Taylor, B. S., Dresdner, G., Gao, J., Gross, B., Seshan, V. E., Ladanyi, M., Reva, B., Sinha, R., Onur Sumer, S., Weinhold, N., Schultz, N., Shen, R., Sander, C., Ng, S., Ma, S., Zhu, J., Radenbaugh, A., Stuart, J. M., Benz, C. C., Yau, C., Haussler, D., Spellman, P. T., Wilkerson, M. D., Parker, J. S., Hoadley, K. A., Kimes, P. K., Neil Hayes, D., Perou, C. M., Broom, B. M., Wang, J., Lu, Y., Kwok Shing Ng, P., Diao, L., Averett Byers, L., Liu, W., Heymach, J. V., Amos, C. I., Weinstein, J. N., Akbani, R., Mills, G. B., Curley, E., Paulauskis, J., Lau, K., Morris, S., Shelton, T., Mallery, D., Gardner, J., Penny, R., Saller, C., Tarvin, K., Richards, W. G., Cerfolio, R., Bryant, A., Raymond, D. P., Pennell, N. A., Farver, C., Czerwinski, C., Huelsenbeck-Dill, L., Iacocca, M., Petrelli, N., Rabeno, B., Brown, J., Bauer, T., Dolzhanskiy, O., Potapova, O., Rotin, D., Voronina, O., Nemirovich-Danchenko, E., Fedosenko, K. V., Gal, A., Behera, M., Ramalingam, S. S., Sica, G., Flieder, D., Boyd, J., Weaver, J., Kohl, B., Huy Quoc Thinh, D., Sandusky, G., Juhl, H., Duhig, E., Illei, P., Gabrielson, E., Shin, J., Lee, B., Rogers, K., Trusty, D., Brock, M. V., Williamson, C., Burks, E., Rieger-Christ, K., Holway, A., Sullivan, T., Wigle, D. A., Asiedu, M. K., Kosari, F., Travis, W. D., Rekhtman, N., Zakowski, M., Rusch, V. W., Zippile, P., Suh, J., Pass, H., Goparaju, C., Owusu-Sarpong, Y., Bartlett, J. M. S., Kodeeswaran, S., Parfitt, J., Sekhon, H., Albert, M., Eckman, J., Myers, J. B., Cheney, R., Morrison, C., Gaudioso, C., Borgia, J. A., Bonomi, P., Pool, M., Liptay, M. J., Moiseenko, F., Zaytseva, I., Dienemann, H., Meister, M., Schnabel, P. A., Muley, T. R., Peifer, M., Gomez-Fernandez, C., Herbert, L., Egea, S., Huang, M., Thorne, L. B., Boice, L., Hill Salazar, A., Funkhouser, W. K., Kimryn Rathmell, W., Dhir, R., Yousem, S. A., Dacic, S., Schneider, F., Siegfried, J. M., Hajek, R., Watson, M. A., McDonald, S., Meyers, B., Clarke, B., Yang, I. A., Fong, K. M., Hunter, L.,

Windsor, M., Bowman, R. V., Peters, S., Letovanec, I., Khan, K. Z., Jensen, M. A., Snyder, E. E., Srinivasan, D., Kahn, A. B., Baboud, J., Pot, D. A., Mills Shaw, K. R., Sheth, M., Davidsen, T., Demchok, J. A., Yang, L., Wang, Z., Tarnuzzer, R., Claude Zenklusen, J., Ozenberger, B. A., Sofia, H. J., Travis, W. D., Cheney, R., Clarke, B., Dacic, S., Duhig, E., Funkhouser, W. K., Illei, P., Farver, C., Rekhtman, N., Sica, G., Suh, J., & Tsao, M.-S. (2014). Comprehensive molecular profiling of lung adenocarcinoma. *Nature, 511*(7511), 543-550. doi:10.1038/nature13385

Conde, E., Hernandez, S., Prieto, M., Martinez, R., & Lopez-Rios, F. (2016). Profile of Ventana ALK (D5F3) companion diagnostic assay for non-small-cell lung carcinomas. *Expert Rev Mol Diagn, 16*(6), 707-713. doi:10.1586/14737159.2016.1172963

Conklin, C. M., Craddock, K. J., Have, C., Laskin, J., Couture, C., & Ionescu, D. N. (2013). Immunohistochemistry is a reliable screening tool for identification of ALK rearrangement in non-small-cell lung carcinoma and is antibody dependent. *J Thorac Oncol, 8*(1), 45-51. doi:10.1097/JTO.0b013e318274a83e

Cook, N., Jodrell, D. I., & Tuveson, D. A. (2012). Predictive in vivo animal models and translation to clinical trials. *Drug Discov Today, 17*(5-6), 253-260. doi:10.1016/j.drudis.2012.02.003

Costa, D. B., Kobayashi, S., Pandya, S. S., Yeo, W. L., Shen, Z., Tan, W., & Wilner, K. D. (2011). CSF concentration of the anaplastic lymphoma kinase inhibitor crizotinib. *J Clin Oncol, 29*(15), e443-445. doi:10.1200/JCO.2010.34.1313

Costa, D. B., Shaw, A. T., Ou, S. H., Solomon, B. J., Riely, G. J., Ahn, M. J., Zhou, C., Shreeve, S. M., Selaru, P., Polli, A., Schnell, P., Wilner, K. D., Wiltshire, R., Camidge, D. R., & Crino, L. (2015). Clinical Experience With Crizotinib in Patients With Advanced ALK-Rearranged Non-Small-Cell Lung Cancer and Brain Metastases. *J Clin Oncol, 33*(17), 1881-1888. doi:10.1200/JCO.2014.59.0539

Cote, M. L., Liu, M., Bonassi, S., Neri, M., Schwartz, A. G., Christiani, D. C., Spitz, M. R., Muscat, J. E., Rennert, G., Aben, K. K., Andrew, A. S., Bencko, V., Bickeboller, H., Boffetta, P., Brennan, P., Brenner, H., Duell, E. J., Fabianova, E., Field, J. K., Foretova, L., Friis, S., Harris, C. C., Holcatova, I., Hong, Y. C., Isla, D., Janout, V., Kiemeney, L. A., Kiyohara, C., Lan, Q., Lazarus, P., Lissowska, J., Le Marchand, L., Mates, D., Matsuo, K., Mayordomo, J. I., McLaughlin, J. R., Morgenstern, H., Mueller, H., Orlow, I., Park, B. J., Pinchev, M., Raji, O. Y., Rennert, H. S., Rudnai, P., Seow, A., Stucker, I., Szeszenia-Dabrowska, N., Dawn Teare, M., Tjonnelan, A., Ugolini, D., van der Heijden, H. F., Wichmann, E., Wiencke, J. K., Woll, P. J., Yang, P., Zaridze, D., Zhang, Z. F., Etzel, C. J., & Hung, R. J. (2012). Increased risk of lung cancer in individuals with a family history of the disease: a pooled analysis from the International Lung Cancer Consortium. *Eur J Cancer, 48*(13), 1957-1968. doi:10.1016/j.ejca.2012.01.038

Courtin, A., Smyth, T., Hearn, K., Saini, H. K., Thompson, N. T., Lyons, J. F., & Wallis, N. G. (2016). Emergence of resistance to tyrosine kinase inhibitors in non-small-cell lung cancer can be delayed by an upfront combination with the HSP90 inhibitor onalespib. *Br J Cancer, 115*(9), 1069-1077. doi:10.1038/bjc.2016.294

Cozzo, A. J., Sundaram, S., Zattra, O., Qin, Y., Freemerman, A. J., Essaid, L., Darr, D. B., Montgomery, S. A., McNaughton, K. K., Ezzell, J. A., Galanko, J. A., Troester, M. A., & Makowski, L. (2016). cMET inhibitor crizotinib impairs

angiogenesis and reduces tumor burden in the C3(1)-Tag model of basal-like breast cancer. *Springerplus, 5*, 348. doi:10.1186/s40064-016-1920-3

Crino, L., Ahn, M. J., De Marinis, F., Groen, H. J., Wakelee, H., Hida, T., Mok, T., Spigel, D., Felip, E., Nishio, M., Scagliotti, G., Branle, F., Emeremni, C., Quadrigli, M., Zhang, J., & Shaw, A. T. (2016). Multicenter Phase II Study of Whole-Body and Intracranial Activity With Ceritinib in Patients With ALK-Rearranged Non-Small-Cell Lung Cancer Previously Treated With Chemotherapy and Crizotinib: Results From ASCEND-2. *J Clin Oncol, 34*(24), 2866-2873. doi:10.1200/JCO.2015.65.5936

Crockett, D. K., Lin, Z., Elenitoba-Johnson, K. S., & Lim, M. S. (2004). Identification of NPM-ALK interacting proteins by tandem mass spectrometry. *Oncogene, 23*(15), 2617-2629. doi:10.1038/sj.onc.1207398

Crowley, L. C., & Waterhouse, N. J. (2016). Detecting Cleaved Caspase-3 in Apoptotic Cells by Flow Cytometry. *Cold Spring Harb Protoc, 2016*(11). doi:10.1101/pdb.prot087312

Crystal, A. S., Shaw, A. T., Sequist, L. V., Friboulet, L., Niederst, M. J., Lockerman, E. L., Frias, R. L., Gainor, J. F., Amzallag, A., Greninger, P., Lee, D., Kalsy, A., Gomez-Caraballo, M., Elamine, L., Howe, E., Hur, W., Lifshits, E., Robinson, H. E., Katayama, R., Faber, A. C., Awad, M. M., Ramaswamy, S., Mino-Kenudson, M., Iafrate, A. J., Benes, C. H., & Engelman, J. A. (2014). Patient-derived models of acquired resistance can identify effective drug combinations for cancer. *Science, 346*(6216), 1480-1486. doi:10.1126/science.1254721

Cui, J. J., Tran-Dubé, M., Shen, H., Nambu, M., Kung, P. P., Pairish, M., Jia, L., Meng, J., Funk, L., Botrous, I., McTigue, M., Grodsky, N., Ryan, K., Padrique, E., Alton, G., Timofeevski, S., Yamazaki, S., Li, Q., Zou, H., Christensen, J., Mroczkowski, B., Bender, S., Kania, R. S., & Edwards, M. P. (2011). Structure based drug design of crizotinib (PF-02341066), a potent and selective dual inhibitor of mesenchymal-epithelial transition factor (c-MET) kinase and anaplastic lymphoma kinase (ALK). *Journal of Medicinal Chemistry, 54*(18), 6342-6363. doi:10.1021/jm2007613

Curran, M. P. (2012). Crizotinib. *72*(1), 99-107.

Cuyas, E., Perez-Sanchez, A., Micol, V., Menendez, J. A., & Bosch-Barrera, J. (2016). STAT3-targeted treatment with silibinin overcomes the acquired resistance to crizotinib in ALK-rearranged lung cancer. *Cell Cycle, 15*(24), 3413-3418. doi:10.1080/15384101.2016.1245249

D'Arcy, M. S. (2019). Cell death: a review of the major forms of apoptosis, necrosis and autophagy. *Cell Biol Int, 43*(6), 582-592. doi:10.1002/cbin.11137

Dacic, S., Villaruz, L. C., Abberbock, S., Mahaffey, A., Incharoen, P., & Nikiforova, M. N. (2016). ALK FISH patterns and the detection of ALK fusions by next generation sequencing in lung adenocarcinoma. *Oncotarget, 7*(50), 82943-82952. doi:10.18632/oncotarget.12705

Dagogo-Jack, I., & Shaw, A. T. (2016). Crizotinib resistance: implications for therapeutic strategies. *Ann Oncol, 27 Suppl 3*, iii42-iii50. doi:10.1093/annonc/mdw305

Dai, X., Guo, G., Zou, P., Cui, R., Chen, W., Chen, X., Yin, C., He, W., Vinothkumar, R., Yang, F., Zhang, X., & Liang, G. (2017). (S)-crizotinib induces apoptosis in human non-small cell lung cancer cells by activating ROS independent of MTH1. *J Exp Clin Cancer Res, 36*(1), 120. doi:10.1186/s13046-017-0584-3

Daly, N. L., Scanlon, M. J., Djordjevic, J. T., Kroon, P. A., & Smith, R. (1995). Three-dimensional structure of a cysteine-rich repeat from the low-density lipoprotein

receptor. *Proc Natl Acad Sci U S A, 92*(14), 6334-6338. doi:10.1073/pnas.92.14.6334

Das, A., Cheng, R. R., Hilbert, M. L., Dixon-Moh, Y. N., Decandio, M., Vandergrift, W. A., 3rd, Banik, N. L., Lindhorst, S. M., Cachia, D., Varma, A. K., Patel, S. J., & Giglio, P. (2015). Synergistic Effects of Crizotinib and Temozolomide in Experimental FIG-ROS1 Fusion-Positive Glioblastoma. *Cancer Growth Metastasis, 8*, 51-60. doi:10.4137/CGM.S32801

Davies, B. R., Logie, A., McKay, J. S., Martin, P., Steele, S., Jenkins, R., Cockerill, M., Cartlidge, S., & Smith, P. D. (2007). AZD6244 (ARRY-142886), a potent inhibitor of mitogen-activated protein kinase/extracellular signal-regulated kinase kinase 1/2 kinases: mechanism of action in vivo, pharmacokinetic/pharmacodynamic relationship, and potential for combination in preclinical. *Molecular Cancer Therapeutics, 6*(8), 2209-2219. doi:10.1158/1535-7163.MCT-07-0231

de Groot, P. M., Wu, C. C., Carter, B. W., & Munden, R. F. (2018). The epidemiology of lung cancer. *Transl Lung Cancer Res, 7*(3), 220-233. doi:10.21037/tlcr.2018.05.06

De Matteis, S., Consonni, D., & Bertazzi, P. A. (2008). Exposure to occupational carcinogens and lung cancer risk. Evolution of epidemiological estimates of attributable fraction. *Acta Biomed, 79 Suppl 1*, 34-42.

Degterev, A., Boyce, M., & Yuan, J. (2003). A decade of caspases. *Oncogene, 22*(53), 8543-8567. doi:10.1038/sj.onc.1207107

Dhillon, A. S., Hagan, S., Rath, O., & Kolch, W. (2007). MAP kinase signalling pathways in cancer. *Oncogene, 26*(22), 3279-3290. doi:10.1038/sj.onc.1210421

Ding, L., Getz, G., Wheeler, D. A., Mardis, E. R., McLellan, M. D., Cibulskis, K., Sougnez, C., Greulich, H., Muzny, D. M., Morgan, M. B., Fulton, L., Fulton, R. S., Zhang, Q., Wendl, M. C., Lawrence, M. S., Larson, D. E., Chen, K., Dooling, D. J., Sabo, A., Hawes, A. C., Shen, H., Jhangiani, S. N., Lewis, L. R., Hall, O., Zhu, Y., Mathew, T., Ren, Y., Yao, J., Scherer, S. E., Clerc, K., Metcalf, G. A., Ng, B., Milosavljevic, A., Gonzalez-Garay, M. L., Osborne, J. R., Meyer, R., Shi, X., Tang, Y., Koboldt, D. C., Lin, L., Abbott, R., Miner, T. L., Pohl, C., Fewell, G., Haipek, C., Schmidt, H., Dunford-Shore, B. H., Kraja, A., Crosby, S. D., Sawyer, C. S., Vickery, T., Sander, S., Robinson, J., Winckler, W., Baldwin, J., Chirieac, L. R., Dutt, A., Fennell, T., Hanna, M., Johnson, B. E., Onofrio, R. C., Thomas, R. K., Tonon, G., Weir, B. A., Zhao, X., Ziaugra, L., Zody, M. C., Giordano, T., Orringer, M. B., Roth, J. A., Spitz, M. R., Wistuba, II, Ozenberger, B., Good, P. J., Chang, A. C., Beer, D. G., Watson, M. A., Ladanyi, M., Broderick, S., Yoshizawa, A., Travis, W. D., Pao, W., Province, M. A., Weinstock, G. M., Varmus, H. E., Gabriel, S. B., Lander, E. S., Gibbs, R. A., Meyerson, M., & Wilson, R. K. (2008). Somatic mutations affect key pathways in lung adenocarcinoma. *Nature, 455*(7216), 1069-1075. doi:10.1038/nature07423

Dirks, W. G., Fahnrich, S., Lis, Y., Becker, E., MacLeod, R. A., & Drexler, H. G. (2002). Expression and functional analysis of the anaplastic lymphoma kinase (ALK) gene in tumor cell lines. *Int J Cancer, 100*(1), 49-56. doi:10.1002/ijc.10435

Doebele, R. C., Pilling, A. B., Aisner, D. L., Kutateladze, T. G., Le, A. T., Weickhardt, A. J., Kondo, K. L., Linderman, D. J., Heasley, L. E., Franklin, W. A., Varella-Garcia, M., & Camidge, D. R. (2012). Mechanisms of resistance to crizotinib in patients with ALK gene rearranged non-small cell lung cancer. *Clinical Cancer Research, 18*(5), 1472-1482. doi:10.1158/1078-0432.CCR-11-2906

Dong, J., Li, B., Lin, D., Zhou, Q., & Huang, D. (2019). Advances in Targeted Therapy and Immunotherapy for Non-small Cell Lung Cancer Based on Accurate Molecular Typing. *Front Pharmacol, 10*, 230. doi:10.3389/fphar.2019.00230

Drizou, M., Kotteas, E. A., & Syrigos, N. (2017). Treating patients with ALK-rearranged non-small-cell lung cancer: mechanisms of resistance and strategies to overcome it. *Clinical and Translational Oncology, 19*(6), 658-666. doi:http://dx.doi.org/10.1007/s12094-016-1605-y

Du, C., Fang, M., Li, Y., Li, L., & Wang, X. (2000). Smac, a mitochondrial protein that promotes cytochrome c-dependent caspase activation by eliminating IAP inhibition. *Cell, 102*(1), 33-42. doi:10.1016/s0092-8674(00)00008-8

Duma, N., Santana-Davila, R., & Molina, J. R. (2019). Non-Small Cell Lung Cancer: Epidemiology, Screening, Diagnosis, and Treatment. *Mayo Clin Proc, 94*(8), 1623-1640. doi:10.1016/j.mayocp.2019.01.013

Dummer, R., Schadendorf, D., Ascierto, P. A., Arance, A., Dutriaux, C., Di Giacomo, A. M., Rutkowski, P., Del Vecchio, M., Gutzmer, R., Mandala, M., Thomas, L., Demidov, L., Garbe, C., Hogg, D., Liszkay, G., Queirolo, P., Wasserman, E., Ford, J., Weill, M., Sirulnik, L. A., Jehl, V., Bozon, V., Long, G. V., & Flaherty, K. (2017). Binimetinib versus dacarbazine in patients with advanced NRAS-mutant melanoma (NEMO): a multicentre, open-label, randomised, phase 3 trial. *Lancet Oncol, 18*(4), 435-445. doi:10.1016/S1470-2045(17)30180-8

Dymond, A. W., Howes, C., Pattison, C., So, K., Mariani, G., Savage, M., Mair, S., Ford, G., & Martin, P. (2016). Metabolism, Excretion, and Pharmacokinetics of Selumetinib, an MEK1/2 inhibitor, in Healthy Adult Male Subjects. *Clinical Therapeutics, 38*(11), 2447-2458. doi:10.1016/j.clinthera.2016.09.002

Dymond, A. W., So, K., Martin, P., Huang, Y., Severin, P., Mathews, D., Lisbon, E., & Mariani, G. (2017). Effects of cytochrome P450 (CYP3A4 and CYP2C19) inhibition and induction on the exposure of selumetinib, a MEK1/2 inhibitor, in healthy subjects: results from two clinical trials. *Eur J Clin Pharmacol, 73*(2), 175-184. doi:10.1007/s00228-016-2153-7

Ebert, P. J. R., Cheung, J., Yang, Y., McNamara, E., Hong, R., Moskalenko, M., Gould, S. E., Maecker, H., Irving, B. A., Kim, J. M., Belvin, M., & Mellman, I. (2016). MAP Kinase Inhibition Promotes T Cell and Anti-tumor Activity in Combination with PD-L1 Checkpoint Blockade. *Immunity, 44*(3), 609-621. doi:10.1016/j.immuni.2016.01.024

Elledge, S. J. (1996). Cell cycle checkpoints: preventing an identity crisis. *Science, 274*(5293), 1664-1672. doi:10.1126/science.274.5293.1664

Elmore, S. (2007). Apoptosis: a review of programmed cell death. *Toxicol Pathol, 35*(4), 495-516. doi:10.1080/01926230701320337

Evan, G. I., & Vousden, K. H. (2001). Proliferation, cell cycle and apoptosis in cancer. *Nature, 411*(6835), 342-348. doi:10.1038/35077213

Evans, C. E., Palazon, A., Sim, J., Tyrakis, P. A., Prodger, A., Lu, X., Chan, S., Bendahl, P. O., Belting, M., Von Euler, L., Rundqvist, H., Johnson, R. S., & Branco, C. (2017). Modelling pulmonary microthrombosis coupled to metastasis: distinct effects of thrombogenesis on tumorigenesis. *Biol Open, 6*(5), 688-697. doi:10.1242/bio.024653

Ewings, K. E., Hadfield-Moorhouse, K., Wiggins, C. M., Wickenden, J. A., Balmanno, K., Gilley, R., Degenhardt, K., White, E., & Cook, S. J. (2007). ERK1/2-dependent phosphorylation of BimEL promotes its rapid dissociation from Mcl-1 and Bcl-xL. *EMBO J, 26*(12), 2856-2867. doi:10.1038/sj.emboj.7601723

Falasca, M., Logan, S. K., Lehto, V. P., Baccante, G., Lemmon, M. A., & Schlessinger, J. (1998). Activation of phospholipase C gamma by PI 3-kinase-induced PH domain-mediated membrane targeting. *EMBO J, 17*(2), 414-422. doi:10.1093/emboj/17.2.414

Falchook, G. S., Lewis, K. D., Infante, J. R., Gordon, M. S., Vogelzang, N. J., DeMarini, D. J., Sun, P., Moy, C., Szabo, S. A., Roadcap, L. T., Peddareddigari, V. G., Lebowitz, P. F., Le, N. T., Burris, H. A., 3rd, Messersmith, W. A., O'Dwyer, P. J., Kim, K. B., Flaherty, K., Bendell, J. C., Gonzalez, R., Kurzrock, R., & Fecher, L. A. (2012). Activity of the oral MEK inhibitor trametinib in patients with advanced melanoma: a phase 1 dose-escalation trial. *Lancet Oncol, 13*(8), 782-789. doi:10.1016/S1470-2045(12)70269-3

Fan, T. P., Jaggar, R., & Bicknell, R. (1995). Controlling the vasculature: angiogenesis, anti-angiogenesis and vascular targeting of gene therapy. *Trends Pharmacol Sci, 16*(2), 57-66. doi:10.1016/s0165-6147(00)88979-8

Farber, E. (1995). Cell proliferation as a major risk factor for cancer: a concept of doubtful validity. *Cancer Res, 55*(17), 3759-3762.

Farr, M., & Bacon, P. A. (1995). How and when should combination therapy be used? The role of an anchor drug. *Br J Rheumatol, 34 Suppl 2*, 100-103.

Fass, D., Blacklow, S., Kim, P. S., & Berger, J. M. (1997). Molecular basis of familial hypercholesterolaemia from structure of LDL receptor module. *Nature, 388*(6643), 691-693. doi:10.1038/41798

Feitelson, M. A., Arzumanyan, A., Kulathinal, R. J., Blain, S. W., Holcombe, R. F., Mahajna, J., Marino, M., Martinez-Chantar, M. L., Nawroth, R., Sanchez-Garcia, I., Sharma, D., Saxena, N. K., Singh, N., Vlachostergios, P. J., Guo, S., Honoki, K., Fujii, H., Georgakilas, A. G., Bilsland, A., Amedei, A., Niccolai, E., Amin, A., Ashraf, S. S., Boosani, C. S., Guha, G., Ciriolo, M. R., Aquilano, K., Chen, S., Mohammed, S. I., Azmi, A. S., Bhakta, D., Halicka, D., Keith, W. N., & Nowsheen, S. (2015). Sustained proliferation in cancer: Mechanisms and novel therapeutic targets. *Semin Cancer Biol, 35 Suppl*, S25-S54. doi:10.1016/j.semcancer.2015.02.006

Felip, E., Orlov, S., Park, K., Yu, C.-J., Tsai, C.-M., Nishio, M., Dols, M. C., McKeage, M. J., Su, W.-C., Mok, T., Scagliotti, G. V., Spigel, D., Branle, F., Emeremni, C., Quadrigli, M., & Shaw, A. T. (2015). ASCEND-3: A single-arm, open-label, multicenter phase II study of ceritinib in ALKi-naïve adult patients (pts) with ALK-rearranged (ALK+) non-small cell lung cancer (NSCLC). *Journal of Clinical Oncology, 33*(15_suppl), 8060-8060. doi:10.1200/jco.2015.33.15_suppl.8060

Ferlay, J., Soerjomataram, I., Dikshit, R., Eser, S., Mathers, C., Rebelo, M., Parkin, D. M., Forman, D., & Bray, F. (2015). Cancer incidence and mortality worldwide: sources, methods and major patterns in GLOBOCAN 2012. *Int J Cancer, 136*(5), E359-386. doi:10.1002/ijc.29210

Ferrara, N., Gerber, H. P., & LeCouter, J. (2003). The biology of VEGF and its receptors. *Nat Med, 9*(6), 669-676. doi:10.1038/nm0603-669

Ferrara, N., & Kerbel, R. S. (2005). Angiogenesis as a therapeutic target. *Nature, 438*(7070), 967-974. doi:10.1038/nature04483

Fina, L., Molgaard, H. V., Robertson, D., Bradley, N. J., Monaghan, P., Delia, D., Sutherland, D. R., Baker, M. A., & Greaves, M. F. (1990). Expression of the CD34 gene in vascular endothelial cells. *Blood, 75*(12), 2417-2426.

Flaherty, K. T., Infante, J. R., Daud, A., Gonzalez, R., Kefford, R. F., Sosman, J., Hamid, O., Schuchter, L., Cebon, J., Ibrahim, N., Kudchadkar, R., Burris, H. A., 3rd,

Falchook, G., Algazi, A., Lewis, K., Long, G. V., Puzanov, I., Lebowitz, P., Singh, A., Little, S., Sun, P., Allred, A., Ouellet, D., Kim, K. B., Patel, K., & Weber, J. (2012). Combined BRAF and MEK inhibition in melanoma with BRAF V600 mutations. *N Engl J Med, 367*(18), 1694-1703. doi:10.1056/NEJMoa1210093

Flaherty, K. T., Robert, C., Hersey, P., Nathan, P., Garbe, C., Milhem, M., Demidov, L. V., Hassel, J. C., Rutkowski, P., Mohr, P., Dummer, R., Trefzer, U., Larkin, J. M., Utikal, J., Dreno, B., Nyakas, M., Middleton, M. R., Becker, J. C., Casey, M., Sherman, L. J., Wu, F. S., Ouellet, D., Martin, A. M., Patel, K., Schadendorf, D., & Group, M. S. (2012). Improved survival with MEK inhibition in BRAF-mutated melanoma. *N Engl J Med, 367*(2), 107-114. doi:10.1056/NEJMoa1203421

Flanagan, S. P. (1966). 'Nude', a new hairless gene with pleiotropic effects in the mouse. *Genet Res, 8*(3), 295-309. doi:10.1017/s0016672300010168

Folkman, J. (1972). Anti-angiogenesis: new concept for therapy of solid tumors. *Ann Surg, 175*(3), 409-416. doi:10.1097/00000658-197203000-00014

Folkman, J. (1995). Angiogenesis in cancer, vascular, rheumatoid and other disease. *Nat Med, 1*(1), 27-31. doi:10.1038/nm0195-27

Folkman, J., & Shing, Y. (1992). Angiogenesis. *The Journal of Biological Chemistry, 267*(16), 10931-10934.

Frampton, J. E. (2013). Crizotinib: A review of its use in the treatment of anaplastic lymphoma kinase-positive, advanced non-small cell lung cancer. *Drugs, 73*(18), 2031-2051. doi:10.1007/s40265-013-0142-z

Friboulet, L., Li, N., Katayama, R., Lee, C. C., Gainor, J. F., Crystal, A. S., Michellys, P. Y., Awad, M. M., Yanagitani, N., Kim, S., Pferdekamper, A. M. C., Li, J., Kasibhatla, S., Sun, F., Sun, X., Hua, S., McNamara, P., Mahmood, S., Lockerman, E. L., Fujita, N., Nishio, M., Harris, J. L., Shaw, A. T., & Engelman, J. A. (2014). The ALK inhibitor ceritinib overcomes crizotinib resistance in non-small cell lung cancer. *Cancer Discovery, 4*(6), 662-673. doi:10.1158/2159-8290.CD-13-0846

Fruman, D. A., Meyers, R. E., & Cantley, L. C. (1998). Phosphoinositide kinases. *Annu Rev Biochem, 67*, 481-507. doi:10.1146/annurev.biochem.67.1.481

Fu, Z., & Tindall, D. J. (2008). FOXOs, cancer and regulation of apoptosis. *Oncogene, 27*(16), 2312-2319. doi:10.1038/onc.2008.24

Fujimoto, J., Shiota, M., Iwahara, T., Seki, N., Satoh, H., Mori, S., & Yamamoto, T. (1996). Characterization of the transforming activity of p80, a hyperphosphorylated protein in a Ki-1 lymphoma cell line with chromosomal translocation t(2;5). *Proc Natl Acad Sci U S A, 93*(9), 4181-4186. doi:10.1073/pnas.93.9.4181

Fujimoto, J., & Wistuba, II. (2014). Current concepts on the molecular pathology of non-small cell lung carcinoma. *Semin Diagn Pathol, 31*(4), 306-313. doi:10.1053/j.semdp.2014.06.008

Fujishita, T., Loda, M., Turner, R. E., Gentler, M., Kashii, T., Breathnach, O. S., & Johnson, B. E. (2003). Sensitivity of non-small-cell lung cancer cell lines established from patients treated with prolonged infusions of Paclitaxel. *ONCOLOGY, 64*(4), 399-406. doi:10.1159/000070299

Fulda, S., & Debatin, K. M. (2006). Extrinsic versus intrinsic apoptosis pathways in anticancer chemotherapy. *Oncogene, 25*(34), 4798-4811. doi:10.1038/sj.onc.1209608

Gadgeel, S. M., Gandhi, L., Riely, G. J., Chiappori, A. A., West, H. L., Azada, M. C., Morcos, P. N., Lee, R. M., Garcia, L., Yu, L., Boisserie, F., Di Laurenzio, L., Golding, S., Sato, J., Yokoyama, S., Tanaka, T., & Ou, S. H. (2014). Safety and activity of alectinib against systemic disease and brain metastases in patients with crizotinib-resistant ALK-rearranged non-small-cell lung cancer (AF-002JG): results from the dose-finding portion of a phase 1/2 study. *Lancet Oncol, 15*(10), 1119-1128. doi:10.1016/S1470-2045(14)70362-6

Gainor, J. F., Dardaei, L., Yoda, S., Friboulet, L., Leshchiner, I., Katayama, R., Dagogo-Jack, I., Gadgeel, S., Schultz, K., Singh, M., Chin, E., Parks, M., Lee, D., DiCecca, R. H., Lockerman, E., Huynh, T., Logan, J., Ritterhouse, L. L., Le, L. P., Muniappan, A., Digumarthy, S., Channick, C., Keyes, C., Getz, G., Dias-Santagata, D., Heist, R. S., Lennerz, J., Sequist, L. V., Benes, C. H., Iafrate, A. J., Mino-Kenudson, M., Engelman, J. A., & Shaw, A. T. (2016). Molecular Mechanisms of Resistance to First- and Second-Generation ALK Inhibitors in ALK-Rearranged Lung Cancer. *Cancer Discov, 6*(10), 1118-1133. doi:10.1158/2159-8290.CD-16-0596

Gainor, J. F., & Shaw, A. T. (2013). Emerging paradigms in the development of resistance to tyrosine kinase inhibitors in lung cancer. *J Clin Oncol, 31*(31), 3987-3996. doi:10.1200/JCO.2012.45.2029

Gainor, J. F., Varghese, A. M., Ou, S. H. I., Kabraji, S., Awad, M. M., Katayama, R., Pawlak, A., Mino-Kenudson, M., Yeap, B. Y., Riely, G. J., Iafrate, A. J., Arcila, M. E., Ladanyi, M., Engelman, J. A., Dias-Santagata, D., & Shaw, A. T. (2013). ALK rearrangements are mutually exclusive with mutations in EGFR or KRAS: An analysis of 1,683 patients with non-small cell lung cancer. *Clinical Cancer Research, 19*(15), 4273-4281. doi:10.1158/1078-0432.CCR-13-0318

Gandhi, S., Chen, H., Zhao, Y., & Dy, G. K. (2015). First-line treatment of advanced ALK-positive non-small-cell lung cancer. *Lung Cancer: Targets and Therapy, 6*(pp 71-82). doi:http://dx.doi.org/10.2147/LCTT.S63491

Garon, E. B., Finn, R. S., Hosmer, W., Dering, J., Ginther, C., Adhami, S., Kamranpour, N., Pitts, S., Desai, A., Elashoff, D., French, T., Smith, P., & Slamon, D. J. (2010). Identification of Common Predictive Markers of In vitro Response to the Mek Inhibitor Selumetinib (AZD6244; ARRY-142886) in Human Breast Cancer and Non-Small Cell Lung Cancer Cell Lines. *Molecular Cancer Therapeutics, 9*(7), 1985-1994. doi:10.1158/1535-7163.MCT-10-0037

Garrido, C., Galluzzi, L., Brunet, M., Puig, P. E., Didelot, C., & Kroemer, G. (2006). Mechanisms of cytochrome c release from mitochondria. *Cell Death Differ, 13*(9), 1423-1433. doi:10.1038/sj.cdd.4401950

Gavrieli, Y., Sherman, Y., & Ben-Sasson, S. A. (1992). Identification of programmed cell death in situ via specific labeling of nuclear DNA fragmentation. *J Cell Biol, 119*(3), 493-501. doi:10.1083/jcb.119.3.493

Gazdar, A. F., Bunn, P. A., & Minna, J. D. (2017). Small-cell lung cancer: what we know, what we need to know and the path forward. *Nat Rev Cancer, 17*(12), 725-737. doi:10.1038/nrc.2017.87

George, J., Lim, J. S., Jang, S. J., Cun, Y., Ozretic, L., Kong, G., Leenders, F., Lu, X., Fernandez-Cuesta, L., Bosco, G., Muller, C., Dahmen, I., Jahchan, N. S., Park, K. S., Yang, D., Karnezis, A. N., Vaka, D., Torres, A., Wang, M. S., Korbel, J. O., Menon, R., Chun, S. M., Kim, D., Wilkerson, M., Hayes, N., Engelmann, D., Putzer, B., Bos, M., Michels, S., Vlasic, I., Seidel, D., Pinther, B., Schaub, P., Becker, C., Altmuller, J., Yokota, J., Kohno, T., Iwakawa, R., Tsuta, K., Noguchi, M., Muley, T., Hoffmann, H., Schnabel, P. A., Petersen, I., Chen, Y., Soltermann,

A., Tischler, V., Choi, C. M., Kim, Y. H., Massion, P. P., Zou, Y., Jovanovic, D., Kontic, M., Wright, G. M., Russell, P. A., Solomon, B., Koch, I., Lindner, M., Muscarella, L. A., la Torre, A., Field, J. K., Jakopovic, M., Knezevic, J., Castanos-Velez, E., Roz, L., Pastorino, U., Brustugun, O. T., Lund-Iversen, M., Thunnissen, E., Kohler, J., Schuler, M., Botling, J., Sandelin, M., Sanchez-Cespedes, M., Salvesen, H. B., Achter, V., Lang, U., Bogus, M., Schneider, P. M., Zander, T., Ansen, S., Hallek, M., Wolf, J., Vingron, M., Yatabe, Y., Travis, W. D., Nurnberg, P., Reinhardt, C., Perner, S., Heukamp, L., Buttner, R., Haas, S. A., Brambilla, E., Peifer, M., Sage, J., & Thomas, R. K. (2015). Comprehensive genomic profiles of small cell lung cancer. *Nature, 524*(7563), 47-53. doi:10.1038/nature14664

Gerdes, J., Schwab, U., Lemke, H., & Stein, H. (1983). Production of a mouse monoclonal antibody reactive with a human nuclear antigen associated with cell proliferation. *Int J Cancer, 31*(1), 13-20. doi:10.1002/ijc.2910310104

Gettinger, S. N., Bazhenova, L. A., Langer, C. J., Salgia, R., Gold, K. A., Rosell, R., Shaw, A. T., Weiss, G. J., Tugnait, M., Narasimhan, N. I., Dorer, D. J., Kerstein, D., Rivera, V. M., Clackson, T., Haluska, F. G., & Camidge, D. R. (2016). Activity and safety of brigatinib in ALK-rearranged non-small-cell lung cancer and other malignancies: a single-arm, open-label, phase 1/2 trial. *Lancet Oncol, 17*(12), 1683-1696. doi:10.1016/S1470-2045(16)30392-8

Gilley, J., Coffer, P. J., & Ham, J. (2003). FOXO transcription factors directly activate bim gene expression and promote apoptosis in sympathetic neurons. *J Cell Biol, 162*(4), 613-622. doi:10.1083/jcb.200303026

Gillings, A. S., Balmanno, K., Wiggins, C. M., Johnson, M., & Cook, S. J. (2009). Apoptosis and autophagy: BIM as a mediator of tumour cell death in response to oncogene-targeted therapeutics. *FEBS J, 276*(21), 6050-6062. doi:10.1111/j.1742-4658.2009.07329.x

Gilmartin, A. G., Bleam, M. R., Groy, A., Moss, K. G., Minthorn, E. A., Kulkarni, S. G., Rominger, C. M., Erskine, S., Fisher, K. E., Yang, J., Zappacosta, F., Annan, R., Sutton, D., & Laquerre, S. G. (2011). GSK1120212 (JTP-74057) is an inhibitor of MEK activity and activation with favorable pharmacokinetic properties for sustained in vivo pathway inhibition. *Clin Cancer Res, 17*(5), 989-1000. doi:10.1158/1078-0432.CCR-10-2200

Gimbrone, M. A., Jr., Leapman, S. B., Cotran, R. S., & Folkman, J. (1972). Tumor dormancy in vivo by prevention of neovascularization. *J Exp Med, 136*(2), 261-276. doi:10.1084/jem.136.2.261

Goldoni, M., & Johansson, C. (2007). A mathematical approach to study combined effects of toxicants in vitro: evaluation of the Bliss independence criterion and the Loewe additivity model. *Toxicol In Vitro, 21*(5), 759-769. doi:10.1016/j.tiv.2007.03.003

Goldstraw, P., Chansky, K., Crowley, J., Rami-Porta, R., Asamura, H., Eberhardt, W. E., Nicholson, A. G., Groome, P., Mitchell, A., Bolejack, V., International Association for the Study of Lung Cancer, S., Prognostic Factors Committee, A. B., Participating, I., International Association for the Study of Lung Cancer, S., Prognostic Factors Committee Advisory, B., & Participating, I. (2016). The IASLC Lung Cancer Staging Project: Proposals for Revision of the TNM Stage Groupings in the Forthcoming (Eighth) Edition of the TNM Classification for Lung Cancer. *J Thorac Oncol, 11*(1), 39-51. doi:10.1016/j.jtho.2015.09.009

Golias, C. H., Charalabopoulos, A., & Charalabopoulos, K. (2004). Cell proliferation and cell cycle control: a mini review. *Int J Clin Pract, 58*(12), 1134-1141. doi:10.1111/j.1742-1241.2004.00284.x

Gridelli, C., Rossi, A., Carbone, D. P., Guarize, J., Karachaliou, N., Mok, T., Petrella, F., Spaggiari, L., & Rosell, R. (2015). Non-small-cell lung cancer. *Nat Rev Dis Primers, 1*, 15009. doi:10.1038/nrdp.2015.9

Gu, T. L., Tothova, Z., Scheijen, B., Griffin, J. D., Gilliland, D. G., & Sternberg, D. W. (2004). NPM-ALK fusion kinase of anaplastic large-cell lymphoma regulates survival and proliferative signaling through modulation of FOXO3a. *Blood, 103*(12), 4622-4629. doi:10.1182/blood-2003-03-0820

Guengerich, P. F. (2014). Analysis and Characterization of Enzymes and Nucleic Acids Relevant to Toxicology. In A. W. Hayes & C. L. Kruger (Eds.), *Hayes' Principles and Methods of Toxicology, Sixth Edition* (pp. 1905-1964): Taylor & Francis.

Guillaud, P., du Manoir, S., & Seigneurin, D. (1989). Quantification and topographical description of Ki-67 antibody labelling during the cell cycle of normal fibroblastic (MRC-5) and mammary tumour cell lines (MCF-7). *Anal Cell Pathol, 1*(1), 25-39.

Guo, Y. J., Pan, W. W., Liu, S. B., Shen, Z. F., Xu, Y., & Hu, L. L. (2020). ERK/MAPK signalling pathway and tumorigenesis. *Exp Ther Med, 19*(3), 1997-2007. doi:10.3892/etm.2020.8454

Haass, N. K., Sproesser, K., Nguyen, T. K., Contractor, R., Medina, C. A., Nathanson, K. L., Herlyn, M., & Smalley, K. S. (2008). The mitogen-activated protein/extracellular signal-regulated kinase kinase inhibitor AZD6244 (ARRY-142886) induces growth arrest in melanoma cells and tumor regression when combined with docetaxel. *Clin Cancer Res, 14*(1), 230-239. doi:10.1158/1078-0432.CCR-07-1440

Hainsworth, J. D., Cebotaru, C. L., Kanarev, V., Ciuleanu, T. E., Damyanov, D., Stella, P., Ganchev, H., Pover, G., Morris, C., & Tzekova, V. (2010). A phase II, open-label, randomized study to assess the efficacy and safety of AZD6244 (ARRY-142886) versus pemetrexed in patients with non-small cell lung cancer who have failed one or two prior chemotherapeutic regimens. *J Thorac Oncol, 5*(10), 1630-1636. doi:10.1097/JTO.0b013e3181e8b3a3

Hallberg, B., & Palmer, R. H. (2011). ALK and NSCLC: targeted therapy with ALK inhibitors. *F1000 Medicine Reports, 3*.

Hallberg, B., & Palmer, R. H. (2013). Mechanistic insight into ALK receptor tyrosine kinase in human cancer biology. *Nat Rev Cancer, 13*(10), 685-700. doi:10.1038/nrc3580

Hamedani, F. S., Cinar, M., Mo, Z., Cervania, M. A., Amin, H. M., & Alkan, S. (2014). Crizotinib (PF-2341066) induces apoptosis due to downregulation of pSTAT3 and BCL-2 family proteins in NPM-ALK(+) anaplastic large cell lymphoma. *Leuk Res, 38*(4), 503-508. doi:10.1016/j.leukres.2013.12.027

Hamilton, G., Rath, B., & Burghuber, O. (2015). Pharmacokinetics of crizotinib in NSCLC patients. *Expert Opinion on Drug Metabolism & Toxicology, 11*(5), 835-842. doi:10.1517/17425255.2015.1021685

Hammerman, P. S., Sos, M. L., Ramos, A. H., Xu, C., Dutt, A., Zhou, W., Brace, L. E., Woods, B. A., Lin, W., Zhang, J., Deng, X., Lim, S. M., Heynck, S., Peifer, M., Simard, J. R., Lawrence, M. S., Onofrio, R. C., Salvesen, H. B., Seidel, D., Zander, T., Heuckmann, J. M., Soltermann, A., Moch, H., Koker, M., Leenders, F., Gabler, F., Querings, S., Ansen, S., Brambilla, E., Brambilla, C., Lorimier, P., Brustugun, O. T., Helland, A., Petersen, I., Clement, J. H., Groen, H., Timens,

W., Sietsma, H., Stoelben, E., Wolf, J., Beer, D. G., Tsao, M. S., Hanna, M., Hatton, C., Eck, M. J., Janne, P. A., Johnson, B. E., Winckler, W., Greulich, H., Bass, A. J., Cho, J., Rauh, D., Gray, N. S., Wong, K. K., Haura, E. B., Thomas, R. K., & Meyerson, M. (2011). Mutations in the DDR2 kinase gene identify a novel therapeutic target in squamous cell lung cancer. *Cancer Discov, 1*(1), 78-89. doi:10.1158/2159-8274.CD-11-0005

Hanahan, D., & Folkman, J. (1996). Patterns and emerging mechanisms of the angiogenic switch during tumorigenesis. *Cell, 86*(3), 353-364. doi:10.1016/s0092-8674(00)80108-7

Hanahan, D., & Weinberg, R. A. (2000). The hallmarks of cancer. *Cell, 100*(1), 57-70. doi:10.1016/s0092-8674(00)81683-9

Hanahan, D., & Weinberg, R. A. (2011). Hallmarks of cancer: the next generation. *Cell, 144*(5), 646-674. doi:10.1016/j.cell.2011.02.013

Harrison, D. A. (2012). The Jak/STAT pathway. *Cold Spring Harb Perspect Biol, 4*(3). doi:10.1101/cshperspect.a011205

Hartwell, L. H., & Weinert, T. A. (1989). Checkpoints: controls that ensure the order of cell cycle events. *Science, 246*(4930), 629-634. doi:10.1126/science.2683079

Hassan, M., Watari, H., AbuAlmaaty, A., Ohba, Y., & Sakuragi, N. (2014). Apoptosis and molecular targeting therapy in cancer. *Biomed Res Int, 2014*, 150845. doi:10.1155/2014/150845

Hecht, S. S. (1999). Tobacco smoke carcinogens and lung cancer. *J Natl Cancer Inst, 91*(14), 1194-1210. doi:10.1093/jnci/91.14.1194

Hengartner, M. O. (2000). The biochemistry of apoptosis. *Nature, 407*(6805), 770-776. doi:10.1038/35037710

Henry, C. J., Billups, L. H., Avery, M. D., Rude, T. H., Dansie, D. R., Lopez, A., Sass, B., Whitmire, C. E., & Kouri, R. E. (1981). Lung cancer model system using 3-methylcholanthrene in inbred strains of mice. *Cancer Res, 41*(12 Pt 1), 5027-5032.

Herbst, R. S., Heymach, J. V., & Lippman, S. M. (2008). Lung cancer. *The New England journal of medicine, 359*(13), 1367-1380. doi:10.1056/NEJMra0802714

Heuckmann, J. M., Balke-Want, H., Malchers, F., Peifer, M., Sos, M. L., Koker, M., Meder, L., Lovly, C. M., Heukamp, L. C., Pao, W., Küppers, R., & Thomas, R. K. (2012). Differential protein stability and ALK inhibitor sensitivity of EML4-ALK fusion variants. *Clinical Cancer Research, 18*(17), 4682-4690. doi:10.1158/1078-0432.CCR-11-3260

Heuckmann, J. M., Hölzel, M., Sos, M. L., Heynck, S., Balke-Want, H., Koker, M., Peifer, M., Weiss, J., Lovly, C. M., Grütter, C., Rauh, D., Pao, W., & Thomas, R. K. (2011). ALK mutations conferring differential resistance to structurally diverse ALK inhibitors. *Clinical Cancer Research, 17*(23), 7394-7401. doi:10.1158/1078-0432.CCR-11-1648

Hida, T., Nokihara, H., Kondo, M., Kim, Y. H., Azuma, K., Seto, T., Takiguchi, Y., Nishio, M., Yoshioka, H., Imamura, F., Hotta, K., Watanabe, S., Goto, K., Satouchi, M., Kozuki, T., Shukuya, T., Nakagawa, K., Mitsudomi, T., Yamamoto, N., Asakawa, T., Asabe, R., Tanaka, T., & Tamura, T. (2017). Alectinib versus crizotinib in patients with ALK-positive non-small-cell lung cancer (J-ALEX): an open-label, randomised phase 3 trial. *Lancet, 390*(10089), 29-39. doi:10.1016/S0140-6736(17)30565-2

Hilger, R. A., Scheulen, M. E., & Strumberg, D. (2002). The Ras-Raf-MEK-ERK pathway in the treatment of cancer. *Onkologie, 25*(6), 511-518. doi:10.1159/000068621

Hoeflich, K. P., Merchant, M., Orr, C., Chan, J., Den Otter, D., Berry, L., Kasman, I., Koeppen, H., Rice, K., Yang, N. Y., Engst, S., Johnston, S., Friedman, L. S., & Belvin, M. (2012). Intermittent administration of MEK inhibitor GDC-0973 plus PI3K inhibitor GDC-0941 triggers robust apoptosis and tumor growth inhibition. *Cancer Res, 72*(1), 210-219. doi:10.1158/0008-5472.CAN-11-1515

Hofer, E., & Schweighofer, B. (2007). Signal transduction induced in endothelial cells by growth factor receptors involved in angiogenesis. *Thromb Haemost, 97*(3), 355-363.

Holt, S. V., Logie, A., Davies, B. R., Alferez, D., Runswick, S., Fenton, S., Chresta, C. M., Gu, Y., Zhang, J., Wu, Y. L., Wilkinson, R. W., Guichard, S. M., & Smith, P. D. (2012). Enhanced apoptosis and tumor growth suppression elicited by combination of MEK (selumetinib) and mTOR kinase inhibitors (AZD8055). *Cancer Res, 72*(7), 1804-1813. doi:10.1158/0008-5472.CAN-11-1780

Holt, S. V., Logie, A., Odedra, R., Heier, A., Heaton, S. P., Alferez, D., Davies, B. R., Wilkinson, R. W., & Smith, P. D. (2012). The MEK1/2 inhibitor, selumetinib (AZD6244; ARRY-142886), enhances anti-tumour efficacy when combined with conventional chemotherapeutic agents in human tumour xenograft models. *Br J Cancer, 106*(5), 858-866. doi:10.1038/bjc.2012.8

Hoshino, R., Chatani, Y., Yamori, T., Tsuruo, T., Oka, H., Yoshida, O., Shimada, Y., Ari-i, S., Wada, H., Fujimoto, J., & Kohno, M. (1999). Constitutive activation of the 41-/43-kDa mitogen-activated protein kinase signaling pathway in human tumors. *Oncogene, 18*(3), 813-822. doi:10.1038/sj.onc.1202367

Houtman, S. H., Rutteman, M., De Zeeuw, C. I., & French, P. J. (2007). Echinoderm microtubule-associated protein like protein 4, a member of the echinoderm microtubule-associated protein family, stabilizes microtubules. *Neuroscience, 144*(4), 1373-1382. doi:10.1016/j.neuroscience.2006.11.015

Hrustanovic, G., Olivas, V., Pazarentzos, E., Tulpule, A., Asthana, S., Blakely, C. M., Okimoto, R. A., Lin, L., Neel, D. S., Sabnis, A., Flanagan, J., Chan, E., Varella-Garcia, M., Aisner, D. L., Vaishnavi, A., Ou, S.-H. I., Collisson, E. A., Ichihara, E., Mack, P. C., Lovly, C. M., Karachaliou, N., Rosell, R., Riess, J. W., Doebele, R. C., & Bivona, T. G. (2015). RAS-MAPK dependence underlies a rational polytherapy strategy in EML4-ALK–positive lung cancer. *Nature Medicine, 21*(9), 1038-1047. doi:10.1038/nm.3930

Hsu, H., Xiong, J., & Goeddel, D. V. (1995). The TNF receptor 1-associated protein TRADD signals cell death and NF-kappa B activation. *Cell, 81*(4), 495-504. doi:10.1016/0092-8674(95)90070-5

Huang, W. S., Liu, S., Zou, D., Thomas, M., Wang, Y., Zhou, T., Romero, J., Kohlmann, A., Li, F., Qi, J., Cai, L., Dwight, T. A., Xu, Y., Xu, R., Dodd, R., Toms, A., Parillon, L., Lu, X., Anjum, R., Zhang, S., Wang, F., Keats, J., Wardwell, S. D., Ning, Y., Xu, Q., Moran, L. E., Mohemmad, Q. K., Jang, H. G., Clackson, T., Narasimhan, N. I., Rivera, V. M., Zhu, X., Dalgarno, D., & Shakespeare, W. C. (2016). Discovery of Brigatinib (AP26113), a Phosphine Oxide-Containing, Potent, Orally Active Inhibitor of Anaplastic Lymphoma Kinase. *J Med Chem, 59*(10), 4948-4964. doi:10.1021/acs.jmedchem.6b00306

Huang, X. X., Xie, F. F., Hou, L. J., Chen, X. X., Ou, R. Y., Yu, J. T., Qiu, J. G., Zhang, W. J., Jiang, Q. W., Yang, Y., Zheng, D. W., Chen, Y., Huang, J. R., Wang, K., Wei, M. N., Li, W. F., Shi, Z., & Yan, X. J. (2017). Crizotinib synergizes with cisplatin in preclinical models of ovarian cancer. *Am J Transl Res, 9*(4), 1667-1679.

Hubbard, S. R. (1999). Structural analysis of receptor tyrosine kinases. *Progress in Biophysics and Molecular Biology, 71*(3-4), 343-358. doi:10.1016/S0079-6107(98)00047-9

Hubbard, S. R., & Miller, W. T. (2007). Receptor tyrosine kinases: mechanisms of activation and signaling. *Current Opinion in Cell Biology, 19*(2), 117-123. doi:10.1016/j.ceb.2007.02.010

Humphrey, L. L., Teutsch, S., Johnson, M., & Force, U. S. P. S. T. (2004). Lung cancer screening with sputum cytologic examination, chest radiography, and computed tomography: an update for the U.S. Preventive Services Task Force. *Ann Intern Med, 140*(9), 740-753. doi:10.7326/0003-4819-140-9-200405040-00015

Hung, R. J., McKay, J. D., Gaborieau, V., Boffetta, P., Hashibe, M., Zaridze, D., Mukeria, A., Szeszenia-Dabrowska, N., Lissowska, J., Rudnai, P., Fabianova, E., Mates, D., Bencko, V., Foretova, L., Janout, V., Chen, C., Goodman, G., Field, J. K., Liloglou, T., Xinarianos, G., Cassidy, A., McLaughlin, J., Liu, G., Narod, S., Krokan, H. E., Skorpen, F., Elvestad, M. B., Hveem, K., Vatten, L., Linseisen, J., Clavel-Chapelon, F., Vineis, P., Bueno-de-Mesquita, H. B., Lund, E., Martinez, C., Bingham, S., Rasmuson, T., Hainaut, P., Riboli, E., Ahrens, W., Benhamou, S., Lagiou, P., Trichopoulos, D., Holcátová, I., Merletti, F., Kjaerheim, K., Agudo, A., Macfarlane, G., Talamini, R., Simonato, L., Lowry, R., Conway, D. I., Znaor, A., Healy, C., Zelenika, D., Boland, A., Delepine, M., Foglio, M., Lechner, D., Matsuda, F., Blanche, H., Gut, I., Heath, S., Lathrop, M., & Brennan, P. (2008). A susceptibility locus for lung cancer maps to nicotinic acetylcholine receptor subunit genes on 15q25. *Nature, 452*(7187), 633-637. doi:10.1038/nature06885

Hunter, T. (1998). THE CROONIAN LECTURE 1997. The phosphorylation of proteins on tyrosine: its role in cell growth and disease. *Philosophical Transactions of the Royal Society B: Biological Sciences, 353*(1368), 583-605. doi:10.1098/rstb.1998.0228

Huynh, H., Soo, K. C., Chow, P. K., & Tran, E. (2007). Targeted inhibition of the extracellular signal-regulated kinase kinase pathway with AZD6244 (ARRY-142886) in the treatment of hepatocellular carcinoma. *Mol Cancer Ther, 6*(1), 138-146. doi:10.1158/1535-7163.MCT-06-0436

Hwang, S. J., Cheng, L. S. C., Lozano, G., Amos, C. I., Gu, X., & Strong, L. C. (2003). Lung cancer risk in germline p53 mutation carriers: Association between an inherited cancer predisposition, cigarette smoking, and cancer risk. *Human Genetics, 113*(3), 238-243. doi:10.1007/s00439-003-0968-7

Ignatius Ou, S. H., Azada, M., Hsiang, D. J., Herman, J. M., Kain, T. S., Siwak-Tapp, C., Casey, C., He, J., Ali, S. M., Klempner, S. J., & Miller, V. A. (2014). Next-generation sequencing reveals a Novel NSCLC ALK F1174V mutation and confirms ALK G1202R mutation confers high-level resistance to alectinib (CH5424802/RO5424802) in ALK-rearranged NSCLC patients who progressed on crizotinib. *J Thorac Oncol, 9*(4), 549-553. doi:10.1097/JTO.0000000000000094

Igney, F. H., & Krammer, P. H. (2002). Death and anti-death: tumour resistance to apoptosis. *Nat Rev Cancer, 2*(4), 277-288. doi:10.1038/nrc776

Imielinski, M., Berger, A. H., Hammerman, P. S., Hernandez, B., Pugh, T. J., Hodis, E., Cho, J., Suh, J., Capelletti, M., Sivachenko, A., Sougnez, C., Auclair, D., Lawrence, M. S., Stojanov, P., Cibulskis, K., Choi, K., de Waal, L., Sharifnia, T., Brooks, A., Greulich, H., Banerji, S., Zander, T., Seidel, D., Leenders, F., Ansen, S., Ludwig, C., Engel-Riedel, W., Stoelben, E., Wolf, J., Goparju, C., Thompson,

K., Winckler, W., Kwiatkowski, D., Johnson, B. E., Janne, P. A., Miller, V. A., Pao, W., Travis, W. D., Pass, H. I., Gabriel, S. B., Lander, E. S., Thomas, R. K., Garraway, L. A., Getz, G., & Meyerson, M. (2012). Mapping the hallmarks of lung adenocarcinoma with massively parallel sequencing. *Cell, 150*(6), 1107-1120. doi:10.1016/j.cell.2012.08.029

Infante, J. R., Cohen, R. B., Kim, K. B., Burris, H. A., 3rd, Curt, G., Emeribe, U., Clemett, D., Tomkinson, H. K., & LoRusso, P. M. (2017). A phase I dose-escalation study of Selumetinib in combination with Erlotinib or Temsirolimus in patients with advanced solid tumors. *Invest New Drugs, 35*(5), 576-588. doi:10.1007/s10637-017-0459-7

Infante, J. R., Fecher, L. A., Falchook, G. S., Nallapareddy, S., Gordon, M. S., Becerra, C., DeMarini, D. J., Cox, D. S., Xu, Y., Morris, S. R., Peddareddigari, V. G., Le, N. T., Hart, L., Bendell, J. C., Eckhardt, G., Kurzrock, R., Flaherty, K., Burris, H. A., 3rd, & Messersmith, W. A. (2012). Safety, pharmacokinetic, pharmacodynamic, and efficacy data for the oral MEK inhibitor trametinib: a phase 1 dose-escalation trial. *Lancet Oncol, 13*(8), 773-781. doi:10.1016/S1470-2045(12)70270-X

International Breast Cancer Study, G. (2002). Endocrine responsiveness and tailoring adjuvant therapy for postmenopausal lymph node-negative breast cancer: a randomized trial. *J Natl Cancer Inst, 94*(14), 1054-1065. doi:10.1093/jnci/94.14.1054

International Breast Cancer Study, G., Castiglione-Gertsch, M., O'Neill, A., Price, K. N., Goldhirsch, A., Coates, A. S., Colleoni, M., Nasi, M. L., Bonetti, M., & Gelber, R. D. (2003). Adjuvant chemotherapy followed by goserelin versus either modality alone for premenopausal lymph node-negative breast cancer: a randomized trial. *J Natl Cancer Inst, 95*(24), 1833-1846. doi:10.1093/jnci/djg119

Iwahara, T., Fujimoto, J., Wen, D., Cupples, R., Bucay, N., Arakawa, T., Mori, S., Ratzkin, B., & Yamamoto, T. (1997). Molecular characterization of ALK, a receptor tyrosine kinase expressed specifically in the nervous system. *Oncogene, 14*(4), 439-449. doi:10.1038/sj.onc.1200849

Iyevleva, A. G., Raskin, G. A., Tiurin, V. I., Sokolenko, A. P., Mitiushkina, N. V., Aleksakhina, S. N., Garifullina, A. R., Strelkova, T. N., Merkulov, V. O., Ivantsov, A. O., Kuligina, E., Pozharisski, K. M., Togo, A. V., & Imyanitov, E. N. (2015). Novel ALK fusion partners in lung cancer. *Cancer Lett, 362*(1), 116-121. doi:10.1016/j.canlet.2015.03.028

Janne, P. A., Shaw, A. T., Pereira, J. R., Jeannin, G., Vansteenkiste, J., Barrios, C., Franke, F. A., Grinsted, L., Zazulina, V., Smith, P., Smith, I., & Crino, L. (2013). Selumetinib plus docetaxel for KRAS-mutant advanced non-small-cell lung cancer: a randomised, multicentre, placebo-controlled, phase 2 study. *Lancet Oncol, 14*(1), 38-47. doi:10.1016/S1470-2045(12)70489-8

Janne, P. A., van den Heuvel, M. M., Barlesi, F., Cobo, M., Mazieres, J., Crino, L., Orlov, S., Blackhall, F., Wolf, J., Garrido, P., Poltoratskiy, A., Mariani, G., Ghiorghiu, D., Kilgour, E., Smith, P., Kohlmann, A., Carlile, D. J., Lawrence, D., Bowen, K., & Vansteenkiste, J. (2017). Selumetinib Plus Docetaxel Compared With Docetaxel Alone and Progression-Free Survival in Patients With KRAS-Mutant Advanced Non-Small Cell Lung Cancer: The SELECT-1 Randomized Clinical Trial. *Jama, 317*(18), 1844-1853. doi:10.1001/jama.2017.3438

Jiang, J., Wu, X., Tong, X., Wei, W., Chen, A., Wang, X., Shao, Y. W., & Huang, J. (2018). GCC2-ALK as a targetable fusion in lung adenocarcinoma and its

enduring clinical responses to ALK inhibitors. *Lung Cancer, 115*, 5-11. doi:10.1016/j.lungcan.2017.10.011

Jiao, Q., Bi, L., Ren, Y., Song, S., Wang, Q., & Wang, Y. S. (2018). Advances in studies of tyrosine kinase inhibitors and their acquired resistance. *Mol Cancer, 17*(1), 36. doi:10.1186/s12943-018-0801-5

Jin, G., Kim, M. J., Jeon, H. S., Choi, J. E., Kim, D. S., Lee, E. B., Cha, S. I., Yoon, G. S., Kim, C. H., Jung, T. H., & Park, J. Y. (2010). PTEN mutations and relationship to EGFR, ERBB2, KRAS, and TP53 mutations in non-small cell lung cancers. *Lung Cancer, 69*(3), 279-283. doi:10.1016/j.lungcan.2009.11.012

Jin, Z., & El-Deiry, W. S. (2005). Overview of cell death signaling pathways. *Cancer Biol Ther, 4*(2), 139-163. doi:10.4161/cbt.4.2.1508

Joazeiro, C. A., Wing, S. S., Huang, H., Leverson, J. D., Hunter, T., & Liu, Y. C. (1999). The tyrosine kinase negative regulator c-Cbl as a RING-type, E2-dependent ubiquitin-protein ligase. *Science, 286*(5438), 309-312. doi:10.1126/science.286.5438.309

Johnson, D. B., Flaherty, K. T., Weber, J. S., Infante, J. R., Kim, K. B., Kefford, R. F., Hamid, O., Schuchter, L., Cebon, J., Sharfman, W. H., McWilliams, R. R., Sznol, M., Lawrence, D. P., Gibney, G. T., Burris, H. A., 3rd, Falchook, G. S., Algazi, A., Lewis, K., Long, G. V., Patel, K., Ibrahim, N., Sun, P., Little, S., Cunningham, E., Sosman, J. A., Daud, A., & Gonzalez, R. (2014). Combined BRAF (Dabrafenib) and MEK inhibition (Trametinib) in patients with BRAFV600-mutant melanoma experiencing progression with single-agent BRAF inhibitor. *J Clin Oncol, 32*(33), 3697-3704. doi:10.1200/JCO.2014.57.3535

Johnson, T. R., Tan, W., Goulet, L., Smith, E. B., Yamazaki, S., Walker, G. S., O'Gorman, M. T., Bedarida, G., Zou, H. Y., Christensen, J. G., Nguyen, L. N., Shen, Z., Dalvie, D., Bello, A., & Smith, B. J. (2015). Metabolism, excretion and pharmacokinetics of [14C]crizotinib following oral administration to healthy subjects. *Xenobiotica, 45*(1), 45-59. doi:10.3109/00498254.2014.941964

Johnson, T. W., Richardson, P. F., Bailey, S., Brooun, A., Burke, B. J., Collins, M. R., Cui, J. J., Deal, J. G., Deng, Y. L., Dinh, D., Engstrom, L. D., He, M., Hoffman, J., Hoffman, R. L., Huang, Q., Kania, R. S., Kath, J. C., Lam, H., Lam, J. L., Le, P. T., Lingardo, L., Liu, W., McTigue, M., Palmer, C. L., Sach, N. W., Smeal, T., Smith, G. L., Stewart, A. E., Timofeevski, S., Zhu, H., Zhu, J., Zou, H. Y., & Edwards, M. P. (2014). Discovery of (10R)-7-amino-12-fluoro-2,10,16-trimethyl-15-oxo-10,15,16,17-tetrahydro-2H-8,4-(m etheno)pyrazolo[4,3-h][2,5,11]-benzoxadiazacyclotetradecine-3-carbonitrile (PF-06463922), a macrocyclic inhibitor of anaplastic lymphoma kinase (ALK) and c-ros oncogene 1 (ROS1) with preclinical brain exposure and broad-spectrum potency against ALK-resistant mutations. *J Med Chem, 57*(11), 4720-4744. doi:10.1021/jm500261q

Jung, Y., Kim, P., Jung, Y., Keum, J., Kim, S. N., Choi, Y. S., Do, I. G., Lee, J., Choi, S. J., Kim, S., Lee, J. E., Kim, J., Lee, S., & Kim, J. (2012). Discovery of ALK-PTPN3 gene fusion from human non-small cell lung carcinoma cell line using next generation RNA sequencing. *Genes Chromosomes Cancer, 51*(6), 590-597. doi:10.1002/gcc.21945

Kandoth, C., McLellan, M. D., Vandin, F., Ye, K., Niu, B., Lu, C., Xie, M., Zhang, Q., McMichael, J. F., Wyczalkowski, M. A., Leiserson, M. D. M., Miller, C. A., Welch, J. S., Walter, M. J., Wendl, M. C., Ley, T. J., Wilson, R. K., Raphael, B. J., & Ding, L. (2013). Mutational landscape and significance across 12 major cancer types. *Nature, 502*(7471), 333-339. doi:10.1038/nature12634

Kang, J., Chen, H. J., Zhang, X. C., Su, J., Zhou, Q., Tu, H. Y., Wang, Z., Wang, B. C., Zhong, W. Z., Yang, X. N., Chen, Z. H., Ding, Y., Wu, X., Wang, M., Fu, J. G., Yang, Z., Zhang, X., Shao, Y. W., Wu, Y. L., & Yang, J. J. (2018). Heterogeneous responses and resistant mechanisms to crizotinib in ALK-positive advanced non-small cell lung cancer. *Thorac Cancer, 9*(9), 1093-1103. doi:10.1111/1759-7714.12791

Kang, Y., Omura, M., Suzuki, A., Oka, T., Nakagami, Y., Cheng, C., Nagashima, Y., & Inoue, T. (2006). Development of an orthotopic transplantation model in nude mice that simulates the clinical features of human lung cancer. *Cancer Sci, 97*(10), 996-1001. doi:10.1111/j.1349-7006.2006.00276.x

Kanteti, R., Riehm, J. J., Dhanasingh, I., Lennon, F. E., Mirzapoiazova, T., Mambetsariev, B., Kindler, H. L., & Salgia, R. (2016). PI3 Kinase Pathway and MET Inhibition is Efficacious in Malignant Pleural Mesothelioma. *Sci Rep, 6*, 32992. doi:10.1038/srep32992

Karachaliou, N., Pilotto, S., Lazzari, C., Bria, E., de Marinis, F., & Rosell, R. (2016). Cellular and molecular biology of small cell lung cancer: an overview. *Transl Lung Cancer Res, 5*(1), 2-15. doi:10.3978/j.issn.2218-6751.2016.01.02

Katayama, R., Friboulet, L., Koike, S., Lockerman, E. L., Khan, T. M., Gainor, J. F., Iafrate, A. J., Takeuchi, K., Taiji, M., Okuno, Y., Fujita, N., Engelman, J. A., & Shaw, A. T. (2014). Two novel ALK mutations mediate acquired resistance to the next-generation ALK inhibitor alectinib. *Clinical Cancer Research, 20*(22), 5686-5696. doi:10.1158/1078-0432.CCR-14-1511

Katayama, R., Khan, T. M., Benes, C., Lifshits, E., Ebi, H., Rivera, V. M., Shakespeare, W. C., Iafrate, A. J., Engelman, J. A., & Shaw, A. T. (2011). Therapeutic strategies to overcome crizotinib resistance in non-small cell lung cancers harboring the fusion oncogene EML4-ALK. *Proceedings of the National Academy of Sciences, 108*(18), 7535-7540. doi:10.1073/pnas.1019559108

Katayama, R., Lovly, C. M., & Shaw, A. T. (2015). Therapeutic targeting of anaplastic lymphoma kinase in lung cancer: A paradigm for precision cancer medicine. *Clinical Cancer Research, 21*(10), 2227-2235. doi:10.1158/1078-0432.CCR-14-2791

Katayama, R., Shaw, A. T., Khan, T. M., Mino-Kenudson, M., Solomon, B. J., Halmos, B., Jessop, N. A., Wain, J. C., Yeo, A. T., Benes, C., Drew, L., Saeh, J. C., Crosby, K., Sequist, L. V., Iafrate, A. J., & Engelman, J. A. (2012). Mechanisms of Acquired Crizotinib Resistance in ALK-Rearranged Lung Cancers. *Science Translational Medicine, 4*(120), 120ra117-120ra117. doi:10.1126/scitranslmed.3003316

Kaufmann, S. H., & Earnshaw, W. C. (2000). Induction of apoptosis by cancer chemotherapy. *Exp Cell Res, 256*(1), 42-49. doi:10.1006/excr.2000.4838

Kawano, O., Sasaki, H., Endo, K., Suzuki, E., Haneda, H., Yukiue, H., Kobayashi, Y., Yano, M., & Fujii, Y. (2006). PIK3CA mutation status in Japanese lung cancer patients. *Lung Cancer, 54*(2), 209-215. doi:10.1016/j.lungcan.2006.07.006

Kazandjian, D., Blumenthal, G. M., Chen, H. Y., He, K., Patel, M., Justice, R., Keegan, P., & Pazdur, R. (2014). FDA Approval Summary: Crizotinib for the Treatment of Metastatic Non-Small Cell Lung Cancer With Anaplastic Lymphoma Kinase Rearrangements. *The Oncologist, 19*(10), e5-e11. doi:10.1634/theoncologist.2014-0241

Kellar, A., Egan, C., & Morris, D. (2015). Preclinical Murine Models for Lung Cancer: Clinical Trial Applications. *Biomed Res Int, 2015*, 621324. doi:10.1155/2015/621324

Kenfield, S. A., Wei, E. K., Stampfer, M. J., Rosner, B. A., & Colditz, G. A. (2008). Comparison of aspects of smoking among the four histological types of lung cancer. *Tob Control, 17*(3), 198-204. doi:10.1136/tc.2007.022582

Kerr, J. F., Wyllie, A. H., & Currie, A. R. (1972). Apoptosis: a basic biological phenomenon with wide-ranging implications in tissue kinetics. *Br J Cancer, 26*(4), 239-257. doi:10.1038/bjc.1972.33

Kerr, K. M. (2014). ALK Testing in Non-Small Cell Lung Carcinoma: What Now? *Journal of Thoracic Oncology, 9*(5), 593-595. doi:10.1097/JTO.0000000000000171

Khan, M., Lin, J., Liao, G., Tian, Y., Liang, Y., Li, R., Liu, M., & Yuan, Y. (2018). ALK Inhibitors in the Treatment of ALK Positive NSCLC. *Front Oncol, 8*, 557. doi:10.3389/fonc.2018.00557

Kim, C., & Giaccone, G. (2018). MEK inhibitors under development for treatment of non-small-cell lung cancer. *Expert Opin Investig Drugs, 27*(1), 17-30. doi:10.1080/13543784.2018.1415324

Kim, D. W., Mehra, R., Tan, D. S. W., Felip, E., Chow, L. Q. M., Camidge, D. R., Vansteenkiste, J., Sharma, S., De Pas, T., Riely, G. J., Solomon, B. J., Wolf, J., Thomas, M., Schuler, M., Liu, G., Santoro, A., Sutradhar, S., Li, S., Szczudlo, T., Yovine, A., & Shaw, A. T. (2016). Activity and safety of ceritinib in patients with ALK-rearranged non-small-cell lung cancer (ASCEND-1): updated results from the multicentre, open-label, phase 1 trial. *Lancet Oncol, 17*(4), 452-463. doi:10.1016/S1470-2045(15)00614-2

Kim, D. W., Tiseo, M., Ahn, M. J., Reckamp, K. L., Hansen, K. H., Kim, S. W., Huber, R. M., West, H. L., Groen, H. J. M., Hochmair, M. J., Leighl, N. B., Gettinger, S. N., Langer, C. J., Paz-Ares Rodriguez, L. G., Smit, E. F., Kim, E. S., Reichmann, W., Haluska, F. G., Kerstein, D., & Camidge, D. R. (2017). Brigatinib in Patients With Crizotinib-Refractory Anaplastic Lymphoma Kinase-Positive Non-Small-Cell Lung Cancer: A Randomized, Multicenter Phase II Trial. *J Clin Oncol, 35*(22), 2490-2498. doi:10.1200/JCO.2016.71.5904

Kim, H., Rafiuddin-Shah, M., Tu, H. C., Jeffers, J. R., Zambetti, G. P., Hsieh, J. J., & Cheng, E. H. (2006). Hierarchical regulation of mitochondrion-dependent apoptosis by BCL-2 subfamilies. *Nat Cell Biol, 8*(12), 1348-1358. doi:10.1038/ncb1499

Kischkel, F. C., Hellbardt, S., Behrmann, I., Germer, M., Pawlita, M., Krammer, P. H., & Peter, M. E. (1995). Cytotoxicity-dependent APO-1 (Fas/CD95)-associated proteins form a death-inducing signaling complex (DISC) with the receptor. *EMBO J, 14*(22), 5579-5588.

Kisseleva, T., Bhattacharya, S., Braunstein, J., & Schindler, C. W. (2002). Signaling through the JAK/STAT pathway, recent advances and future challenges. *Gene, 285*(1-2), 1-24. doi:10.1016/s0378-1119(02)00398-0

Kitada, M., Igoshi, N., Kamataki, T., Itahashi, K., Imaoka, S., Komori, M., Funae, Y., Rikihisa, T., & Kanakubo, Y. (1988). Immunochemical similarity of P-450 HFLa, a form of cytochrome P-450 in human fetal livers, to a form of rat liver cytochrome P-450 inducible by macrolide antibiotics. *Arch Biochem Biophys, 264*(1), 61-66. doi:10.1016/0003-9861(88)90570-x

Kodama, T., Tsukaguchi, T., Yoshida, M., Kondoh, O., & Sakamoto, H. (2014). Selective ALK inhibitor alectinib with potent antitumor activity in models of crizotinib resistance. *Cancer Letters, 351*(2), 215-221. doi:10.1016/j.canlet.2014.05.020

Kohno, T., Ichikawa, H., Totoki, Y., Yasuda, K., Hiramoto, M., Nammo, T., Sakamoto, H., Tsuta, K., Furuta, K., Shimada, Y., Iwakawa, R., Ogiwara, H., Oike, T., Enari, M., Schetter, A. J., Okayama, H., Haugen, A., Skaug, V., Chiku, S., Yamanaka, I., Arai, Y., Watanabe, S., Sekine, I., Ogawa, S., Harris, C. C., Tsuda, H., Yoshida, T., Yokota, J., & Shibata, T. (2012). KIF5B-RET fusions in lung adenocarcinoma. *Nat Med, 18*(3), 375-377. doi:10.1038/nm.2644

Koivunen, J. P., Mermel, C., Zejnullahu, K., Murphy, C., Lifshits, E., Holmes, A. J., Choi, H. G., Kim, J., Chiang, D., Thomas, R., Lee, J., Richards, W. G., Sugarbaker, D. J., Ducko, C., Lindeman, N., Marcoux, J. P., Engelman, J. A., Gray, N. S., Lee, C., Meyerson, M., & Jänne, P. A. (2008). EML4-ALK fusion gene and efficacy of an ALK kinase inhibitor in lung cancer. *Clinical Cancer Research, 14*(13), 4275-4283. doi:10.1158/1078-0432.CCR-08-0168

Kominami, K., Nakabayashi, J., Nagai, T., Tsujimura, Y., Chiba, K., Kimura, H., Miyawaki, A., Sawasaki, T., Yokota, H., Manabe, N., & Sakamaki, K. (2012). The molecular mechanism of apoptosis upon caspase-8 activation: quantitative experimental validation of a mathematical model. *Biochim Biophys Acta, 1823*(10), 1825-1840. doi:10.1016/j.bbamcr.2012.07.003

Kroemer, G., Galluzzi, L., & Brenner, C. (2007). Mitochondrial membrane permeabilization in cell death. *Physiol Rev, 87*(1), 99-163. doi:10.1152/physrev.00013.2006

Kuwana, T., Bouchier-Hayes, L., Chipuk, J. E., Bonzon, C., Sullivan, B. A., Green, D. R., & Newmeyer, D. D. (2005). BH3 domains of BH3-only proteins differentially regulate Bax-mediated mitochondrial membrane permeabilization both directly and indirectly. *Mol Cell, 17*(4), 525-535. doi:10.1016/j.molcel.2005.02.003

Kuwana, T., Mackey, M. R., Perkins, G., Ellisman, M. H., Latterich, M., Schneiter, R., Green, D. R., & Newmeyer, D. D. (2002). Bid, Bax, and lipids cooperate to form supramolecular openings in the outer mitochondrial membrane. *Cell, 111*(3), 331-342. doi:10.1016/s0092-8674(02)01036-x

Kwak, E. L., Bang, Y.-J., Camidge, D. R., Shaw, A. T., Solomon, B., Maki, R. G., Ou, S.-H. I., Dezube, B. J., Jänne, P. A., & Costa, D. B. (2010). Anaplastic lymphoma kinase inhibition in non–small-cell lung cancer. *New England Journal of Medicine, 363*(18), 1693-1703.

Kwak, E. L., Camidge, D., Clark, J., Shapiro, G., Maki, R., Ratain, M., Solomon, B., Bang, Y., Ou, S., & Salgia, R. (2009). G6 Clinical activity observed in a phase I dose escalation trial of an oral c-met and ALK inhibitor, PF-02341066. *European Journal of Cancer Supplements, 7*(3), 8.

Kwon, J., & Meagher, A. (2012). Crizotinib: a breakthrough for targeted therapies in lung cancer. *J Adv Pract Oncol, 3*(4), 267-272. doi:10.6004/jadpro.2012.3.4.8

Laemmli, U. K. (1970). Cleavage of structural proteins during the assembly of the head of bacteriophage T4. *Nature, 227*(5259), 680-685. doi:10.1038/227680a0

Langer, C. J., Besse, B., Gualberto, A., Brambilla, E., & Soria, J. C. (2010). The evolving role of histology in the management of advanced non-small-cell lung cancer. *J Clin Oncol, 28*(36), 5311-5320. doi:10.1200/JCO.2010.28.8126

Larkins, E., Blumenthal, G. M., Chen, H., He, K., Agarwal, R., Gieser, G., Stephens, O., Zahalka, E., Ringgold, K., Helms, W., Shord, S., Yu, J., Zhao, H., Davis, G., McKee, A. E., Keegan, P., & Pazdur, R. (2016). FDA Approval: Alectinib for the Treatment of Metastatic, ALK-Positive Non-Small Cell Lung Cancer Following Crizotinib. *Clin Cancer Res, 22*(21), 5171-5176. doi:10.1158/1078-0432.CCR-16-1293

Lavoie, J. N., L'Allemain, G., Brunet, A., Muller, R., & Pouyssegur, J. (1996). Cyclin D1 expression is regulated positively by the p42/p44MAPK and negatively by the p38/HOGMAPK pathway. *J Biol Chem, 271*(34), 20608-20616. doi:10.1074/jbc.271.34.20608

Lee, C. C., Jia, Y., Li, N., Sun, X., Ng, K., Ambing, E., Gao, M. Y., Hua, S., Chen, C., Kim, S., Michellys, P. Y., Lesley, S. A., Harris, J. L., & Spraggon, G. (2010). Crystal structure of the ALK (anaplastic lymphoma kinase) catalytic domain. *Biochem J, 430*(3), 425-437. doi:10.1042/BJ20100609

Lee, P. A., Wallace, E., Marlow, A., Yeh, T., Marsh, V., Anderson, D., Woessner, R., Hurley, B., Lyssikatos, J., Poch, G., Gross, S., Rana, S., Winski, S., & Koch, K. (2010). Abstract 2515: Preclinical Development of ARRY-162, A Potent and Selective MEK 1/2 Inhibitor. *Cancer Research, 70*(8 Supplement), 2515-2515. doi:10.1158/1538-7445.Am10-2515

Lees, E. (1995). Cyclin dependent kinase regulation. *Current Opinion in Cell Biology, 7*(6), 773-780. doi:https://doi.org/10.1016/0955-0674(95)80060-3

Leijen, S., Soetekouw, P. M., Jeffry Evans, T. R., Nicolson, M., Schellens, J. H., Learoyd, M., Grinsted, L., Zazulina, V., Pwint, T., & Middleton, M. (2011). A phase I, open-label, randomized crossover study to assess the effect of dosing of the MEK 1/2 inhibitor Selumetinib (AZD6244; ARRY-142866) in the presence and absence of food in patients with advanced solid tumors. *Cancer Chemother Pharmacol, 68*(6), 1619-1628. doi:10.1007/s00280-011-1732-7

Ley, R., Balmanno, K., Hadfield, K., Weston, C., & Cook, S. J. (2003). Activation of the ERK1/2 signaling pathway promotes phosphorylation and proteasome-dependent degradation of the BH3-only protein, Bim. *J Biol Chem, 278*(21), 18811-18816. doi:10.1074/jbc.M301010200

Li, T., Kang, G., Wang, T., & Huang, H. (2018). Tumor angiogenesis and anti-angiogenic gene therapy for cancer. *Oncol Lett, 16*(1), 687-702. doi:10.3892/ol.2018.8733

Liao, E. H., Hung, W., Abrams, B., & Zhen, M. (2004). An SCF-like ubiquitin ligase complex that controls presynaptic differentiation. *Nature, 430*(6997), 345-350. doi:10.1038/nature02647

Lim, W., Ridge, C. A., Nicholson, A. G., & Mirsadraee, S. (2018). The 8(th) lung cancer TNM classification and clinical staging system: review of the changes and clinical implications. *Quant Imaging Med Surg, 8*(7), 709-718. doi:10.21037/qims.2018.08.02

Lin, C., Shi, X., Yang, S., Zhao, J., He, Q., Jin, Y., & Yu, X. (2019). Comparison of ALK detection by FISH, IHC and NGS to predict benefit from crizotinib in advanced non-small-cell lung cancer. *Lung Cancer, 131*, 62-68. doi:10.1016/j.lungcan.2019.03.018

Lin, J. J., Riely, G. J., & Shaw, A. T. (2017). Targeting ALK: Precision medicine takes on drug resistance. *Cancer Discovery, 7*(2), 137-155. doi:10.1158/2159-8290.CD-16-1123

Lindeman, N. I., Cagle, P. T., Beasley, M. B., Chitale, D. A., Dacic, S., Giaccone, G., Jenkins, R. B., Kwiatkowski, D. J., Saldivar, J. S., Squire, J., Thunnissen, E., & Ladanyi, M. (2013). Molecular testing guideline for selection of lung cancer patients for EGFR and ALK tyrosine kinase inhibitors: guideline from the College of American Pathologists, International Association for the Study of Lung Cancer, and Association for Molecular Pathology. *J Thorac Oncol, 8*(7), 823-859. doi:10.1097/JTO.0b013e318290868f

Lindenmayer, A. E., & Miettinen, M. (1995). Immunophenotypic features of uterine stromal cells. CD34 expression in endocervical stroma. *Virchows Arch, 426*(5), 457-460. doi:10.1007/BF00193168

Linsell, O., & Ashton, J. C. (2014). Cerebral hypoxia-ischemia causes cardiac damage in a rat model. *Neuroreport, 25*(10), 796-800. doi:10.1097/WNR.0000000000000190

Liu, C., Pepper, K., Hendrickson, H., Cagle, P. T., & Portier, B. P. (2016). Clinical Validation of a Novel Commercial Reverse Transcription-Quantitative Polymerase Chain Reaction Screening Assay for Detection of ALK Translocations and Amplifications in Non-Small Cell Lung Carcinomas. *Arch Pathol Lab Med, 140*(7), 690-693. doi:10.5858/arpa.2015-0419-OA

Liu, X., Liu, J., Guan, Y., Li, H., Huang, L., Tang, H., & He, J. (2012). Establishment of an orthotopic lung cancer model in nude mice and its evaluation by spiral CT. *J Thorac Dis, 4*(2), 141-145. doi:10.3978/j.issn.2072-1439.2012.03.04

Loren, C. E., Scully, A., Grabbe, C., Edeen, P. T., Thomas, J., McKeown, M., Hunter, T., & Palmer, R. H. (2001). Identification and characterization of DAlk: a novel Drosophila melanogaster RTK which drives ERK activation in vivo. *Genes Cells, 6*(6), 531-544. doi:10.1046/j.1365-2443.2001.00440.x

LoRusso, P. M., Infante, J. R., Kim, K. B., Burris, H. A., 3rd, Curt, G., Emeribe, U., Clemett, D., Tomkinson, H. K., & Cohen, R. B. (2017). A phase I dose-escalation study of selumetinib in combination with docetaxel or dacarbazine in patients with advanced solid tumors. *BMC Cancer, 17*(1), 173. doi:10.1186/s12885-017-3143-6

Lou-Qian, Z., Rong, Y., Ming, L., Xin, Y., Feng, J., & Lin, X. (2013). The prognostic value of epigenetic silencing of p16 gene in NSCLC patients: a systematic review and meta-analysis. *PLoS ONE, 8*(1), e54970. doi:10.1371/journal.pone.0054970

Lovly, C. M., McDonald, N. T., Chen, H., Ortiz-Cuaran, S., Heukamp, L. C., Yan, Y., Florin, A., Ozretić, L., Lim, D., Wang, L., Chen, Z., Chen, X., Lu, P., Paik, P. K., Shen, R., Jin, H., Buettner, R., Ansén, S., Perner, S., Brockmann, M., Bos, M., Wolf, J., Gardizi, M., Wright, G. M., Solomon, B., Russell, P. A., Rogers, T.-M., Suehara, Y., Red-Brewer, M., Tieu, R., de Stanchina, E., Wang, Q., Zhao, Z., Johnson, D. H., Horn, L., Wong, K.-K., Thomas, R. K., Ladanyi, M., & Pao, W. (2014). Rationale for co-targeting IGF-1R and ALK in ALK fusion–positive lung cancer. *Nature Medicine, 20*(9), 1027-1034. doi:10.1038/nm.3667

Lovly, C. M., & Pao, W. (2012). Escaping ALK inhibition: mechanisms of and strategies to overcome resistance. *Sci Transl Med, 4*(120), 120ps122. doi:10.1126/scitranslmed.3003728

Lovly, C. M., & Shaw, A. T. (2014). Molecular pathways: resistance to kinase inhibitors and implications for therapeutic strategies. *Clin Cancer Res, 20*(9), 2249-2256. doi:10.1158/1078-0432.CCR-13-1610

Lu, Z., & Xu, S. (2006). ERK1/2 MAP kinases in cell survival and apoptosis. *IUBMB Life, 58*(11), 621-631. doi:10.1080/15216540600957438

Luciano, F., Jacquel, A., Colosetti, P., Herrant, M., Cagnol, S., Pages, G., & Auberger, P. (2003). Phosphorylation of Bim-EL by Erk1/2 on serine 69 promotes its degradation via the proteasome pathway and regulates its proapoptotic function. *Oncogene, 22*(43), 6785-6793. doi:10.1038/sj.onc.1206792

Lugano, R., Ramachandran, M., & Dimberg, A. (2020). Tumor angiogenesis: causes, consequences, challenges and opportunities. *Cell Mol Life Sci, 77*(9), 1745-1770. doi:10.1007/s00018-019-03351-7

Lung Foundation NZ. (2020). Lung Health Lung Cancer Lung disease. Retrieved from https://lungfoundation.org.nz/lung-health/

Maae, E., Nielsen, M., Steffensen, K. D., Jakobsen, E. H., Jakobsen, A., & Sorensen, F. B. (2011). Estimation of immunohistochemical expression of VEGF in ductal carcinomas of the breast. *J Histochem Cytochem, 59*(8), 750-760. doi:10.1369/0022155411412599

Maillet, D., Martel-Lafay, I., Arpin, D., & Perol, M. (2013). Ineffectiveness of crizotinib on brain metastases in two cases of lung adenocarcinoma with EML4-ALK rearrangement. *J Thorac Oncol, 8*(4), e30-31. doi:10.1097/JTO.0b013e318288dc2d

Mak, I. W., Evaniew, N., & Ghert, M. (2014). Lost in translation: animal models and clinical trials in cancer treatment. *Am J Transl Res, 6*(2), 114-118.

Mao, J., Johnson, T. R., Shen, Z., & Yamazaki, S. (2013). Prediction of crizotinib-midazolam interaction using the Simcyp population-based simulator: comparison of CYP3A time-dependent inhibition between human liver microsomes versus hepatocytes. *Drug Metab Dispos, 41*(2), 343-352. doi:10.1124/dmd.112.049114

Marani, M., Hancock, D., Lopes, R., Tenev, T., Downward, J., & Lemoine, N. R. (2004). Role of Bim in the survival pathway induced by Raf in epithelial cells. *Oncogene, 23*(14), 2431-2441. doi:10.1038/sj.onc.1207364

Marchetti, A., Di Lorito, A., Pace, M. V., Iezzi, M., Felicioni, L., D'Antuono, T., Filice, G., Guetti, L., Mucilli, F., & Buttitta, F. (2016). ALK Protein Analysis by IHC Staining after Recent Regulatory Changes: A Comparison of Two Widely Used Approaches, Revision of the Literature, and a New Testing Algorithm. *J Thorac Oncol, 11*(4), 487-495. doi:10.1016/j.jtho.2015.12.111

Marsilje, T. H., Pei, W., Chen, B., Lu, W., Uno, T., Jin, Y., Jiang, T., Kim, S., Li, N., Warmuth, M., Sarkisova, Y., Sun, F., Ste, A., Pferdekamper, A. C., Li, A. G., Joseph, S. B., Kim, Y., Liu, B., Tuntland, T., Cui, X., Gray, N. S., Steensma, R., Wan, Y., Jiang, J., Chopiuk, G., Li, J., Gordon, W. P., Richmond, W., Johnson, K., Chang, J., Groessl, T., He, Y.-q., Phimister, A., Aycinena, A., Lee, C. C., Bursulaya, B., Karanewsky, D. S., Seidel, H. M., & Harris, J. L. (2013). Genomics Institute of the Novartis Research Foundation, 10675 John Jay Hopkins Drive, San Diego, California 92121, United States. *Journal of Medicinal Chemistry, 56*, 5675-5690.

Martelli, M. P., Sozzi, G., Hernandez, L., Pettirossi, V., Navarro, A., Conte, D., Gasparini, P., Perrone, F., Modena, P., Pastorino, U., Carbone, A., Fabbri, A., Sidoni, A., Nakamura, S., Gambacorta, M., Fernandez, P. L., Ramirez, J., Chan, J. K., Grigioni, W. F., Campo, E., Pileri, S. A., & Falini, B. (2009). EML4-ALK rearrangement in non-small cell lung cancer and non-tumor lung tissues. *Am J Pathol, 174*(2), 661-670. doi:10.2353/ajpath.2009.080755

Martey, O., Greish, K., Smith, P. F., & Rosengren, R. J. (2019). A multivariate statistical analysis of the effects of styrene maleic acid encapsulated RL71 in a xenograft model of triple negative breast cancer. *J Biol Methods, 6*(4), e121. doi:10.14440/jbm.2019.306

Martey, O., Nimick, M., Taurin, S., Sundararajan, V., Greish, K., & Rosengren, R. J. (2017). Styrene maleic acid-encapsulated RL71 micelles suppress tumor growth in a murine xenograft model of triple negative breast cancer. *Int J Nanomedicine, 12*, 7225-7237. doi:10.2147/IJN.S148908

Marzec, M., Kasprzycka, M., Liu, X., El-Salem, M., Halasa, K., Raghunath, P. N., Bucki, R., Wlodarski, P., & Wasik, M. A. (2007). Oncogenic tyrosine kinase NPM/ALK

induces activation of the rapamycin-sensitive mTOR signaling pathway. *Oncogene, 26*(38), 5606-5614. doi:10.1038/sj.onc.1210346

Marzec, M., Kasprzycka, M., Liu, X., Raghunath, P. N., Wlodarski, P., & Wasik, M. A. (2007). Oncogenic tyrosine kinase NPM/ALK induces activation of the MEK/ERK signaling pathway independently of c-Raf. *Oncogene, 26*(6), 813-821. doi:10.1038/sj.onc.1209843

Marzec, M., Kasprzycka, M., Ptasznik, A., Wlodarski, P., Zhang, Q., Odum, N., & Wasik, M. A. (2005). Inhibition of ALK enzymatic activity in T-cell lymphoma cells induces apoptosis and suppresses proliferation and STAT3 phosphorylation independently of Jak3. *Lab Invest, 85*(12), 1544-1554. doi:10.1038/labinvest.3700348

Mascaux, C., Iannino, N., Martin, B., Paesmans, M., Berghmans, T., Dusart, M., Haller, A., Lothaire, P., Meert, A. P., Noel, S., Lafitte, J. J., & Sculier, J. P. (2005). The role of RAS oncogene in survival of patients with lung cancer: a systematic review of the literature with meta-analysis. *Br J Cancer, 92*(1), 131-139. doi:10.1038/sj.bjc.6602258

Mathivet, T., Mazot, P., & Vigny, M. (2007). In contrast to agonist monoclonal antibodies, both C-terminal truncated form and full length form of Pleiotrophin failed to activate vertebrate ALK (anaplastic lymphoma kinase)? *Cell Signal, 19*(12), 2434-2443. doi:10.1016/j.cellsig.2007.07.011

McCune, J. S., Hawke, R. L., LeCluyse, E. L., Gillenwater, H. H., Hamilton, G., Ritchie, J., & Lindley, C. (2000). In vivo and in vitro induction of human cytochrome P4503A4 by dexamethasone. *Clin Pharmacol Ther, 68*(4), 356-366. doi:10.1067/mcp.2000.110215

McCusker, M. G., Russo, A., Scilla, K. A., Mehra, R., & Rolfo, C. (2019). How I treat ALK-positive non-small cell lung cancer. *ESMO Open, 4*(Suppl 2), e000524. doi:10.1136/esmoopen-2019-000524

McDermott, U., Iafrate, A. J., Gray, N. S., Shioda, T., Classon, M., Maheswaran, S., Zhou, W., Choi, H. G., Smith, S. L., & Dowell, L. (2008). Genomic alterations of anaplastic lymphoma kinase may sensitize tumors to anaplastic lymphoma kinase inhibitors. *Cancer Research, 68*(9), 3389-3395.

McDonnell, S. R., Hwang, S. R., Basrur, V., Conlon, K. P., Fermin, D., Wey, E., Murga-Zamalloa, C., Zeng, Z., Zu, Y., Elenitoba-Johnson, K. S., & Lim, M. S. (2012). NPM-ALK signals through glycogen synthase kinase 3beta to promote oncogenesis. *Oncogene, 31*(32), 3733-3740. doi:10.1038/onc.2011.542

McKeage, M. J., Tin Tin, S., Khwaounjoo, P., Sheath, K., Dixon-McIver, A., Ng, D., Sullivan, R., Cameron, L., Shepherd, P., Laking, G. R., Kingston, N., Strauss, M., Lewis, C., Elwood, M., & Love, D. R. (2019). Screening for Anaplastic Lymphoma Kinase (ALK) gene rearrangements in non-small cell lung cancer (NSCLC) in New Zealand. *Intern Med J*. doi:10.1111/imj.14435

McLemore, T. L., Liu, M. C., Blacker, P. C., Gregg, M., Alley, M. C., Abbott, B. J., Shoemaker, R. H., Bohlman, M. E., Litterst, C. C., Hubbard, W. C., & et al. (1987). Novel intrapulmonary model for orthotopic propagation of human lung cancers in athymic nude mice. *Cancer Res, 47*(19), 5132-5140.

Melosky, B. (2018). Rapidly changing treatment algorithms for metastatic nonsquamous non-small-cell lung cancer. *Curr Oncol, 25*(Suppl 1), S68-S76. doi:10.3747/co.25.3839

Meng, J., Dai, B., Fang, B., Nebiyou Bekele, B., Bornmann, W. G., Sun, D., Peng, Z., Herbst, R. S., Papadimitrakopoulou, V., Minna, J. D., Peyton, M., & Roth, J. A. (2010). Combination treatment with MEK and AKT inhibitors is more effective

than each drug alone in human non- small cell lung cancer in vitro and in vivo. *PLoS ONE, 5*(11), 1-10. doi:10.1371/journal.pone.0014124

Meng, J., Fang, B., Liao, Y., Chresta, C. M., Smith, P. D., & Roth, J. A. (2010). Apoptosis induction by MEK inhibition in human lung cancer cells is mediated by Bim. *PLoS ONE, 5*(9), e13026. doi:10.1371/journal.pone.0013026

Menzies, A. M., & Long, G. V. (2014). Dabrafenib and trametinib, alone and in combination for BRAF-mutant metastatic melanoma. *Clin Cancer Res, 20*(8), 2035-2043. doi:10.1158/1078-0432.CCR-13-2054

Merino, D., Giam, M., Hughes, P. D., Siggs, O. M., Heger, K., O'Reilly, L. A., Adams, J. M., Strasser, A., Lee, E. F., Fairlie, W. D., & Bouillet, P. (2009). The role of BH3-only protein Bim extends beyond inhibiting Bcl-2-like prosurvival proteins. *J Cell Biol, 186*(3), 355-362. doi:10.1083/jcb.200905153

Metcalfe, E., Arik, D., Oge, T., Etiz, D., Yalcin, O. T., Kabukcuoglu, S., Pasaoglu, O., & Ozalp, S. S. (2018). CD105 (endoglin) expression as a prognostic marker of angiogenesis in squamous cell cervical cancer treated with radical radiotherapy. *J Cancer Res Ther, 14*(6), 1373-1378. doi:10.4103/0973-1482.203602

Metro, G., Tazza, M., Matocci, R., Chiari, R., & Crinò, L. (2017). Optimal management of ALK-positive NSCLC progressing on crizotinib. *Lung Cancer, 106*, 58-66. doi:10.1016/j.lungcan.2017.02.003

Mikhailov, V., Mikhailova, M., Degenhardt, K., Venkatachalam, M. A., White, E., & Saikumar, P. (2003). Association of Bax and Bak homo-oligomers in mitochondria. Bax requirement for Bak reorganization and cytochrome c release. *J Biol Chem, 278*(7), 5367-5376. doi:10.1074/jbc.M203392200

Minca, E. C., Portier, B. P., Wang, Z., Lanigan, C., Farver, C. F., Feng, Y., Ma, P. C., Arrossi, V. A., Pennell, N. A., & Tubbs, R. R. (2013). ALK status testing in non-small cell lung carcinoma: correlation between ultrasensitive IHC and FISH. *J Mol Diagn, 15*(3), 341-346. doi:10.1016/j.jmoldx.2013.01.004

Mino-Kenudson, M., Chirieac, L. R., Law, K., Hornick, J. L., Lindeman, N., Mark, E. J., Cohen, D. W., Johnson, B. E., Janne, P. A., Iafrate, A. J., & Rodig, S. J. (2010). A novel, highly sensitive antibody allows for the routine detection of ALK-rearranged lung adenocarcinomas by standard immunohistochemistry. *Clin Cancer Res, 16*(5), 1561-1571. doi:10.1158/1078-0432.CCR-09-2845

Mitsudomi, T., Hamajima, N., Ogawa, M., & Takahashi, T. (2000). Prognostic significance of p53 alterations in patients with non-small cell lung cancer: a meta-analysis. *Clin Cancer Res, 6*(10), 4055-4063.

Miyata, Y., Sagara, Y., Watanabe, S., Asai, A., Matsuo, T., Ohba, K., Hayashi, T., & Sakai, H. (2013). CD105 is a more appropriate marker for evaluating angiogenesis in urothelial cancer of the upper urinary tract than CD31 or CD34. *Virchows Arch, 463*(5), 673-679. doi:10.1007/s00428-013-1463-8

Molina, J. R., & Adjei, A. A. (2006). The Ras/Raf/MAPK pathway. *J Thorac Oncol, 1*(1), 7-9.

Moog-Lutz, C., Degoutin, J., Gouzi, J. Y., Frobert, Y., Brunet-de Carvalho, N., Bureau, J., Creminon, C., & Vigny, M. (2005). Activation and inhibition of anaplastic lymphoma kinase receptor tyrosine kinase by monoclonal antibodies and absence of agonist activity of pleiotrophin. *J Biol Chem, 280*(28), 26039-26048. doi:10.1074/jbc.M501972200

Moran, T., & Sequist, L. V. (2012). Timing of epidermal growth factor receptor tyrosine kinase inhibitor therapy in patients with lung cancer with EGFR mutations. *J Clin Oncol, 30*(27), 3330-3336. doi:10.1200/JCO.2012.43.1858

Morris, S. W., Kirstein, M. N., Valentine, M. B., Dittmer, K. G., Shapiro, D. N., Saltman, D. L., & Look, A. T. (1994). Fusion of a kinase gene, ALK, to a nucleolar protein gene, NPM, in non-Hodgkin's lymphoma. *SCIENCE-NEW YORK THEN WASHINGTON-*, 1281-1281.

Morris, S. W., Naeve, C., Mathew, P., James, P. L., Kirstein, M. N., Cui, X., & Witte, D. P. (1997). ALK, the chromosome 2 gene locus altered by the t(2;5) in non-Hodgkin's lymphoma, encodes a novel neural receptor tyrosine kinase that is highly related to leukocyte tyrosine kinase (LTK). *Oncogene, 14*(18), 2175-2188. doi:10.1038/sj.onc.1201062

Morrison, D. K. (2012). MAP kinase pathways. *Cold Spring Harb Perspect Biol, 4*(11). doi:10.1101/cshperspect.a011254

Morton, C. L., & Houghton, P. J. (2007). Establishment of human tumor xenografts in immunodeficient mice. *Nat Protoc, 2*(2), 247-250. doi:10.1038/nprot.2007.25

Motegi, A., Fujimoto, J., Kotani, M., Sakuraba, H., & Yamamoto, T. (2004). ALK receptor tyrosine kinase promotes cell growth and neurite outgrowth. *J Cell Sci, 117*(Pt 15), 3319-3329. doi:10.1242/jcs.01183

Munoz-Chapuli, R., Quesada, A. R., & Angel Medina, M. (2004). Angiogenesis and signal transduction in endothelial cells. *Cell Mol Life Sci, 61*(17), 2224-2243. doi:10.1007/s00018-004-4070-7

Murphy, D. A., Makonnen, S., Lassoued, W., Feldman, M. D., Carter, C., & Lee, W. M. (2006). Inhibition of tumor endothelial ERK activation, angiogenesis, and tumor growth by sorafenib (BAY43-9006). *Am J Pathol, 169*(5), 1875-1885. doi:10.2353/ajpath.2006.050711

Murray, P. B., Lax, I., Reshetnyak, A., Ligon, G. F., Lillquist, J. S., Natoli, E. J., Jr., Shi, X., Folta-Stogniew, E., Gunel, M., Alvarado, D., & Schlessinger, J. (2015). Heparin is an activating ligand of the orphan receptor tyrosine kinase ALK. *Sci Signal, 8*(360), ra6. doi:10.1126/scisignal.2005916

Muscat, J. E., Stellman, S. D., Zhang, Z. F., Neugut, A. I., & Wynder, E. L. (1997). Cigarette smoking and large cell carcinoma of the lung. *Cancer Epidemiol Biomarkers Prev, 6*(7), 477-480.

Nagasaka, M., & Gadgeel, S. M. (2018). Role of chemotherapy and targeted therapy in early-stage non-small cell lung cancer. *Expert Rev Anticancer Ther, 18*(1), 63-70. doi:10.1080/14737140.2018.1409624

Nagashima, O., Ohashi, R., Yoshioka, Y., Inagaki, A., Tajima, M., Koinuma, Y., Iwakami, S., Iwase, A., Sasaki, S., Tominaga, S., & Takahashi, K. (2013). High prevalence of gene abnormalities in young patients with lung cancer. *J Thorac Dis, 5*(1), 27-30. doi:10.3978/j.issn.2072-1439.2012.12.02

Nair, A., Morsy, M. A., & Jacob, S. (2018). Dose translation between laboratory animals and human in preclinical and clinical phases of drug development. *Drug Dev Res*. doi:10.1002/ddr.21461

Nakajima, T., Anayama, T., Matsuda, Y., Hwang, D. M., McVeigh, P. Z., Wilson, B. C., Zheng, G., Keshavjee, S., & Yasufuku, K. (2014). Orthotopic lung cancer murine model by nonoperative transbronchial approach. *Ann Thorac Surg, 97*(5), 1771-1775. doi:10.1016/j.athoracsur.2014.01.048

Nassiri, F., Cusimano, M. D., Scheithauer, B. W., Rotondo, F., Fazio, A., Yousef, G. M., Syro, L. V., Kovacs, K., & Lloyd, R. V. (2011). Endoglin (CD105): a review of its role in angiogenesis and tumor diagnosis, progression and therapy. *Anticancer Res, 31*(6), 2283-2290.

National Lung Screening Trial Research, T., Aberle, D. R., Adams, A. M., Berg, C. D., Black, W. C., Clapp, J. D., Fagerstrom, R. M., Gareen, I. F., Gatsonis, C., Marcus,

P. M., & Sicks, J. D. (2011). Reduced lung-cancer mortality with low-dose computed tomographic screening. *N Engl J Med, 365*(5), 395-409. doi:10.1056/NEJMoa1102873

NCCN Clinical Practice Guidelines in Oncology (NCCN Guidelines®). (2020). Non-Small Cell Lung Cancer V.3.2020. Retrieved from www.nccn.org

Nencioni, A., Caffa, I., Raffaghello, L., Montecucco, F., Cea, M., Monacelli, F., Grossi, F., Patrone, F., Odetti, P., Ballestrero, A., & Longo, V. (2014). Potentiation of crizotinib activity by fasting cycles in an ALK+ lung cancer model. *Journal of Clinical Oncology, 32*(15_suppl), e13511-e13511. doi:10.1200/jco.2014.32.15_suppl.e13511

Nesbitt, J. C., Putnam, J. B., Jr., Walsh, G. L., Roth, J. A., & Mountain, C. F. (1995). Survival in early-stage non-small cell lung cancer. *Ann Thorac Surg, 60*(2), 466-472. doi:10.1016/0003-4975(95)00169-l

Nigg, E. A. (1995). Cyclin-dependent protein kinases: key regulators of the eukaryotic cell cycle. *Bioessays, 17*(6), 471-480. doi:10.1002/bies.950170603

Nishida, N., Yano, H., Nishida, T., Kamura, T., & Kojiro, M. (2006). Angiogenesis in cancer. *Vasc Health Risk Manag, 2*(3), 213-219. doi:10.2147/vhrm.2006.2.3.213

Nishizuka, Y. (1995). Protein kinase C and lipid signaling for sustained cellular responses. *FASEB J, 9*(7), 484-496.

Noguchi, M., Morikawa, A., Kawasaki, M., Matsuno, Y., Yamada, T., Hirohashi, S., Kondo, H., & Shimosato, Y. (1995). Small adenocarcinoma of the lung. Histologic characteristics and prognosis. *Cancer, 75*(12), 2844-2852. doi:10.1002/1097-0142(19950615)75:12<2844::aid-cncr2820751209>3.0.co;2-#

Norbury, C., & Nurse, P. (1992). ANIMAL CELL CYCLES AND THEIR CONTROL. *Annual Review of Biochemistry, 61*(1), 441-468. doi:10.1146/annurev.bi.61.070192.002301

Norbury, C. J., & Hickson, I. D. (2001). Cellular responses to DNA damage. *Annu Rev Pharmacol Toxicol, 41*, 367-401. doi:10.1146/annurev.pharmtox.41.1.367

O'Connor, L., Strasser, A., O'Reilly, L. A., Hausmann, G., Adams, J. M., Cory, S., & Huang, D. C. (1998). Bim: a novel member of the Bcl-2 family that promotes apoptosis. *EMBO J, 17*(2), 384-395. doi:10.1093/emboj/17.2.384

Oberst, A., Pop, C., Tremblay, A. G., Blais, V., Denault, J. B., Salvesen, G. S., & Green, D. R. (2010). Inducible dimerization and inducible cleavage reveal a requirement for both processes in caspase-8 activation. *J Biol Chem, 285*(22), 16632-16642. doi:10.1074/jbc.M109.095083

Ollauri-Ibanez, C., Nunez-Gomez, E., Egido-Turrion, C., Silva-Sousa, L., Diaz-Rodriguez, E., Rodriguez-Barbero, A., Lopez-Novoa, J. M., & Pericacho, M. (2020). Continuous endoglin (CD105) overexpression disrupts angiogenesis and facilitates tumor cell metastasis. *Angiogenesis, 23*(2), 231-247. doi:10.1007/s10456-019-09703-y

Olson, B., Li, Y., Lin, Y., Liu, E. T., & Patnaik, A. (2018). Mouse Models for Cancer Immunotherapy Research. *Cancer Discov, 8*(11), 1358-1365. doi:10.1158/2159-8290.CD-18-0044

Onn, A., Isobe, T., Itasaka, S., Wu, W., O'Reilly, M. S., Ki Hong, W., Fidler, I. J., & Herbst, R. S. (2003). Development of an orthotopic model to study the biology and therapy of primary human lung cancer in nude mice. *Clin Cancer Res, 9*(15), 5532-5539.

Orellana, E. A., & Kasinski, A. L. (2016). Sulforhodamine B (SRB) Assay in Cell Culture to Investigate Cell Proliferation. *Bio Protoc, 6*(21). doi:10.21769/BioProtoc.1984

Pacheco, J. M., Gao, D., Smith, D., Purcell, T., Hancock, M., Bunn, P., Robin, T., Liu, A., Karam, S., Gaspar, L., Kavanagh, B., Rusthoven, C., Aisner, D., Doebele, R., & Camidge, D. R. (2019). Natural History and Factors Associated with Overall Survival in Stage IV ALK-Rearranged Non-Small Cell Lung Cancer. *J Thorac Oncol, 14*(4), 691-700. doi:10.1016/j.jtho.2018.12.014

Padma, V. V. (2015). An overview of targeted cancer therapy. *Biomedicine (Taipei), 5*(4), 19. doi:10.7603/s40681-015-0019-4

Paez, J. G., Janne, P. A., Lee, J. C., Tracy, S., Greulich, H., Gabriel, S., Herman, P., Kaye, F. J., Lindeman, N., Boggon, T. J., Naoki, K., Sasaki, H., Fujii, Y., Eck, M. J., Sellers, W. R., Johnson, B. E., & Meyerson, M. (2004). EGFR mutations in lung cancer: correlation with clinical response to gefitinib therapy. *Science, 304*(5676), 1497-1500. doi:10.1126/science.1099314

Paik, P. K., Arcila, M. E., Fara, M., Sima, C. S., Miller, V. A., Kris, M. G., Ladanyi, M., & Riely, G. J. (2011). Clinical characteristics of patients with lung adenocarcinomas harboring BRAF mutations. *J Clin Oncol, 29*(15), 2046-2051. doi:10.1200/JCO.2010.33.1280

Palmer, R. H., Vernersson, E., Grabbe, C., & Hallberg, B. (2009). Anaplastic lymphoma kinase: signalling in development and disease. *Biochemical Journal, 420*(3), 345-361.

Pao, W., & Girard, N. (2011). New driver mutations in non-small-cell lung cancer. *Lancet Oncol, 12*(2), 175-180. doi:10.1016/S1470-2045(10)70087-5

Papadimitrakopoulou, V. (2012). Development of PI3K/AKT/mTOR pathway inhibitors and their application in personalized therapy for non-small-cell lung cancer. *J Thorac Oncol, 7*(8), 1315-1326. doi:10.1097/JTO.0b013e31825493eb

Park, H. S., Lee, J. K., Kim, D. W., Kulig, K., Kim, T. M., Lee, S. H., Jeon, Y. K., Chung, D. H., & Heo, D. S. (2012). Immunohistochemical screening for anaplastic lymphoma kinase (ALK) rearrangement in advanced non-small cell lung cancer patients. *Lung Cancer, 77*(2), 288-292. doi:10.1016/j.lungcan.2012.03.004

Park, K. S., Liang, M. C., Raiser, D. M., Zamponi, R., Roach, R. R., Curtis, S. J., Walton, Z., Schaffer, B. E., Roake, C. M., Zmoos, A. F., Kriegel, C., Wong, K. K., Sage, J., & Kim, C. F. (2011). Characterization of the cell of origin for small cell lung cancer. *Cell Cycle, 10*(16), 2806-2815. doi:10.4161/cc.10.16.17012

Patz, E. F., Jr. (2000). Imaging bronchogenic carcinoma. *Chest, 117*(4 Suppl 1), 90S-95S. doi:10.1378/chest.117.4_suppl_1.90s

Peled, N., Palmer, G., Hirsch, F. R., Wynes, M. W., Ilouze, M., Varella-Garcia, M., Soussan-Gutman, L., Otto, G. A., Stephens, P. J., Ross, J. S., Cronin, M. T., Lipson, D., & Miller, V. A. (2012). Next-generation sequencing identifies and immunohistochemistry confirms a novel crizotinib-sensitive ALK rearrangement in a patient with metastatic non-small-cell lung cancer. *J Thorac Oncol, 7*(9), e14-16. doi:10.1097/JTO.0b013e3182614ab5

Perner, S., Wagner, P. L., Demichelis, F., Mehra, R., Lafargue, C. J., Moss, B. J., Arbogast, S., Soltermann, A., Weder, W., Giordano, T. J., Beer, D. G., Rickman, D. S., Chinnaiyan, A. M., Moch, H., & Rubin, M. A. (2008). EML4-ALK fusion lung cancer: a rare acquired event. *Neoplasia, 10*(3), 298-302. doi:10.1593/neo.07878

Peters, S., Camidge, D. R., Shaw, A. T., Gadgeel, S., Ahn, J. S., Kim, D. W., Ou, S. H. I., Perol, M., Dziadziuszko, R., Rosell, R., Zeaiter, A., Mitry, E., Golding, S., Balas, B., Noe, J., Morcos, P. N., & Mok, T. (2017). Alectinib versus crizotinib in untreated ALK-positive non-small-cell lung cancer. *New England Journal of Medicine, 377*(9), 829-838. doi:http://dx.doi.org/10.1056/NEJMoa1704795

Pfeffer, C. M., & Singh, A. T. K. (2018). Apoptosis: A Target for Anticancer Therapy. *Int J Mol Sci, 19*(2). doi:10.3390/ijms19020448

Pfizer Inc. (2012). XALKORI® (crizotinib) capsules, for oral use Initial U.S. Approval: 2011. Retrieved from https://www.accessdata.fda.gov/drugsatfda_docs/label/2012/202570s002lbl.pdf

Pfizer Inc. (2019). XALKORI® (crizotinib) capsules, for oral use Initial U.S. Approval: 2011. Retrieved from http://labeling.pfizer.com/showlabeling.aspx?id=676

Pirker, R., & Filipits, M. (2019). From crizotinib to lorlatinib: continuous improvement in precision treatment of ALK-positive non-small cell lung cancer. *ESMO Open, 4*(5), e000548. doi:10.1136/esmoopen-2019-000548

Polgar, D., Leisser, C., Maier, S., Strasser, S., Ruger, B., Dettke, M., Khorchide, M., Simonitsch, I., Cerni, C., & Krupitza, G. (2005). Truncated ALK derived from chromosomal translocation t(2;5)(p23;q35) binds to the SH3 domain of p85-PI3K. *Mutat Res, 570*(1), 9-15. doi:10.1016/j.mrfmmm.2004.09.011

Pollmann, M., Parwaresch, R., Adam-Klages, S., Kruse, M. L., Buck, F., & Heidebrecht, H. J. (2006). Human EML4, a novel member of the EMAP family, is essential for microtubule formation. *Exp Cell Res, 312*(17), 3241-3251. doi:10.1016/j.yexcr.2006.06.035

Porta, C., Paglino, C., & Mosca, A. (2014). Targeting PI3K/Akt/mTOR Signaling in Cancer. *Front Oncol, 4*, 64. doi:10.3389/fonc.2014.00064

Rashid, O. M., Nagahashi, M., Ramachandran, S., Dumur, C. I., Schaum, J. C., Yamada, A., Aoyagi, T., Milstien, S., Spiegel, S., & Takabe, K. (2013). Is tail vein injection a relevant breast cancer lung metastasis model? *J Thorac Dis, 5*(4), 385-392. doi:10.3978/j.issn.2072-1439.2013.06.17

Rawlings, J. S., Rosler, K. M., & Harrison, D. A. (2004). The JAK/STAT signaling pathway. *J Cell Sci, 117*(Pt 8), 1281-1283. doi:10.1242/jcs.00963

Recondo, G., Mezquita, L., Facchinetti, F., Planchard, D., Gazzah, A., Bigot, L., Rizvi, A. Z., Frias, R. L., Thiery, J. P., Scoazec, J. Y., Sourisseau, T., Howarth, K., Deas, O., Samofalova, D., Galissant, J., Tesson, P., Braye, F., Naltet, C., Lavaud, P., Mahjoubi, L., Abou Lovergne, A., Vassal, G., Bahleda, R., Hollebecque, A., Nicotra, C., Ngo-Camus, M., Michiels, S., Lacroix, L., Richon, C., Auger, N., De Baere, T., Tselikas, L., Solary, E., Angevin, E., Eggermont, A. M., Andre, F., Massard, C., Olaussen, K. A., Soria, J. C., Besse, B., & Friboulet, L. (2020). Diverse Resistance Mechanisms to the Third-Generation ALK Inhibitor Lorlatinib in ALK-Rearranged Lung Cancer. *Clin Cancer Res, 26*(1), 242-255. doi:10.1158/1078-0432.CCR-19-1104

Reiner, D. J., Ailion, M., Thomas, J. H., & Meyer, B. J. (2008). C. elegans anaplastic lymphoma kinase ortholog SCD-2 controls dauer formation by modulating TGF-beta signaling. *Curr Biol, 18*(15), 1101-1109. doi:10.1016/j.cub.2008.06.060

Reshetnyak, A. V., Murray, P. B., Shi, X., Mo, E. S., Mohanty, J., Tome, F., Bai, H., Gunel, M., Lax, I., & Schlessinger, J. (2015). Augmentor alpha and beta (FAM150) are ligands of the receptor tyrosine kinases ALK and LTK: Hierarchy and specificity of ligand-receptor interactions. *Proc Natl Acad Sci U S A, 112*(52), 15862-15867. doi:10.1073/pnas.1520099112

Rice, K. D., Aay, N., Anand, N. K., Blazey, C. M., Bowles, O. J., Bussenius, J., Costanzo, S., Curtis, J. K., Defina, S. C., Dubenko, L., Engst, S., Joshi, A. A., Kennedy, A. R., Kim, A. I., Koltun, E. S., Lougheed, J. C., Manalo, J. C., Martini, J. F., Nuss, J. M., Peto, C. J., Tsang, T. H., Yu, P., & Johnston, S. (2012). Novel Carboxamide-Based Allosteric MEK Inhibitors: Discovery and Optimization

Efforts toward XL518 (GDC-0973). *ACS Med Chem Lett, 3*(5), 416-421. doi:10.1021/ml300049d

Richmond, A., & Su, Y. (2008). Mouse xenograft models vs GEM models for human cancer therapeutics. *Dis Model Mech, 1*(2-3), 78-82. doi:10.1242/dmm.000976

Riedl, S. J., & Salvesen, G. S. (2007). The apoptosome: signalling platform of cell death. *Nat Rev Mol Cell Biol, 8*(5), 405-413. doi:10.1038/nrm2153

Riely, G. J., Kris, M. G., Rosenbaum, D., Marks, J., Li, A., Chitale, D. A., Nafa, K., Riedel, E. R., Hsu, M., Pao, W., Miller, V. A., & Ladanyi, M. (2008). Frequency and distinctive spectrum of KRAS mutations in never smokers with lung adenocarcinoma. *Clin Cancer Res, 14*(18), 5731-5734. doi:10.1158/1078-0432.CCR-08-0646

Riera, L., Lasorsa, E., Ambrogio, C., Surrenti, N., Voena, C., & Chiarle, R. (2010). Involvement of Grb2 adaptor protein in nucleophosmin-anaplastic lymphoma kinase (NPM-ALK)-mediated signaling and anaplastic large cell lymphoma growth. *J Biol Chem, 285*(34), 26441-26450. doi:10.1074/jbc.M110.116327

Rikova, K., Guo, A., Zeng, Q., Possemato, A., Yu, J., Haack, H., Nardone, J., Lee, K., Reeves, C., Li, Y., Hu, Y., Tan, Z., Stokes, M., Sullivan, L., Mitchell, J., Wetzel, R., Macneill, J., Ren, J. M., Yuan, J., Bakalarski, C. E., Villen, J., Kornhauser, J. M., Smith, B., Li, D., Zhou, X., Gygi, S. P., Gu, T. L., Polakiewicz, R. D., Rush, J., & Comb, M. J. (2007). Global survey of phosphotyrosine signaling identifies oncogenic kinases in lung cancer. *Cell, 131*(6), 1190-1203. doi:10.1016/j.cell.2007.11.025

Robert, C., Karaszewska, B., Schachter, J., Rutkowski, P., Mackiewicz, A., Stroiakovski, D., Lichinitser, M., Dummer, R., Grange, F., Mortier, L., Chiarion-Sileni, V., Drucis, K., Krajsova, I., Hauschild, A., Lorigan, P., Wolter, P., Long, G. V., Flaherty, K., Nathan, P., Ribas, A., Martin, A. M., Sun, P., Crist, W., Legos, J., Rubin, S. D., Little, S. M., & Schadendorf, D. (2015). Improved overall survival in melanoma with combined dabrafenib and trametinib. *N Engl J Med, 372*(1), 30-39. doi:10.1056/NEJMoa1412690

Rosen, L. S., LoRusso, P., Ma, W. W., Goldman, J. W., Weise, A., Colevas, A. D., Adjei, A., Yazji, S., Shen, A., Johnston, S., Hsieh, H. J., Chan, I. T., & Sikic, B. I. (2016). A first-in-human phase I study to evaluate the MEK1/2 inhibitor, cobimetinib, administered daily in patients with advanced solid tumors. *Invest New Drugs, 34*(5), 604-613. doi:10.1007/s10637-016-0374-3

Roskoski, R. (2013). Anaplastic lymphoma kinase (ALK): Structure, oncogenic activation, and pharmacological inhibition. *Pharmacological Research, 68*(1), 68-94. doi:10.1016/j.phrs.2012.11.007

Rossing, H. H., Grauslund, M., Urbanska, E. M., Melchior, L. C., Rask, C. K., Costa, J. C., Skov, B. G., Sørensen, J. B., & Santoni-Rugiu, E. (2013). Concomitant occurrence of EGFR (epidermal growth factor receptor) and KRAS (V-Ki-ras2 Kirsten rat sarcoma viral oncogene homolog) mutations in an ALK (anaplastic lymphoma kinase)-positive lung adenocarcinoma patient with acquired resistance to crizotinib: a case report. *BMC research notes, 6*(1), 489.

Roux, P. P., & Blenis, J. (2004). ERK and p38 MAPK-activated protein kinases: a family of protein kinases with diverse biological functions. *Microbiol Mol Biol Rev, 68*(2), 320-344. doi:10.1128/MMBR.68.2.320-344.2004

Rubin, S. A. (1991). Lung cancer: past, present, and future. *J Thorac Imaging, 7*(1), 1-8.

Ruggeri, B. A., Camp, F., & Miknyoczki, S. (2014). Animal models of disease: pre-clinical animal models of cancer and their applications and utility in drug discovery. *Biochem Pharmacol, 87*(1), 150-161. doi:10.1016/j.bcp.2013.06.020

Sabir, S. R., Yeoh, S., Jackson, G., & Bayliss, R. (2017). EML4-ALK Variants: Biological and Molecular Properties, and the Implications for Patients. *Cancers (Basel), 9*(9). doi:10.3390/cancers9090118

Sahnane, N., Frattini, M., Bernasconi, B., Zappa, F., Schiavone, G., Wannesson, L., Antonelli, P., Balzarini, P., Sessa, F., Mazzucchelli, L., Tibiletti, M. G., & Martin, V. (2016). EGFR and KRAS Mutations in ALK-Positive Lung Adenocarcinomas: Biological and Clinical Effect. *Clinical Lung Cancer, 17*(1), 56-61. doi:http://dx.doi.org/10.1016/j.cllc.2015.08.001

Saka, W. O., Pacey, S., Blackhall, F. H., Garcia-Corbacho, J., Fusi, A., Karydis, I., Hategan, M., Laviste, G., Halford, S. E. R., Foxton, C., McLeod, R., Wan, S., & Talbot, D. C. (2015). A phase I dose escalation study of the tolerability of the oral VEGFR and EGFR inhibitor vandetanib (V) in combination with the oral MEK inhibitor selumetinib (S) in solid tumors. *Journal of Clinical Oncology, 33*(15_suppl), 2583-2583. doi:10.1200/jco.2015.33.15_suppl.2583

Sakamoto, H., Tsukaguchi, T., Hiroshima, S., Kodama, T., Kobayashi, T., Fukami, T. A., Oikawa, N., Tsukuda, T., Ishii, N., & Aoki, Y. (2011). CH5424802, a Selective ALK Inhibitor Capable of Blocking the Resistant Gatekeeper Mutant. *Cancer Cell, 19*(5), 679-690. doi:10.1016/j.ccr.2011.04.004

Sale, M. J., & Cook, S. J. (2013). The BH3 mimetic ABT-263 synergizes with the MEK1/2 inhibitor selumetinib/AZD6244 to promote BIM-dependent tumour cell death and inhibit acquired resistance. *Biochem J, 450*(2), 285-294. doi:10.1042/BJ20121212

Sanchez-Cespedes, M., Parrella, P., Esteller, M., Nomoto, S., Trink, B., Engles, J. M., Westra, W. H., Herman, J. G., & Sidransky, D. (2002). Inactivation of LKB1/STK11 is a common event in adenocarcinomas of the lung. *Cancer Res, 62*(13), 3659-3662.

Sanders, B. M., Jay, M., Draper, G. J., & Roberts, E. M. (1989). Non-ocular cancer in relatives of retinoblastoma patients. *British Journal of Cancer, 60*, 358-365. doi:10.1007/BF00206747

Sanders, H. R., Li, H. R., Bruey, J. M., Scheerle, J. A., Meloni-Ehrig, A. M., Kelly, J. C., Novick, C., & Albitar, M. (2011). Exon scanning by reverse transcriptase-polymerase chain reaction for detection of known and novel EML4-ALK fusion variants in non-small cell lung cancer. *Cancer Genet, 204*(1), 45-52. doi:10.1016/j.cancergencyto.2010.08.024

Saputra, E. C., Huang, L., Chen, Y., & Tucker-Kellogg, L. (2018). Combination Therapy and the Evolution of Resistance: The Theoretical Merits of Synergism and Antagonism in Cancer. *Cancer Res, 78*(9), 2419-2431. doi:10.1158/0008-5472.CAN-17-1201

Sasaki, T., Koivunen, J., Ogino, A., Yanagita, M., Nikiforow, S., Zheng, W., Lathan, C., Marcoux, J. P., Du, J., Okuda, K., Capelletti, M., Shimamura, T., Ercan, D., Stumpfova, M., Xiao, Y., Weremowicz, S., Butaney, M., Heon, S., Wilner, K., Christensen, J. G., Eck, M. J., Wong, K. K., Lindeman, N., Gray, N. S., Rodig, S. J., & Jänne, P. A. (2011). A novel ALK secondary mutation and EGFR signaling cause resistance to ALK kinase inhibitors. *Cancer Research, 71*(18), 6051-6060. doi:10.1158/0008-5472.CAN-11-1340

Sasaki, T., Rodig, S. J., Chirieac, L. R., & Janne, P. A. (2010). The biology and treatment of EML4-ALK non-small cell lung cancer. *Eur J Cancer, 46*(10), 1773-1780. doi:10.1016/j.ejca.2010.04.002

Schafer, K. A. (1998). The cell cycle: a review. *Vet Pathol, 35*(6), 461-478. doi:10.1177/030098589803500601

Schiller, J. H., Harrington, D., Belani, C. P., Langer, C., Sandler, A., Krook, J., Zhu, J., Johnson, D. H., & Eastern Cooperative Oncology, G. (2002). Comparison of four chemotherapy regimens for advanced non-small-cell lung cancer. *N Engl J Med, 346*(2), 92-98. doi:10.1056/NEJMoa011954

Schirrmacher, V. (2019). From chemotherapy to biological therapy: A review of novel concepts to reduce the side effects of systemic cancer treatment (Review). *Int J Oncol, 54*(2), 407-419. doi:10.3892/ijo.2018.4661

Schlessinger, J. (2000). Cell Signaling by Receptor Tyrosine Kinases. *October, 103*(2), 211-225. doi:10.1016/j.cell.2010.06.011

Scripture, C. D., & Figg, W. D. (2006). Drug interactions in cancer therapy. *Nat Rev Cancer, 6*(7), 546-558. doi:10.1038/nrc1887

Seger, R., & Krebs, E. G. (1995). The MAPK signaling cascade. *FASEB J, 9*(9), 726-735.

Shaw, A. T., & Engelman, J. A. (2013). ALK in lung cancer: Past, present, and future. *Journal of Clinical Oncology, 31*(8), 1105-1111. doi:10.1200/JCO.2012.44.5353

Shaw, A. T., & Engelman, J. A. (2014). Ceritinib in ALK-rearranged non-small-cell lung cancer. *N Engl J Med, 370*(26), 2537-2539. doi:10.1056/NEJMc1404894

Shaw, A. T., Felip, E., Bauer, T. M., Besse, B., Navarro, A., Postel-Vinay, S., Gainor, J. F., Johnson, M., Dietrich, J., James, L. P., Clancy, J. S., Chen, J., Martini, J. F., Abbattista, A., & Solomon, B. J. (2017). Lorlatinib in non-small-cell lung cancer with ALK or ROS1 rearrangement: an international, multicentre, open-label, single-arm first-in-man phase 1 trial. *Lancet Oncol, 18*(12), 1590-1599. doi:10.1016/S1470-2045(17)30680-0

Shaw, A. T., Friboulet, L., Leshchiner, I., Gainor, J. F., Bergqvist, S., Brooun, A., Burke, B. J., Deng, Y. L., Liu, W., Dardaei, L., Frias, R. L., Schultz, K. R., Logan, J., James, L. P., Smeal, T., Timofeevski, S., Katayama, R., Iafrate, A. J., Le, L., McTigue, M., Getz, G., Johnson, T. W., & Engelman, J. A. (2016). Resensitization to crizotinib by the lorlatinib ALK resistance mutation L1198F. *New England Journal of Medicine, 374*(1), 54-61. doi:http://dx.doi.org/10.1056/NEJMoa1508887

Shaw, A. T., Gandhi, L., Gadgeel, S., Riely, G. J., Cetnar, J., West, H., Camidge, D. R., Socinski, M. A., Chiappori, A., Mekhail, T., Chao, B. H., Borghaei, H., Gold, K. A., Zeaiter, A., Bordogna, W., Balas, B., Puig, O., Henschel, V., & Ou, S. H. I. (2016). Alectinib in ALK-positive, crizotinib-resistant, non-small-cell lung cancer: A single-group, multicentre, phase 2 trial. *The Lancet Oncology, 17*(2), 234-242. doi:http://dx.doi.org/10.1016/S1470-2045%2815%2900488-X

Shaw, A. T., Kim, D.-W., Nakagawa, K., Seto, T., Crinó, L., Ahn, M.-J., De Pas, T., Besse, B., Solomon, B. J., & Blackhall, F. (2013). Crizotinib versus chemotherapy in advanced ALK-positive lung cancer. *New England Journal of Medicine, 368*(25), 2385-2394.

Shaw, A. T., Kim, T. M., Crino, L., Gridelli, C., Kiura, K., Liu, G., Novello, S., Bearz, A., Gautschi, O., Mok, T., Nishio, M., Scagliotti, G., Spigel, D. R., Deudon, S., Zheng, C., Pantano, S., Urban, P., Massacesi, C., Viraswami-Appanna, K., & Felip, E. (2017). Ceritinib versus chemotherapy in patients with ALK-rearranged non-small-cell lung cancer previously given chemotherapy and crizotinib (ASCEND-5): a randomised, controlled, open-label, phase 3 trial. *Lancet Oncol, 18*(7), 874-886. doi:10.1016/S1470-2045(17)30339-X

Shaw, A. T., & Solomon, B. (2011). Targeting anaplastic lymphoma kinase in lung cancer. *Clinical Cancer Research, 17*(8), 2081-2086. doi:10.1158/1078-0432.CCR-10-1591

Shaw, A. T., Solomon, B. J., Besse, B., Bauer, T. M., Lin, C. C., Soo, R. A., Riely, G. J., Ou, S. I., Clancy, J. S., Li, S., Abbattista, A., Thurm, H., Satouchi, M., Camidge, D. R., Kao, S., Chiari, R., Gadgeel, S. M., Felip, E., & Martini, J. F. (2019). ALK Resistance Mutations and Efficacy of Lorlatinib in Advanced Anaplastic Lymphoma Kinase-Positive Non-Small-Cell Lung Cancer. *J Clin Oncol, 37*(16), 1370-1379. doi:10.1200/JCO.18.02236

Shaw, A. T., Yeap, B. Y., Mino-Kenudson, M., Digumarthy, S. R., Costa, D. B., Heist, R. S., Solomon, B., Stubbs, H., Admane, S., McDermott, U., Settleman, J., Kobayashi, S., Mark, E. J., Rodig, S. J., Chirieac, L. R., Kwak, E. L., Lynch, T. J., & Iafrate, A. J. (2009). Clinical features and outcome of patients with non-small-cell lung cancer who harbor EML4-ALK. *Journal of Clinical Oncology, 27*(26), 4247-4253. doi:10.1200/JCO.2009.22.6993

Shaw, A. T., Yeap, B. Y., Solomon, B. J., Riely, G. J., Gainor, J., Engelman, J. A., Shapiro, G. I., Costa, D. B., Ou, S. H., Butaney, M., Salgia, R., Maki, R. G., Varella-Garcia, M., Doebele, R. C., Bang, Y. J., Kulig, K., Selaru, P., Tang, Y., Wilner, K. D., Kwak, E. L., Clark, J. W., Iafrate, A. J., & Camidge, D. R. (2011). Effect of crizotinib on overall survival in patients with advanced non-small-cell lung cancer harbouring ALK gene rearrangement: a retrospective analysis. *Lancet Oncol, 12*(11), 1004-1012. doi:10.1016/S1470-2045(11)70232-7

Shi, Y. (2002). Mechanisms of caspase activation and inhibition during apoptosis. *Mol Cell, 9*(3), 459-470. doi:10.1016/s1097-2765(02)00482-3

Shweiki, D., Itin, A., Soffer, D., & Keshet, E. (1992). Vascular endothelial growth factor induced by hypoxia may mediate hypoxia-initiated angiogenesis. *Nature, 359*(6398), 843-845. doi:10.1038/359843a0

Siegel, R. L., Miller, K. D., & Jemal, A. (2019). Cancer statistics, 2019. *CA Cancer J Clin, 69*(1), 7-34. doi:10.3322/caac.21551

Singh, A., Misra, V., Thimmulappa, R. K., Lee, H., Ames, S., Hoque, M. O., Herman, J. G., Baylin, S. B., Sidransky, D., Gabrielson, E., Brock, M. V., & Biswal, S. (2006). Dysfunctional KEAP1-NRF2 interaction in non-small-cell lung cancer. *PLoS Med, 3*(10), e420. doi:10.1371/journal.pmed.0030420

Sionov, R. V., Vlahopoulos, S. A., & Granot, Z. (2015). Regulation of Bim in Health and Disease. *Oncotarget, 6*(27), 23058-23134. doi:10.18632/oncotarget.5492

Skehan, P., Storeng, R., Scudiero, D., Monks, A., McMahon, J., Vistica, D., Warren, J. T., Bokesch, H., Kenney, S., & Boyd, M. R. (1990). New colorimetric cytotoxicity assay for anticancer-drug screening. *J Natl Cancer Inst, 82*(13), 1107-1112. doi:10.1093/jnci/82.13.1107

Slupianek, A., Nieborowska-Skorska, M., Hoser, G., Morrione, A., Majewski, M., Xue, L., Morris, S. W., Wasik, M. A., & Skorski, T. (2001). Role of phosphatidylinositol 3-kinase-Akt pathway in nucleophosmin/anaplastic lymphoma kinase-mediated lymphomagenesis. *Cancer Res, 61*(5), 2194-2199.

Smith, P. K., Krohn, R. I., Hermanson, G. T., Mallia, A. K., Gartner, F. H., Provenzano, M. D., Fujimoto, E. K., Goeke, N. M., Olson, B. J., & Klenk, D. C. (1985). Measurement of protein using bicinchoninic acid. *Anal Biochem, 150*(1), 76-85. doi:10.1016/0003-2697(85)90442-7

Smulson, M. E., Simbulan-Rosenthal, C. M., Boulares, A. H., Yakovlev, A., Stoica, B., Iyer, S., Luo, R., Haddad, B., Wang, Z. Q., Pang, T., Jung, M., Dritschilo, A., & Rosenthal, D. S. (2000). Roles of poly(ADP-ribosyl)ation and PARP in apoptosis, DNA repair, genomic stability and functions of p53 and E2F-1. *Adv Enzyme Regul, 40*, 183-215. doi:10.1016/s0065-2571(99)00024-2

Soda, M., Choi, Y. L., Enomoto, M., Takada, S., Yamashita, Y., Ishikawa, S., Fujiwara, S.-i., Watanabe, H., Kurashina, K., Hatanaka, H., Bando, M., Ohno, S., Ishikawa, Y., Aburatani, H., Niki, T., Sohara, Y., Sugiyama, Y., & Mano, H. (2007). Identification of the transforming EML4–ALK fusion gene in non-small-cell lung cancer. *Nature, 448*(7153), 561-566. doi:10.1038/nature05945

Soda, M., Isobe, K., Inoue, A., Maemondo, M., Oizumi, S., Fujita, Y., Gemma, A., Yamashita, Y., Ueno, T., Takeuchi, K., Choi, Y. L., Miyazawa, H., Tanaka, T., Hagiwara, K., Mano, H., North-East Japan Study, G., & Group, A. L. K. L. C. S. (2012). A prospective PCR-based screening for the EML4-ALK oncogene in non-small cell lung cancer. *Clin Cancer Res, 18*(20), 5682-5689. doi:10.1158/1078-0432.CCR-11-2947

Soda, M., Takada, S., Takeuchi, K., Choi, Y. L., Enomoto, M., Ueno, T., Haruta, H., Hamada, T., Yamashita, Y., & Ishikawa, Y. (2008). A mouse model for EML4-ALK-positive lung cancer. *Proceedings of the National Academy of Sciences, 105*(50), 19893-19897.

Solary, E., Dubrez, L., & Eymin, B. (1996). The role of apoptosis in the pathogenesis and treatment of diseases. *Eur Respir J, 9*(6), 1293-1305. doi:10.1183/09031936.96.09061293

Solomon, B. (2020, Jan 30, 2020). Anaplastic lymphoma kinase (ALK) fusion oncogene positive non-small cell lung cancer. Retrieved from https://www.uptodate.com/contents/anaplastic-lymphoma-kinase-alk-fusion-oncogene-positive-non-small-cell-lung-cancer

Solomon, B., Varella-Garcia, M., & Camidge, D. R. (2009). ALK gene rearrangements: a new therapeutic target in a molecularly defined subset of non-small cell lung cancer. *Journal of Thoracic Oncology, 4*(12), 1450-1454.

Solomon, B., Wilner, K. D., & Shaw, A. T. (2014). Current status of targeted therapy for anaplastic lymphoma kinase-rearranged non-small cell lung cancer. *Clin Pharmacol Ther, 95*(1), 15-23. doi:10.1038/clpt.2013.200

Solomon, B. J., Besse, B., Bauer, T. M., Felip, E., Soo, R. A., Camidge, D. R., Chiari, R., Bearz, A., Lin, C. C., Gadgeel, S. M., Riely, G. J., Tan, E. H., Seto, T., James, L. P., Clancy, J. S., Abbattista, A., Martini, J. F., Chen, J., Peltz, G., Thurm, H., Ou, S. I., & Shaw, A. T. (2018). Lorlatinib in patients with ALK-positive non-small-cell lung cancer: results from a global phase 2 study. *Lancet Oncol, 19*(12), 1654-1667. doi:10.1016/S1470-2045(18)30649-1

Solomon, B. J., Mok, T., Kim, D.-W., Wu, Y.-L., Nakagawa, K., Mekhail, T., Felip, E., Cappuzzo, F., Paolini, J., Usari, T., Iyer, S., Reisman, A., Wilner, K. D., Tursi, J., & Blackhall, F. (2014). First-Line Crizotinib versus Chemotherapy in ALK -Positive Lung Cancer. *New England Journal of Medicine, 371*(23), 2167-2177. doi:10.1056/NEJMoa1408440

Soria, J. C., Tan, D. S. W., Chiari, R., Wu, Y. L., Paz-Ares, L., Wolf, J., Geater, S. L., Orlov, S., Cortinovis, D., Yu, C. J., Hochmair, M., Cortot, A. B., Tsai, C. M., Moro-Sibilot, D., Campelo, R. G., McCulloch, T., Sen, P., Dugan, M., Pantano, S., Branle, F., Massacesi, C., & de Castro, G., Jr. (2017). First-line ceritinib versus platinum-based chemotherapy in advanced ALK-rearranged non-small-cell lung cancer (ASCEND-4): a randomised, open-label, phase 3 study. *Lancet, 389*(10072), 917-929. doi:10.1016/S0140-6736(17)30123-X

Spitz, M. R., Wei, Q., Dong, Q., Amos, C. I., & Wu, X. (2003). Genetic susceptibility to lung cancer: The role of DNA damage and repair. *Cancer Epidemiology Biomarkers and Prevention, 12*(8), 689-698.

Staber, P. B., Vesely, P., Haq, N., Ott, R. G., Funato, K., Bambach, I., Fuchs, C., Schauer, S., Linkesch, W., Hrzenjak, A., Dirks, W. G., Sexl, V., Bergler, H., Kadin, M. E., Sternberg, D. W., Kenner, L., & Hoefler, G. (2007). The oncoprotein NPM-ALK of anaplastic large-cell lymphoma induces JUNB transcription via ERK1/2 and JunB translation via mTOR signaling. *Blood, 110*(9), 3374-3383. doi:10.1182/blood-2007-02-071258

Steuer, C. E., & Ramalingam, S. S. (2014). ALK-positive non-small cell lung cancer: Mechanisms of resistance and emerging treatment options. *Cancer, 120*(16), 2392-2402. doi:10.1002/cncr.28597

Stoica, G. E., Kuo, A., Aigner, A., Sunitha, I., Souttou, B., Malerczyk, C., Caughey, D. J., Wen, D., Karavanov, A., Riegel, A. T., & Wellstein, A. (2001). Identification of anaplastic lymphoma kinase as a receptor for the growth factor pleiotrophin. *J Biol Chem, 276*(20), 16772-16779. doi:10.1074/jbc.M010660200

Stoica, G. E., Kuo, A., Powers, C., Bowden, E. T., Sale, E. B., Riegel, A. T., & Wellstein, A. (2002). Midkine binds to anaplastic lymphoma kinase (ALK) and acts as a growth factor for different cell types. *J Biol Chem, 277*(39), 35990-35998. doi:10.1074/jbc.M205749200

Strasser, A., Puthalakath, H., Bouillet, P., Huang, D. C., O'Connor, L., O'Reilly, L. A., Cullen, L., Cory, S., & Adams, J. M. (2000). The role of bim, a proapoptotic BH3-only member of the Bcl-2 family in cell-death control. *Ann N Y Acad Sci, 917*, 541-548. doi:10.1111/j.1749-6632.2000.tb05419.x

Sullivan, I., & Planchard, D. (2015). ALK inhibitors in non-small cell lung cancer: the latest evidence and developments. *Therapeutic Advances in Medical Oncology*, 32-47. doi:10.1177/1758834015617355

Sun, J. M., Choi, Y. L., Won, J. K., Hirsch, F. R., Ahn, J. S., Ahn, M. J., & Park, K. (2012). A dramatic response to crizotinib in a non-small-cell lung cancer patient with IHC-positive and FISH-negative ALK. *J Thorac Oncol, 7*(12), e36-e38. doi:10.1097/JTO.0b013e318274694e

Sun S, S. J. H. G. A. F. (2007). Lung cancer in never smokers--a different disease. [Nat Rev Cancer. 2007] - PubMed Result. *Nat Rev Cancer., 7*(10), 778-790.

Sun, Y., Ren, Y., Fang, Z., Li, C., Fang, R., Gao, B., Han, X., Tian, W., Pao, W., Chen, H., & Ji, H. (2010). Lung adenocarcinoma from East Asian never-smokers is a disease largely defined by targetable oncogenic mutant kinases. *J Clin Oncol, 28*(30), 4616-4620. doi:10.1200/JCO.2010.29.6038

Suzuki, Y., Imai, Y., Nakayama, H., Takahashi, K., Takio, K., & Takahashi, R. (2001). A serine protease, HtrA2, is released from the mitochondria and interacts with XIAP, inducing cell death. *Mol Cell, 8*(3), 613-621. doi:10.1016/s1097-2765(01)00341-0

Takahashi, O., Komaki, R., Smith, P. D., Jurgensmeier, J. M., Ryan, A., Bekele, B. N., Wistuba, II, Jacoby, J. J., Korshunova, M. V., Biernacka, A., Erez, B., Hosho, K., Herbst, R. S., & O'Reilly, M. S. (2012). Combined MEK and VEGFR inhibition in orthotopic human lung cancer models results in enhanced inhibition of tumor angiogenesis, growth, and metastasis. *Clin Cancer Res, 18*(6), 1641-1654. doi:10.1158/1078-0432.CCR-11-2324

Takahashi, T., Nau, M. M., Chiba, I., Birrer, M. J., Rosenberg, R. K., Vinocour, M., Levitt, M., Pass, H., Gazdar, A. F., & Minna, J. D. (1989). p53: a frequent target for genetic abnormalities in lung cancer. *Science, 246*(4929), 491-494. doi:10.1126/science.2554494

Takamochi, K., Ohmiya, H., Itoh, M., Mogushi, K., Saito, T., Hara, K., Mitani, K., Kogo, Y., Yamanaka, Y., Kawai, J., Hayashizaki, Y., Oh, S., Suzuki, K., & Kawaji, H.

(2016). Novel biomarkers that assist in accurate discrimination of squamous cell carcinoma from adenocarcinoma of the lung. *BMC Cancer, 16*(1), 760. doi:10.1186/s12885-016-2792-1

Takeuchi, K., Choi, Y. L., Soda, M., Inamura, K., Togashi, Y., Hatano, S., Enomoto, M., Takada, S., Yamashita, Y., Satoh, Y., Okumura, S., Nakagawa, K., Ishikawa, Y., & Mano, H. (2008). Multiplex reverse transcription-PCR screening for EML4-ALK fusion transcripts. *Clin Cancer Res, 14*(20), 6618-6624. doi:10.1158/1078-0432.CCR-08-1018

Takeuchi, K., Choi, Y. L., Togashi, Y., Soda, M., Hatano, S., Inamura, K., Takada, S., Ueno, T., Yamashita, Y., Satoh, Y., Okumura, S., Nakagawa, K., Ishikawa, Y., & Mano, H. (2009). KIF5B-ALK, a novel fusion oncokinase identified by an immunohistochemistry-based diagnostic system for ALK-positive lung cancer. *Clin Cancer Res, 15*(9), 3143-3149. doi:10.1158/1078-0432.CCR-08-3248

Takeuchi, K., Soda, M., Togashi, Y., Suzuki, R., Sakata, S., Hatano, S., Asaka, R., Hamanaka, W., Ninomiya, H., Uehara, H., Lim Choi, Y., Satoh, Y., Okumura, S., Nakagawa, K., Mano, H., & Ishikawa, Y. (2012). RET, ROS1 and ALK fusions in lung cancer. *Nat Med, 18*(3), 378-381. doi:10.1038/nm.2658

Tan, W., Wilner, K. D., Bang, Y., Kwak, E. L., Maki, R. G., Camidge, D. R., Solomon, B. J., Ou, S. I., Salgia, R., & Clark, J. W. (2010). Pharmacokinetics (PK) of PF-02341066, a dual ALK/MET inhibitor after multiple oral doses to advanced cancer patients. *Journal of Clinical Oncology, 28*, 2596.

Tang, Z., Wang, L., Tang, G., & Medeiros, L. J. (2019). Fluorescence in Situ Hybridization (FISH) for Detecting Anaplastic Lymphoma Kinase (ALK) Rearrangement in Lung Cancer: Clinically Relevant Technical Aspects. *Int J Mol Sci, 20*(16). doi:10.3390/ijms20163939

Tanizaki, J., Okamoto, I., Okabe, T., Sakai, K., Tanaka, K., Hayashi, H., Kaneda, H., Takezawa, K., Kuwata, K., Yamaguchi, H., Hatashita, E., Nishio, K., & Nakagawa, K. (2012). Activation of HER family signaling as a mechanism of acquired resistance to ALK inhibitors in EML4-ALK-positive non-small cell lung cancer. *Clinical Cancer Research, 18*(22), 6219-6226. doi:10.1158/1078-0432.CCR-12-0392

Tanizaki, J., Okamoto, I., Okamoto, K., Takezawa, K., Kuwata, K., Yamaguchi, H., & Nakagawa, K. (2011). MET tyrosine kinase inhibitor crizotinib (PF-02341066) shows differential antitumor effects in non-small cell lung cancer according to MET alterations. *Journal of Thoracic Oncology, 6*(10), 1624-1631.

Tanizaki, J., Okamoto, I., Takezawa, K., Sakai, K., Azuma, K., Kuwata, K., Yamaguchi, H., Hatashita, E., Nishio, K., Janne, P. A., & Nakagawa, K. (2012). Combined effect of ALK and MEK inhibitors in EML4-ALK-positive non-small-cell lung cancer cells. *Br J Cancer, 106*(4), 763-767. doi:10.1038/bjc.2011.586

Terada, Y., Inoshita, S., Nakashima, O., Kuwahara, M., Sasaki, S., & Marumo, F. (1999). Regulation of cyclin D1 expression and cell cycle progression by mitogen-activated protein kinase cascade. *Kidney Int, 56*(4), 1258-1261. doi:10.1046/j.1523-1755.1999.00704.x

To, K. F., Tong, J. H., Yeung, K. S., Lung, R. W., Law, P. P., Chau, S. L., Kang, W., Tong, C. Y., Chow, C., Chan, A. W., Leung, L. K., & Mok, T. S. (2013). Detection of ALK rearrangement by immunohistochemistry in lung adenocarcinoma and the identification of a novel EML4-ALK variant. *J Thorac Oncol, 8*(7), 883-891. doi:10.1097/JTO.0b013e3182904e22

Togashi, Y., Soda, M., Sakata, S., Sugawara, E., Hatano, S., Asaka, R., Nakajima, T., Mano, H., & Takeuchi, K. (2012). KLC1-ALK: a novel fusion in lung cancer

identified using a formalin-fixed paraffin-embedded tissue only. *PLoS ONE, 7*(2), e31323. doi:10.1371/journal.pone.0031323

Tonini, T., Rossi, F., & Claudio, P. P. (2003). Molecular basis of angiogenesis and cancer. *Oncogene, 22*(42), 6549-6556. doi:10.1038/sj.onc.1206816

Torii, S., Yamamoto, T., Tsuchiya, Y., & Nishida, E. (2006). ERK MAP kinase in G cell cycle progression and cancer. *Cancer Sci, 97*(8), 697-702. doi:10.1111/j.1349-7006.2006.00244.x

Toyokawa, G., Hirai, F., Inamasu, E., Yoshida, T., Nosaki, K., Takenaka, T., Yamaguchi, M., Seto, T., Takenoyama, M., & Ichinose, Y. (2014). Secondary mutations at I1171 in the ALK gene confer resistance to both Crizotinib and Alectinib. *J Thorac Oncol, 9*(12), e86-87. doi:10.1097/JTO.0000000000000358

Toyokawa, G., & Seto, T. (2014a). ALK inhibitors: what is the best way to treat patients with ALK+ non–small-cell lung cancer? *Clinical Lung Cancer, 15*(5), 313-319.

Toyokawa, G., & Seto, T. (2014b). Anaplastic lymphoma kinase rearrangement in lung Cancer: Its biological and clinical significance. *Respiratory Investigation, 52*(6), 330-338. doi:10.1016/j.resinv.2014.06.005

Travis, W. D., Brambilla, E., Nicholson, A. G., Yatabe, Y., Austin, J. H. M., Beasley, M. B., Chirieac, L. R., Dacic, S., Duhig, E., Flieder, D. B., Geisinger, K., Hirsch, F. R., Ishikawa, Y., Kerr, K. M., Noguchi, M., Pelosi, G., Powell, C. A., Tsao, M. S., Wistuba, I., & Panel, W. H. O. (2015). The 2015 World Health Organization Classification of Lung Tumors: Impact of Genetic, Clinical and Radiologic Advances Since the 2004 Classification. *J Thorac Oncol, 10*(9), 1243-1260. doi:10.1097/JTO.0000000000000630

Travis, W. D., Brambilla, E., & Riely, G. J. (2013). New pathologic classification of lung cancer: Relevance for clinical practice and clinical trials. *Journal of Clinical Oncology, 31*(8), 992-1001. doi:10.1200/JCO.2012.46.9270

Tzifi, F., Economopoulou, C., Gourgiotis, D., Ardavanis, A., Papageorgiou, S., & Scorilas, A. (2012). The Role of BCL2 Family of Apoptosis Regulator Proteins in Acute and Chronic Leukemias. *Adv Hematol, 2012*, 524308. doi:10.1155/2012/524308

U.S. Food and Drug Administration. (2017a). Alectinib approved for (ALK) positive metastatic non-small cell lung cancer (NSCLC). Retrieved from https://www.fda.gov/drugs/resources-information-approved-drugs/alectinib-approved-alk-positive-metastatic-non-small-cell-lung-cancer-nsclc

U.S. Food and Drug Administration. (2017b). Brigatinib. Retrieved from https://www.fda.gov/drugs/resources-information-approved-drugs/brigatinib

U.S. Food and Drug Administration. (2017c). FDA broadens ceritinib indication to previously untreated ALK-positive metastatic NSCLC. Retrieved from https://www.fda.gov/drugs/resources-information-approved-drugs/fda-broadens-ceritinib-indication-previously-untreated-alk-positive-metastatic-nsclc

U.S. Food and Drug Administration. (2017d). FDA grants regular approval to dabrafenib and trametinib combination for metastatic NSCLC with BRAF V600E mutation. Retrieved from https://www.fda.gov/drugs/resources-information-approved-drugs/fda-grants-regular-approval-dabrafenib-and-trametinib-combination-metastatic-nsclc-braf-v600e

U.S. Food and Drug Administration. (2018a). FDA approves encorafenib and binimetinib in combination for unresectable or metastatic melanoma with BRAF mutations. Retrieved from https://www.fda.gov/drugs/resources-information-approved-drugs/fda-approves-encorafenib-and-binimetinib-combination-unresectable-or-metastatic-melanoma-

braf#:~:text=On%20June%2027%2C%202018%2C%20the,by%20an%20FDA%2Dapproved%20test.

U.S. Food and Drug Administration. (2018b). FDA approves lorlatinib for second- or third-line treatment of ALK-positive metastatic NSCLC. Retrieved from https://www.fda.gov/drugs/fda-approves-lorlatinib-second-or-third-line-treatment-alk-positive-metastatic-nsclc

U.S. Food and Drug Administration. (2020a). FDA approves atezolizumab for BRAF V600 unresectable or metastatic melanoma. Retrieved from https://www.fda.gov/drugs/resources-information-approved-drugs/fda-approves-atezolizumab-braf-v600-unresectable-or-metastatic-melanoma

U.S. Food and Drug Administration. (2020b). Foundation One CDX. Retrieved from https://www.accessdata.fda.gov/cdrh_docs/pdf17/P170019a.pdf

Valentine, S. P., Le Nedelec, M. J., Menzies, A. R., Scandlyn, M. J., Goodin, M. G., & Rosengren, R. J. (2006). Curcumin modulates drug metabolizing enzymes in the female Swiss Webster mouse. *Life Sci, 78*(20), 2391-2398. doi:10.1016/j.lfs.2005.09.017

Vendrell, J. A., Taviaux, S., Beganton, B., Godreuil, S., Audran, P., Grand, D., Clermont, E., Serre, I., Szablewski, V., Coopman, P., Mazieres, J., Costes, V., Pujol, J. L., Brousset, P., Rouquette, I., & Solassol, J. (2017). Detection of known and novel ALK fusion transcripts in lung cancer patients using next-generation sequencing approaches. *Sci Rep, 7*(1), 12510. doi:10.1038/s41598-017-12679-8

Verhagen, A. M., Ekert, P. G., Pakusch, M., Silke, J., Connolly, L. M., Reid, G. E., Moritz, R. L., Simpson, R. J., & Vaux, D. L. (2000). Identification of DIABLO, a mammalian protein that promotes apoptosis by binding to and antagonizing IAP proteins. *Cell, 102*(1), 43-53. doi:10.1016/s0092-8674(00)00009-x

Vermeulen, K., Van Bockstaele, D. R., & Berneman, Z. N. (2003). The cell cycle: a review of regulation, deregulation and therapeutic targets in cancer. *Cell Prolif, 36*(3), 131-149. doi:10.1046/j.1365-2184.2003.00266.x

Viale, G., Regan, M. M., Mastropasqua, M. G., Maffini, F., Maiorano, E., Colleoni, M., Price, K. N., Golouh, R., Perin, T., Brown, R. W., Kovacs, A., Pillay, K., Ohlschlegel, C., Gusterson, B. A., Castiglione-Gertsch, M., Gelber, R. D., Goldhirsch, A., Coates, A. S., & International Breast Cancer Study, G. (2008). Predictive value of tumor Ki-67 expression in two randomized trials of adjuvant chemoendocrine therapy for node-negative breast cancer. *J Natl Cancer Inst, 100*(3), 207-212. doi:10.1093/jnci/djm289

Vichai, V., & Kirtikara, K. (2006). Sulforhodamine B colorimetric assay for cytotoxicity screening. *Nat Protoc, 1*(3), 1112-1116. doi:10.1038/nprot.2006.179

Vigneswaran, J., Tan, Y. H., Murgu, S. D., Won, B. M., Patton, K. A., Villaflor, V. M., Hoffman, P. C., Hensing, T., Hogarth, D. K., Malik, R., MacMahon, H., Mueller, J., Simon, C. A., Vigneswaran, W. T., Wigfield, C. H., Ferguson, M. K., Husain, A. N., Vokes, E. E., & Salgia, R. (2016). Comprehensive genetic testing identifies targetable genomic alterations in most patients with non-small cell lung cancer, specifically adenocarcinoma, single institute investigation. *Oncotarget, 7*(14), 18876-18886. doi:10.18632/oncotarget.7739

Villanueva, J., Yung, Y., Walker, J. L., & Assoian, R. K. (2007). ERK activity and G1 phase progression: identifying dispensable versus essential activities and primary versus secondary targets. *Mol Biol Cell, 18*(4), 1457-1463. doi:10.1091/mbc.e06-10-0908

Wajant, H. (2002). The Fas signaling pathway: more than a paradigm. *Science, 296*(5573), 1635-1636. doi:10.1126/science.1071553

Walczak, H., & Sprick, M. R. (2001). Biochemistry and function of the DISC. *Trends Biochem Sci, 26*(7), 452-453. doi:10.1016/s0968-0004(01)01895-3

Walters, S., Maringe, C., Coleman, M. P., Peake, M. D., Butler, J., Young, N., Bergstrom, S., Hanna, L., Jakobsen, E., Kolbeck, K., Sundstrom, S., Engholm, G., Gavin, A., Gjerstorff, M. L., Hatcher, J., Johannesen, T. B., Linklater, K. M., McGahan, C. E., Steward, J., Tracey, E., Turner, D., Richards, M. A., Rachet, B., & Group, I. M. W. (2013). Lung cancer survival and stage at diagnosis in Australia, Canada, Denmark, Norway, Sweden and the UK: a population-based study, 2004-2007. *Thorax, 68*(6), 551-564. doi:10.1136/thoraxjnl-2012-202297

Wang, D., Boerner, S. A., Winkler, J. D., & LoRusso, P. M. (2007). Clinical experience of MEK inhibitors in cancer therapy. *Biochim Biophys Acta, 1773*(8), 1248-1255. doi:10.1016/j.bbamcr.2006.11.009

Wang, H. Y., Ross, H. M., Ng, B., & Burt, M. E. (1997). Establishment of an experimental intrapulmonary tumor nodule model. *Ann Thorac Surg, 64*(1), 216-219. doi:10.1016/s0003-4975(97)00343-3

Wang, X. (2001). The expanding role of mitochondria in apoptosis. *Genes Dev, 15*(22), 2922-2933.

Wang, Y., Liu, Y., Zhao, C., Li, X., Wu, C., Hou, L., Zhang, S., Jiang, T., Chen, X., Su, C., Gao, G., Li, W., Wu, F., Li, A., Ren, S., Zhou, C., & Zhang, J. (2016). Feasibility of cytological specimens for ALK fusion detection in patients with advanced NSCLC using the method of RT-PCR. *Lung Cancer, 94*, 28-34. doi:10.1016/j.lungcan.2016.01.014

Warren, C. F. A., Wong-Brown, M. W., & Bowden, N. A. (2019). BCL-2 family isoforms in apoptosis and cancer. *Cell Death Dis, 10*(3), 177. doi:10.1038/s41419-019-1407-6

Watanabe, K., Otsu, S., Hirashima, Y., Morinaga, R., Nishikawa, K., Hisamatsu, Y., Shimokata, T., Inada-Inoue, M., Shibata, T., Takeuchi, H., Watanabe, T., Tokushige, K., Maacke, H., Shiaro, K., & Ando, Y. (2016). A phase I study of binimetinib (MEK162) in Japanese patients with advanced solid tumors. *Cancer Chemother Pharmacol, 77*(6), 1157-1164. doi:10.1007/s00280-016-3019-5

Weber, J. D., Raben, D. M., Phillips, P. J., & Baldassare, J. J. (1997). Sustained activation of extracellular-signal-regulated kinase 1 (ERK1) is required for the continued expression of cyclin D1 in G1 phase. *Biochem J, 326 (Pt 1)*, 61-68. doi:10.1042/bj3260061

Weickhardt, A. J., Aisner, D. L., Franklin, W. A., Varella-Garcia, M., Doebele, R. C., & Camidge, D. R. (2013). Diagnostic assays for identification of anaplastic lymphoma kinase-positive non-small cell lung cancer. *Cancer, 119*(8), 1467-1477. doi:10.1002/cncr.27913

Weis, S. M., & Cheresh, D. A. (2011). Tumor angiogenesis: molecular pathways and therapeutic targets. *Nat Med, 17*(11), 1359-1370. doi:10.1038/nm.2537

Weiss, J., Sos, M. L., Seidel, D., Peifer, M., Zander, T., Heuckmann, J. M., Ullrich, R. T., Menon, R., Maier, S., Soltermann, A., Moch, H., Wagener, P., Fischer, F., Heynck, S., Koker, M., Schottle, J., Leenders, F., Gabler, F., Dabow, I., Querings, S., Heukamp, L. C., Balke-Want, H., Ansen, S., Rauh, D., Baessmann, I., Altmuller, J., Wainer, Z., Conron, M., Wright, G., Russell, P., Solomon, B., Brambilla, E., Brambilla, C., Lorimier, P., Sollberg, S., Brustugun, O. T., Engel-Riedel, W., Ludwig, C., Petersen, I., Sanger, J., Clement, J., Groen, H., Timens, W., Sietsma, H., Thunnissen, E., Smit, E., Heideman, D., Cappuzzo, F., Ligorio, C., Damiani, S., Hallek, M., Beroukhim, R., Pao, W., Klebl, B., Baumann, M., Buettner, R., Ernestus, K., Stoelben, E., Wolf, J., Nurnberg, P., Perner, S., &

Thomas, R. K. (2010). Frequent and focal FGFR1 amplification associates with therapeutically tractable FGFR1 dependency in squamous cell lung cancer. *Sci Transl Med, 2*(62), 62ra93. doi:10.1126/scitranslmed.3001451

Willis, S. N., Chen, L., Dewson, G., Wei, A., Naik, E., Fletcher, J. I., Adams, J. M., & Huang, D. C. (2005). Proapoptotic Bak is sequestered by Mcl-1 and Bcl-xL, but not Bcl-2, until displaced by BH3-only proteins. *Genes Dev, 19*(11), 1294-1305. doi:10.1101/gad.1304105

Wilson, C., Nimick, M., Nehoff, H., & Ashton, J. C. (2017). ALK and IGF-1R as independent targets in crizotinib resistant lung cancer. *Sci Rep, 7*(1), 13955. doi:10.1038/s41598-017-14289-w

Witek, B., El Wakil, A., Nord, C., Ahlgren, U., Eriksson, M., Vernersson-Lindahl, E., Helland, A., Alexeyev, O. A., Hallberg, B., & Palmer, R. H. (2015). Targeted Disruption of ALK Reveals a Potential Role in Hypogonadotropic Hypogonadism. *PLoS ONE, 10*(5), e0123542. doi:10.1371/journal.pone.0123542

Wong, D. W., Leung, E. L., So, K. K., Tam, I. Y., Sihoe, A. D., Cheng, L. C., Ho, K. K., Au, J. S., Chung, L. P., Pik Wong, M., & University of Hong Kong Lung Cancer Study, G. (2009). The EML4-ALK fusion gene is involved in various histologic types of lung cancers from nonsmokers with wild-type EGFR and KRAS. *Cancer, 115*(8), 1723-1733. doi:10.1002/cncr.24181

Wright, C. J., & McCormack, P. L. (2013). Trametinib: first global approval. *Drugs, 73*(11), 1245-1254. doi:10.1007/s40265-013-0096-1

Wu, P. K., & Park, J. I. (2015). MEK1/2 Inhibitors: Molecular Activity and Resistance Mechanisms. *Semin Oncol, 42*(6), 849-862. doi:10.1053/j.seminoncol.2015.09.023

Xu, W., Kim, J. W., Jung, W. J., Koh, Y., & Yoon, S. S. (2018). Crizotinib in Combination with Everolimus Synergistically Inhibits Proliferation of Anaplastic Lymphoma KinasePositive Anaplastic Large Cell Lymphoma. *Cancer Res Treat, 50*(2), 599-613. doi:10.4143/crt.2016.357

Xu, Y., Zhang, Y. F., Chen, X. Y., & Zhong, D. F. (2018). CYP3A4 inducer and inhibitor strongly affect the pharmacokinetics of triptolide and its derivative in rats. *Acta Pharmacol Sin, 39*(8), 1386-1392. doi:10.1038/aps.2017.170

Yamaguchi, N., Lucena-Araujo, A. R., Nakayama, S., de Figueiredo-Pontes, L. L., Gonzalez, D. A., Yasuda, H., Kobayashi, S., & Costa, D. B. (2014). Dual ALK and EGFR inhibition targets a mechanism of acquired resistance to the tyrosine kinase inhibitor crizotinib in ALK rearranged lung cancer. *Lung Cancer, 83*(1), 37-43. doi:10.1016/j.lungcan.2013.09.019

Yamaguchi, T., Kakefuda, R., Tajima, N., Sowa, Y., & Sakai, T. (2011). Antitumor activities of JTP-74057 (GSK1120212), a novel MEK1/2 inhibitor, on colorectal cancer cell lines in vitro and in vivo. *Int J Oncol, 39*(1), 23-31. doi:10.3892/ijo.2011.1015

Yan, H. H., Jung, K. H., Son, M. K., Fang, Z., Kim, S. J., Ryu, Y. L., Kim, J., Kim, M. H., & Hong, S. S. (2014). Crizotinib exhibits antitumor activity by targeting ALK signaling not c-MET in pancreatic cancer. *Oncotarget, 5*(19), 9150-9168. doi:10.18632/oncotarget.2363

Yancopoulos, G. D., Davis, S., Gale, N. W., Rudge, J. S., Wiegand, S. J., & Holash, J. (2000). Vascular-specific growth factors and blood vessel formation. *Nature, 407*(6801), 242-248. doi:10.1038/35025215

Yang, J.-J., Zhang, X.-C., Su, J., Xu, C.-R., Zhou, Q., Tian, H.-X., Xie, Z., Chen, H.-J., Huang, Y.-S., & Jiang, B.-Y. (2014). Lung cancers with concomitant EGFR mutations and ALK rearrangements: diverse responses to EGFR-TKI and

crizotinib in relation to diverse receptors phosphorylation. *Clinical Cancer Research, 20*(5), 1383-1392.

Yang, J. Y., Zong, C. S., Xia, W., Yamaguchi, H., Ding, Q., Xie, X., Lang, J. Y., Lai, C. C., Chang, C. J., Huang, W. C., Huang, H., Kuo, H. P., Lee, D. F., Li, L. Y., Lien, H. C., Cheng, X., Chang, K. J., Hsiao, C. D., Tsai, F. J., Tsai, C. H., Sahin, A. A., Muller, W. J., Mills, G. B., Yu, D., Hortobagyi, G. N., & Hung, M. C. (2008). ERK promotes tumorigenesis by inhibiting FOXO3a via MDM2-mediated degradation. *Nat Cell Biol, 10*(2), 138-148. doi:10.1038/ncb1676

Yang, Q. H., Church-Hajduk, R., Ren, J., Newton, M. L., & Du, C. (2003). Omi/HtrA2 catalytic cleavage of inhibitor of apoptosis (IAP) irreversibly inactivates IAPs and facilitates caspase activity in apoptosis. *Genes Dev, 17*(12), 1487-1496. doi:10.1101/gad.1097903

Yeh, T. C., Marsh, V., Bernat, B. A., Ballard, J., Colwell, H., Evans, R. J., Parry, J., Smith, D., Brandhuber, B. J., Gross, S., Marlow, A., Hurley, B., Lyssikatos, J., Lee, P. A., Winkler, J. D., Koch, K., & Wallace, E. (2007). Biological characterization of ARRY-142886 (AZD6244), a potent, highly selective mitogen-activated protein kinase kinase 1/2 inhibitor. *Clin Cancer Res, 13*(5), 1576-1583. doi:10.1158/1078-0432.CCR-06-1150

Yerushalmi, R., Woods, R., Ravdin, P. M., Hayes, M. M., & Gelmon, K. A. (2010). Ki67 in breast cancer: prognostic and predictive potential. *Lancet Oncol, 11*(2), 174-183. doi:10.1016/S1470-2045(09)70262-1

Yip, P. Y. (2015). Phosphatidylinositol 3-kinase-AKT-mammalian target of rapamycin (PI3K-Akt-mTOR) signaling pathway in non-small cell lung cancer. *Transl Lung Cancer Res, 4*(2), 165-176. doi:10.3978/j.issn.2218-6751.2015.01.04

Yoshida, T., Oya, Y., Tanaka, K., Shimizu, J., Horio, Y., Kuroda, H., Sakao, Y., Hida, T., & Yatabe, Y. (3383). Differential crizotinib response duration among ALK fusion variants in ALK-positive non-small-cell lung cancer. *Journal of Clinical Oncology, 34*(28), 3383-3389. doi:http://dx.doi.org/10.1200/JCO.2015.65.8732

Yu, D., Zhang, X., Liu, J., Yuan, P., Tan, W., Guo, Y., Sun, T., Zhao, D., Yang, M., Liu, J., Xu, B., & Lin, D. (2008). Characterization of functional excision repair cross-complementation group 1 variants and their association with lung cancer risk and prognosis. *Clinical Cancer Research, 14*(9), 2878-2886. doi:10.1158/1078-0432.CCR-07-1612

Zamo, A., Chiarle, R., Piva, R., Howes, J., Fan, Y., Chilosi, M., Levy, D. E., & Inghirami, G. (2002). Anaplastic lymphoma kinase (ALK) activates Stat3 and protects hematopoietic cells from cell death. *Oncogene, 21*(7), 1038-1047. doi:10.1038/sj.onc.1205152

Zhang, L., Jiang, T., Li, X., Wang, Y., Zhao, C., Zhao, S., Xi, L., Zhang, S., Liu, X., Jia, Y., Yang, H., Shi, J., Su, C., Ren, S., & Zhou, C. (2017). Clinical features of Bim deletion polymorphism and its relation with crizotinib primary resistance in Chinese patients with ALK/ROS1 fusion-positive non-small cell lung cancer. *Cancer, 123*(15), 2927-2935. doi:10.1002/cncr.30677

Zhang, S., Anjum, R., Squillace, R., Nadworny, S., Zhou, T., Keats, J., Ning, Y., Wardwell, S. D., Miller, D., Song, Y., Eichinger, L., Moran, L., Huang, W. S., Liu, S., Zou, D., Wang, Y., Mohemmad, Q., Jang, H. G., Ye, E., Narasimhan, N., Wang, F., Miret, J., Zhu, X., Clackson, T., Dalgarno, D., Shakespeare, W. C., & Rivera, V. M. (2016). The Potent ALK Inhibitor Brigatinib (AP26113) Overcomes Mechanisms of Resistance to First- and Second-Generation ALK Inhibitors in Preclinical Models. *Clin Cancer Res, 22*(22), 5527-5538. doi:10.1158/1078-0432.CCR-16-0569

Zhang, S., Wang, F., Keats, J., Zhu, X., Ning, Y., Wardwell, S. D., Moran, L., Mohemmad, Q. K., Anjum, R., Wang, Y., Narasimhan, N. I., Dalgarno, D., Shakespeare, W. C., Miret, J. J., Clackson, T., & Rivera, V. M. (2011). Crizotinib-resistant mutants of EML4-ALK identified through an accelerated mutagenesis screen. *Chemical Biology and Drug Design, 78*(6), 999-1005. doi:10.1111/j.1747-0285.2011.01239.x

Zhang, W., & Liu, H. T. (2002). MAPK signal pathways in the regulation of cell proliferation in mammalian cells. *Cell Res, 12*(1), 9-18. doi:10.1038/sj.cr.7290105

Zhang, W., Moore, L., & Ji, P. (2011). Mouse models for cancer research. *Chinese Journal of Cancer, 30*(3), 149-152.

Zhang, W., Ruvolo, V. R., Gao, C., Zhou, L., Bornmann, W., Tsao, T., Schober, W. D., Smith, P., Guichard, S., Konopleva, M., & Andreeff, M. (2014). Evaluation of apoptosis induction by concomitant inhibition of MEK, mTOR, and Bcl-2 in human acute myelogenous leukemia cells. *Mol Cancer Ther, 13*(7), 1848-1859. doi:10.1158/1535-7163.MCT-13-0576

Zhang, X., Zhang, S., Yang, X., Yang, J., Zhou, Q., Yin, L., An, S., Lin, J., Chen, S., Xie, Z., Zhu, M., Zhang, X., & Wu, Y. L. (2010). Fusion of EML4 and ALK is associated with development of lung adenocarcinomas lacking EGFR and KRAS mutations and is correlated with ALK expression. *Mol Cancer, 9*, 188. doi:10.1186/1476-4598-9-188

Zhao, M., Suetsugu, A., Ma, H., Zhang, L., Liu, F., Zhang, Y., Tran, B., & Hoffman, R. M. (2012). Efficacy against lung metastasis with a tumor-targeting mutant of Salmonella typhimurium in immunocompetent mice. *Cell Cycle, 11*(1), 187-193. doi:10.4161/cc.11.1.18667

Zhao, Y., & Adjei, A. A. (2015). Targeting Angiogenesis in Cancer Therapy: Moving Beyond Vascular Endothelial Growth Factor. *Oncologist, 20*(6), 660-673. doi:10.1634/theoncologist.2014-0465

Zheng, X., He, K., Zhang, L., & Yu, J. (2013). Crizotinib induces PUMA-dependent apoptosis in colon cancer cells. *Mol Cancer Ther, 12*(5), 777-786. doi:10.1158/1535-7163.MCT-12-1146

Zhou, B., & Cox, A. D. (2015). Up-front polytherapy for ALK-positive lung cancer. *Nature Medicine, 21*(9), 974-975. doi:10.1038/nm.3942

Zhou, W. J., Zhang, X., Cheng, C., Wang, F., Wang, X. K., Liang, Y. J., To, K. K., Zhou, W., Huang, H. B., & Fu, L. W. (2012). Crizotinib (PF-02341066) reverses multidrug resistance in cancer cells by inhibiting the function of P-glycoprotein. *Br J Pharmacol, 166*(5), 1669-1683. doi:10.1111/j.1476-5381.2012.01849.x

Zhou, Y., Lin, S., Tseng, K. F., Han, K., Wang, Y., Gan, Z. H., Min, D. L., & Hu, H. Y. (2016). Selumetinib suppresses cell proliferation, migration and trigger apoptosis, G1 arrest in triple-negative breast cancer cells. *BMC Cancer, 16*(1), 818. doi:10.1186/s12885-016-2773-4

Ziogas, D. C., Tsiara, A., Tsironis, G., Lykka, M., Liontos, M., Bamias, A., & Dimopoulos, M. A. (2018). Treating ALK-positive non-small cell lung cancer. *Ann Transl Med, 6*(8), 141. doi:10.21037/atm.2017.11.34

Zou, H. Y., Friboulet, L., Kodack, D. P., Engstrom, L. D., Li, Q., West, M., Tang, R. W., Wang, H., Tsaparikos, K., Wang, J., Timofeevski, S., Katayama, R., Dinh, D. M., Lam, H., Lam, J. L., Yamazaki, S., Hu, W., Patel, B., Bezwada, D., Frias, R. L., Lifshits, E., Mahmood, S., Gainor, J. F., Affolter, T., Lappin, P. B., Gukasyan, H., Lee, N., Deng, S., Jain, R. K., Johnson, T. W., Shaw, A. T., Fantin, V. R., & Smeal, T. (2015). PF-06463922, an ALK/ROS1 Inhibitor, Overcomes Resistance

to First and Second Generation ALK Inhibitors in Preclinical Models. *Cancer Cell, 28*(1), 70-81. doi:10.1016/j.ccell.2015.05.010

Zou, H. Y., Li, Q., Lee, J. H., Arango, M. E., McDonnell, S. R., Yamazaki, S., Koudriakova, T. B., Alton, G., Cui, J. J., & Kung, P.-P. (2007). An orally available small-molecule inhibitor of c-Met, PF-2341066, exhibits cytoreductive antitumor efficacy through antiproliferative and antiangiogenic mechanisms. *Cancer Research, 67*(9), 4408-4417.